ENTERIC NERVOUS SYSTEM DEFICITS IN THE GANGLIONATED BOWEL OF HIRSCHSPRUNG MOUSE MODELS AND PATIENTS.

By

Melissa Anne Musser

Dissertation

Submitted to the Faculty of the

Graduate School of Vanderbilt University

in partial fulfillment of the requirements

for the degree of

DOCTOR OF PHILOSOPHY

in

Human Genetics

December, 2014

Nashville, Tennessee

Approved:

E. Michelle Southard-Smith, PhD

Maureen Gannon, PhD

Jennifer Kearney, PhD

Doug Mortlock, PhD

Sari Acra, MD, MPH

DEDICATION

to Alex, for his frequently tested but always immeasurable love and support

to my family, especially my parents David & Tammy Musser, who always nourished my insatiable curiosity and pursuits to cure it

ACKNOWLEDGEMENTS

First, none of this work would be possible without my funding sources. I would like to thank the following funding sources for science $$$ and for supporting my coffee addiction: March of Dimes FY12-450, NIH R01 DK60047, NIH F30 DK096831, VICTR award from the CTSA award No. UL1TR000445, T32 GM07347.

I have to thank all my previous science mentors for taking me into their labs and introducing me to the wonderful (and not so wonderful) aspects of research! Ola Fincke was instrumental in teaching me about experimental set up and planning and also introduced me to the fascinating world of “evo-devo” and population genetics. David McCauley elicited a love for all things neural crest. I am thankful that he took a chance on me as his first undergraduate student, and I am forever grateful for not being delegated to typical undergraduate grunt work and actually participating fully in experiments and having a skill set to take along when I left OU. I truly appreciate Marilyn Menotti-Raymond and lab member Victor David for giving me a chance in a genetics lab when I had absolutely no genetics lab background.

There are several programs, administrators, and individuals I would like to thank that made my PhD training bearable and even quite enjoyable at times. First, the CHGR and HGEN faculty, staff, and students have always been incredible. It has been hard to see so many changes in program personnel over the last couple years, but I hope our paths will cross in the future. I also owe a shout out to the PDB program, especially Chris Wright and David Bader. PDB has kept my love for development alive and continually challenges me to think creatively and critically about my science.

Several Vanderbilt labs and individuals within those labs have helped me learn new techniques or have been crazy enough to collaborate with me. Thanks to Byron Knowles (Jim Goldenring lab) for expert Western Blot advice, Joan Breyers (Jeff Smith

lab) for help with the LJL analyst, and Jumpei Kondo (Bob Coffey lab) for diving into the world of ICC. A special thanks to Elaine Shelton (Jeff Reese lab) for going out on a limb to help develop a new technique and Eric “Awesome” Armour (Kevin Ess/Rob Carson labs) for “secret science” and being an incredible roommate. Externally, several individuals and lab groups have given me science and career advice. There are too many to list here without being afraid of missing someone! But, I do need to personally thank Sam Li and Mike Gershon for letting me visit the lab in NY to learn gut motility assays.

A BIG shout out to the Core staff who made the majority of this study possible. In particular, I want to thank Carol Ann Bonner and Bob Matthews (CISR) and Sherry Smith (TPSR) for all their help as well as Jenny Taylor for taking great care of our mice. Other staff also made my life much more fun and amusing—especially “Danny” Kai and J.J. as well as a host of other custodial staff. Thanks for keeping me company at night and reminding me that most of the important and memorable things in life take place outside of school.

I have an amazing thesis committee! Doug Mortlock and Jennifer Kearney not only helped me navigate graduate school during thesis committee meetings, but were great teachers and I enjoyed having both of them as course directors. Sari Acra’s questions and advice always made me think about the clinical picture (and realize how much I did not always think about the clinical picture!) Thanks for helping to direct my attention and for jumping onto my committee at such short notice. Although an *ex officio* member, I appreciate Al George’s time on my committee and his ability to make me think critically and devise future directions. And, I cannot thank my chair, Maureen Gannon, enough for the time, support, and life advice she provided throughout graduate school.

I rotated in the Southard-Smith lab almost two years before I started my PhD studies! I would like to thank members of the lab during my rotation—Dustin Temple, Alex Nickle, Sarah Ireland and Jennifer Corpenning Rosebrock— for the warm welcome and

providing me with a great lab environment to work in. I have to give an even bigger shout out to Stephanie “Bizzle” Byers and Lauren C. Walters for not only welcoming me during my rotation, but sticking around long enough to be in lab when I joined. Even though the time we overlapped was brief, I gained two really great friends and am truly grateful for everything you guys taught me before you left lab. I’m still trying to “Suck it up and make it work!” and I hope our paths cross in the future, whether professionally or just over margaritas. Carrie Weise—I am so happy I got to now you before you ran off to graduate school and that we now have gotten to be jaded graduate students together. I wish you the best of luck in your future science endeavors and know you have the capabilities to go far.

I would like to thank Jean-Marc DeKeyser for his great stories, good sense of humor, and love for molecular science. Lab is always entertaining if you are around. Also, thank you for saving me from “early mornings” during motility assays. I also want to thank Dennis Buehler for always being dependable. Dennis—you have great science hands and can think very critically about science. Whether you continue as a lab tech or take your expertise elsewhere, you will do well. Noah Lawler, Kate Jones, and Makenzie Beaman are all great new additions to the lab; I am sad our time does not overlap more. And, I cannot thank Elaine “Kritter” Ritter enough. Elaine has been a rock of support in matters scientific, social, religious, intellectual, etc. and has become one of my best friends at school. I hope she never loses her love for science or sight of her goals. I look forward to our DERKIN DERNITS dates in the future. Derp.

I would be amiss if I did not thank my mentor, Michelle Southard-Smith, for the excellent training I received in her lab. Not only did I learn “how to do science” in Michelle’s lab, but Michelle provided me with several professional training opportunities that I believe many graduate students miss out on, including attending conferences, meeting leaders in

the field, allowing me to write a review, contributing to a book chapter, reviewing grants and paper, etc. I hope to stay in touch and that our paths will cross frequently in the future.

I lucked out when I was accepted to Vanderbilt's MSTP training program. I truly believe the MSTP leadership team here offers one of the most supportive and encouraging environments and MSTP could ask for. I would like to individually thank Michelle Grundy and Melissa Krasnove for their amazing abilities to keep everything organized and always make events run smoothly, Jim Bills for his sense of humor and always making feel reassured that everything will work out, and Terry Dermody for his always useful advice and keen insight. I also want to thank previous MSTP co-director Larry Swift for his contagious smile and encouragement. His calm demeanor and sound advice could put any type A, anxiety ridden MSTP student at ease. And, although I have only briefly interacted with Danny Winder, I was excited to hear of his addition the MSTP and look forward to working with him in the future. Finally, I love my MSTP class (2016!) and am thankful to have had such great people to share the journey with.

I would like to thank all my immediate family—Tom & Ginny Musser, Dick & Yvonne Tillemans, Rebecca, Jon, Catherine and Margaret—for always being supportive and keeping me in your thoughts and prayers. (Can you believe I am actually finishing my PhD? It's about time.) I also wanted to give a special thank you to my parents, Dave and Tammy Musser. No matter what crazy idea I had—from pageants, to taking a year after school to live in Maryland, to moving to Nashville for an 8+ year dual degree program—you were supportive. Thanks for your financial support, fun holidays, for believing in me, and never questioning why I still do not have a "real job."

And of course, this section would not be complete if I did not thank my better half, Alex Schenkman. Thank you for letting me practice my talks in front of you and discuss scientific ideas (even when you had no idea what I was talking about.) Thank you for putting up with me when I come home grumpy. Thank you for permitting my crazy work

hours. Thank you for moving to Nashville. I could keep going on forever in regard to the love and support you show me on a daily basis, but I was told the majority of this dissertation should pertain to my thesis work and should not be an in depth study of how awesome you are. So with that, I will say one last thank you, and I love you.

And…thank you mice. If IACUC allowed it, I would feed you all cheesecake.

TABLE OF CONTENTS

Page

LIST OF TABLES

LIST OF FIGURES

LIST OF ABBREVIATIONS

Abbreviation	
129Sv	129S6/SvEvTac mouse strain
5-HT	serotonin
AChE	acetylcholinesterase
Ascl1	achaete-scute homolog 1 (formerly Mash1)
B6	C57BL/6J mouse strain
BAC	bacterial artificial chromosome
BLPB	brain lipid binding protein
BMP	bone morphogenetic protein
bp	base pairs
BSA	bovine serum albumin
C3Fe	C3HeB/FeJ mouse strain
C57/B6	C57BL/6J mouse strain
CD1	Crl: CD1 (ICR) mouse strain
ChAT	choline acetyltransferase
CFP	cyan fluorescent protein
CGRP	calcitonin gene related peptide
CISR	Cell Imaging Shared Resource
cKIT	CD117; tyrosine-protein kinase kit; mast/stem cell growth factor receptor
CMMC	colonic migrating motor complexes
CCHD	Congenital Central Hypoventilation Disorder

Cre	Cre recombinase
DA	dopamine
D2 or Drd2	dopamine receptor 2
DS	Down Syndrome
DSS	dextran sodium sulphate
DNA	deoxyribonucleic acid
E	embryonic age
Edn3 or ET-3	endothelin 3
Ednrb	endothelin receptor type B
ENP	enteric neural progenitor
ENS	enteric nervous system
EtOH	ethanol
FABP7	fatty acid binding protein 7
Fgf-2	fibroblast growth factor 2 (basic)
FoxD3	forkhead box D3
GABA	gamma-aminobutyric acid
GADPH	glyceraldehyde 3-phosphate dehydrogenase
Gdnf	glial cell line-derived neurotrophic factor
Gfap	glial fibrillary acidic protein
Gfra1	Gdnf family receptor alpha-1
Gfra2	Gdnf family receptor alpha-2

GFP	green fluorescent protein
GI	gastrointestinal
GPI	glycophosphatidylinositol
GMS	gut muscle strip
H&E	hematoxylin and eosin stain
HAEC	Hirschprung associated-enterocolitis
Hand2	heart- and neural crest derivatives-expressed protein 2
HRP	horse radish peroxidase
HSCR	Hirschsprung disease
Hu	HuD; ELAV (embryonic lethal, abnormal vision, Drosophila)-like protein 4
ICC	interstitial cells of cajal
IHC	immunohistochemistry
IND	intestinal neuronal dysplasia
KO	knock-out
LacZ	β-galactosidase
Mash1	achaete-scute homolog 1
MEN2A	Multiple Endocrine Neoplasia Type 2a
MEN2B	Multiple Endocrine Neoplasia Type 2b
MP	myenteric plexus
NADPH	nicotinamide adenine dinucleotide phosphate
NBF	neutral buffered formalin

NC	neural crest
NCC	neural crest cell(s)
NCP	neural crest-derived progenitor
NDS	normal donkey serum
Neo	neomycin
Nestin	a type VI intermediate filament
NET	norepinephrine transporter
nNOS	neural nitric oxide synthase
NO	nitric oxide
Nrtn	neurturin
O/N	overnight
P	postnatal day (age)
PBS	phosphate buffered saline
PCR	polymerase chain reaction
PFA	paraformaldehyde
PGP9.5	UCH-L1; protein gene product 9.5
Phox2b	paired-like homeobox 2b
Rapsyn	receptor-associated protein of the synapse
REDCap	Research Electronic Data Capture
Ret	rearranged during transfection' receptor tyrosine kinase
RT	room temperature

s100	S100 calcium binding protein
SB	Laemli sample buffer
SDS-PAGE	sodium dodecyl sulfate-polyacrylamide gel electrophoresis
SERT	serotonin transporter
SEM	standard error of the mean
Shh	sonic hedgehog
Sox10	SRY (sex determining region Y)-box 10
Sox10-Cre	Sox10CrehGH BAC transgene
TBST	tris buffered saline with Tween20
tdTOM	tdTomato fluorophore
TE	tris & edta
TGS	tris-gylcine sodium dodecyl sulfate buffer
TH	tyrosine hydroxylase
TNBS	trinitrobenzene sulfonic acid
Tph1	tryptophan hydroxylase 1
Tph2	tryptophan hydroxylase 2
TPSR	Translational Pathology Shared Resource
TrkC	neurotrophic tyrosine kinase receptor type 3
TX-100	Triton X-100
vAChT	vesicular acetyl choline transporter
VENT	ventral neural tube

VIP	vasoactive intestinal polypeptide
WS4	Waardenburg-Shah Syndrome Type 4
WB	western blot
Wnt1	Wingless-type MMTV integration site family, member 1
WT	wildtype
YFP	yellow fluorescent protein

CHAPTER I

INTRODUCTION

This chapter is a modified version of a published review article (1). The journal, *Developmental Biology*, grants permission for reproduction within doctoral candidate theses.

Enteric Nervous System

The enteric nervous system (ENS) is a complex network of ganglia intrinsic to the intestinal wall that is necessary for normal motility and homeostasis of the gastrointestinal (GI) tract. The ENS originates from vagal, rostral truncal, and sacral neural crest (NC) populations that migrate to the fetal gut in the developing embryo (2). In the mouse, vagal and rostral trunk neural crest cells (NCC) emigrate from the neural tube to the foregut and migrate caudally to populate the entire gut. Sacral NCC delaminate later from the neural tube, enter the hindgut, and migrate rostrally, opposite the vagal NCC, to co-populate the post-umbilical portion of the gut. As these populations migrate from the neural tube and along the gut, cell-autonomous signaling as well as cues from the environment play a role in their lineage divergence (2). NCC contributing to the ENS, appropriately called enteric neural progenitors (ENPs), differentiate from a stem cell-like state to give rise to glia and numerous neuronal types (3-5). For successful ENS development, correct timing and dosage of gene expression affecting ENP survival, proliferation, and differentiation is essential. The necessity of balancing these processes is clearly seen in the human functional bowel disorder, Hirschsprung disease (HSCR), which is clinically recognized by the absence of ganglia in a variable portion of the distal intestine.

Research in ENS development has previously focused on HSCR in part because of the dramatic megacolon phenotype that results from aganglionosis of the distal bowel. This spotlight has remained trained on HSCR as a GI disorder due to success in identifying susceptibility genes

in patients and the recapitulation of aganglionosis in rodent models bearing mutations in homologous genes (6). Concurrent advances in treating HSCR patients through surgical removal of distal aganglionic bowel followed by reattachment of ganglionated proximal intestine to the anus has led to increased survival (7). Yet long term clinical follow-up of HSCR patients has found that surgical intervention does not completely "cure" intestinal symptoms in these individuals who continue to suffer from intestinal disorders, such as enterocolitis and chronic constipation, despite successful surgical removal of the aganglionic gut segment (7-10). The occurrence of such chronic bowel dysfunction across a variety of surgical procedures (10) and evidence from developmental studies of HSCR mouse models (11-13) hint that defects in ENS development in the proximal, ganglionated portions of the intestine may be causative. In particular, mechanistic analyses of HSCR mouse models indicate that defects in ENP developmental potential, the ability of NCC to differentiate into a variety of cell types, contribute to HSCR. Moreover, the concept that imbalance of NC-derived cell types within the ENS could lead to GI dysfunction is gaining strength, fueled by evidence from gene-specific mouse mutants that lack aganglionosis yet show deficits in ENS lineages, GI motility, and immune response (Table 1.1). This chapter collates multiple studies whose evidence adds weight to this concept and raises future questions for the field to address.

Enteric NCC deficits in Hirschsprung mouse models

Early studies in HSCR mouse models focused on determining the genetic causes of aganglionosis in spontaneously occurring mutants as a means to identify genes that contribute to development of the ENS. Initially, little thought was given to the possibility that ENS defects in ganglionated regions of the bowel might contribute to intestinal dysfunction. However, more recently, abnormalities in proximal ganglionated regions of the intestine have been recognized (12, 14, 15). This discovery led investigators to hypothesize that long term complications in HSCR patients could result from deficiencies in ganglia that had been formed in the proximal intestine

Allele	ENS density	ENS architecture	NCC lineage balance	Effect on GI function	Inflammatory response	References
Sox10$^{Dom/+}$	Decrease in ENPs	Variable disorganized patterning observed	*In vitro* data	Unknown	Unknown	Kapur, (1999), Southard-Smith et al., (1998), Walters et al., (2010)
Sox10$^{lacZ/+}$	Decrease in ENPs	Postnatal unknown	*In vitro* data; increase in immature neuronal markers *in vivo*	Unknown	Unknown	Paratore et al., (2002) Paratore et al., (2001)
Ednrb$^{s-l/s-l}$	Decreased intensity of AChE fibers	Abnormal patterning	Unknown	Unknown	Unknown	Cantrell et al., (2004))
EdnrB$^{s-l/s-l}$ *or* *EdnrB*$^{sl/+}$	Decreased through colon	Unknown	Unknown	Absent or impaired colonic migrating motor complexes	Subset susceptible to enterocolitis	Cantrell et al., (2004), Fujimoto, (1988a), Fujimoto et al., (1988b), Hosoda et al., (1994)
Ednrb$^{tm1Ywa/+}$ or *Ednrb*$^{tm1Ywa/tm1Ywa}$	Unknown	Unknown	Unknown	Unknown	Subset susceptible to enterocolitis	Cheng et al., (2010), Hosoda et al., (1994), Zhao et al., (2010)
ET-3$^{-/-}$	Decreased neuronal numbers	Unknown	Increased NOS+ neurons	Absent colonic migrating motor complexes	Unknown	Roberts et al., (2008)
Ret$^{tm1Cos/+}$	Normal neuronal numbers	Decreased neuron size and cholinergic fibers	Unknown	Reduced contractility; but ENS signaling aberrant	Unknown	Gianino et al., (2003)
Ret $^{DN/+}$	Decreased neuronal numbers	Decreased neuronal fiber density	Unknown	Unknown	Unknown	Jain et al., (2004)
Ret$^{CS20R/+}$	Decreased neuronal numbers	Decreased neuronal fiber density	Unknown	Unknown	Unknown	Carniti et al., (2006)
Gfra$^{+/-}$	Normal neuronal numbers	Decreased neuron size	Unknown	Reduced contractility; ENS signaling aberrant; delayed GI transit	Unknown	Gianino et al., (2003) Wang et al., (2010)
Gdnf $^{+/-}$	Decreased neuronal numbers	Alterations observed, but not significant	Reduction in NOS+ and CHAT+ neurons, but proportional to overall neuronal decreases	Reduced contractility; ENS signaling aberrant	Unknown	(Gianino et al., (2003), Shen et al., (2002); Wang et al., (2010)
Gdnf over expression	Neuronal numbers increased	Changes in fiber density with increased Gdnf expression	Increases in late born neuron subtypes	Stronger contractility; increased VIP and Substance P release; accelerated GI transit	Unknown	Wang et al., (2010)
Ascl1$^{-/-}$ (*Mash1*$^{-/-}$)	Decreased neuronal numbers	Wide spacing, erratic arrangement of ganglia	CGRP+ neuronal numbers normal, other subtypes unknown	Unknown	Unknown	Blaugrund et al., (1996)
TPH2 $^{-/-}$	Decreased neuronal density in ileum	Unknown	Decreased dopaminergic neurons	Slowed total GI transit and colonic emptying; accelerated gastric emptying	Unknown	Li et al., (2011)
D$_2^{-/-}$	Unknown	Unknown	Unknown	Faster total GI transit and colonic emptying; absorption affected	Unknown	Li et al., (2006)
Hand2 (*Nestin-del*)	Decreased neuronal numbers	Disorganized plexi	Decreased CHAT+, NOS+, and calretinin+ neurons and glia	Unknown	Unknown	Lei and Howard, (2011)
Hand2$^{+/-}$ *or* *Hand2*$^{flox/-}$	Decreased neuronal numbers	Disorganized plexi	Significant decrease in NOS+ neurons	Decreased GI motility	Decreased susceptibility to induced inflammation	D'Autreaux et al., (2011)
BMP over expression	No changes in neuronal density	Unknown	Region specific increases in dopaminergic, 5-HT+ and TrkC+ neurons; glia increased	Unknown	Unknown	Chalazonitis et al., (2004), Chalazonitis et al., (2011), Chalazonitis et al., (2008)
Noggin over expression	Increased neuronal numbers	Increased density	Increased TrkC+, 5-HT+ neurons, decreased GABA+ and CGRP+ neurons	Irregular transit; increased stool frequency, weight and water content	Increased susceptibility to induced inflammation	Chalazonitis et al., (2004), Chalazonitis et al., (2011), Chalazonitis et al., (2008), Margolis et al., (2011)
Fgf-2$^{-/-}$	Decreased neuronal numbers	Changes in neurite length; larger neurons	Decreased calbindin+ neurons	Reduced chloride-ion secretion; mucosal barrier defects	Unknown	Hagl et al., (2008), Hagl et al., (2012)
NET$^{-/-}$	Decrease in myenteric neuronal numbers	Unknown	5-HT+ and calretinin+ neurons reduced	Unknown	Unknown	Li et al., (2010)

Table 1.1. Summary of mutant allele effects on enteric nervous system structure and function. Changes in ENS architecture and density apply to ganglionated regions of the bowel for HSCR mouse models. Fields marked as "uknown" indicate data not reported or mouse model not tested.

(12, 15). As the field has learned more about the developmental processes that contribute to aganglionosis in mouse models, evidence for effects of individual HSCR genes on NCC lineage divergence in the fetal intestine has emerged.

Sox10

Sox10 is a SRY-related High Mobility Group-box transcription factor putatively expressed in all neural crest cells. Mice with a loss-of-function *Sox10*$^{+/-}$ (*Sox10*^{Lacz} *or Sox10*^{tm1Weg}) (11, 13) or a dominant-negative allele of *Sox10* (*Sox10*$^{Dom/+}$) (16, 17) both recapitulate the HSCR phenotype of distal bowel aganglionosis. Specifically, *Sox10Dom* is a dominant-negative mutation wherein an insertion mutation leads to an intact DNA binding domain, but a novel tail in the transcription activating domain (16, 18). The first clue that perturbations in normal Sox10 levels could produce alterations in development potential came from *in vitro* studies conducted on neural crest-derived progenitors isolated from dorsal root ganglia of *Sox10*$^{-/-}$, *Sox10*$^{+/-}$, and *Sox10*$^{+/+}$ mice (11). These isolated cells were allowed to grow and then differentiate in culture. The developmental potential of isolated progenitors was scored by the differentiated cell types these cultured cells produced. Sox10 deficient NCC showed altered developmental potential and were deficient in gliogenesis at both high and low plating densities. While this study focused on neural crest-derived cells collected from dorsal root ganglia, a subsequent effort by the same group determined that the temporal appearance of early and late neuronal differentiation markers within the fetal foregut and midgut of *Sox10*$^{+/-}$ mutants *in vivo* was also disrupted (13). Careful analysis revealed that neural progenitor cells expressing early neuronal markers like PGP9.5 were increased in frequency among *Sox10*$^{+/-}$ mutants, while more mature neurons marked by expression of neurofilament 160 were reduced. Interestingly, although the NC progenitor pool was decreased in *Sox10*$^{+/-}$ mutants, total neuronal numbers were not, suggesting that reduction of Sox10 promotes a neural fate, but may not contribute to later neural differentiation processes.

Whether these fetal irregularities persist in the postnatal intestine of *Sox10*$^{+/-}$ mutants remains in question.

An independent study assessed developmental potential of ENPs for the dominant-negative allele of *Sox10*, *Sox10*$^{Dom/+}$, while concurrently investigating the effects of genetic strain background on ENS development (12). This analysis found that ENPs from *Sox10*$^{Dom/+}$ mutants also had altered developmental potential *in vivo* and documented ENS irregularities in fetal and postnatal intestine of heterozygous *Sox10*$^{Dom/+}$ mice. Moreover, the authors reported atypical myofibroblast-like cells with cytoplasmic Phox2b expression in and around myenteric ganglia. While similar cells were also observed in wild type littermates, the overall number of these unusual cells was increased in *Sox10*$^{Dom/+}$ mutants. Taken together the studies by Paratore et al., (2001, 2002), and Walters et al., (2010), suggest that altered developmental potential of NCC, including enteric cell types, occurs in HSCR individuals carrying *Sox10* mutations. However, whether this altered developmental potential ultimately disrupts the balance of cell types in the postnatal enteric ganglia *in vivo* and how such alterations would affect intestinal function has not previously been explored. To this end, I explicitly analyzed neuron, glia, and specific neuronal subtype populations as well as motility and inflammation in the *Sox10*$^{Dom/+}$ mouse model (Chapter 2).

Ednrb/Edn3

Endothelin receptor B (*Ednrb*) is expressed in migrating NCC while its preferred ligand, Endothelin 3 (*Edn3*) is expressed in the gut wall. Several spontaneously occurring and genetically modified rodent models with altered *Ednrb* or *Edn3* expression exist (19-23). One study has documented alterations in proximal ENS density and patterning among *Ednrb*$^{s-l/s-l}$ homozygous mutants (14) and a more recent study has shown that *Ednrb*$^{-/-}$ have fewer cholinergic neurons in the colon, but more colonic VIP neurons compared to *Ednrb*$^{+/-}$ littermates (24). In regard to functional outcomes, *Ednrb* mutants do exhibit enterocolitis that leads to early death. Fujimoto et. al., (25) first described the presence of enterocolitis in the piebald lethal (*Ednrb*$^{s-l/s-l}$) mouse.

Ednrb$^{s\text{-}l/s\text{-}l}$ mice have an increase in enterocolitis compared to wild-type littermates and a subset of *Ednrb*$^{s\text{-}l/s\text{-}l}$ mice die presumably due to acute infectious processes as they have no gross megacolon, but exhibit acute splenitis and an increase in intestinal Ig-A secreting plasma cells at time of death (26). Similarly, a subset of Ednrb-null (*Ednrb*$^{Tm1Ywa/Tm1Ywa}$, hereafter referred to as *Ednrb*$^{-/-}$) mice die prematurely with signs of widespread bacteremia (27). Interestingly, these inflammatory processes appear mediated, at least in part, by ganglionated portions of the intestine as ~40% of *Ednrb*$^{-/-}$ mice that undergo corrective pull-through surgery to remove aganglionic bowel still go on to develop enterocolitis (28). Mice with mutations in *Edn3 (Et-3)* have not been assessed for enterocolitis, but have been evaluated for altered GI motility and proportions of enteric neurons. *ET-3* $^{-/-}$ (*Edn3*$^{tm1Ywa/tm1Ywa}$) lack colonic migrating motor complexes in the ganglionated portions of their bowel. Additionally, despite having a lower density of neurons in the myenteric plexus, they have twice as many NOS expressing neurons compared to their wild-type littermates (22).

Ret Signaling Pathway

Gene deficits among members of the Ret signaling pathway have been the most extensively studied models for HSCR phenotypes. Ret is a receptor tyrosine kinase expressed on ENPs that has documented roles in proliferation, migration, and survival of these cells. Although several Ret ligands and co-receptors exist, Ret signaling in the development of the ENS primarily occurs in conjunction with its Gfra1 co-receptor and its preferred ligand, Gdnf (29).

In humans, a single functional mutation in *RET* is sufficient to cause HSCR. In mice, gene targeting of *Ret* (*Ret*$^{tm1Cos/tm1Cos}$ *,* commonly referred to as *Ret*$^{-/-}$*)* results in complete loss of the ENS in the small and large intestines (30, 31). However, mice with heterozygous loss (*Ret*$^{+/-}$) appear normal and healthy, with no aganglionosis or loss of neuron numbers in either myenteric or submucosal ganglia (29). Whether the proportions of various neuron subtypes in *Ret*$^{+/+}$ and *Ret*$^{+/-}$ are equivalent remains unknown. Interestingly, *Ret*$^{+/-}$ mice do show a reduction in neuron

size and cholinergic neuronal fiber count in certain regions of the bowel and also exhibit deficits of intestinal contractility (29). The cellular basis of the motility deficits observed in heterozygous *Ret*$^{+/-}$ mutants is of interest not only from a mechanistic standpoint, but also because heterozygous deficiencies are more prevalent in patient populations.

Intermediate phenotypes in *Ret* mutant mice that exhibit the distal aganglionosis present in human HSCR patients have been generated. These include the *Ret*$^{DN/+}$ (*Ret*$^{tm3.1Jmi/+}$) mouse that harbors a dominant-negative mutation (15) and the *Ret*$^{C620R/+}$ (*Ret*$^{tm1Cti/+}$) mouse that carries a gain-of-function point mutation (32). NC lineage segregation has not been evaluated in either of these two models. However, the ENS in the proximal bowel of the *Ret*$^{DN/+}$ mouse contains fewer neurons and exhibits decreased neuronal fiber density. These heterozygous models provide an ideal opportunity to investigate roles for *Ret* in NC lineage segregation.

Gfra1 (Gdnf receptor alpha-1) is a GPI-linked co-receptor that preferentially binds Gdnf (glial derived neurotrophic factor) with Ret (33, 34). Deficits in ENS development in *Gfra1* mutants tend to recapitulate those found in *Ret* mutants. This evidence supports the theory that Ret signaling through Gfra1 and Gdnf, not other co-receptor:ligand pairs, is largely acting in early ENS development. Similar to complete loss of *Ret*, ablation of *Gfra1* (*Gfra*$^{tm3Jmi/tm3Jmi}$, commonly called *Gfra*$^{-/-}$) leads to a nearly complete absence of neurons in the small intestine and colon (35, 36). And, as is seen for *Ret* heterozygous mutants, animals lacking a single copy of *Gfra1* possess normal numbers of neurons in both myenteric and submucosal plexi, but significant reductions in neuron cell size are evident in some regions of the intestine and contractility of the intestine is abnormal in these animals (29).

Studies from mouse models with altered Gdnf expression, particularly those that disrupt levels or timing of Gdnf production, provide the best evidence to date that Ret signaling influences ENP lineage divergence. Similar to *Ret* and *Gfra1* knockouts, *Gdnf* null mice (*Gdnf*$^{tm1Rosl/tm1Rosl}$ knockout mutants, commonly called *Gdnf*$^{-/-}$) do not develop enteric ganglia caudal to the stomach and exhibit early lethality. However *Gdnf*$^{+/-}$ mice, in contrast to *Ret*$^{+/-}$ and *Gfra-1*$^{+/-}$ mutants, do

exhibit hypoganglionosis throughout the intestine (37). To investigate the effect of Gdnf expression levels on ENS development, Wang and colleagues (38) over-expressed Gdnf in the fetal intestine. Overexpression starting at embryonic day 17 was accomplished using transgene constructs that conferred expression in enteric glia or the muscle cells, while postnatal, global Gdnf expression was accomplished through daily peritoneal injections starting at birth. Both modes of Gdnf overexpression resulted in increased neuronal proliferation in submucosal neurons of the small intestine as well as neurons of both plexi in the colon. While myenteric neurons in the small intestine showed no significant increases in proliferation, the timing of GDNF overexpression affected submucosal neuronal subtypes. Early born neuron subtypes that were established before the onset of GDNF overexpression, such as serotonergic neurons, and ChAT expressing neurons, were not significantly affected. However, neurons that appear early but also continue to be born in the postnatal period, such as NOS+ neurons, were significantly increased in number in both Gdnf overexpression models. In addition, gross intestinal contractility changes were found in mice with Gfap-driven Gdnf overexpression. While the altered contractility may indirectly correlate with increased numbers of NOS neurons, the mechanistic basis remains to be determined as electrical properties of specific neuronal subtypes were not evaluated and multiple neuronal subtypes were not examined. It will be interesting to determine if overexpression of Gdnf before embryonic day 17 alters ratios and functionality of earlier born neuronal subtypes or if postnatal reduction of Gdnf levels cause reductions in late born neuron types.

It is worth noting that while Ret signaling through the Gfra1:Gdnf (co-receptor:ligand) combination plays an early and major role in ENS development, signaling through interactions with Gfra2:Nrtn plays a later role. This is especially relevant for the maintenance and proliferation of neurons in the submucosal plexus of the small intestine and both plexi of the colon (29). The possibility that Gfra2:Nrtn are able to compensate for a loss of Gdnf in late stages of development expression or whether this axis selectively affects NC subtypes is yet to be determined. While heterozygous *Ret*$^{+/-}$, *Gfra-1*$^{+/-}$, and *Gdnf* $^{+/-}$ mouse mutants do not exhibit absence of enteric

ganglia in the distal intestine that is characteristic of HSCR, all of these models share loss of intestinal contractility and exhibit reduced release of neurotransmitters *in vitro* (29). Understanding the causes of altered GI motility is crucial for developing strategies to treat patients with functional GI deficits that comprise a substantial proportion of the population. The realization that heterozygous deficiency of *Ret*, *Gfra1*, and *Gdnf* alter the composition and functionality of the ENS likely would not have come about without studies to better understand the rare disorder HSCR. These results nicely illustrate how studies of rare disorders can inform common problems.

Enteric NCC deficits in non-Hirschsprung Mouse Models

Although mouse mutants have been used to model the obvious aganglionosis that occurs in human HSCR, studies in non-HSCR mouse models provide the most substantial evidence that disruption of NC-derived lineages can occur in the ENS and that these imbalances can alter GI function. Understanding the etiology of GI dysmotility is relevant to a large fraction of the population as millions of people suffer from intestinal motility disorders. Surprisingly, the etiologies of chronic constipation, pseudo-obstruction, Crohn's disease, ulcerative colitis, and other GI disorders that appear to have genetic components remain relatively obscure (39-42). Given the evidence detailed below, it is likely that ENS defects, including abnormal NC lineage segregation, contribute significantly to many GI disorders. Discoveries in non-HSCR mouse models should aid in teasing apart the etiologies of these disorders.

Ascl1 (formerly Mash-1)

Ascl1 (*Mash-1*) is a basic helix-loop-helix transcription factor most extensively studied for its role in neurogenesis in the central and sympathetic nervous systems (43). However, *Ascl1* also largely influences development in a subpopulation of ENPs. Blaugrund et al., (1996) determined that *Ascl1*-dependent enteric progenitors give rise to a subset of transiently

catecholaminergic cells which differentiate into serotonergic neurons. Transiently catecholaminergic cells initially express catecholaminergic gene products, such as tyrosine hydroxylase, but lose catecholominergic gene expression upon differentiation. *Ascl1* null embryos (*Ascl1*$^{tm1And/tm1And}$, commonly referred to as *Ascl1*$^{-/-}$) have severely reduced neuronal serotonin (5-HT) expression and exhibit gross ENS deficits, such as a reduction in overall neuronal number and more widely spaced and erratically arranged ganglia. This study only evaluated one other neuronal subtype, the late born CGRP (calcitonin gene related peptide) expressing neurons, which appeared unaffected in *Ascl1* null mutants. Recent studies described below have found that perturbations in neuronal serotonin expression alter neuronal subtype proportions and development; thus, it would be interesting to evaluate other neuronal subtypes in the *Ascl1*$^{-/-}$ mutants.

Serotonin (5-HT)

Although serotonergic neurons only comprise 1-2% of the myenteric plexus in rodents (44), they are one of the earliest types of neurons that exit the cell cycle in the developing ENS (3) and they also affect the development of later born neurons, GI motility (45), and GI epithelial growth (46). The exact role 5-HT plays in GI development and function has been somewhat obscured by the fact that two 5-HT expressing cell types exist in the gut — enterochromaffin cells within the gut epithelium and neurons within the myenteric and submucosal plexi. The recent, fortuitous discovery that 5-HT expressing epithelial cells rely on the enzyme Tph1 (tryptophan hydroxylase 1) for 5-HT synthesis while enteric neurons rely on the enzyme Tph2 (tryptophan hydroxylase 2) (47, 48) has permitted a more thorough investigation of 5-HT in ENS development. Li et al., (2011) conducted a study utilizing *Tph1*, *Tph2*, and *Tph1/2* knockout (KO) mice to determine the effects of 5-HT depletion (epithelial vs neuronal vs total gut respectively) on enteric development and GI motility. These studies identified perturbations of both ENS development and GI motility in the *Tph2* KO (neuronal 5-HT depleted) mice. In contrast such perturbations

were not seen in *Tph1* single knockout or exacerbated in the *Tph1/2* double knockouts. In comparison to wild-type ENS development, *Tph2* KO mice had a significantly lower neuronal density in the ileum and a significant decrease in the late born dopaminergic neurons. Complementary gain-of-function experiments using ENPs isolated from *Slc6a*$^{-/-}$ (serotonin transporter) mutants, as well as treatment of ENP cultures with 5-HT both confirmed and extended the finding that 5-HT impacts development of dopaminergic neurons in the fetal intestine. Functional deficits due to loss of neuronal 5-HT were also documented in *Tph2* KO mice including significantly faster gastric emptying but overall slower total GI transit and colonic emptying. How disruption of one enteric neuronal population, like 5-HT+ neurons, might impact cell types within the ganglia is diagrammed in Figure 1.1. Experiments to investigate the effect of neuronal 5-HT overexpression on ENS development and GI motility have yet to be conducted.

Dopamine Receptor 2 (Drd2)

Do alterations of ENS dopaminergic signaling significantly alter GI function? Li et al, (49) conducted a study in which dopaminergic signaling was disrupted through dopamine receptor 2 (Drd2) knockouts. Five dopaminergic receptors (Drd1a-5) are expressed in the gut, but Drd2 is restricted to enteric neurons. *Drd2*$^{-/-}$ (allele name *Drd2*$^{tm1Schm/tm1Schm}$) knockout mice had faster total GI transit times as well as faster colonic motility when compared to wild type littermates. Absorption of food was affected as *Drd*$_2^{-/-}$ mice were runted although they ate more food and drank more water than wild type siblings. Other neurons and other cell types receiving signals from dopaminergic neurons in the bowel may be able to compensate for changes in dopaminergic neuron number or function by altering dopamine (DA) receptor expression. However, this possibility remains to be investigated in detail.

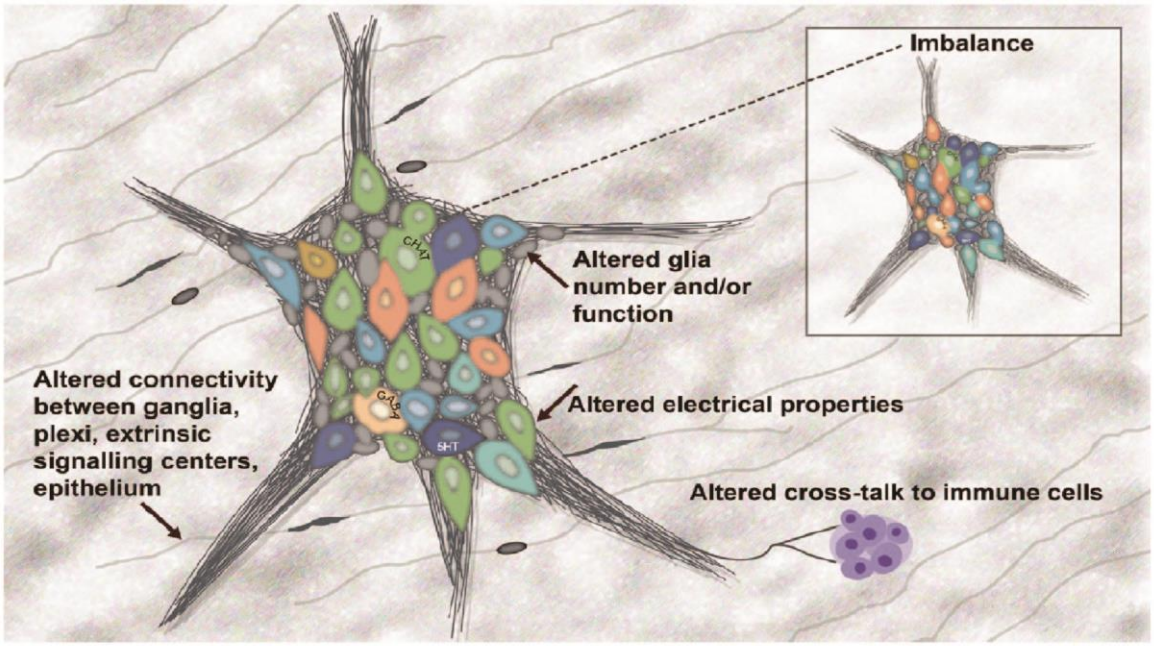

Figure 1.1. Potential mechanisms by which alterations in gene expression or function could lead to multiple ENS defects. A typical normal myenteric ganglia is shown consisting of multiple neuronal subtypes (ChAT+ green, 5-HT+ dark blue, and GABA+ peach). Enteric glia normally reside within the ganglia, along inter-ganglia fibers, and within the underlying muscle (grey ovals/stellate cell shapes). Changes in neuron and glia numbers and imbalance of specific neuronal subtypes (such as the decrease in CHAT+ neurons seen in the inset, fewer green neuronal cell bodies) have already been described in some mouse mutants. These alterations — as well as more subtle changes — could disrupt the electrical properties of neurons and glia thus interfering with signaling between ENS components and other cell types like those of the immune system. Such changes could ultimately result in GI dysfunction due to deficits in motility and inappropriate immune response.

Hand2

Hand2 (heart- and neural crest derivatives-expressed protein 2) is a basic helix-loop-helix DNA binding protein that plays a role in neurogenesis and proliferation (50). Several studies in recent years have implicated *Hand2* in lineage divergence among ENS progenitors (45, 51-53). Collectively, these efforts demonstrate how loss of a single gene can alter proportions of specific neuronal classes in the ENS with a significant impact on intestinal motility.

Initially, Hendershot et al (2007) ablated Hand2 expression in NC derivatives through crosses of a conditional floxed allele (*Hand2*$^{tm1.1MajH:Wnt1-Cre}$) with a *Wnt1* promoter driven-Cre transgene (54). This strategic approach removed *Hand2* from all NCC with the result that organization and connectivity of enteric ganglia was disturbed accompanied by an overall reduction in neuron numbers. Complete absence of VIP expressing neurons from the fetal intestines of these mutants, while ChAT+ neurons were maintained, was the first indication that loss of *Hand2* could have a specific effect on a discrete neuron lineage. In subsequent analyses, Lei et al (2011) depleted *Hand2* from a specific subset of progenitors during ENS development using a Nestin-Cre driver (allele *Hand2*$^{tm1.1MajH:Nestin-Cre}$). Through this refined ablation of Hand2, a Nestin-independent population of ENPs that accounted for approximately 15% of total enteric neural precursors was revealed. In *Hand2* depleted mutants, this population was able to proliferate and compensate for a decrease in nestin-dependent neurons. However, this compensatory effect was unique to specific subsets of neurons in *Hand2* mutants. For example, Nestin-independent precursors were able to proliferate and compensate for the loss in nestin-dependent ChAT neurons, but could not compensate for the loss of NOS or calretinin expressing neurons. Additionally, Nestin-independent precursors appeared skewed towards a neuronal fate. In wild type animals and Nestin-driven *Hand2* depleted mice, greater than 90% of glia were Nestin-dependent. Glia were reduced overall in Nestin-driven Hand2 depleted animals and nestin-independent precursors did not compensate for this loss of glia. In addition to skewed ratios of NC derivatives, Nestin-driven Hand2 depleted mice had an overall disorganized plexus and

typically died by postnatal day 20. While the cause of death was uncertain, these animals exhibited massive distension of the entire GI tract, and it is certainly plausible that GI dysfunction contributed to their premature death.

D'Autreaux et al., (2007) also observed that NC-specific depletion of Hand2 disrupted terminal differentiation of enteric neurons. Moreover, this group later demonstrated that *Hand2* depletion in the ENS impacted not only GI motility, but inflammation as well (45). Similar to the Lei et al., (2011), they observed disruption of enteric plexus organization as well as a significant decrease in NOS expressing neurons in *Hand2* deficient mice (*Hand2*$^{+/-}$ and *Hand2*$^{flox/-}$). However, they also found that neuronal subtype specification is *Hand2* dosage specific by analyzing ratios of NOS+ neurons in various combinations of *Hand2* targeted alleles. In contrast to the Lei et al., (2011) study, D'Autreaux et al., (2011), found glia numbers were not significantly reduced in the myenteric plexus of *Hand2* haplo-insufficient mutants. This finding could either reflect the capacity of enteric glia to differentiate despite low levels of Hand2, temporal effects of Hand2, and/or the effect of differential Hand2 expression levels in distinct NCC subpopulations. Effects of transcription factor levels and timing have previously been shown to play a role in cell lineage segregation in the pancreas (55-58). And, differential expression of transcription factor levels may be functional in the ENS as well since this phenomenon has been documented in ENPs at stages concurrent with lineage segregation (59). Regardless of the underlying mechanism, the D'Autreaux and Lei studies also differ since Nestin-Hand2 depleted mutants die near weaning with gross bowel distention, but *Hand2*$^{+/-}$ mice are fertile and have a normal lifespan. However, despite a normal lifespan, *Hand2*$^{+/-}$ heterozygotes do not have normal intestinal function, as D'Autreaux et al., (2011) documented these mutants have a significant increase in total GI transit time and markedly slower colonic motility compared to wild type littermates. Surprisingly, despite a reduction in overall neuronal density and decrease in GI motility, *Hand2*$^{+/-}$ mice are protected against TNBS induced inflammation when compared to wild type littermates (60). This finding was unexpected as increased gut motility is thought to protect against microbial overgrowth and

infection (61). Margolis et al., (2011) concluded that an overall decrease in neuronal density is protective against GI inflammation despite the decrease in motility seen in these mutants. Indeed, neurons have been implicated in GI inflammation (62). For example, T cell activation in the intestine leads to an altered electrical response from the ENS and post-ganglionic sympathetic innervation is known to regulate mast cell actions (reviewed in Sharkey & Mawe, 2002). However, the specific mechanisms and theneuron subtypes contributing to inflammatory processes remain largely unknown. Future studies elucidating roles for distinct neuronal subtypes and enteric glia in initiating and propagating inflammation will be essential to understanding how the ENS mediates enterocolitis.

Bone Morphogenic Proteins (BMPs)

BMPs orchestrate several developmental programs in a dosage and time specific manner during the course of development including neurogenesis in the developing gut. ENPs encounter BMP signaling throughout development as the notochord and somites mature (63). In addition, it is known that BMP 2, 4, and 7 are expressed in the developing fetal intestine (64, 65).

The influence of BMPs agonists and antagonists on ENP lineage segregation has been studied *in vitro* and *in vivo* for multiple enteric lineages. *In vitro,* isolated rat ENPs treated with BMP2 and BMP4 levels above those normally encountered *in vivo* appear to specify TrkC expressing neurons prematurely and cause an overall increase the number of TrkC expressing neurons (64). Mouse models with neuronal BMP4 overexpression show no changes in ENS neuronal density *in vivo*; however, neuronal subtype proportions are skewed with significant increases in dopaminergic neurons, serotonergic neurons, and TrkC expressing neurons in specific gut regions (65). Additionally, BMP4 overexpression causes glial numbers to increase markedly at the expense of neurons (66).

Antagonsim of BMP signaling in neurons through neuron specific enolase (NSE)-driven noggin overexpression corroborated findings in regard to the role of BMPs in ENS development.

Noggin overexpression in neurons increases overall ENS neuronal density which is consistent with BMPs' opposing role in promoting neural differentiation at the expense of proliferation (67). Noggin overexpression increased the proportion of serotonergic neurons (65), but led to decreases in TrkC and GABA and CGRP expressing neurons (64) (65) as well as the glia to neuron ratio (66). Importantly, these mice also exhibited irregular bowel transit (65) as well as increased sensitivity to chemically induced inflammation (60). It is clear that decreased BMP signaling tips the balance to favor more neurons and glia as well as certain neuronal subtypes; however, we can only speculate now as to how these imbalances are exactly influencing GI function. Also, it is imperative to mention that these studies (64-66) and others (67) note the dosage and timing of BMP expression affects the timing and differentiation capacity of cell types.

Norepinephrine Transporter (NET)

Although the ENS is not known to house any intrinsic norepinephrine producing neurons, developing transiently catecholaminergic neural precursors express norepinephrine transporter (NET). Transiently catecholaminergic subtypes include, but are not limited to, 5-HT expressing neurons and some (but not all) Calretinin and NOS expressing subtypes (68, 69). To determine if NET is essential for the specification of these transiently catecholaminergic neuronal subtypes, Li et. al., (69) evaluated transiently catecholaminergic subtypes in the myenteric plexus of NET null mice (*Slc6a2*^{tm1Mca}, common name *NET*$^{-/-}$). *NET*$^{-/-}$ mice have an overall decrease in myenteric neuron numbers, with 5-HT and Calretinin+ subsets significantly reduced in number. In *NET*$^{-/-}$ mutants, NOS+ neurons were observed to be slightly reduced in number, but the reduction was not significant. These results indicate that NET is essential for certain transiently catecholaminergic subtypes. However, it is unknown whether both the transiently catecholaminergic NOS and non-transiently catecholaminergic NOS populations of neurons were largely unaffected by the NET deficiency or if one of these populations was able to proliferate and compensate for an undocumented loss in the other population.

Fgf2 and Sprouty2

Mutations in *Sprouty2*, an FGF2 antagonist, have been associated with intestinal neuronal dysplasia (IND) in humans (70) and *Fgf-2*$^{-/-}$ (*Fgf2*$^{tm1Zllr/tm1Zllr}$) mice similarly exhibit abnormally large ganglia that contain fewer, but larger, neurons than wild-type mice (71). Hagl and colleagues (72) classified enteric neurons in *Fgf-2*$^{-/-}$ mice based on morphology measures (73) and found a significant decrease in calbindin expressing Dogiel Type 2 neurons . Neurons may be classified by their shape, function, neurotransmitters, electrical properties, and/or gene expression patterns. Most of the studies mentioned previously used gene expression detected by immunohistochemistry to classify neurons. Because the studies by Hagl et al (2012) assessed morphology and calbindin expression as characteristic features, the authors hypothesized that the neuronal population lost was sensory in nature. Additionally, *Fgf-2*$^{-/-}$ mice exhibit alterations in chloride secretion and translocation of bacteria across the mucosal barrier. How the ENS modulates permeability to bacterial penetration has not been determined (71).

Transgenic Models

Recent development of fluorescent transgenic mouse models (59, 74, 75) has permitted refined analyses of ENS development that were not previously possible by immunohistochemical studies of mutant strains. In particular, it has long been accepted that ENPs either enter the foregut mesenchyme proximally and migrate down its length in a rostral to caudal fashion (vagal ENPs) or they enter the gut at the distal end and migrate caudal to rostral (sacral ENPs). These processes left unexplained how subsets of HSCR patients exhibit 'skip segment' aganglionosis where small region(s) of the colon contain ganglia (O'Donnell & Puri, 2010) instead of continuous aganglionosis that is typically seen in the distal colon. How skip segment aganglionosis might arise given known mechanisms remained a quandary although several groups suggested that extramural ENPs could account for the ganglionated 'skip segments' seen in some HSCR cases (76, 77). Synthesis of information from multiple transgenic models now suggests these skip

regions occur because normal migration of ENPs across the mesentery between the small intestine and the colon occurs, but subsequent filling of the proximal colon by ENPs that migrate from the cecum fails. Mesenteric ENPs were initially reported by Drukenbrod & Epstein (75). However, only recently has mechanistic data emerged that can explain the role of these mesenteric ENPs in skip segment aganglionosis. Recent analysis by Nishiyama et al., (78) using elegant live cell imaging, has unequivocally shown that ENPs migrate across gut mesentery to populate the majority of the colon before cells migrating down the length of the gut tube arrive. The integration of these analyses is just one more example of how studying fundamental processes in normal development can serve to elaborate the etiology of disease.

Summary

Post-surgery, chronic constipation and/or enterocolitis afflicts many HSCR patients, and some *Ednrb* mouse models suffer from enterocolitis as well despite surgical removal of the aganglionic segment (28). Because the distal aganglionic region has been removed in these patients and mouse models, the effect of and role played by ganglionated proximal intestine in long-term GI function has to be considered. To date, evidence suggests the balance of cell types within enteric ganglia that derive from NC during lineage segregation can significantly alter the ENS. Studies from mouse models that mimic the diagnostic feature of HSCR, aganglionosis, are in their infancy, but recent studies and additional data presented within subsequent chapters are consistent with the possibility of disrupted lineage segregation in at least some HSCR mutants. Specifically, Chapter 2 herein is an in depth study in regard to enteric neural crest-derived lineage imbalance and alterations in gastric emptying and small intestine transit in the *Sox10*$^{Dom/+}$ HSCR mouse model. In the same vein, Chapter 4 details aberrant pyloric sphincter function in the *Sox10*$^{Dom/+}$ HSCR mouse.

Likewise, analysis of enteric development in mouse mutants that do not exhibit overt aganglionosis (non-HSCR) also indicates that any one of several gene deficits can disrupt the

normal processes of ENS ontogeny and skew the resulting profile of neurons and glia away from normal composites. It should be emphasized that while several non-HSCR mouse mutants exhibit alterations in enteric neural crest lineages, how these imbalances directly or indirectly cause GI dysfunction remains to be determined. Many studies evaluating ENS architecture and composition do not assess GI function and those preliminary studies that do focus on gross assessments, such as overall changes in GI transit time or colonic motility. A need for further histological, physiological, and electrophysiological studies to determine exactly how certain populations and imbalances in these populations affect GI function would be valuable for better understanding the etiology of intestinal dysmotility.

As the ENS field moves forward, we must consider several factors. How much does one need to tilt the balance of neural crest derivatives for GI dysmotility to occur? The answer to this question is paramount. Some variability in neural crest derivative portions is expected since different inbred mouse strains may have slight differences in neuronal subtypes proportions but still have normal bowel function (48). It may be that only certain environmental stressors, such as infection, cause certain imbalances to manifest as disease. Reduced penetrance seen in some human diseases could be due to a slight tip of the balance by genetic modifiers, causing the balance to wax and wane between disease and unaffected amongst family members. Other functional bowel disorders in humans appear to have a genetic component, but the genetic etiologies and risk factors remain unknown. Small perturbations that do not lead to overt aganglionosis, but cause imbalances of cell types or alterations in ENS signaling, could explain disorders such as chronic constipation despite the presence of detectable enteric ganglia throughout the intestine. This possibility is likely given a recent case study documenting chronic constipation in a patient with a *RET* mutation, but no detectable HSCR disease (79). In Chapter 3, I present data further corroborating this possibility as I observed increased total gut transit times in *Ret* deficient male mice compared to wild type littermates.

Additionally, recent studies have unearthed previously unrecognized ENP subpopulations that appear to be distinct in their developmental capacity. It was formerly believed that ENPs were homogenous with regard to expression of Nestin, but Lei et al (2011) identified a previously unknown ENP nestin-independent population. A study by Mundell and colleagues (80) revealed a distinct ENP population that does not express *Ednrb* and appears to have substantial capacity to compensate for loss of other enteric progenitors during ENS development. The ability to fate-map, isolate, and manipulate these and other subpopulations as the ENS forms will be important and is explored in Chapter 6. In the future, such efforts will provide insight into how and when subpopulations are specified, how distinct subpopulations influence lineage diversification, and define the ability of distinct subpopulations to compensate for disturbances in other enteric cell types that might otherwise derail GI motility and immune response.

Of ultimate importance in patient care is determining how study findings in HSCR and non-HSCR mouse models relate to human disease. Most histological studies in human tissues utilize cross sections. This type of section limits the ability to analyze the patterning, cell connectives, and density of the ENS. Few studies have attempted laminar visualization and analysis of cell types in the ENS in human tissues (81, 82). Thus, true proportions of specific ENS cell types are unknown in humans in non-disease and disease states and can only be estimated from cross section studies and studies in other animals. In Chapter 8, experimental techniques are described where such laminar analysis of the ENS in human tissue (HSCR and non-HSCR) is attempted.

Currently, HSCR patients are not genetically screened and standard histology for disease diagnosis and determining surgical boundaries only calls for assessing for presence or absence of ganglia. However, the type of genetic mutation, histological findings (such as eosinophilia), and other clinical information could inform clinicians as to what patients are most likely to suffer from adverse outcomes post-surgery. To begin to address these questions and issues, I define and describe a HSCR cohort in Chapter 5. Ultimately, efforts to elucidate the developmental processes affected in HSCR disease will call for future studies to be conducted in both animal

models as well as patient populations and such potential future studies are detailed within Chapter 7. A clearer understanding of such processes should lead to better outcomes for HSCR patients as well as non-HSCR patients who suffer from inflammation and aberrant GI motility.

References

1. Musser, M.A., and Michelle Southard-Smith, E. 2013. Balancing on the crest - Evidence for disruption of the enteric ganglia via inappropriate lineage segregation and consequences for gastrointestinal function. *Dev Biol* 382:356-364.
2. Burns, A.J. 2005. Migration of neural crest-derived enteric nervous system precursor cells to and within the gastrointestinal tract. *Int J Dev Biol* 49:143-150.
3. Pham, T.D., Gershon, M.D., and Rothman, T.P. 1991. Time of origin of neurons in the murine enteric nervous system: sequence in relation to phenotype. *J Comp Neurol* 314:789-798.
4. Sang, Q., and Young, H.M. 1996. Chemical coding of neurons in the myenteric plexus and external muscle of the small and large intestine of the mouse. *Cell Tissue Res* 284:39-53.
5. Heanue, T.A., and Pachnis, V. 2011. Prospective identification and isolation of enteric nervous system progenitors using Sox2. *Stem Cells* 29:128-140.
6. Chakravarti, A., McCallion, A., and Lyonnet, S. 2006. Multisystem Inborn Errors of Development: Hirschsprung. In *Scriver's Online Metabolic & Molecular Bases of Inherited Disease*. B.A. Valle D, Vogelstein B, Kinzler KW, et al,, editor: McGraw Hill Education.
7. Amiel, J., Sproat-Emison, E., Garcia-Barcelo, M., Lantieri, F., Burzynski, G., Borrego, S., Pelet, A., Arnold, S., Miao, X., Griseri, P., et al. 2008. Hirschsprung disease, associated syndromes and genetics: a review. *J Med Genet* 45:1-14.
8. Austin, K.M. 2012. The pathogenesis of Hirschsprung's disease-associated enterocolitis. *Semin Pediatr Surg* 21:319-327.
9. Kaul, A., Garza, J.M., Connor, F.L., Cocjin, J.T., Flores, A.F., Hyman, P.E., and Di Lorenzo, C. 2011. Colonic hyperactivity results in frequent fecal soiling in a subset of

children after surgery for Hirschsprung disease. *J Pediatr Gastroenterol Nutr* 52:433-436.

10. Chumpitazi, B.P., and Nurko, S. 2011. Defecation disorders in children after surgery for Hirschsprung disease. *J Pediatr Gastroenterol Nutr* 53:75-79.
11. Paratore, C., Goerich, D.E., Suter, U., Wegner, M., and Sommer, L. 2001. Survival and glial fate acquisition of neural crest cells are regulated by an interplay between the transcription factor Sox10 and extrinsic combinatorial signaling. *Development* 128:3949-3961.
12. Walters, L.C., Cantrell, V.A., Weller, K.P., Mosher, J.T., and Southard-Smith, E.M. 2010. Genetic background impacts developmental potential of enteric neural crest-derived progenitors in the Sox10Dom model of Hirschsprung disease. *Hum Mol Genet* 19:4353-4372.
13. Paratore, C., Eichenberger, C., Suter, U., and Sommer, L. 2002. Sox10 haploinsufficiency affects maintenance of progenitor cells in a mouse model of Hirschsprung disease. *Hum Mol Genet* 11:3075-3085.
14. Cantrell, V.A., Owens, S.E., Chandler, R.L., Airey, D.C., Bradley, K.M., Smith, J.R., and Southard-Smith, E.M. 2004. Interactions between Sox10 and EdnrB modulate penetrance and severity of aganglionosis in the Sox10Dom mouse model of Hirschsprung disease. *Hum Mol Genet* 13:2289-2301.
15. Jain, S., Naughton, C.K., Yang, M., Strickland, A., Vij, K., Encinas, M., Golden, J., Gupta, A., Heuckeroth, R., Johnson, E.M., Jr., et al. 2004. Mice expressing a dominant-negative Ret mutation phenocopy human Hirschsprung disease and delineate a direct role of Ret in spermatogenesis. *Development* 131:5503-5513.
16. Southard-Smith, E.M., Kos, L., and Pavan, W.J. 1998. Sox10 mutation disrupts neural crest development in Dom Hirschsprung mouse model. *Nat Genet* 18:60-64.

17. Kapur, R.P. 1999. Early death of neural crest cells is responsible for total enteric aganglionosis in Sox10(Dom)/Sox10(Dom) mouse embryos. *Pediatr Dev Pathol* 2:559-569.

18. Southard-Smith, E.M., Angrist, M., Ellison, J.S., Agarwala, R., Baxevanis, A.D., Chakravarti, A., and Pavan, W.J. 1999. The Sox10(Dom) mouse: modeling the genetic variation of Waardenburg-Shah (WS4) syndrome. *Genome Res* 9:215-225.

19. Hosoda, K., Hammer, R.E., Richardson, J.A., Baynash, A.G., Cheung, J.C., Giaid, A., and Yanagisawa, M. 1994. Targeted and natural (piebald-lethal) mutations of endothelin-B receptor gene produce megacolon associated with spotted coat color in mice. *Cell* 79:1267-1276.

20. Druckenbrod, N.R., Powers, P.A., Bartley, C.R., Walker, J.W., and Epstein, M.L. 2008. Targeting of endothelin receptor-B to the neural crest. *Genesis* 46:396-400.

21. Rothman, T.P., and Gershon, M.D. 1984. Regionally defective colonization of the terminal bowel by the precursors of enteric neurons in lethal spotted mutant mice. *Neuroscience* 12:1293-1311.

22. Roberts, R.R., Bornstein, J.C., Bergner, A.J., and Young, H.M. 2008. Disturbances of colonic motility in mouse models of Hirschsprung's disease. *Am J Physiol Gastrointest Liver Physiol* 294:G996-G1008.

23. Baynash, A.G., Hosoda, K., Giaid, A., Richardson, J.A., Emoto, N., Hammer, R.E., and Yanagisawa, M. 1994. Interaction of endothelin-3 with endothelin-B receptor is essential for development of epidermal melanocytes and enteric neurons. *Cell* 79:1277-1285.

24. Zaitoun, I., Erickson, C.S., Barlow, A.J., Klein, T.R., Heneghan, A.F., Pierre, J.F., Epstein, M.L., and Gosain, A. 2013. Altered neuronal density and neurotransmitter expression in the ganglionated region of Ednrb null mice: implications for Hirschsprung's disease. *Neurogastroenterol Motil* 25:e233-244.

25. Fujimoto, T. 1988. Natural history and pathophysiology of enterocolitis in the piebald lethal mouse model of Hirschsprung's disease. *J Pediatr Surg* 23:237-242.

26. Fujimoto, T., Reen, D.J., and Puri, P. 1988. Inflammatory response in enterocolitis in the piebald lethal mouse model of Hirschsprung's disease. *Pediatr Res* 24:152-155.

27. Cheng, Z., Dhall, D., Zhao, L., Wang, H.L., Doherty, T.M., Bresee, C., and Frykman, P.K. 2010. Murine model of Hirschsprung-associated enterocolitis. I: phenotypic characterization with development of a histopathologic grading system. *J Pediatr Surg* 45:475-482.

28. Zhao, L., Dhall, D., Cheng, Z., Wang, H.L., Doherty, T.M., Bresee, C., and Frykman, P.K. 2010. Murine model of Hirschsprung-associated enterocolitis II: Surgical correction of aganglionosis does not eliminate enterocolitis. *J Pediatr Surg* 45:206-211; discussion 211-202.

29. Gianino, S., Grider, J.R., Cresswell, J., Enomoto, H., and Heuckeroth, R.O. 2003. GDNF availability determines enteric neuron number by controlling precursor proliferation. *Development* 130:2187-2198.

30. Schuchardt, A., D'Agati, V., Larsson-Blomberg, L., Costantini, F., and Pachnis, V. 1994. Defects in the kidney and enteric nervous system of mice lacking the tyrosine kinase receptor Ret. *Nature* 367:380-383.

31. Schuchardt, A., D'Agati, V., Larsson-Blomberg, L., Costantini, F., and Pachnis, V. 1995. RET-deficient mice: an animal model for Hirschsprung's disease and renal agenesis. *J Intern Med* 238:327-332.

32. Carniti, C., Belluco, S., Riccardi, E., Cranston, A.N., Mondellini, P., Ponder, B.A., Scanziani, E., Pierotti, M.A., and Bongarzone, I. 2006. The Ret(C620R) mutation affects renal and enteric development in a mouse model of Hirschsprung's disease. *Am J Pathol* 168:1262-1275.

33. Jing, S., Wen, D., Yu, Y., Holst, P.L., Luo, Y., Fang, M., Tamir, R., Antonio, L., Hu, Z., Cupples, R., et al. 1996. GDNF-induced activation of the ret protein tyrosine kinase is mediated by GDNFR-alpha, a novel receptor for GDNF. *Cell* 85:1113-1124.

34. Treanor, J.J., Goodman, L., de Sauvage, F., Stone, D.M., Poulsen, K.T., Beck, C.D., Gray, C., Armanini, M.P., Pollock, R.A., Hefti, F., et al. 1996. Characterization of a multicomponent receptor for GDNF. *Nature* 382:80-83.

35. Cacalano, G., Farinas, I., Wang, L.C., Hagler, K., Forgie, A., Moore, M., Armanini, M., Phillips, H., Ryan, A.M., Reichardt, L.F., et al. 1998. GFRalpha1 is an essential receptor component for GDNF in the developing nervous system and kidney. *Neuron* 21:53-62.

36. Enomoto, H., Araki, T., Jackman, A., Heuckeroth, R.O., Snider, W.D., Johnson, E.M., Jr., and Milbrandt, J. 1998. GFR alpha1-deficient mice have deficits in the enteric nervous system and kidneys. *Neuron* 21:317-324.

37. Shen, L., Pichel, J.G., Mayeli, T., Sariola, H., Lu, B., and Westphal, H. 2002. Gdnf haploinsufficiency causes Hirschsprung-like intestinal obstruction and early-onset lethality in mice. *Am J Hum Genet* 70:435-447.

38. Wang, H., Hughes, I., Planer, W., Parsadanian, A., Grider, J.R., Vohra, B.P., Keller-Peck, C., and Heuckeroth, R.O. 2010. The timing and location of glial cell line-derived neurotrophic factor expression determine enteric nervous system structure and function. *J Neurosci* 30:1523-1538.

39. Ostwani, W., Dolan, J., and Elitsur, Y. 2010. Familial clustering of habitual constipation: a prospective study in children from West Virginia. *J Pediatr Gastroenterol Nutr* 50:287-289.

40. Van Limbergen, J., Wilson, D.C., and Satsangi, J. 2009. The genetics of Crohn's disease. *Annu Rev Genomics Hum Genet* 10:89-116.

41. Karban, A.S., Okazaki, T., Panhuysen, C.I., Gallegos, T., Potter, J.J., Bailey-Wilson, J.E., Silverberg, M.S., Duerr, R.H., Cho, J.H., Gregersen, P.K., et al. 2004. Functional

annotation of a novel NFKB1 promoter polymorphism that increases risk for ulcerative colitis. *Hum Mol Genet* 13:35-45.

42. Villani, A.C., Lemire, M., Thabane, M., Belisle, A., Geneau, G., Garg, A.X., Clark, W.F., Moayyedi, P., Collins, S.M., Franchimont, D., et al. 2010. Genetic risk factors for post-infectious irritable bowel syndrome following a waterborne outbreak of gastroenteritis. *Gastroenterology* 138:1502-1513.

43. Bertrand, N., Castro, D.S., and Guillemot, F. 2002. Proneural genes and the specification of neural cell types. *Nat Rev Neurosci* 3:517-530.

44. Furness, J.B. 2006. *The Enteric Nervous System.* . Malden, Massachusetts: Blackwell Publishing Inc.

45. D'Autreaux, F., Margolis, K.G., Roberts, J., Stevanovic, K., Mawe, G., Li, Z., Karamooz, N., Ahuja, A., Morikawa, Y., Cserjesi, P., et al. 2011. Expression level of Hand2 affects specification of enteric neurons and gastrointestinal function in mice. *Gastroenterology* 141:576-587, 587 e571-576.

46. Gross, E.R., Gershon, M.D., Margolis, K.G., Gertsberg, Z.V., and Cowles, R.A. 2012. Neuronal serotonin regulates growth of the intestinal mucosa in mice. *Gastroenterology* 143:408-417 e402.

47. Gershon, M.D., and Tack, J. 2007. The serotonin signaling system: from basic understanding to drug development for functional GI disorders. *Gastroenterology* 132:397-414.

48. Neal, K.B., Parry, L.J., and Bornstein, J.C. 2009. Strain-specific genetics, anatomy and function of enteric neural serotonergic pathways in inbred mice. *J Physiol* 587:567-586.

49. Li, Z.S., Schmauss, C., Cuenca, A., Ratcliffe, E., and Gershon, M.D. 2006. Physiological modulation of intestinal motility by enteric dopaminergic neurons and the D2 receptor: analysis of dopamine receptor expression, location, development, and function in wild-type and knock-out mice. *J Neurosci* 26:2798-2807.

50. Rohrer, H. 2011. Transcriptional control of differentiation and neurogenesis in autonomic ganglia. *Eur J Neurosci* 34:1563-1573.

51. Hendershot, T.J., Liu, H., Sarkar, A.A., Giovannucci, D.R., Clouthier, D.E., Abe, M., and Howard, M.J. 2007. Expression of Hand2 is sufficient for neurogenesis and cell type-specific gene expression in the enteric nervous system. *Dev Dyn* 236:93-105.

52. D'Autreaux, F., Morikawa, Y., Cserjesi, P., and Gershon, M.D. 2007. Hand2 is necessary for terminal differentiation of enteric neurons from crest-derived precursors but not for their migration into the gut or for formation of glia. *Development* 134:2237-2249.

53. Lei, J., and Howard, M.J. 2011. Targeted deletion of Hand2 in enteric neural precursor cells affects its functions in neurogenesis, neurotransmitter specification and gangliogenesis, causing functional aganglionosis. *Development* 138:4789-4800.

54. Danielian, P.S., Echelard, Y., Vassileva, G., and McMahon, A.P. 1997. A 5.5-kb enhancer is both necessary and sufficient for regulation of Wnt-1 transcription in vivo. *Dev Biol* 192:300-309.

55. Pan, F.C., and Wright, C. 2011. Pancreas organogenesis: from bud to plexus to gland. *Dev Dyn* 240:530-565.

56. Collombat, P., Mansouri, A., Hecksher-Sorensen, J., Serup, P., Krull, J., Gradwohl, G., and Gruss, P. 2003. Opposing actions of Arx and Pax4 in endocrine pancreas development. *Genes Dev* 17:2591-2603.

57. Hang, Y., and Stein, R. 2011. MafA and MafB activity in pancreatic beta cells. *Trends Endocrinol Metab* 22:364-373.

58. Liu, B.Y., Jiang, Y., Lu, Z., Li, S., Lu, D., and Chen, B. 2011. Down-regulation of zinc transporter 8 in the pancreas of db/db mice is rescued by Exendin-4 administration. *Mol Med Report* 4:47-52.

59. Corpening, J.C., Cantrell, V.A., Deal, K.K., and Southard-Smith, E.M. 2008. A Histone2BCerulean BAC transgene identifies differential expression of Phox2b in migrating enteric neural crest derivatives and enteric glia. *Dev Dyn* 237:1119-1132.

60. Margolis, K.G., Stevanovic, K., Karamooz, N., Li, Z.S., Ahuja, A., D'Autreaux, F., Saurman, V., Chalazonitis, A., and Gershon, M.D. 2011. Enteric neuronal density contributes to the severity of intestinal inflammation. *Gastroenterology* 141:588-598, 598 e581-582.

61. Powell, D.W. 1995. Neuroimmunophysiology of the gastrointestinal mucosa: implications for inflammatory diseases. *Trans Am Clin Climatol Assoc* 106:124-138; discussion 138-140.

62. Lakhan, S.E., and Kirchgessner, A. 2010. Neuroinflammation in inflammatory bowel disease. *J Neuroinflammation* 7:37.

63. Faure, S., de Santa Barbara, P., Roberts, D.J., and Whitman, M. 2002. Endogenous patterns of BMP signaling during early chick development. *Dev Biol* 244:44-65.

64. Chalazonitis, A., D'Autreaux, F., Guha, U., Pham, T.D., Faure, C., Chen, J.J., Roman, D., Kan, L., Rothman, T.P., Kessler, J.A., et al. 2004. Bone morphogenetic protein-2 and -4 limit the number of enteric neurons but promote development of a TrkC-expressing neurotrophin-3-dependent subset. *J Neurosci* 24:4266-4282.

65. Chalazonitis, A., Pham, T.D., Li, Z., Roman, D., Guha, U., Gomes, W., Kan, L., Kessler, J.A., and Gershon, M.D. 2008. Bone morphogenetic protein regulation of enteric neuronal phenotypic diversity: relationship to timing of cell cycle exit. *J Comp Neurol* 509:474-492.

66. Chalazonitis, A., D'Autreaux, F., Pham, T.D., Kessler, J.A., and Gershon, M.D. 2011. Bone morphogenetic proteins regulate enteric gliogenesis by modulating ErbB3 signaling. *Dev Biol* 350:64-79.

67. Chen, H.L., and Panchision, D.M. 2007. Concise review: bone morphogenetic protein pleiotropism in neural stem cells and their derivatives--alternative pathways, convergent signals. *Stem Cells* 25:63-68.

68. Blaugrund, E., Pham, T.D., Tennyson, V.M., Lo, L., Sommer, L., Anderson, D.J., and Gershon, M.D. 1996. Distinct subpopulations of enteric neuronal progenitors defined by time of development, sympathoadrenal lineage markers and Mash-1-dependence. *Development* 122:309-320.

69. Li, Z., Caron, M.G., Blakely, R.D., Margolis, K.G., and Gershon, M.D. 2010. Dependence of serotonergic and other nonadrenergic enteric neurons on norepinephrine transporter expression. *J Neurosci* 30:16730-16740.

70. Borghini, S., Duca, M.D., Pini Prato, A., Lerone, M., Martucciello, G., Jasonni, V., Ravazzolo, R., and Ceccherini, I. 2009. Search for pathogenetic variants of the SPRY2 gene in intestinal innervation defects. *Intern Med J* 39:335-337.

71. Hagl, C.I., Klotz, M., Wink, E., Kranzle, K., Holland-Cunz, S., Gretz, N., Diener, M., and Schafer, K.H. 2008. Temporal and regional morphological differences as a consequence of FGF-2 deficiency are mirrored in the myenteric proteome. *Pediatr Surg Int* 24:49-60.

72. Hagl, C.I., Wink, E., Scherf, S., Heumuller-Klug, S., Hausott, B., and Schafer, K.H. 2012. FGF2 deficit during development leads to specific neuronal cell loss in the enteric nervous system. *Histochem Cell Biol*.

73. Hanani, M., and Reichenbach, A. 1994. Morphology of horseradish peroxidase (HRP)-injected glial cells in the myenteric plexus of the guinea-pig. *Cell Tissue Res* 278:153-160.

74. Enomoto, H., Crawford, P.A., Gorodinsky, A., Heuckeroth, R.O., Johnson, E.M., Jr., and Milbrandt, J. 2001. RET signaling is essential for migration, axonal growth and axon guidance of developing sympathetic neurons. *Development* 128:3963-3974.

75. Druckenbrod, N.R., and Epstein, M.L. 2005. The pattern of neural crest advance in the cecum and colon. *Dev Biol* 287:125-133.

76. Coventry, S., Yost, C., Palmiter, R.D., and Kapur, R.P. 1994. Migration of ganglion cell precursors in the ileoceca of normal and lethal spotted embryos, a murine model for Hirschsprung disease. *Lab Invest* 71:82-93.

77. O'Donnell, A.M., and Puri, P. 2010. Skip segment Hirschsprung's disease: a systematic review. *Pediatr Surg Int* 26:1065-1069.

78. Nishiyama, C., Uesaka, T., Manabe, T., Yonekura, Y., Nagasawa, T., Newgreen, D.F., Young, H.M., and Enomoto, H. 2012. Trans-mesenteric neural crest cells are the principal source of the colonic enteric nervous system. *Nat Neurosci* 15:1211-1218.

79. King, S.K., Southwell, B.R., and Hutson, J.M. 2006. An association of multiple endocrine neoplasia 2B, a RET mutation; constipation; and low substance P-nerve fiber density in colonic circular muscle. *J Pediatr Surg* 41:437-442.

80. Mundell, N.A., Plank, J.L., LeGrone, A.W., Frist, A.Y., Zhu, L., Shin, M.K., Southard-Smith, E.M., and Labosky, P.A. 2012. Enteric nervous system specific deletion of Foxd3 disrupts glial cell differentiation and activates compensatory enteric progenitors. *Dev Biol* 363:373-387.

81. Wester, T., O'Briain, S., and Puri, P. 1998. NADPH diaphorase-containing nerve fibers and neurons in the myenteric plexus are resistant to postmortem changes: studies in Hirschsprung's disease and normal autopsy material. *Arch Pathol Lab Med* 122:461-466.

82. Wester, T., O'Briain, D.S., and Puri, P. 1999. Notable postnatal alterations in the myenteric plexus of normal human bowel. *Gut* 44:666-674.

CHAPTER II

DEFECITS IN THE GANGLIONATED REGIONS OF THE *SOX10*$^{DOM/+}$ MOUSE INTESTINE

This chapter is a modified version of an article *in press* (1).

Introduction

The ENS regulates multiple gastrointestinal (GI) functions including motility, secretion, and inflammatory processes (2). The ENS originates from neural crest-derived progenitors (NCPs) that migrate from the neural tube to colonize the entire intestine (2). Normal function of the ENS relies upon complete colonization of the bowel as well as appropriate lineage segregation of NCPs to generate a balanced repertoire of distinct neuron classes and glial cell proportions.

In Hirschsprung disease (HSCR), migrating NCPs fail to populate the distal intestine leading to a variable length of aganglionic bowel (3). Mutations in *RET, EDNRB, EDN3,* or *SOX10* cause HSCR in patients, although other genetic variants influence disease penetrance and extent of aganglionosis (3-7). Despite surgical resection of the aganglionic segment, many HSCR patients suffer from residual chronic constipation (5-33% of patients) and decreased bowel function (8). In addition, a substantial number of patients suffer from Hirschsprung associated-enterocolitis (HAEC) (9). Differences in surgical procedures and recovery explain some adverse outcomes. Yet, many patients suffer from residual symptoms where no iatrogenic cause is found. An understanding of the processes that contribute to residual symptoms in HSCR patients would serve to better predict which patients will suffer from HSCR-related sequelae and guide treatment options.

Prior evidence from mouse models with mutations that affect the ENS, yet exhibit no overt aganglionosis, suggests that deficits in enteric NCP lineage segregation contribute to GI dysmotility (10). Chronic GI dysfunction in HSCR patients after surgery suggests that HSCR

susceptibility genes (e.g., *SOX10*) not only contribute to aganglionosis, but may also affect ganglionated regions of the bowel. It has been suggested that Sox10 affects multipotency of NC-derived cells and neuronal and glial specification. However, these implications are derived from *in vitro* experiments or from other NC-derived structures, such as dorsal root ganglia (11-13), While Sox10 is essential for enteric NCP migration and colonization of the bowel, studies to elucidate the role of Sox10 in NCP fate specification in the ENS *in vivo* have not been undertaken. Given established roles for Sox10 outside the ENS and the presence of residual symptoms in HSCR patients, we hypothesized that perturbations in *Sox10* disrupt NCP lineage segregation and alter the function of ganglionated bowel in the $Sox10^{Dom/+}$ HSCR mouse model. To test this hypothesis, we fate-mapped NCPs using a Cre-LoxP system. Fate-mapping and immunohistochemical labeling of cell types in the myenteric plexus revealed that the normal complement of NC-derived lineages is disrupted in the enteric ganglia of $Sox10^{Dom/+}$ mutants. These changes are region specific and disturbances in specific cell types in the colon correlate with extent of aganglionosis. Alterations seen in neuronal subtype proportions in $Sox10^{Dom/+}$ animals suggest a novel role for Sox10 in neuronal class specification. Since changes in neuron ratios within enteric ganglia can alter GI motility, we investigated the potential for aberrant intestinal transit in the proximal small intestine of this HSCR model. GI motility assays exposed alterations in gastric emptying and small intestine transit that were age- and sex-dependent. Our results show that the $Sox10^{Dom}$ HSCR mutation alters NC lineage segregation and GI motility despite the presence and normal density of ENS ganglia in the proximal small intestine. Such changes could partially explain adverse outcomes in surgically treated HSCR patients and help clinicians better identify and treat patients at high risk for experiencing post-surgical GI dysfunction.

Methods

Animals

Sox10$^{Dom/+}$ and homozygous *B6.Cg-Gt(ROSA)26Sor*$^{tm9(CAG-tdTomato/Hze/J)}$, hereafter *R26R*^{tdTom}, were maintained on a C57BL/6J background. *Wnt1*^{tm1Amc}, hereafter *Wnt1*-Cre, mice were maintained on a Crl:CD1(ICR) background. The *Sox10*-Cre BAC construct was generated by linking nuclear localized Cre joined to a human growth hormone mRNA stabilization sequence (14, 15) to the regulatory elements of *Sox10* within a well-characterized *Sox10* BAC (Figure 2.1). The resulting Tg$^{(Sox10\text{-}CrehGH)1Sout}$ line, hereafter *Sox10*-Cre, was made congenic on the C3HeB/FeJ background. Transgene driven reporter expression mirrors known Sox10 expression in NC-derived lineages. (Corpening Rosebrock J et al., 2014. *In preparation*). Experimental animals for NC-derived lineage quantification were from crosses between *Sox10*$^{Dom/+}$*; Sox10*-Cre or *Sox10*$^{Dom/+}$*; Sox10*-Cre/Cre mice to *R26Rt*^{dTom} mice. *Sox10*$^{Dom/+}$ mice were identified by the presence of white feet and belly spotting as well as discernable hypoaganglionosis and/or aganglionosis revealed by the absence of tdTomato fluorescent ganglia in the distal intestine. The *Sox10*$^{Dom/+}$ recapitulates HSCR in humans with animals exhibiting varying lengths of aganglionosis within the bowel despite harboring the same HSCR causing mutation. *Sox10*-Cre transgene presence was verified by PCR genotyping (Table 2.1). The Institutional Animal Care and Use Committee at Vanderbilt University approved all experimental protocols. *Wnt1*-Cre genotyping information and detailed methods and materials in regard to this chapter can be found within Chapter 7 Extended Methods.

Table 2.1. Primers for PCR amplification of the *Sox10*-Cre transgene.

Mouse line	Product Amplified	Forward primer (5' to 3')	Reverse primer (5' to 3')
Sox10CreHGH BAC Transgenic	Transgene-Sp6 arm	GTTTTTTGCGATCTGCCGTTTC	GGCACTTTCATGTTATCTGAGG
Sox10CreHGH BAC Transgenic	Transgene-T7 arm	AAGAGCAAGCCTTGGAACTG	TCGAGCTTGACATTGTAGGAC
Sox10CreHGH BAC Transgenic	Transgene-Cre Recombinase Fragment	GCGGCATGGTGCAAGTTGAAT	CGTTCACCGGCATCAACGTTT

Thermocycler conditions for all primers sets listed: 94°C for 5 min, [(94°C for 30 sec, 55°C for 30 sec, 0.5 sec ramp up to 72°C, 72°C for 30 sec, 0.5 sec ramp up to 94°C) 35 times] 72°C for 10 min, 4°C indefinitely.

Immunohistochemistry

Regions of the duodenum, ileum, and mid-colon were collected from postnatal (P) 15-19 day *Sox10*$^{Dom/+}$ and *Sox10*$^{+/+}$ littermates. Laminar muscle preparations containing myenteric plexus were isolated and subjected to immunohistochemistry (IHC)(16) (Tables 2.2 & 2.3). Z-stack images of samples were captured on a Zeiss LSM 510 confocal microscope (20X objective with 1.5X software zoom) to quantify NC derivatives within the ganglia and primary connectives of the myenteric plexus. Image brightness and contrast were adjusted in Adobe Photoshop to aid in cell quantification. We quantified n=5-6 samples per genotype for all duodenum and ileum NC lineage analyses and n=5-6 *Sox10*$^{+/+}$ and n=10-11 for *Sox10*$^{Dom/+}$ samples for colon NC lineage analyses.

Table 2.2. Primary antibodies for immunohistochemistry.

Antigen	Host	Supplier	Catalog #	Dilution	Tissue fix times
Phox2b	Rabbit (polyclonal)	gift of A. Pattyn	n/a	1:750	20-25 min at RT
HuC/D	Human	gift of V. Lennon	n/a	1:10000	20-25 min at RT or O/N at 4°C
FoxD3	Rabbit (polyclonal)	gift of T. Labosky	n/a	1:400	O/N at 4°C
Calretinin	Goat (polyclonal)	Millipore	AB1550	1:2500	20-25 min at RT
NOS1 (K-20)	Rabbit (polyclonal)	Santa Cruz	sc-1025	1:600	O/N at 4°C
s100A1	Sheep (polyclonal)	QED Biosciences	56201	1:3000	O/N at 4°C

RT = room temperature. O/N = overnight. All tissues used in immunohistochemistry were blocked for 1-2 hours at RT (1XPBS/0.1% Trixton X-100/5% NDS/1% BSA) followed by incubation in the primary antibody dilution in block for at least 4 hours at RT or a minimum of O/N at 4°C.

Table 2.3. Secondary antibodies for immunohistochemistry.

Detection and Type	Supplier	Catalog #	*Dilution
Alexa488 Donkey Anti-Rabbit IgG (H+L)	Jackson Immuno	711-545-152	1:400
Alexa488 Donkey Anti-Sheep IgG (H+L)	Jackson Immuno	713-545-147	1:400
Alexa647 Donkey Anti-Rabbit IgG (H+L)	Jackson Immuno	711-605-152	1:200
DyLight649 Donkey Anti-Human IgG (H+L)	Jackson Immuno	709-495-149	1:200
Cy2 Donkey Anti-Goat	Jackson Immuno	705-225-147	1:600

*All secondary antibody dilutions listed are based on an initial 1:1 dilution in glycerol.

Gastrointestinal transit assays

To determine gastric emptying and small intestine transit rates, 4-week (27-30 days) or 6-week (42-48 days) mice were gavaged with a rhodamine dextran fluorescence containing meal following established procedures (17, 18). Fifteen minutes post-gavage, the stomach and 10 equal segments of small intestine were collected and homogenized separately. Fluorescence signal from the stomach and each intestinal segment was read on a Molecular Devices/LJL Analyst HT (Molecular Devices, Union City, CA, USA). Gastric emptying percent was determined by calculating the proportion of fluorescence that had left the stomach to total recovered fluorescence. A small intestine transit score was assigned by determining the geometric mean of fluorescence within the 10 equal small intestine segments. Miller and Burk originally described this method in rats (18). Full details for this procedure in mice can be found in recent studies (19, 20). To depict small intestine transit rates, the average percent contribution of each individual intestine segment to the motility score was calculated. A heat map was generated using MATLAB (Mathworks, Natick, MA, USA), where intestine segment numbers contributing the most to the small intestine transit score are shown in darker red and those contributing little or none to the score in lighter red. Color intensity in between segment number hashes was interpolated to create each heat map. n=6-8 mice per genotype, sex, and age.

Inflammation

Transverse sections (~5 µM) of entire colon from 6 week or older *Sox10*$^{Dom/+}$ and *Sox10*$^{+/+}$ littermates were stained with hematoxylin and eosin. An expert pathologist blinded to genotype scored sample inflammation based on a previously developed scoring system utilizing Hirschsprung mouse models (21). Specifically, a final score of 0-7 was assigned by assessing severity of inflammation (0-3 with 0 = no inflammation or rare neutrophils; 1 =mild inflammatory infiltrates, no necrosis; 2 = moderate to marked inflammatory infiltrates and mucosal necrosis and

3 = transmural necrosis) and depth of inflammation (0-4 with 0 = none, 1 = mucosa, 2 = submucosa, 3 = muscularis propia; 4 = subserosa/serosa). n=6-9 mice per genotype and per sex.

Statistics

For NC lineage quantification, 5 duodenal, 3 ileal, and 2 colonic images were manually counted for each animal. For *Sox10*$^{Dom/+}$ mice with hypoganglionosis in the mid-colon, additional images were quantified so a comparable number of neurons were counted between *Sox10*$^{+/+}$ and *Sox10*$^{Dom/+}$ mice. We tested for differences in cell type proportions, gastric emptying rates, small intestine transit rates, and inflammation scores using a Student's t-test assuming unequal variance (Welch's t-test). ANOVA (F-test) was used to test for significance of slope and to determine coefficients of determination (r^2). Statistical analysis was performed using JMP (version 10) software. Variance is reported as ±SEM.

Results

Validation of the Sox10-Cre BAC transgene system

Studies to assess alterations in enteric cell types *in vivo* have largely focused on comparing total numbers of neurons and glia, although a few studies have assessed neuronal subtypes (20, 22). While informative, IHC alone may not comprehensively identify all NC derivatives in the ENS and may miss alterations in patterning and distribution of enteric ganglia depending on the marker used. The *Wnt1*-Cre transgene has been the gold standard for labeling NC derivatives since its introduction in 1997 (23). However, *Wnt1*-Cre transgenic animals suffer neurological developmental defects (24) and both heterozygotes and homozygotes are susceptible to early death due to seizures (personal communications, Elise Pfaltzgraff). Additionally, Cre expression through the *Wnt1*-Cre transgene is driven by a single *Wnt1* enhancer; thus, important regulatory regions that could drive *Wnt1* expression in specific cell types may be excluded within the *Wnt1*-Cre transgene (23). To avoid potential confounders that accompany

use of the *Wnt1*-Cre transgene line, other members of the Southard-Smith lab generated a *Sox10*-Cre BAC transgenic line to label NC derivatives (Figure 2.1). Because *Sox10* is ubiquitously expressed in NC cells emerging from the neural tube, the use of *Sox10* regulatory regions linked to a Cre driver enables extensive labeling of NC derivatives. (Corpening Rosebrock et al., 2014 *in preparation)*(25, 26). (Further details in regard to generation of the *Sox10*-Cre transgene can be found in the "Methods" section of this chapter as well as in Figure 2.1).

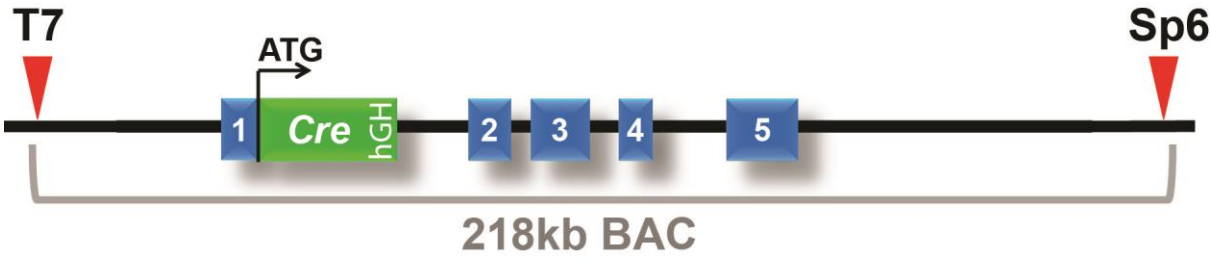

Figure 2.1. Overview of the *Sox10*-Cre transgene. The *Sox10*-Cre transgene is built from a 218 kb BAC ecompassing the *Sox10* gene. The transgene inlcudes a Cre-Recombinase sequence insertion in frame at the ATG start site as well as an human growth hormone (hGH) sequence to enhance mRNA stability.

Because the *Wnt1*-Cre transgene has been the standard for labeling NC derivatives, we compared the labeling of NC derivatives in the ENS in the duodenum, ileum, and colon in *Wnt1*-Cre or *Sox10*-Cre lines crossed to a *R26R*^{tdTom} line. In these crosses, we compared *R26R*^{tdTom} expression with IHC labeling of NC derivatives by an antibody to Phox2b. All NC derivatives express Phox2b although enteric neurons express Phox2b at high levels and enteric glia express Phox2b at relatively low levels (27) (Figure 2.2). Both transgenes were expressed in the vast majority of enteric Phox2b+ cells (>97%) in all regions of the intestine examined. However, the *Sox10*-Cre transgene performed significantly better in the ileum (*$P<0.05$) and the colon (*$P<0.02$) (Table 2.4).

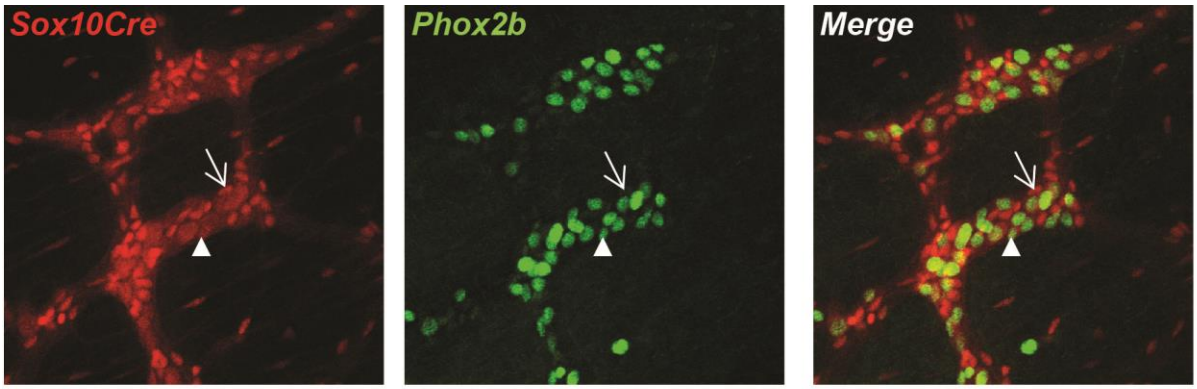

Figure 2.2. *Sox10*-Cre and Phox2b labeling of enteric NC derivatives. Duodenum of a P17 pup from a *R26R*^{tdTom} x *Sox10*-Cre cross. *R26R*^{tdTom} expression, through *Sox10*-Cre action, labels NC-derived lineages, including neurons with high Phox2b expression (arrowhead) and glia with relatively low Phox2b expression (arrow).

Table 2.4. Comparison of *R26R*^{tdTom} reporter labeled enteric NC derivatives between *Sox10*-Cre and *Wnt1*-Cre transgenes.

	***Sox10*-Cre**	***Wnt1*-Cre**	
	mean ± std dev	*mean ± std dev*	*p-value*
Duodenum	97.6% ± 2.2	97.9% ± 0.9	>0.85
Ileum	99.1% ± 0.6	97.3% ± 0.8	*<0.05
Colon	97.8% ± 0.3	96.1% ± 0.5	*<0.02

Mean and standard deviation (std dev) measurements refer to the average percent of *R26R*^{tdTom} reporter+ cells out of total Phox2b+ cells. n=3 for each genotype.

Sox10-Cre presence does not lead to adverse phenotypes

After validation of transgene expression in enteric NC derivatives, we attempted to generate mice homozygous for the *Sox10*-Cre transgene. Transgenic homozygote breeders are desirable in a study where many mice are needed, but where litter sizes (such as those on a C57/BL6 background) are small. A limitation of the *Wnt1*-Cre transgene is that attempts to generate *Wnt1*-Cre homozygotes have been difficult. *Wnt1*-Cre homozygotes typically succumb to seizure induced death before they are able to breed (personal communications, Elise Pfaltzgraff). We successfully crossed $Sox10^{Dom/+}$; *Sox10*-Cre males to *Sox10*-Cre females to generate mice homozygous for the *Sox10*-Cre transgene. Mice were first screened for homozygosity of the transgene through semi-quantitative PCR. (See Extended Methods.) Homozygosity was validated by crossing a $Sox10^{Dom/+}$; *Sox10*-Cre/Cre male to a homozygous $R26R^{tdTom}$ female. We observed tdTomato fluorescence in NC derivates in all progeny of the two litters produced from this cross. *Sox10*-Cre transgene presence in progeny was also verified by PCR genotyping.

Sox protein family members are known to regulate each other and to self-regulate (reviewed in (28)). Thus, the *Sox10Dom* mutation could potentially affect *Sox10*-Cre transgene expression. In order to study NC derivatives in $Sox10^{Dom/+}$; *Sox10*-Cre animals, we first needed to verify that the *Sox10*-Cre transgene and the *Sox10Dom* mutation do not interact and affect reporter expression in our study. In our crosses, we observed expression of $R26R^{tdTom}$ in the ENS in all mice carrying the *Sox10Dom* mutation and *Sox10*-Cre transgene and reporter expression appeared equivalent between wildtype and mutant animals, suggesting no or little interaction of the transgene and mutated Sox10.

Additionally, random integration of transgenes during generation of transgenic lines can alter or ablate expression of other genes depending on integration location. And because the *Sox10*-Cre transgene requires the same transcriptional machinery as the endogenous *Sox10* loci, transgene presence in a cell could potentially hijack transcriptional machinery needed for Sox10

expression or expression of other genes. This hijacking could lead to a more severe phenotype and thus higher death rates in *Sox10*$^{Dom/+}$ mice. To rule out potential effects of the *Sox10*-Cre transgene on our study, we monitored *Sox10*-Cre mouse viability and fertility. We noticed no viability or growth defects nor any other additional phenotypes in the *Sox10*-Cre line (line F) used in this study. To test if the *Sox10*-Cre transgene affected the *Sox10*$^{Dom/+}$ phenotype, we monitored the number of *Sox10*$^{Dom/+}$*; Sox10*-Cre+ and *Sox10*$^{Dom/+;}$ *Sox10*-Cre- pups that reached experimental age (P15-19). If *Sox10*-Cre were to increase the severity of the *Sox10*$^{Dom/+}$ phenotype, we would expect fewer pups harboring the *Sox10*$^{Dom/+}$ mutation and transgene to reach experimental age than pups with the mutation but not the transgene. When we compared our expected progeny ratios to observed, we found no statistical difference (*P=0.2413*; X^2 goodness of fit) (Table 2.5).

Genotype	Expected pups	Observed pups	P-value
Sox10$^{Dom/+}$*; Sox10*-Cre	29.5	25	*0.2413*
Sox10$^{Dom/+}$	29.5	34	

Table 2.5. Expected and observed survival of *Sox10*$^{Dom/+}$ pups with or without the *Sox10*-Cre transgene. Survival of *Sox10*$^{Dom/+}$ pups with or without the *Sox10*-Cre transgene was documented for several litters. The transgene does not appear to have an affect on *Sox10*$^{Dom/+}$ pup survival. (Chi squared goodness of fit test)

Fate-mapping enteric NC derivatives in Sox10$^{+/+}$ *and Sox10*$^{Dom/+}$ *mice*

Once we validated the *Sox10*-Cre transgene as an effective means to label enteric NC derivatives, we combined a *Sox10*-Cre BAC transgene with a Cre-dependent *R26R*^{tdTom} reporter in crosses with *Sox10*$^{Dom/+}$ mice to evaluate NC derivatives within enteric ganglia between *Sox10*$^{+/+}$ and *Sox10*$^{Dom/+}$ mice. Analysis of *Sox10*$^{Dom/+}$ mutants, on a mixed background in these crosses, is advantageous since this model recapitulates the variable penetrance and severity of

aganglionosis seen in human HSCR patients (5, 29). In the resulting progeny, the cytoplasmic reporter, tdTomato, which is concentrated in the cell soma and labels cellular processes, reveals ganglia structure, density and connectives of cells in which Cre is expressed. We collected laminar gut muscle preparations in postnatal pups between postnatal days (P)15-19 before the majority of these animals develop and perish due to megacolon at weaning. We observed similar myenteric ganglia density, spacing between ganglia, and overall architecture of ganglia in the duodenum, ileum, and ganglionated regions of the colon in both *Sox10*$^{+/+}$ and *Sox10*$^{Dom/+}$ pups (Figure 2.3). While comparable ganglia patterning and density were seen, the possibility remained that total numbers of myenteric NCPs might differ between *Sox10*$^{+/+}$ and *Sox10*$^{Dom/+}$ animals and could lead to altered GI function. We compared total numbers of enteric NC-derived cells between *Sox10*$^{+/+}$ and *Sox10*$^{Dom/+}$ pups. This analysis revealed similar total numbers of NC-derived cells between *Sox10*$^{+/+}$ and *Sox10*$^{Dom/+}$ mice in both duodenum and ileum (Table 2.6).

Correlation between disease severity and neuron or glia proportions

In vitro and in peripheral nervous structures outside the ENS, timing and levels of *Sox10* expression affect neuronal and glial fate acquisition from NC progenitors (11-13, 30, 31). However, the role of *Sox10* in neuronal and glial fate acquisition in the ENS *in vivo* has not been determined. Feasibly, disruption of *Sox10* could alter the ratios of these cell types and contribute to GI dysfunction by impacting motility or by contributing to inflammation secondary to perturbing enteric glia (32). To examine the possibility that ratios of enteric neurons and glia are abnormal in *Sox10*$^{Dom/+}$ pups, we quantified the proportions of neurons and glia out of total NC derivatives within the myenteric plexus at P15-17. Because different regions of the bowel have distinct functions and it is unknown how proximal to regions of aganglionosis aberrancies in lineage segregation might occur, we assessed neuron and glia proportions in the duodenum, ileum, and mid-colon. Enteric neurons (Hu+) (20) and glia (FoxD3+) (33) (Figure 2.4) were IHC labeled, counted, and their proportions out of total NC derivatives calculated (Figure 2.5A). Proportions

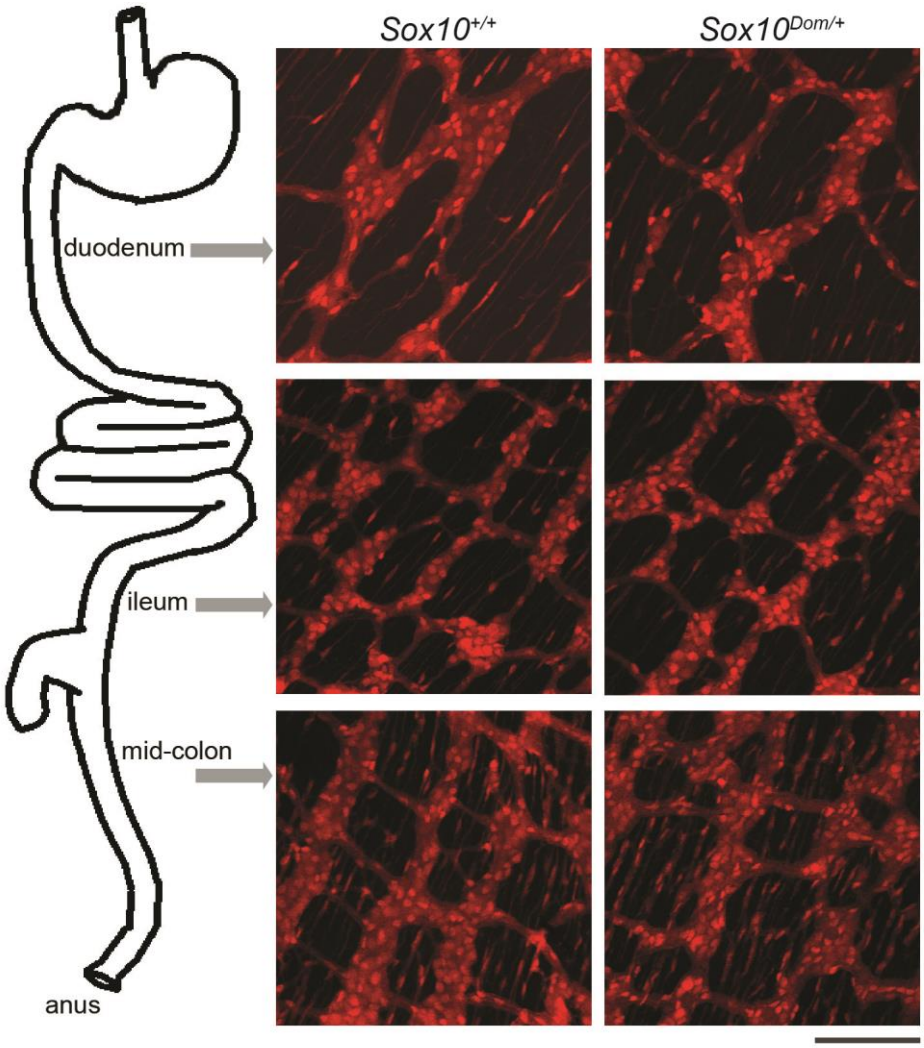

Figure 2.3. The *Sox10*-Cre transgene system enables visualization of enteric NC derivatives and ENS patterning. Images of P16 *Sox10*$^{+/+}$ and *Sox10*$^{Dom/+}$ mouse duodenum, ileum, and colon are shown. NC derivatives are labeled by activation of the *R26R*^{tdTom} reporter following *Sox10*-Cre transgene expression. Scale bar = 100 µm. *Sox10*$^{+/+}$ and *Sox10*$^{Dom/+}$ mice have comparable ENS patterning and overall numbers of NC derivatives in the duodenum (*P=0.86)* and in the ileum (*P=0.55)*. (n=5 per genotype)

Table 2.6. Comparison of total NC derivatives beween *Sox10*$^{+/+}$ and *Sox10*$^{Dom/+}$.

Genotype	Region	Avg. NC derivatives/mm^2	SEM	p-value
Sox10$^{+/+}$	duodenum	3155	±57	0.86
Sox10$^{Dom/+}$	duodenum	3194	±41	
Sox10$^{+/+}$	ileum	4555	±26	0.55
Sox10$^{Dom/+}$	ileum	4384	±44	

n=5 per genotype. Comparisons for the mid-colon were not made because many *Sox10*$^{Dom/+}$ mice are hypoganglionic in this region.

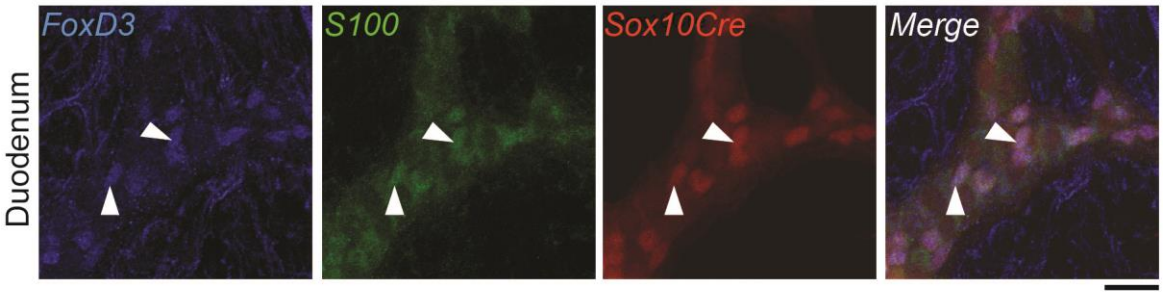

Figure 2.4. FoxD3 expression overlaps with S100. FoxD3 and S100, a known glial marker in the ENS, readily identify enteric glia that derive from NCPs permanently labeled by *Sox10*-Cre action on *R26R*^{tdTom} in the wildtype duodenum. (arrowheads) (n=3) Scale bar = 20 µm.

of neurons and glia were found to be comparable within the duodenum (neurons *P=0.28*; glia *P=0.36*) and the ileum (neuron *P=0.78*; glia *P=0.50*) between *Sox10*$^{Dom/+}$ and *Sox10*$^{+/+}$ animals (Figure 2.5B & C).

While neuronal and glial proportions in the mid-colon revealed no statistical difference between *Sox10*$^{Dom/+}$ and *Sox10*$^{+/+}$ animals (neurons *P=0.06*; glia *P=0.37)*, we noted an overall decrease in neuron proportions and an overall increase in glia proportions in *Sox10*$^{Dom/+}$ mice (Figure 2.5B & C). Given the variable length of aganglionosis present in HSCR *Sox10*$^{Dom/+}$ mice, which models that seen in HSCR patients, we compared colonic neuronal and glial proportions against the length of colonic aganglionosis for each *Sox10*$^{Dom/+}$ mouse. This analysis detected a

strong inverse correlation between neuron proportions and length of colonic aganglionosis (*$*P<0.003; r^2=0.70$*) (Figure 2.5D). Conversely, a strong direct relationship is present between glia proportions and extent of colonic aganglionosis (*$*P<0.005; r^2=0.66$*) (Figure 2.5D). Thus, while neuron and glia proportions in the *$Sox10^{Dom/+}$* small intestine are not altered and do not correlate with aganglionosis, in the colon, neuronal numbers decrease in concert with an increase in glial numbers as the area of the bowel affected by aganglionosis increases. Correlation scores for cell type proportions and extent of aganglionosis for each region of the bowel examined are summarized in Table 2.7.

Rare, enteric NC derived cell types in $Sox10^{+/+}$ and $Sox10^{Dom/+}$ mice.

Given the presence of multiple lineages, including myofibroblasts, in colonies grown from cultured enteric NCPs *in vitro*,(12, 13, 34, 35) we anticipated the possibility of identifying cells within the ENS that express neither neuronal nor glial markers. Use of the *Sox10*-Cre transgene system revealed enteric NC derivatives that were not labeled by neuronal (Hu+) or glial (FoxD3+) immunoreagents. However, these cells were extremely rare within myenteric ganglia and primary connectives with an average incidence of 1.5 cells in 1000 NC derivatives in the duodenum, 0.6 cells in 1000 in the ileum, and 6 cells in 1000 in the colon. The presence of this cell type did not significantly differ between *$Sox10^{+/+}$* and *$Sox10^{Dom/+}$* in any region of the intestine tested (duodenum *P=0.41*; ileum *P=0.90*; colon *P=0.23*) (Figure 2.6A). Furthermore, proportions of this cell type did not correlate with length of aganglionosis (Table 2.7).

Concurrently, while evaluating neuron and glia proportions, we documented a relatively infrequent population of enteric NC-derived cells that expressed both neuronal (Hu+) and glial (FoxD3+) markers. These cells were typically found in small clusters —mainly as couplets, triplets or quadruplets—but on occasion were found singularly (Figure 2.6B). This cell type was very rare in both *$Sox10^{+/+}$* and *$Sox10^{Dom/+}$* mice and its rate of appearance did not differ between *$Sox10^{+/+}$* and *$Sox10^{Dom/+}$* mice in the duodenum (*P=0.71*) or ileum (*P=0.12*). While still rare, *$Sox10^{Dom/+}$*

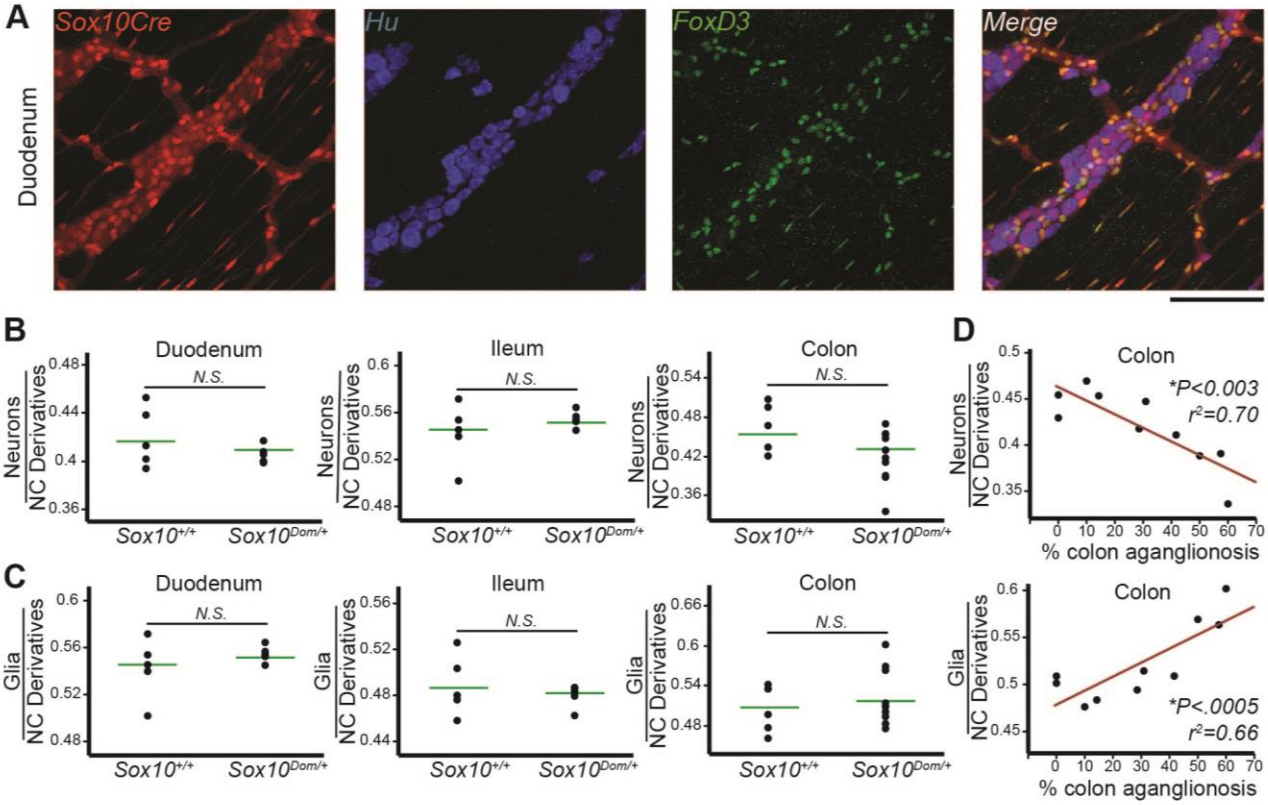

Figure 2.5. Proportions of neurons and glia in the colon correlate with length of aganglionosis in *Sox10$^{Dom/+}$* mice. The proportions of enteric neurons and glia relative to the total number of NC derivatives labeled by the recombined *R26R^{tdTom}* were quantified by immunofluorescent labeling of neurons (Hu+) and glia (FoxD3+). (**A**) Representative image of *Sox10$^{+/+}$* duodenum IHC. Scale bar = 100 µm. (**B**) Mean proportions of neurons (Hu+) were comparable between *Sox10$^{+/+}$* and *Sox10$^{Dom/+}$* mice in the duodenum (*P=0.28)* and ileum (*P=0.78)*, but decreased in the colon *(P=0.063)*. (n=5 per genotype) (**C**) Mean proportions of glia (FoxD3+) were comparable between *Sox10$^{+/+}$* and *Sox10$^{Dom/+}$* mice in the duodenum *(P=0.36)*, ileum *(P=0.50)*, and colon *(P=0.37)*. (**D**) Plots of neuron and glia proportions relative to length of colon aganglionosis. The proportion of NC derivatives that are neurons (Hu+) decreases as the length of colon affected by aganglionosis increases *(*P<0.0003; r^2=0.70).* Conversely, proportions of glia (FoxD3+) increase as the severity of the disease increases *(*P<0.005; r^2=0.66)*. (n=10) N.S.= Not significant. Asterisks denote significant P-values.

mice had more of these double positive cells within the colon (**P<0.005).* On average, *Sox10$^{Dom/+}$* colon samples contained 40 Hu+FoxD3+ cells per 1000 NC derivatives while *Sox10$^{+/+}$* colons only contained 25 Hu+FoxD3+ cells per 1000 NC derivatives. Unlike neurons and glia, the proportion of this cell type did not correlate with disease severity in the colon of *Sox10$^{Dom/+}$* mice (*P=0.80; r^2<0.01*). Additionally, no correlations were seen for this cell type in regions of the small intestine (Table 2.7).

Table 2.7. Correlation scores for NC-derived cell types and length of aganglionosis in the duodenum, ileum, and colon.

Cell type	*Duodenum*		*Ileum*		*Colon*	
	r^2	*p-value*	r^2	*p-value*	r^2	*p-value*
Neurons (all)	0.43	0.23	0.29	0.35	*0.70*	**<0.003*
Glia	0.43	0.23	0.12	0.57	*0.66*	**<0.005*
Hu+FoxD3+ NC derivatives	0.01	0.91	0.22	0.43	0.01	0.80
Hu-FoxD3- NC derivatives	0.07	0.66	0.07	0.66	0.07	0.46
Calretinin+ neurons	0.09	0.56	0.11	0.51	*0.84*	**<0.0001*
nNOS+ neurons	0.07	0.68	0.18	0.48	*0.74*	**<0.0014*

Regional alterations among enteric neuronal subtypes in Sox10$^{Dom/+}$ mice

Because clinicians have identified chronic constipation and incontinence as problematic long term outcomes in Hirschsprung patients (8), we examined the relative proportions of two neuronal subtypes in *Sox10$^{Dom/+}$* mutants with well-known roles in GI motility. Calretinin is expressed in cholinergic neurons and its presence identifies excitatory muscle motor neurons within the myenteric plexus as well as some interneurons and intrinsic primary afferent neurons (2, 36). Therefore, alterations in Calretinin expressing (Calretinin+) neuron numbers could affect intestinal contraction dynamics and overall motility. Proportions of Calretinin+ neurons out of total neurons (Hu+) in the myenteric plexus were quantified through IHC (Figure 2.7A). The proportion of Calretinin+ neurons in *Sox10$^{Dom/+}$* mice duodenum was significantly greater compared to

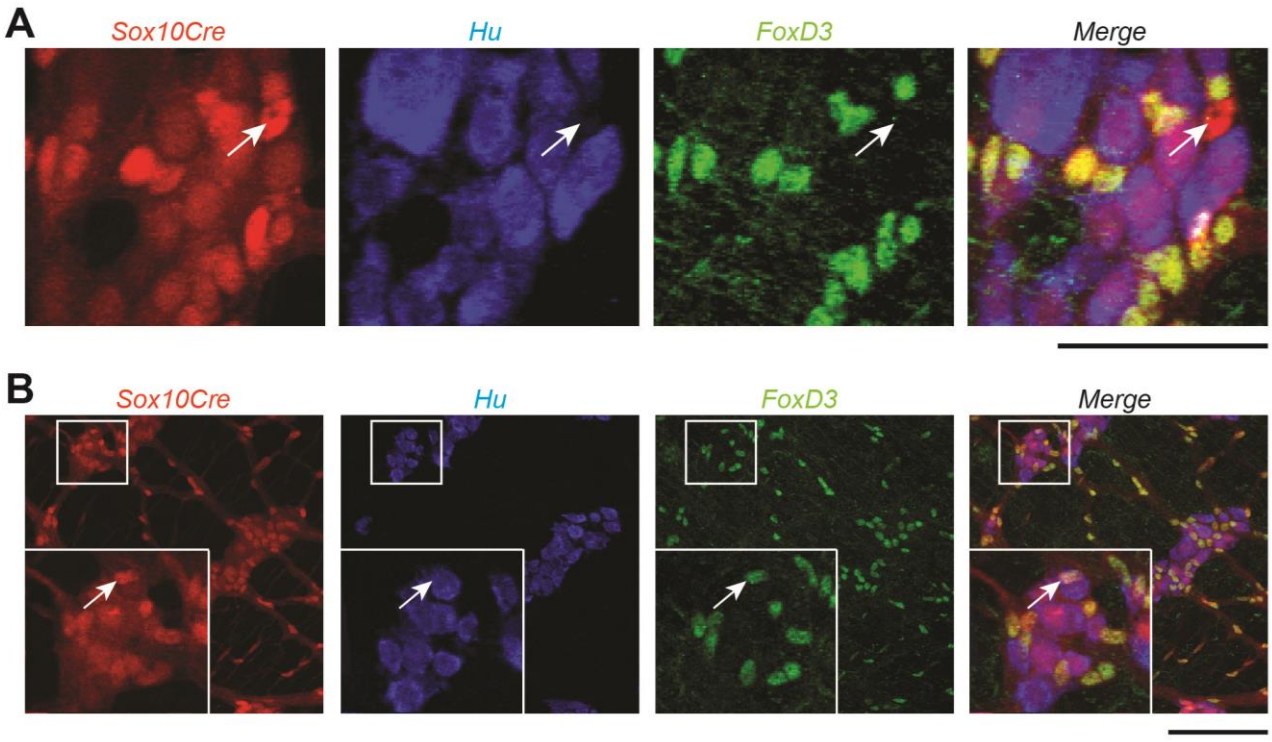

Figure 2.6. Rare NC derivatives in the ENS. (**A**) In this representative image of the duodenum in a *Sox10*$^{+/+}$ mouse, all neural crest derivatives are labeled by *Sox10*-Cre transgene driven expression of the *R26R*^{tdTom} reporter. Immunohistochemistry was used to label neurons (Hu+) and glia (FoxD3+). The arrow denotes a NC-derived cell that does not immunohistochemically label with a neuronal (Hu+) or glial (FoxD3+) marker. These cells were extremely rare in both *Sox10*$^{+/+}$ and *Sox10*$^{Dom/+}$ mice, and the proportion of this cell type to total NC derivatives did not differ between the two phenotypes in any region of the intestine (duodenum *P=0.41*, ileum *P=0.90*, colon *P=0.23*). (**B**) The arrow in the inset denotes NC-derived cells that label with both a neuronal (Hu+) and glial (FoxD3+) marker. These cells were sometimes found alone, but many times found in groups, such as couplets. (n=5 per genotype). Scale bar = 100 μm.

Sox10$^{+/+}$ littermates (**P<0.05*) (Figure 2.7B). Calretinin+ neurons were also present in higher proportions in the ileum of *Sox10*$^{Dom/+}$ mice (**P<0.03*) (Figure 2.7C). In sharp contrast to findings in the small intestine, an overall decrease in the proportion of Calretinin+ neurons was evident in the colon. (**P<0.03*) (Figure 2.7D). Concurrently, greater variance in colonic Calretinin+ neuronal subtype proportions was present in *Sox10*$^{Dom/+}$ mutants compared to *Sox10*$^{+/+}$ samples, similar to the effect seen for colonic neuronal and glial proportions. We also tested the relationship between Calretinin+ neuron proportions and length of aganglionosis. This analysis revealed that Calretinin+ neuron proportions decrease dramatically as the length of aganglionosis increases (**P<0.0001. r*^{2}*=0.84*) (Figure 2.7E). This effect was limited to the colon as Calretinin+ neuron proportions did not correlate with length of aganglionosis in the duodenum nor ileum (Table 2.7).

To further define alterations in other motor neuron types, we evaluated nNOS expressing neurons in *Sox10*$^{Dom/+}$ mutants (Figure 2.8A). Nitrergic (nNOS+) neurons in the myenteric plexus are primarily inhibitory motor neurons responsible for the relaxation of intestinal smooth muscle and also include some interneurons (2). Interestingly, although Calretinin+ neuron proportions were altered in the duodenum in *Sox10*$^{Dom/+}$ mice, nNOS+ neuron proportions were comparable between *Sox10*$^{+/+}$ and *Sox10*$^{Dom/+}$ animals (*P=0.68*) (Figure 2.8B). Similarly, nNOS+ proportions were nearly identical in the ileum between the two genotypes (*P=0.51*) (Figure 2.8C). However, there was a trending increase in nNOS+ neuron proportions in the colon of *Sox10*$^{Dom/+}$ mice compared to *Sox10*$^{+/+}$ controls (*P=0.099*) (Figure 2.8D). While Calretinin+ neuron proportions in the colon decreased as length of aganglionosis increased, the opposite was true for nNOS+ neurons. Animals with greater extents of aganglionosis also exhibited greater proportions of colonic nNOS+ neurons (**P=0.0014; r*^{2}*=0.74)* (Figure 2.8E). Like the majority of cell types we evaluated, correlations for nNOS+ neurons were only detected in the colon and not the duodenum and ileum (Table 2.7).

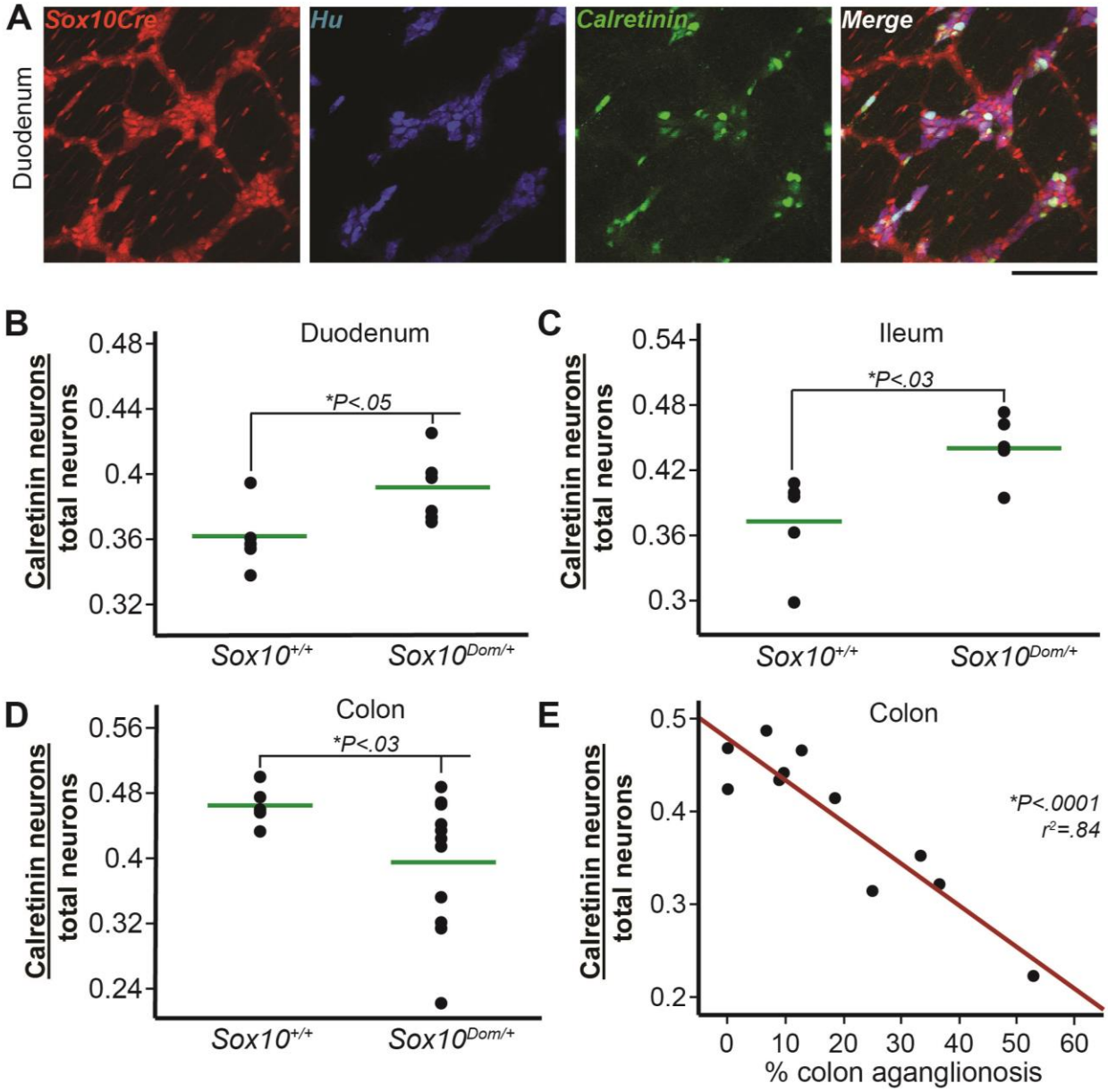

Figure 2.7. Comparision of Calretinin neuron proportions in *Sox10*$^{+/+}$ and *Sox10*$^{Dom/+}$. In *Sox10*$^{Dom/+}$ mice, Calretinin neuron proportions are more abundant in the duodenum and ileum, but decreased in the colon. (**A**) Co-localization of *R26R*^{tdTom} reporter labeled enteric NC with total neurons (Hu+) and Calretinin expressing neurons (Calretinin+) allows quantitation of Calretinin+ neuron proportions as illustrated in representative images of *Sox10*$^{+/+}$ duodenum. Scale bar = 100 μm. *Sox10*$^{Dom/+}$ mice have an increase in Calretinin+ neurons in the (**B**) duodenum (**P<0.05*)and (**C**) ileum (**P<0.03*), but exhibit a decrease in the (**D**) colon (**P<0.03)*. (n=5-6 per genotype) (**E**) Plot of Calretinin+ neuron proportions versus length of aganglionic colon segment reveals a sharp decrease in Calretinin+ neurons as disease severity increases in *Sox10*$^{Dom/+}$ mice. (**P<0.0001; r^2=0.84).* (n=11)

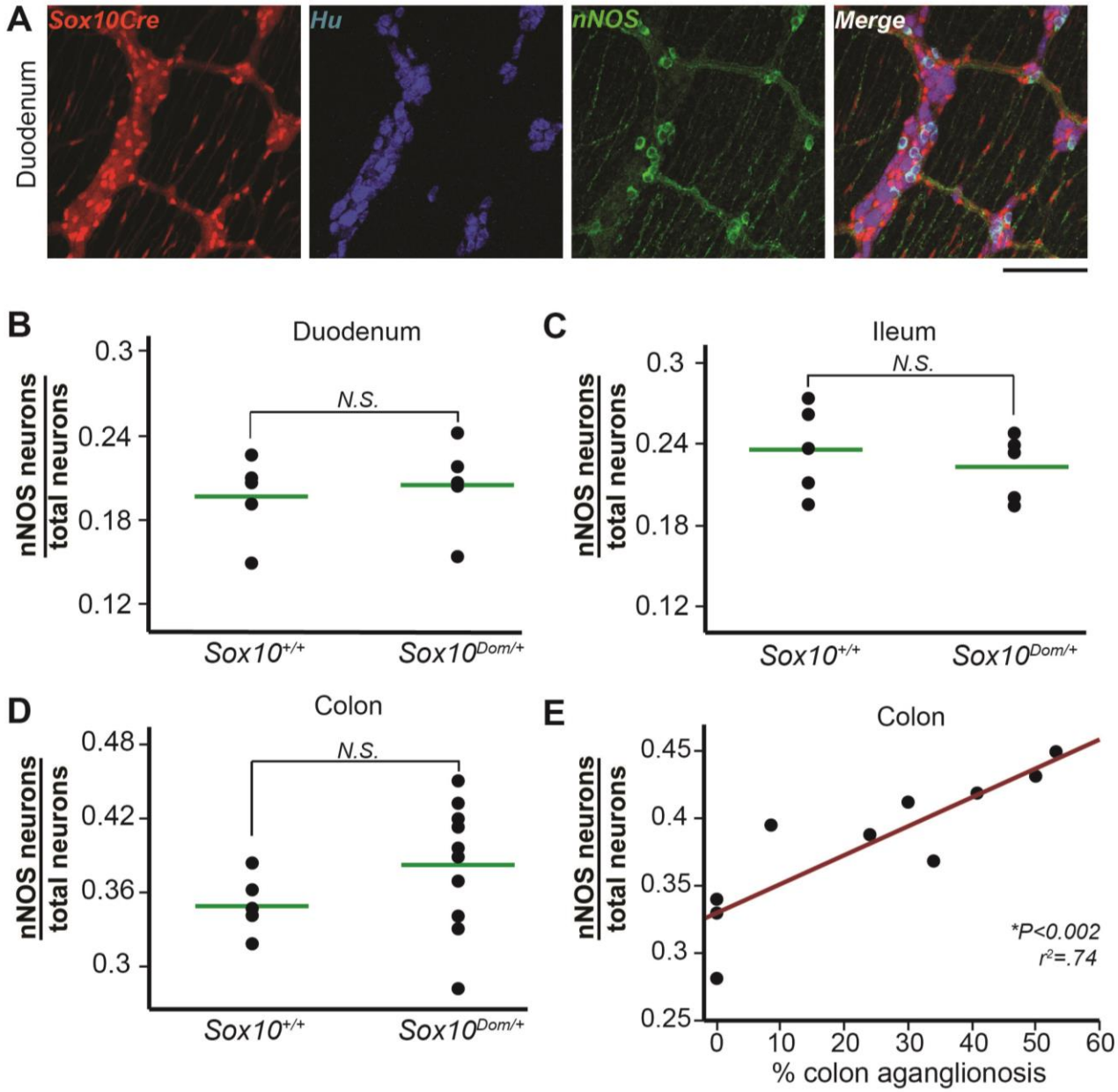

Figure 2.8. Comparison of nNOS neuron proportions in *Sox10*$^{+/+}$ and *Sox10*$^{Dom/+}$ mice. nNOS+ neuron proportions are comparable in *Sox10*$^{+/+}$ and *Sox10*$^{Dom/+}$ duodenum and ileum, although nNOS+ neuron proportions in the colon increase with aganglionosis length in *Sox10*$^{Dom/+}$ colon. (**A**) Co-labeling by the *Sox10*-Cre transgene system and nNOS IHC to quantify nNOS neuron proportions is shown in a *Sox10*$^{+/+}$ duodenum. Scale bar = 100 µm. Comparison of nNOS+ neuron proportions in the (**B**) duodenum (*P=0.68)*, (**C**) ileum (*P=0.51)* and (**D**) colon (*P=0.099)*. (n=5 per genotype) (**E**) Plot of nNOS+ neurons versus length of aganglionic colon segment reveals an increase in nNOS+ neuron proportions as length of colonic aganglionosis increases in *Sox10*$^{Dom/+}$ mice (*$P<0.002$; $r^2=0.74$). (n=10)

Gastric emptying and small intestinal transit in Sox10$^{Dom/+}$ mice

Substantial numbers of HSCR patients suffer GI dysfunction even after surgical resection of aganglionic regions. Given the skewing of neuron proportions observed in *Sox10$^{Dom/+}$* animals resulting from increased Calretinin+ neurons in the duodenum and ileum, we examined GI motility dynamics proximal to the colon in *Sox10$^{Dom/+}$* mice. To evaluate gastric emptying and small intestine transit rates, fasted mice were gavaged with a non-absorbable fluorescent meal. Gastric emptying was determined by calculating the proportion of fluorescent signal that had left the stomach to the total recovered fluorescence, and small intestine transit rates were determined by calculating the geometric mean of fluorescence within the small intestine (18-20). Because distal intestinal obstruction can affect GI transit more proximally and pups with severe aganglionosis often succumb to megacolon around weaning, we chose to limit our analysis to more mature *Sox10$^{Dom/+}$* mice that survived past weaning to 4-weeks or 6-weeks of age. *Sox10$^{Dom/+}$* animals that survive to adulthood typically have short lengths of aganglionosis, reach full adult size, and feed and breed normally.

Initially, gastric emptying and small intestine transit rates were compared in 4-week old *Sox10$^{Dom/+}$* and *Sox10$^{+/+}$* animals. Because HSCR shows a sex bias in humans with three in four HSCR patients males (3), we chose to evaluate GI motility in both *Sox10$^{Dom/+}$* male and female mice. In 4-week old animals, *Sox10$^{Dom/+}$* males had significantly slower small intestinal transit rates than *Sox10$^{+/+}$* males (*$^{*}P<0.04$*) (Figure 2.9A). Nearly identical results were obtained for females, with 4-week old *Sox10$^{Dom/+}$* females also showing significantly reduced small intestinal transit rates (*$^{*}P<0.006$*) (Figure 2.9B). Gastric emptying rates were comparable between *Sox10$^{Dom/+}$* and *Sox10$^{+/+}$* for both sexes at this age (males: *P=0.96*; females: *P=0.68*) (Figure 2.9A & B).

These findings are not surprising given the skew of neuronal subtypes we observed in the small intestine of *Sox10$^{Dom/+}$* and known outcomes among HSCR patients. However, because neurally mediated traits are susceptible to change upon increased exposure to sex hormones (37,

38), gastric emptying and small intestine transit rates were also evaluated in older, sexually mature (6-week+) animals. For older male mice, we observed statistically comparable small intestine transit rates between *Sox10*$^{Dom/+}$ males and their wild type *Sox10*$^{+/+}$ counterparts (*P=0.57*). But, in contrast to the phenotype of 4-week old males, we observed a marked increase in gastric emptying rates of 6-week old *Sox10*$^{Dom/+}$ males that was not observed in 6-week old normal *Sox10*$^{+/+}$ littermates (**P<0.005*) (Figure 2.9C). Small intestine transit rates were comparable between 6-week old *Sox10*$^{Dom/+}$ and *Sox10*$^{+/+}$ females (*P=0.31*) (Figure 2.9D). And, unlike 6-week old males, gastric emptying rates were comparable in female 6-week old *Sox10*$^{Dom/+}$ and *Sox10*$^{+/+}$ mice (*P=0.58*) (Figure 2.9D). To summarize, at an early age, both female and male *Sox10*$^{Dom/+}$ have significant small intestine transit deficits; however, in older *Sox10*$^{Dom/+}$ animals, only males exhibit any type of motility defect. (See Table 2.8 for a numerical summary of GI transit results.)

Sox10*$^{Dom/+}$ *mice exhibit negligible colonic inflammation

Many Hirschsprung patients suffer from severe bouts of enterocolitis and previous studies reported that some animals with an *Ednrb* HSCR mutation suffer from enterocolitis that can ultimately lead to bowel perforation, sepsis and death (21, 39). Additionally, inflammatory processes within the bowel could potentially affect GI motility, making it difficult to determine if GI motility deficits in *Sox10*$^{Dom/+}$ mice result from changes in electrical properties due to ENS deficits and/or influences of inflammatory processes on the bowel. To determine if enterocolitis could be affecting GI motility in adult *Sox10*$^{Dom/+}$ mice, we harvested entire colons from *Sox10*$^{Dom/+}$ and *Sox10*$^{+/+}$ 6 week+ old littermates. Colons were hematoxylin and eosin stained and scored for inflammation by a pathologist blinded to genotype. We adopted a grading rubric for inflammation based on previous studies in HSCR mouse mutants (21). Briefly, each mouse was assigned an inflammation score (0-7) based on the severity (0-3) and depth (0-4) of inflammation. Interestingly, *Sox10*$^{Dom/+}$ mice had no or very little inflammation, comparable to their WT

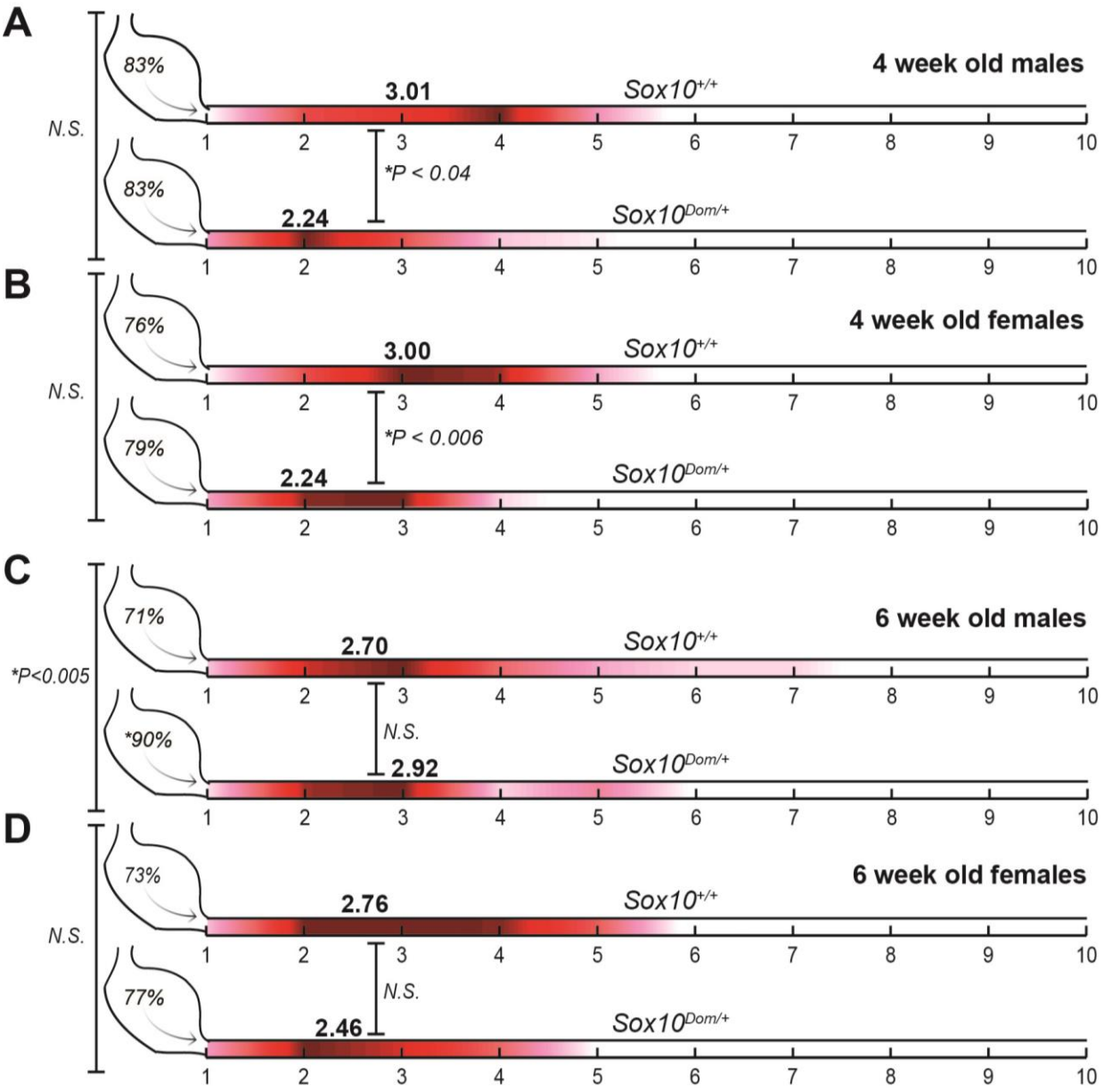

Figure 2.9. Comparison of gastric emptying and small intestinal transit in *Sox10*$^{+/+}$ and *Sox10*$^{Dom/+}$ mice. Schematic illustrating gastric emptying (stomach %) and small intestine transit score (red heat map) in 4-week and 6-week old *Sox10*$^{+/+}$ and *Sox10*$^{Dom/+}$ males and females (n=6-8 mice per genotype, gender, and age). The red heat map was generated by calculating the average contribution (amount of fluorescent signal) to the small intestine transit score; hotter colors (red) indicate high contribution while cool colors (pink) indicate little contribution to the score. Average transit scores (geometric mean of fluorescence) are included in bold lettering above small intestine renditions for each group. Four-week old *Sox10*$^{+/+}$ and *Sox10*$^{Dom/+}$ (**A**) males and (**B**) females have comparable gastric emptying, but both *Sox10*$^{Dom/+}$ sexes show slower intestine transit rates. (**C**) Six-week old *Sox10*$^{Dom/+}$ males have faster gastric emptying, but comparable small intestine transit rates to *Sox10*$^{+/+}$ males. (**D**) Six-week old female genotypes were comparable for both gastric emptying and small intestine transit.

Table 2.8. Comparison of gastric emptying and small intestine transit scores between *Sox10*$^{+/+}$ and *Sox10*$^{Dom/+}$ mice.

Genotype	Age	Sex	Gastric emptying (%)	p-value	Small intestine motility	p-value
Sox10 $^{+/+}$	4 weeks	M	83.09 ±2.68	*0.96*	3.01 ±.23	**0.03*
Sox10 $^{Dom/+}$	4 weeks	M	83.40 ±5.31		2.24 ±.21	
Sox10 $^{+/+}$	4 weeks	F	76.44 ±.4.05	*0.68*	3.00 ±.19	**<0.006*
Sox10 $^{Dom/+}$	4 weeks	F	78.78 ±3.74		2.24 ±.08	
Sox10 $^{+/+}$	6 weeks	M	70.91 ±4.16	**<0.005*	2.70 ±.24	*0.57*
Sox10 $^{Dom/+}$	6 weeks	M	89.50 ±2.14		2.92 ±.29	
Sox10 $^{+/+}$	6 weeks	F	72.94 ±5.56	*0.31*	2.76 ±.20	*0.58*
Sox10 $^{Dom/+}$	6 weeks	F	77.11 ±4.69		2.46 ±.20	

n=6-8 mice per genotype, gender, and age

littermates (*P=0.99*) (Figure 2.10B). Since males and females may differ in the levels of inflammation, we also compared inflammation scores by sex. Even when separated by sex, we observed similar levels of inflammation in *Sox10*$^{Dom/+}$ and *Sox10*$^{+/+}$ mice (Figure 2.10C & D). Other hallmark features of Hirschsprung disease as reported in HSCR patients, such as regions of hypoganglionosis proximal to aganglionosis and thickened muscularis propria were evident (Figure 2.10A). Given the intestinal transit alterations in *Sox10*$^{Dom/+}$ and the lack of inflammation in this HSCR model, our results suggest the motility deficits in this HSCR model are neurally mediated.

Discussion

We utilized the *Sox10*-Cre transgene to evaluate enteric NC derivatives in *Sox10*$^{Dom/+}$ and *Sox10*$^{+/+}$ pups. Both the *Wnt1*-Cre and *Sox10*-Cre transgene label the vast majority of NC derivatives within the ENS. However, we found that the *Sox10*-Cre transgene driven expression of the *R26R*^{tdTom} led to significantly more NC derivative labeling in the ileum and colon than crosses with *Wnt1*-Cre mice (Table 2.4). These findings, along with known neurological developmental defects in the *Wnt1*-Cre line (24), justified our use of the *Sox10*-Cre transgene in

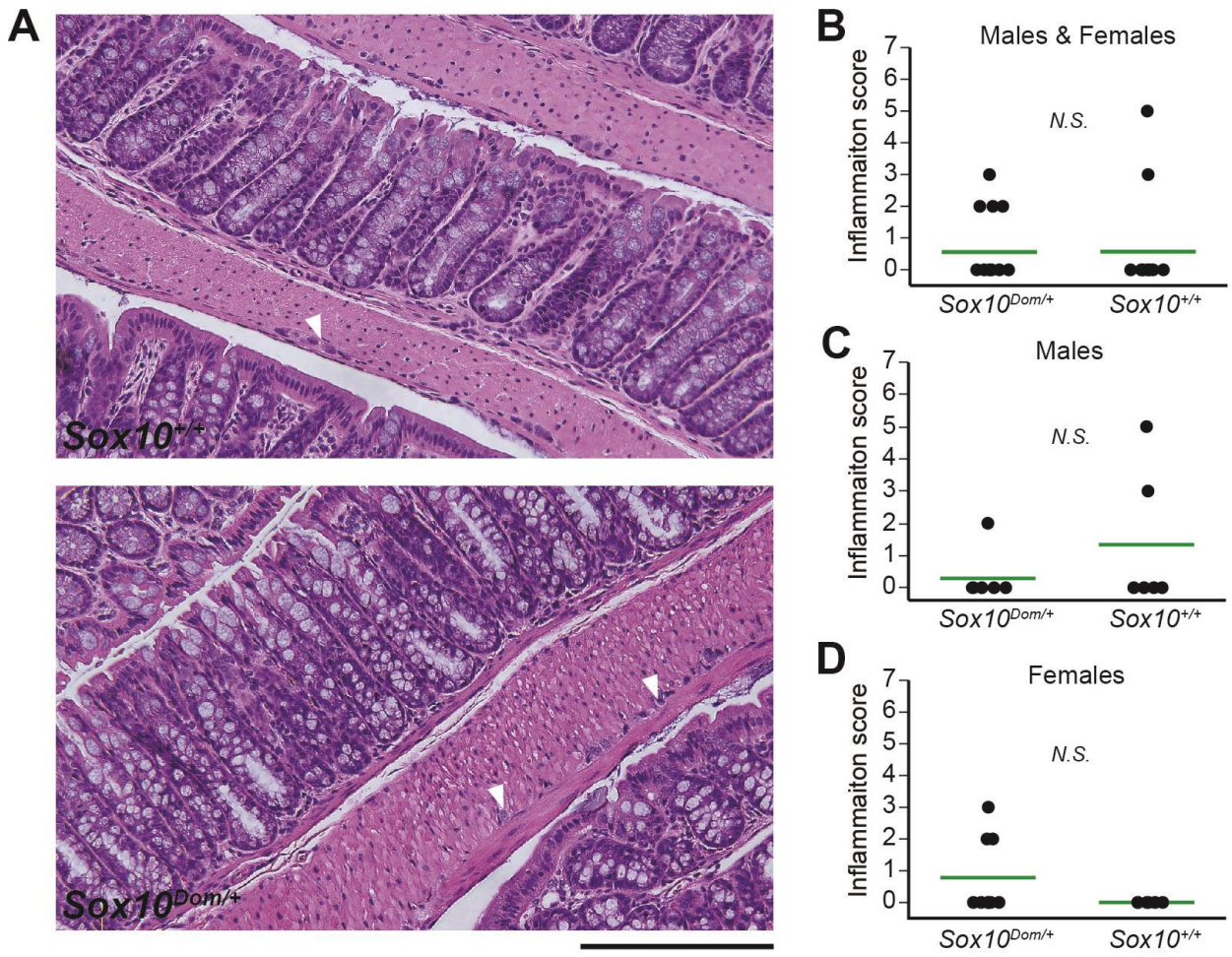

Figure 2.10. Comparison of inflammation in *Sox10*$^{+/+}$ and *Sox10*$^{Dom/+}$ mice. (**A**) H&E stained sections of colon in *Sox10*$^{+/+}$ (upper panel) and *Sox10*$^{Dom/+}$ (lower panel) mice demonstrate no or very little inflammation. However, note the thickened muscle and small ganglia (arrowhead) denoting hypoganglionosis in the *Sox10*$^{Dom/+}$ image, common findings in Hirshsprung disease. Scale bar = 200 µm. (**B**) Comparison of inflammation scores (range 0-7) between genotypes reveals no statistical difference in inflammation levels. *P=0.99*. [*Sox10*$^{Dom/+}$ = 0.56 ±1.03 (n=16) and *Sox10*$^{+/+}$ = 0.57 ±1.50 (n=14)]. (**C**) Comparison of males alone yielded comparable scores between the two genotypes. *P=0.30*. [*Sox10*$^{Dom/+}$ = 0.29 ±0.76 (n=7) and *Sox10*$^{+/+}$ = 1.33 ±2.16 (n=6)]. (**D**) Comparison of females alone also yielded comparable scores between the two genotypes. P=0.09. [*Sox10*$^{Dom/+}$ = 0.78 ±1.20 (n=9) and *Sox10*$^{+/+}$ = 0.00 ±0.00 (n=8)].

this study. However, the biological factors driving the differences we observed between *Wnt1*-Cre and *Sox10*-Cre lines are unknown. It is believed that the neurons and glia of the duodenum derive solely from the vagal NC population, whereas vagal and sacral NC populations contribute to the neurons and glia in the ileum and colon (40). Therefore, differential expression of *Wnt1*-Cre or activation of the *Wnt1*-Cre enhancer in specific sacral NC cells could explain our findings. Alternatively, but possibly related, *Wnt1* expression in sacral NC population is temporally brief (41) compared to *Sox10* expression. Therefore, action of transcription machinery on the *Wnt1*-Cre transgene may be too brief to drive Cre-recombinase expression to levels needed for Cre-LoxP action within $R26R^{tdTom}$. Whatever the reason, this finding highlights the importance of integrating key regulatory regions of a "gene of interest" into a transgene to ensure proper expression of transgene components as well as appropriate transgene choice in studies.

The $Sox10^{Dom/+}$ HSCR mutant is one of several HSCR models frequently studied to better understand the NC deficits that give rise to aganglionosis (3, 10, 31, 42). The $Sox10^{Dom}$ allele disrupts migration of NCPs as they populate the fetal intestine and contribute to extensive colonic aganglionosis (43, 44). Additionally, isolated $Sox10^{Dom/+}$ enteric NPCs do not produce a normal profile of cell lineages when cultured *in vitro* (13). Despite the insights gained from studying fetal effects of Sox10 mutations on NCP migration and consequent aganglionosis, no prior efforts have investigated postnatal consequences of *Sox10* mutations on ganglionated regions. In this study, we undertook a comprehensive assessment of NC derivatives in the proximal, ganglionated intestine of $Sox10^{Dom/+}$ mice to test the hypothesis that the $Sox10^{Dom}$ mutation leads to imbalances in enteric NC derived lineages and deficits in bowel function. Our analysis revealed effects of the *Sox10* mutation on neuronal-glial lineage segregation in the colon, but not the small intestine. Interestingly, this study identified significant imbalances in proportions of excitatory and inhibitory enteric neurons accompanied by deficits in intestinal transit and gastric emptying. Calretinin+ neurons with roles in muscle contraction were significantly increased in the duodenum and ileum while nNOS+ neurons with roles in muscle relaxation were unchanged in these regions.

Sox10 effects on glial cell specification and NCP multipotency are well established in other aspects of the peripheral nervous system, like dorsal root ganglia (11, 30, 31, 45). Surprisingly, our analysis indicated no effect of the *Sox10^{Dom}* mutation on neuronal-glial balance in the duodenum and ileum although there was a significant correlation between proportions of neurons and glia in the *Sox10^{Dom}* colon with overall extent of aganglionosis. It is possible that *Sox10$^{Dom/+}$* neurons and glia are born in equal proportions in the colon, with more neurons subsequently succumbing to apoptosis while glia persist. However, increased apoptosis has not been observed in several ENS mutants to date (13, 46, 47). Moreover, cell death cannot adequately account for observed increases in colonic nNOS+ neuron proportions to levels well above the wild type average in *Sox10$^{Dom/+}$* mice with severe aganglionosis. Our study suggests that timing of NCP lineage choice is likely a key factor in determining not only the length of aganglionosis, but ultimately the proportions of enteric glia, neurons, and neuronal subtypes. It has been postulated that premature neuronal differentiation contributes to HSCR disease by depleting the enteric NCP pool. Premature NCP differentiation would not only exhaust the NCP pool, but may cause certain cell types to be born more or less often based on when (temporally) and where (local environment) lineage choice occurs. This phenomenon could account for the region specific imbalance of different NC-derived cell types we observed in *Sox10$^{Dom/+}$* mice. Such a possibility is corroborated by recent findings in the developing telencephalon, where oscillating or sustained expression of specific transcription factors controls whether neural progenitor cells go on to differentiate into specific cell types or continue to proliferate and give rise to daughter neural progenitor cells (48).

A possibility, not mutually exclusive from our hypothesis above, is that changes in neuron, glia, and neuronal subtype proportions in *Sox10$^{Dom/+}$* animals in the colon are driven by birth dates of NC derivatives. Birth date for a neuron in the ENS can be defined as the point a cell has undergone its last mitotic division and taken on characteristics of a terminally differentiated neuron such as expression of a specific neurotransmitter (49). For example, serotonergic neurons are some of the first neuron subtypes to be born, with birthdates as early as E8 (49). Conversely,

some VIP neurons are extremely late-born with birthdates recorded as late as P5 (49). Therefore, it could be in hypoganglionic regions of the colon in HSCR mouse models, we would see early born neuronal subtypes to be in greater proportions than those born at later stages because the progenitor pool is depleted before it can give rise to these late-born neuron types. If this were the case, then neuron subtype proportions in hypoganglionic regions should correlate directly with the ganglion size (ie extremely hypoganglionic areas with very few cells per ganglia would have more early born neurons while less hypoganglionoic areas with larger ganglia would have a near normal complement of neuron subtypes with only a few late-born neuron subtypes missing.) The birth dates of glia are still unknown in the ENS, but this hypothesis is testable by comparing the proportions of a neuron subtype to the relative ganglia size (NC derivatives within an image.) We performed this analysis for nNOS neuron proportions in the colon and found no correlation between nNOS neuron proportions and relative ganglia size (*P=0.1031; r^2=0.08*) (Figure 2.11). Although this finding rules out the possibility that birthdates of neuronal subtypes exclusively drives our phenotype, this does not mean that birth dating does not play a role. In fact, it is known that early born neuron subtypes affect the fate of later born neuron subtypes. For example, ablation of enteric serotonergic neurons (early born) in embryonic development leads to decreases in dopaminergic neurons and increases in CGRP neuron types (50). Rather, this finding suggests, as above, that multiple factors including timing and environment (intra- and extracellular) are influencing fate choice.

Given the diversity of cell types that can arise from cultured NC progenitors *in vitro* (51), we were not surprised to identify NC-derived cells in the intestine that did not label with neuronal or glial immunoreagents. These cells are infrequent and might represent a novel cell type or possibly cell turnover within ganglia. Because proportions of these NC-derived cells were equivalent between *$Sox10^{Dom/+}$* and *$Sox10^{+/+}$* animals and because they were so rare, we did not attempt to characterize this lineage further. Interestingly, in both *$Sox10^{Dom/+}$* and *$Sox10^{+/+}$* mice, we observed cells that double-labeled with neuronal (Hu+) and glial (FoxD3+) markers. This cell

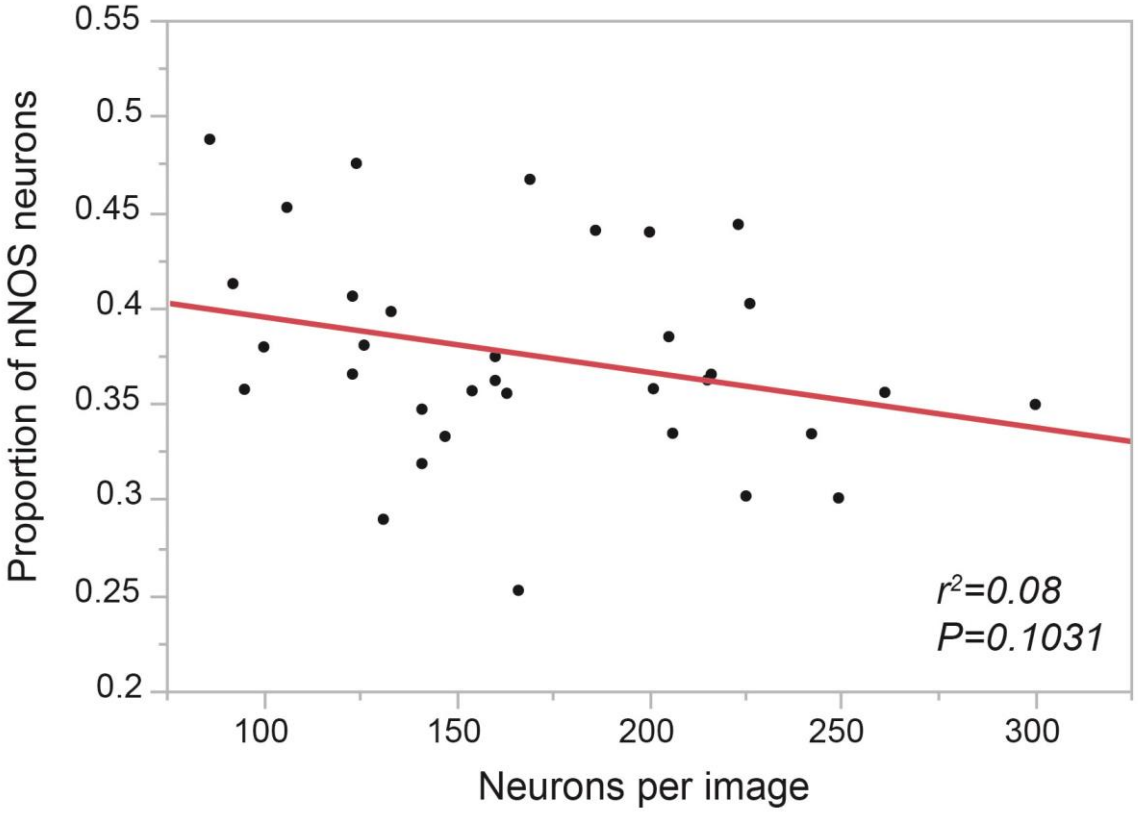

Figure 2.11. Correlation between nNOS neuron proportions and neuron density in *Sox10*$^{Dom/+}$ mice. To test whether neuron subtype proportion and neuron birthdate could be related, neuron density (neurons per 300 um^2 image) was compared to nNOS neuron proportions in each image. No correlation existed, indicating birthdates cannot exclusively be driving nNOS proportions changes in the colon of *Sox10*$^{Dom/+}$ mice.

type may represent either a novel lineage or a progenitor(s) undergoing differentiation. Given their morphology and tendency to be found in clusters, these cells could also represent neural progenitors with adjacent daughter progenitors or daughter cells not fully committed to a specific cell type. The latter is certainly feasible given that Foxd3 is expressed in enteric NCPs as well as enteric glia (33, 52). Enteric neural progenitors certainly exist in the adult intestine, and their exact location and nature are being actively investigated (17, 25, 34). However, no markers have been found that exclusively label neural stem cells in the intestine, convoluting efforts to characterize this cell type. If truly an enteric neural stem cell, the increase in this cell type in the *Sox10*$^{Dom/+}$ colon might represent a futile attempt by the remaining neural stem cells to populate the hypoganglionic or aganglionic areas of the distal intestine.

Because HSCR is an oligogenic disorder, whereby an independent variant in any one of several genes can produce aganglionosis, our findings are potentially of broad relevance to other HSCR models. To our knowledge, this is the first study to examine NC derivative imbalance and GI function in the proximal intestine of a HSCR model. Previous studies in *Gdnf*, *Edn3,* and *Ednrb* HSCR mouse models have noted distal intestinal changes in neuron types, neurotransmitter expression, and/or colonic migratory complexes (22, 53-55). These initial studies were important and our findings corroborate their results. Sandgren and colleagues (53) noted changes in neuron types within a HSCR mouse model, specifically mice with the *Edn3 lethal spotted* mutation. Specifically, Sandgren et al., found that homozygous *lethal spotted* mice had higher proportions of nNOS+ neurons in the ileum and distal colon compared to heterozygous *lethal spotted* mice. In EdnrB deficient mice, Zaitoun et al., (22) identified a decrease in colonic ChAT expressing (cholinergic) neurons somewhat analogous to the decreased proportions of Calretinin (cholinergic) neurons we documented in colon of *Sox10*$^{Dom/+}$ mice. Increased numbers of colonic nNOS+ neurons were also observed. Although these studies are informative, our study is the first to examine the relationship between NC derivative proportions in the colon and aganglionosis length. Our analysis benefited from the varying levels of aganglionosis present with the *Sox10*$^{Dom/+}$

mutation on a mixed background and may not have been possible in other HSCR mouse models where extent of aganglionosis does not differ markedly between littermates.

Recent studies show that prenatal obstruction (atresia) affects NC derivatives in rats (56) and extent of aganglionosis in our HSCR mouse model could be viewed as varying lengths of obstruction. Although we realize obstruction cannot be excluded as a factor that impacts NC derivative choice in the colon, *Sox10*$^{Dom/+}$ are born in Mendelian ratios to their WT littermates, suggesting obstruction does not play a large role prenatally. We also chose P15-19 pups for NC derivative studies to ensure that the ENS was fully developed and to try to avoid influences of obstruction on the ENS. (The majority of *Sox10*$^{Dom/+}$ mice suffer from obstruction and expire due to megacolon near or at weaning when they transition to solid food.) Future studies will be needed to elucidate how different types of obstruction, such as constipation or atresia, affect ENS constituents. Additionally, whether all changes in NC derivatives, gastric emptying, small intestine transit, and colonic motility are comparable among HSCR mutant alleles remains to be seen. Although we are the first to characterize gastric emptying and small intestine transit defects in a HSCR mouse model, previous groups have shown colonic motility defects in HSCR models such as those with Ednrb mutations. Ro et al., demonstrated that both heterozygous and homozygous mice with the *Ednrb piebald lethal* mutation exhibit aganglionosis and have severely reduced or completely absent colonic migrating motor complexes (CMMCs) (55). Similarly, Roberts and colleagues demonstrated abnormal or absent CMMCs in *Gdnf*$^{+/-}$ and *Edn3*$^{-/-}$ HSCR model mice respectively (54). Similarities and disparities in outcomes between HSCR mutant models should help elucidate exactly when and where HSCR genes act within HSCR gene pathways.

Mice with deficits in ENS patterning or NCP lineage segregation but no overt aganglionosis can exhibit altered GI motility (10, 20). And, as previously stated, HSCR models have not previously been evaluated for motility deficits within ganglionated regions of the small intestine. While many studies limit their analysis to male mice, we chose to examine both males and females given the difference in incidence of HSCR and other neurodevelopmental disorders

between males and females. In the *Sox10*$^{Dom/+}$ model, we documented slower small intestine transit rates in 4-week old males and females. Because *Sox10*$^{Dom/+}$ mice show increases in excitatory motor neurons (Calretinin+) in the small intestine, but no changes in inhibitory motor neurons (nNOS+), we hypothesize that imbalances in motor neuron cell types cause changes in peristalsis coordination and/or neuron signaling. Because other neuronal subtypes also affect motility, we cannot at this time directly attribute these changes in GI motility to our findings in Calretinin+ and nNOS+ neurons. However, given that Calretinin+ and nNOS+ neurons comprise the majority of motor neurons in the myenteric plexus, our hypothesis provides a plausible and attractive explanation. Future analyses are required to determine the exact electrophysiological changes within the ENS in *Sox10*$^{Dom/+}$ mice and ascertain if other cell types that contribute to motor activity (such as serotonergic neurons or Interstitial Cells of Cajal) are perturbed. In contrast to our results in young animals, mature *Sox10*$^{Dom/+}$ and *Sox10*$^{+/+}$ mice showed comparable small intestine transit rates. It could be that the *Sox10*$^{Dom/+}$ intestine adapts or compensates for deficits as the ENS matures or that we have selected for more mildly affected mice at this age since many severely affected mice succumb to HSCR near weaning. However, we also observed increased gastric emptying in older *Sox10*$^{Dom/+}$ males that we did not see in females, a result that was unexpected. Increased gastric emptying in HSCR mouse models has not previously been reported and the underlying physiological basis for this effect in males is not clear. For many neurodevelopmental diseases, females are postulated to be protected or differentially affected due to circulating sex hormones while males are more susceptible (37, 38). This tendency for males to be more severely affected by neurodevelopmental disorders may explain why males are afflicted more often with HSCR than females (3:1) and could explain why 6-week old *Sox10*$^{Dom/+}$ males have increased gastric emptying rates, but not females. Furthermore, increased gastric emptying rates may confound small intestine transit rates because gastric contents are more rapidly entering the small intestine. Therefore, it is possible that our

Sox10$^{Dom/+}$ males still have a decreased small intestine transit rate compared to their wild type counterparts, but this phenotype is being masked by increased gastric emptying.

Despite the fact that infection and inflammatory processes are known to affect GI transit speed, we saw no difference in colonic inflammation between *Sox10*$^{Dom/+}$ and *Sox10*$^{+/+}$ adult mice. This finding suggests that differences in gastric emptying and small intestine transit are at least partially driven by neural mechanisms. It remains to be seen whether *Sox10*$^{Dom/+}$ mice are more or less susceptible to inflammation when challenged by surgery, infection, or chemical treatment. Some HSCR patients and mouse models have susceptibility to enterocolitis, but the mechanisms driving this susceptibility are still not well understood (8, 21, 39). Future studies should elucidate the etiology of enterocolitis susceptibility and the role the ENS may play in these inflammatory processes.

Collectively, this study demonstrates for the first time skewed enteric NC derivative proportions in the small intestine and altered GI motility in a HSCR mouse model. These findings demonstrate a role for *Sox10* in NC lineage specification *in vivo* in the ENS. Moreover, our results suggest a novel role for *Sox10* in neuronal subtype choice and indicate that perturbations in *Sox10* can affect GI transit in ganglionated regions of the intestine. Distinct regions of the *Sox10*$^{Dom/+}$ intestine were found to have different abnormalities and GI transit assays revealed sex and age dependent effects, suggesting that timing and environment play a key role in not only NC lineage segregation, but ultimately functional outcomes.

References

1. Musser, M.A., Correa, H., and Southard-Smith, E.M. 2014. Enteric neuron imbalance and motility defects in ganglionated intestine of the *Sox10*$^{Dom/+}$ Hirschsprung mouse model. *CMGH* 1.
2. Furness, J.B. 2006. *The enteric nervous system*. Malden, Mass.: Blackwell Pub. xiii, 274 p. pp.
3. Chakravarti, A., McCallion A.S., Lyonett, S. Hirschsprung disease. In *The Online Metaboloic and Molecular Bases of Inherited Disease*: McGraw-Hill Global Education Holdings, LLC.
4. Cantrell, V.A., Owens, S.E., Chandler, R.L., Airey, D.C., Bradley, K.M., Smith, J.R., and Southard-Smith, E.M. 2004. Interactions between Sox10 and EdnrB modulate penetrance and severity of aganglionosis in the Sox10Dom mouse model of Hirschsprung disease. *Hum Mol Genet* 13:2289-2301.
5. Owens, S.E., Broman, K.W., Wiltshire, T., Elmore, J.B., Bradley, K.M., Smith, J.R., and Southard-Smith, E.M. 2005. Genome-wide linkage identifies novel modifier loci of aganglionosis in the Sox10Dom model of Hirschsprung disease. *Hum Mol Genet* 14:1549-1558.
6. Alves, M.M., Sribudiani, Y., Brouwer, R.W., Amiel, J., Antinolo, G., Borrego, S., Ceccherini, I., Chakravarti, A., Fernandez, R.M., Garcia-Barcelo, M.M., et al. 2013. Contribution of rare and common variants determine complex diseases-Hirschsprung disease as a model. *Dev Biol* 382:320-329.
7. Jiang, Q., Ho, Y.Y., Hao, L., Nichols Berrios, C., and Chakravarti, A. 2011. Copy number variants in candidate genes are genetic modifiers of Hirschsprung disease. *PLoS One* 6:e21219.
8. Rintala, R.J., and Pakarinen, M.P. 2012. Long-term outcomes of Hirschsprung's disease. *Semin Pediatr Surg* 21:336-343.

9. Demehri, F.R., Halaweish, I.F., Coran, A.G., and Teitelbaum, D.H. 2013. Hirschsprung-associated enterocolitis: pathogenesis, treatment and prevention. *Pediatr Surg Int* 29:873-881.

10. Musser, M.A., and Michelle Southard-Smith, E. 2013. Balancing on the crest - Evidence for disruption of the enteric ganglia via inappropriate lineage segregation and consequences for gastrointestinal function. *Dev Biol* 382:356-364.

11. Paratore, C., Goerich, D.E., Suter, U., Wegner, M., and Sommer, L. 2001. Survival and glial fate acquisition of neural crest cells are regulated by an interplay between the transcription factor Sox10 and extrinsic combinatorial signaling. *Development* 128:3949-3961.

12. Paratore, C., Eichenberger, C., Suter, U., and Sommer, L. 2002. Sox10 haploinsufficiency affects maintenance of progenitor cells in a mouse model of Hirschsprung disease. *Hum Mol Genet* 11:3075-3085.

13. Walters, L.C., Cantrell, V.A., Weller, K.P., Mosher, J.T., and Southard-Smith, E.M. 2010. Genetic background impacts developmental potential of enteric neural crest-derived progenitors in the Sox10Dom model of Hirschsprung disease. *Hum Mol Genet* 19:4353-4372.

14. Postic, C., Shiota, M., Niswender, K.D., Jetton, T.L., Chen, Y., Moates, J.M., Shelton, K.D., Lindner, J., Cherrington, A.D., and Magnuson, M.A. 1999. Dual roles for glucokinase in glucose homeostasis as determined by liver and pancreatic beta cell-specific gene knock-outs using Cre recombinase. *J Biol Chem* 274:305-315.

15. Crabtree, J.S., Scacheri, P.C., Ward, J.M., McNally, S.R., Swain, G.P., Montagna, C., Hager, J.H., Hanahan, D., Edlund, H., Magnuson, M.A., et al. 2003. Of mice and MEN1: Insulinomas in a conditional mouse knockout. *Mol Cell Biol* 23:6075-6085.

16. Deal, K.K., Cantrell, V.A., Chandler, R.L., Saunders, T.L., Mortlock, D.P., and Southard-Smith, E.M. 2006. Distant regulatory elements in a Sox10-beta GEO BAC transgene are

required for expression of Sox10 in the enteric nervous system and other neural crest-derived tissues. *Dev Dyn* 235:1413-1432.

17. Liu, M.T., Kuan, Y.H., Wang, J., Hen, R., and Gershon, M.D. 2009. 5-HT4 receptor-mediated neuroprotection and neurogenesis in the enteric nervous system of adult mice. *J Neurosci* 29:9683-9699.

18. Miller, M.S., Galligan, J.J., and Burks, T.F. 1981. Accurate measurement of intestinal transit in the rat. *J Pharmacol Methods* 6:211-217.

19. Brun, P., Giron, M.C., Qesari, M., Porzionato, A., Caputi, V., Zoppellaro, C., Banzato, S., Grillo, A.R., Spagnol, L., De Caro, R., et al. 2013. Toll-like receptor 2 regulates intestinal inflammation by controlling integrity of the enteric nervous system. *Gastroenterology* 145:1323-1333.

20. D'Autreaux, F., Margolis, K.G., Roberts, J., Stevanovic, K., Mawe, G., Li, Z., Karamooz, N., Ahuja, A., Morikawa, Y., Cserjesi, P., et al. 2011. Expression level of Hand2 affects specification of enteric neurons and gastrointestinal function in mice. *Gastroenterology* 141:576-587, 587 e571-576.

21. Cheng, Z., Dhall, D., Zhao, L., Wang, H.L., Doherty, T.M., Bresee, C., and Frykman, P.K. 2010. Murine model of Hirschsprung-associated enterocolitis. I: phenotypic characterization with development of a histopathologic grading system. *J Pediatr Surg* 45:475-482.

22. Zaitoun, I., Erickson, C.S., Barlow, A.J., Klein, T.R., Heneghan, A.F., Pierre, J.F., Epstein, M.L., and Gosain, A. 2013. Altered neuronal density and neurotransmitter expression in the ganglionated region of Ednrb null mice: implications for Hirschsprung's disease. *Neurogastroenterol Motil* 25:e233-244.

23. Danielian, P.S., Echelard, Y., Vassileva, G., and McMahon, A.P. 1997. A 5.5-kb enhancer is both necessary and sufficient for regulation of Wnt-1 transcription in vivo. *Dev Biol* 192:300-309.

24. Lewis, A.E., Vasudevan, H.N., O'Neill, A.K., Soriano, P., and Bush, J.O. 2013. The widely used Wnt1-Cre transgene causes developmental phenotypes by ectopic activation of Wnt signaling. *Dev Biol* 379:229-234.

25. Laranjeira, C., Sandgren, K., Kessaris, N., Richardson, W., Potocnik, A., Vanden Berghe, P., and Pachnis, V. 2011. Glial cells in the mouse enteric nervous system can undergo neurogenesis in response to injury. *J Clin Invest* 121:3412-3424.

26. Hari, L., Miescher, I., Shakhova, O., Suter, U., Chin, L., Taketo, M., Richardson, W.D., Kessaris, N., and Sommer, L. 2012. Temporal control of neural crest lineage generation by Wnt/beta-catenin signaling. *Development* 139:2107-2117.

27. Corpening, J.C., Cantrell, V.A., Deal, K.K., and Southard-Smith, E.M. 2008. A Histone2BCerulean BAC transgene identifies differential expression of Phox2b in migrating enteric neural crest derivatives and enteric glia. *Dev Dyn* 237:1119-1132.

28. Kamachi, Y., and Kondoh, H. 2013. Sox proteins: regulators of cell fate specification and differentiation. *Development* 140:4129-4144.

29. Southard-Smith, E.M., Angrist, M., Ellison, J.S., Agarwala, R., Baxevanis, A.D., Chakravarti, A., and Pavan, W.J. 1999. The Sox10(Dom) mouse: modeling the genetic variation of Waardenburg-Shah (WS4) syndrome. *Genome Res* 9:215-225.

30. Kim, J., Lo, L., Dormand, E., and Anderson, D.J. 2003. SOX10 maintains multipotency and inhibits neuronal differentiation of neural crest stem cells. *Neuron* 38:17-31.

31. Bondurand, N., and Sham, M.H. 2013. The role of SOX10 during enteric nervous system development. *Dev Biol* 382:330-343.

32. Sharkey, K.A., and Savidge, T.C. 2014. Role of enteric neurotransmission in host defense and protection of the gastrointestinal tract. *Auton Neurosci* 181C:94-106.

33. Mundell, N.A., Plank, J.L., LeGrone, A.W., Frist, A.Y., Zhu, L., Shin, M.K., Southard-Smith, E.M., and Labosky, P.A. 2012. Enteric nervous system specific deletion of Foxd3

disrupts glial cell differentiation and activates compensatory enteric progenitors. *Dev Biol* 363:373-387.

34. Kruger, G.M., Mosher, J.T., Bixby, S., Joseph, N., Iwashita, T., and Morrison, S.J. 2002. Neural crest stem cells persist in the adult gut but undergo changes in self-renewal, neuronal subtype potential, and factor responsiveness. *Neuron* 35:657-669.

35. Bixby, S., Kruger, G.M., Mosher, J.T., Joseph, N.M., and Morrison, S.J. 2002. Cell-intrinsic differences between stem cells from different regions of the peripheral nervous system regulate the generation of neural diversity. *Neuron* 35:643-656.

36. Qu, Z.D., Thacker, M., Castelucci, P., Bagyanszki, M., Epstein, M.L., and Furness, J.B. 2008. Immunohistochemical analysis of neuron types in the mouse small intestine. *Cell Tissue Res* 334:147-161.

37. Legato, M.J., and Bilezikian, J.P. 2004. *Principles of gender-specific medicine*. Amsterdam ; Boston: Elsevier Academic Press.

38. Gillies, G.E., and McArthur, S. 2010. Estrogen actions in the brain and the basis for differential action in men and women: a case for sex-specific medicines. *Pharmacol Rev* 62:155-198.

39. Zhao, L., Dhall, D., Cheng, Z., Wang, H.L., Doherty, T.M., Bresee, C., and Frykman, P.K. 2010. Murine model of Hirschsprung-associated enterocolitis II: Surgical correction of aganglionosis does not eliminate enterocolitis. *J Pediatr Surg* 45:206-211; discussion 211-202.

40. Furness, J.B. 2006. *The Enteric Nervous System*. Malden, Massachusetts: Blackwell Publishing Inc.

41. McMahon, A.P., and Bradley, A. 1990. The Wnt-1 (int-1) proto-oncogene is required for development of a large region of the mouse brain. *Cell* 62:1073-1085.

42. Amiel, J., Sproat-Emison, E., Garcia-Barcelo, M., Lantieri, F., Burzynski, G., Borrego, S., Pelet, A., Arnold, S., Miao, X., Griseri, P., et al. 2008. Hirschsprung disease, associated syndromes and genetics: a review. *J Med Genet* 45:1-14.

43. Southard-Smith, E.M., Kos, L., and Pavan, W.J. 1998. Sox10 mutation disrupts neural crest development in Dom Hirschsprung mouse model. *Nat Genet* 18:60-64.

44. Kapur, R.P. 1999. Early death of neural crest cells is responsible for total enteric aganglionosis in Sox10(Dom)/Sox10(Dom) mouse embryos. *Pediatr Dev Pathol* 2:559-569.

45. Sonnenberg-Riethmacher, E., Miehe, M., Stolt, C.C., Goerich, D.E., Wegner, M., and Riethmacher, D. 2001. Development and degeneration of dorsal root ganglia in the absence of the HMG-domain transcription factor Sox10. *Mech Dev* 109:253-265.

46. Gianino, S., Grider, J.R., Cresswell, J., Enomoto, H., and Heuckeroth, R.O. 2003. GDNF availability determines enteric neuron number by controlling precursor proliferation. *Development* 130:2187-2198.

47. Uesaka, T., Jain, S., Yonemura, S., Uchiyama, Y., Milbrandt, J., and Enomoto, H. 2007. Conditional ablation of GFRalpha1 in postmigratory enteric neurons triggers unconventional neuronal death in the colon and causes a Hirschsprung's disease phenotype. *Development* 134:2171-2181.

48. Imayoshi, I., Isomura, A., Harima, Y., Kawaguchi, K., Kori, H., Miyachi, H., Fujiwara, T., Ishidate, F., and Kageyama, R. 2013. Oscillatory control of factors determining multipotency and fate in mouse neural progenitors. *Science* 342:1203-1208.

49. Pham, T.D., Gershon, M.D., and Rothman, T.P. 1991. Time of origin of neurons in the murine enteric nervous system: sequence in relation to phenotype. *J Comp Neurol* 314:789-798.

50. Li, Z., Chalazonitis, A., Huang, Y.Y., Mann, J.J., Margolis, K.G., Yang, Q.M., Kim, D.O., Cote, F., Mallet, J., and Gershon, M.D. 2011. Essential roles of enteric neuronal

serotonin in gastrointestinal motility and the development/survival of enteric dopaminergic neurons. *J Neurosci* 31:8998-9009.

51. Coelho-Aguiar, J.M., Le Douarin, N.M., and Dupin, E. 2013. Environmental factors unveil dormant developmental capacities in multipotent progenitors of the trunk neural crest. *Dev Biol* 384:13-25.

52. Teng, L., Mundell, N.A., Frist, A.Y., Wang, Q., and Labosky, P.A. 2008. Requirement for Foxd3 in the maintenance of neural crest progenitors. *Development* 135:1615-1624.

53. Sandgren, K., Larsson, L.T., and Ekblad, E. 2002. Widespread changes in neurotransmitter expression and number of enteric neurons and interstitial cells of Cajal in lethal spotted mice: an explanation for persisting dysmotility after operation for Hirschsprung's disease? *Dig Dis Sci* 47:1049-1064.

54. Roberts, R.R., Bornstein, J.C., Bergner, A.J., and Young, H.M. 2008. Disturbances of colonic motility in mouse models of Hirschsprung's disease. *Am J Physiol Gastrointest Liver Physiol* 294:G996-G1008.

55. Ro, S., Hwang, S.J., Muto, M., Jewett, W.K., and Spencer, N.J. 2006. Anatomic modifications in the enteric nervous system of piebald mice and physiological consequences to colonic motor activity. *Am J Physiol Gastrointest Liver Physiol* 290:G710-718.

56. Khen-Dunlop, N., Sarnacki, S., Victor, A., Grosos, C., Menard, S., Soret, R., Goudin, N., Pousset, M., Sauvat, F., Revillon, Y., et al. 2013. Prenatal intestinal obstruction affects the myenteric plexus and causes functional bowel impairment in fetal rat experimental model of intestinal atresia. *PLoS One* 8:e62292.

CHAPTER III

GASTROINTESTINAL TRANSIT IN *EDNRB*$^{TM1YWA/+}$ AND *RET*$^{TM1COS/+}$ ADULT MICE

Introduction

Hirschsprung disease (HSCR) is a complex disease with several factors influencing disease penetrance and phenotype expressivity (1, 2). HSCR can segregate through multiple generations in families, but most of the cases appear spontaneously (2). To date, the occurrence of HSCR has been attributed to mutations in eleven different genes (1) (Table 3.1). However, several genetic modifiers exist and presence or absence of a known, characterized mutation does not always guarantee HSCR disease manifestation.

Table 3.1. Genes with putative HSCR causing mutations.

Gene	Long Name	Molecular Function
RET	**Re**arranged during **t**ransfection	receptor tyrosine kinase
GDNF	**G**lial cell line-**d**erived **n**eurotrophic **f**actor	RET ligand
NRTN	**N**eur**t**uri**n**	RET ligand
SOX10	**S**RY-related HMG-b**ox 10**	transcription factor
PHOX2B	**P**aired-like **h**omeob**ox 2b**	transcription factor
TCF4	**T**rans**c**ription **f**actor **4**	transcription factor
KIAA1279	**K**inesin family member 1 binding protein	mitochondria transport (putative)
EDNRB	**E**nd**o**thelin **r**eceptor type **B**	G-protein coupled receptor
ECE1	**E**ndothelin **c**onverting **e**nzyme **1**	Proteolytic processing of EDN1-3
EDN3	**E**nd**o**thelin-**3**	EDNRB ligand
ZFHX1B (ZEB2)	**Z**inc **f**inger E-box-binding **h**omeobo**x 2**	transcription factor

RET is arguably one of the most well studied HSCR genes. The *RET* (*RE*arranged during *T*ransfection) proto-oncogene encodes a receptor tyrosine kinase found on the surface of NCC and other cell types (3-6). The first mapping studies within a HSCR family identified an area of Chromosome 10 as a susceptibility locus (7, 8) and later studies identified a mutation in *RET* in this region that accounted for HSCR disease (9, 10). Subsequent studies have gone on to identify over 100 mutations in the *RET* gene in HSCR cases and a well described SNP in an enhancer region of *RET* appears to increase risk of HSCR in at least some ethnicities (reviewed in (1))(11). Not surprisingly, in HSCR cases where patients are genetically screened and mutations are identifed, *RET* mutations account for roughly 50% of familial cases and 15-20% of sporadic cases (1, 11). *Ret* has also been studied extensively in HSCR mouse models. Several HSCR mouse models with targeted *Ret* mutations exist (3, 12, 13) and studies in these mice have aided in understanding the role of the Ret signaling pathway in ENS development and other organ systems.

Another well studied HSCR gene is *EDNRB*. The *EDNRB gene* encodes a G-coupled protein receptor and a mutation in *EDNRB* was linked to HSCR in an Old Order Mennonite community (14). The discovery of *EDNRB* as a HSCR gene was aided by the spontaneously occurring *piebald-lethal* mouse line where mice homozygous for the *piebald-lethal* locus succumbed early in life to megacolon due to aganglionosis. Mapping studies in this mouse model identified a syntenic region identical to the locus mapped in the Old Order Mennonite community, helping researchers hone in on *EDNRB* as a candidate HSCR gene (15). Subsequent studies in mouse models with *Ednrb* deficiency have further solidified this gene as a large player in HSCR occurrence and HSCR associated sequelae (15-21).

Despite enormous efforts to understand HSCR through HSCR cases and mouse models, much remains to be determined in regard to gene function and disease occurrence. In humans, it appears RET haploinsufficiency drives the HSCR phenotype. But not all patients with a *RET* mutation will go on to have HSCR. Furthermore, supposed activating mutations in *RET* can lead

to MEN2A (Multiple Endocrine Neoplasia Type 2A) and HSCR in the same patients (22-24). *EDNRB* mutations also show incomplete penetrance and many patients with EDNRB mutations also show deficits in pigmentation and sensorineural deafness (1, 2). This triad of HSCR disease, lack of pigmentation, and sensorineural deafness is better known as Waardenburg-Shah Syndrome Type 4 (WS4).

Additionally, recent genetic studies have focused on defining what genetic modifiers and environmental influences may ultimately lead to HSCR occurrence and affect severity of the disease (18, 25-32). For the most part, these studies operate within a strict definition of HSCR disease. Patients either have HSCR disease or no disease—aganglionosis occurs with variable lengths of the intestine affected or the ENS is assumed totally unaffected. However, such thinking does not lend itself to the complex nature of HSCR and the multiple genes involved. Subtle disease or phenotypes could exist in the ENS of patients with deficiencies in HSCR genes, but with no aganglionosis. To add credence to this possibility, one case study exists where a patient with MEN2B and chronic constipation had no aganglionosis, but harbored a *RET* mutation and deficiencies of Substance P within ENS neuronal axons (33). Furthermore, constipation has been shown to cluster within families (34, 35), suggesting a heritable factor. However, the etiology of familial constipation has yet to be determined.

Given the complex nature of HSCR disease and HSCR gene pathways as well as the occurrence of heritable constipation with unknown etiology, I hypothesized that ENS driven motility deficits could exist in the presence of altered HSCR gene expression where no detectable aganglionosis was present. To test this hypothesis, I tested GI transit in $Ret^{tm1Cos/+}$ and $Ednrb^{tm1Ywa/+}$ mice. Both of these mouse models have a deficiency in a HSCR gene, but do not exhibit aganglionosis. I found that neither male nor female $Ednrb^{tm1Ywa/+}$ and $Ret^{tm1Cos/+}$ adults had any gastric emptying or small intestine motility deficits by my test methods. However, $Ret^{tm1Cos/+}$ males had significantly slower total intestinal transit time, suggesting slow transit constipation in these mice.

Methods

Methods for GI motility tests are presented here in brief. However, in depth methods in regard to these experiments can be found in Chapter 7.

Animals

Ednrb$^{tm1Ywa/+}$ and *Ret*$^{tm1Cos/+}$ mice were propagated on a 129S6/SvEvTac background. *Ednrb*$^{tm1Ywa/+}$ were generated by Hosoda et al (15) by substituting exon 3 of the *EdnrbB* gene with a Neo cassette, effectively ablating gene function. *Ret*$^{tm1Cos/+}$ were generated by Schuchardt and colleagues (3). A 0.8 kb portion of the *Ret* gene was replaced by a Neo cassette; the deleted portion of the gene includes sequence for a lysine residue required for Ret kinase activity. I genotyped both mouse models by assessing for the presence or absence of the Neo cassette via PCR. Primers to detect part of the Neo cassette (366 bp) are as follows: Forward = CCTGCCGAGAAAGTATCCATC; Reverse = TTCAGCAATATCACGGGTAGC. PCR to detect the *Rapsn* gene (592 bp) was also included in genotyping as a positive control: Forward = AGGACTGGGTGGCTTCCAACTCCCAGACAC and Reverse = AGCTTCTCATTGGTGCGCGCCAGGTTCAGG . Thermocycler conditions were as follows: 94°C for 5 min, [(94°C for 30 seconds, 55°C or 58°C for 30 sec, ramp to 72°C at 0.5°C per second, 72°C for 30 seconds, ramp to 94°C at 0.5°C per second) x 25-35 times], 72°C for 10 minutes, 4°C indefinitely. The Institutional Animal Care and Use Committee at Vanderbilt University approved all experimental protocols.

Small intestine transit

This method was described previously in Chapter 2. A more detailed explanation of this test can be found within Chapter 7.

Total intestinal transit

Briefly, Adult mice were gavaged with a meal of 6% carmine in a 0.5% methylcellulose/0.09% NaCl solution. Start time of transit was recorded as time of gavage. Mice were given free access to water and food during the course of the experiment. Mice were monitored for presence of carmine (bright red) in fecal pellets. Once a red fecal pellet was noted, a stop time was recorded. The difference between start and stop time was recorded as the "total transit time" for each mouse. Detailed methods in regard to this assay can be found in Chapter 7.

Statistics

I tested for differences in gastric emptying rates, small intestine transit rates, and total intestine transit times using a Student's t-test assuming unequal variance (Welch's t-test). JMP (v10 or v11) software was used for statistical testing.

Results

To determine if alterations in HSCR genes could cause alterations in GI motility, but not overt aganglionosis, I evaluated gastric emptying, small intestine transit rates, and total intestinal transit times in *Ednrb*$^{tm1Ywa/+}$ and *Ret*$^{tm1Cos/+}$ adult mice. Because the aganglionosis that defines HSCR disease shows a sex specific prevalence (4:1 males to female), I tested both males and females to determine if any GI motility alterations caused by HSCR gene alterations showed similar sex ratios.

Gastrointestinal transit times are comparable in Ednrb$^{tm1Ywa/+}$ and Ednrb$^{+/+}$ mice.

I first evaluated gastric emptying and small intestine motility rates in adult *Ednrb*$^{tm1Ywa/+}$ and *Ednrb*$^{+/+}$ adult male littermates. Male *Ednrb*$^{tm1Ywa/+}$ mice had comparable gastric emptying

rates (*P=0.41*) and small intestine motility rates (*P=0.44*) to *Ednrb*$^{+/+}$ littermates (Table 3.2). (Variance in small intestine motility scores tended to be large for both genotypes, hence the larger sample number tested for this group compared to females.) In regard to total intestinal transit times, which additionally accounts for colonic transit, I observed nearly equivalent mean lengths of time in *Ednrb*$^{tm1Ywa/+}$ and *Ednrb*$^{+/+}$ male mice (*P=0.92*) (Figure 3.1A; Table 3.2).

Table 3.2. Comparison of gastric emptying, small intestine transit, and total intestine transit between male *Ednrb*$^{tm1Ywa/+}$ and *Ednrb*$^{+/+}$ mice.

Test	Genotype	n	$Mean	St Dev	p-value
Gastric emptying	*Ednrb*$^{tmYwa1/+}$	8	52.15	27.19	0.41
	Ednrb$^{+/+}$	9	62.16	20.26	
Small intestine motility score	*Ednrb*$^{tmYwa1/+}$	8	2.96	0.81	0.44
	Ednrb$^{+/+}$	9	3.33	1.08	
Total gut transit	*Ednrb*$^{tmYwa1/+}$	9	245.56	131.18	0.92
	Ednrb$^{+/+}$	7	251.43	97.05	

$Mean units: motility score = geometric mean; gastric emptying = %; total gut transit = minutes

Next, I evaluated gastric emptying and small intestine motility rates in adult *Ednrb*$^{tm1Ywa/+}$ and *Ednrb*$^{+/+}$ females. Similar to my evaluation in males, I observed no significant difference between gastric emptying rates (*P=0.76*) and small intestine motility scores (*P=0.38*) between *Ednrb*$^{tm1Ywa/+}$ and *Ednrb*$^{+/+}$ females (Table 3.3). Total intestinal transit time was also comparable (*P=0.67*) (Figure 3.1B). Interestingly, I did note three *Ednrb*$^{tm1Ywa/+}$ mice (n=2 female; n=1 male) that had total gut transit times over 400 minutes which is well above all other recorded *Ednrb*$^{tm1Ywa/+}$ and *Ednrb*$^{+/+}$ mice (Figure 3.1A & B). These mice represented roughly 18% (3 of 17) of all *Ednrb*$^{tm1Ywa/+}$ mice tested.

Table 3.3. Comparison of gastric emptying, small intestine transit, and total intestine transit between female *Ednrb*$^{tm1Ywa/+}$ and *Ednrb*$^{+/+}$ mice.

Test	Genotype	n	$Mean	St Dev	p-value
Gastric emptying	*Ednrb*$^{tmYwa1/+}$	6	61.42	19.56	>0.75
	Ednrb$^{+/+}$	6	57.87	20.14	
Small intestine motility score	*Ednrb*$^{tmYwa1/+}$	6	2.23	0.36	>0.38
	Ednrb$^{+/+}$	6	2.41	0.33	
Total gut transit	*Ednrb*$^{tmYwa1/+}$	8	267.13	116.15	>0.66
	Ednrb$^{+/+}$	6	245.33	69.12	

$Mean units: motility score = geometric mean; gastric emptying = %; total gut transit = minutes

Total intestinal transit time is slower in Ret$^{tm1Cos/+}$ males but not Ret$^{tm1Cos/+}$ females.

Next, I evaluated gastric emptying and small intestine motility rates in *Ret*$^{tm1Cos/+}$ and *Ret*$^{+/+}$ adult mice. I observed *Ret*$^{tm1Cos/+}$ males had extremely similar gastric emptying rates (*P=0.94*) and small intestine motility rates (*P=0.98*) when compared to their *Ret*$^{+/+}$ littermates (Table 3.4). Interestingly, comparisons of total intestinal transit times revealed a large increase in total intestinal transit times in *Ret*$^{tm1Cos/+}$ males (*P=0.0062*) (Figure 3.2A; Table 3.4).

Similar to males, I observed comparable gastric emptying rates (*P=0.40*) and small intestine motility rates (*P=0.67*) between female *Ret*$^{tm1Cos/+}$ and *Ret*$^{+/+}$ adult mice (Table 3.5). In stark contrast to findings in males, total intestinal transit time between the two female genotypes did not differ significantly (*P=0.57*) (Figure 3.2B; Table 3.5).

Discussion

I tested gastric emptying, small intestine transit, and total intestinal transit in male and female *Ednrb*$^{tm1Ywa/+}$ and *Ret*$^{tm1Cos/+}$ mice. Both of these mouse models have targeted genetic ablation of one copy of a known HSCR gene. However, they have no overt aganglionosis, making them ideal for studying how alterations in *Ednrb* or *Ret* may affect ENS development and function outside of gross neural crest migration and proliferation defects. Interestingly, I found no statistical

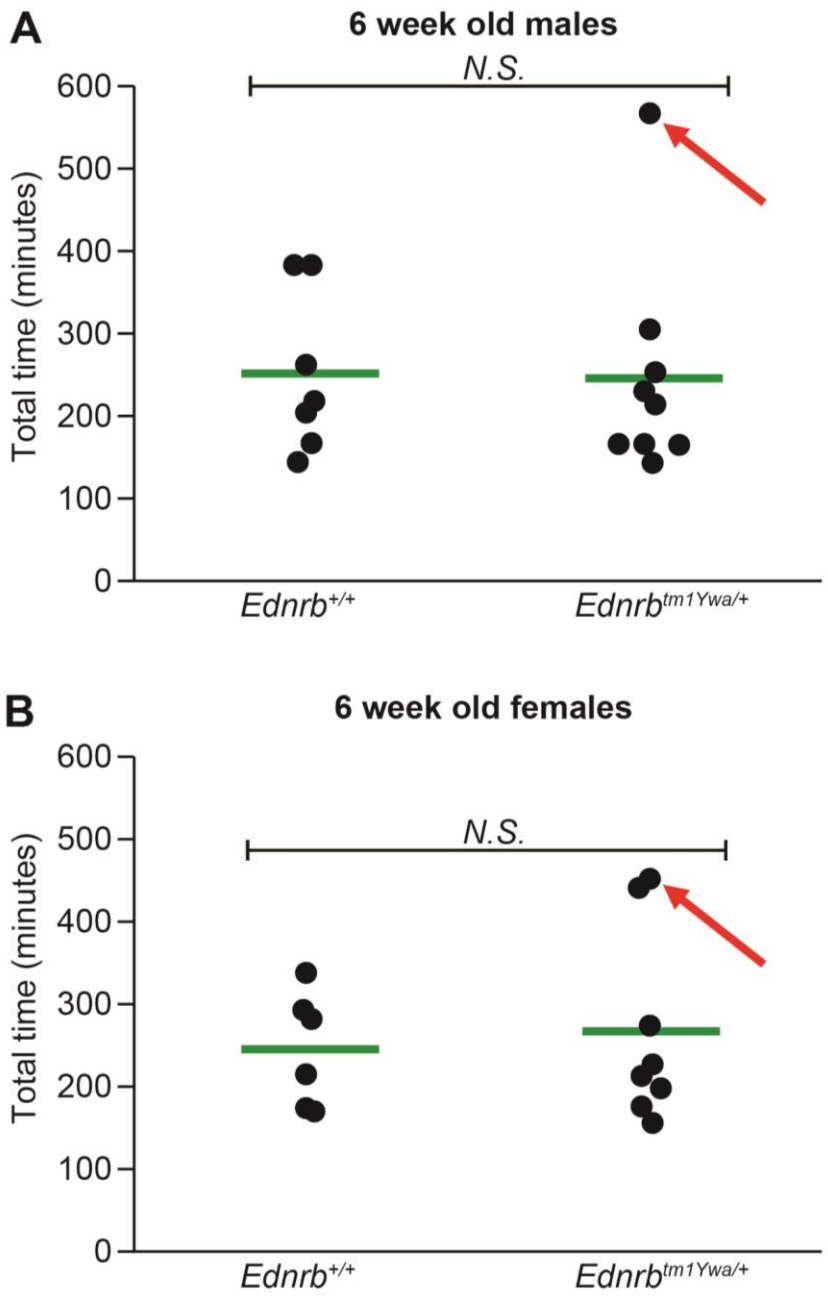

Figure 3.1 Comparsion of total gut transit time between *Ednrb*$^{+/+}$ and *Ednrb*$^{tm1Ywa/+}$ adult mice. (**A**) Total transit time was comparable between *Ednrb*$^{+/+}$ (n=7) and *Ednrb*$^{tmYwa1/+}$ (n=9) males (*P=0.92*). (**B**) Females also demonstrated comparable total transit times between *Ednrb*$^{+/+}$ (n=6) and *Ednrb*$^{tmYwa1/+}$ (n=8) genotypes (*P>0.66*). The green line marks the mean total gut transit time for each group. Interestingly, we observed outliers within *Ednrb*$^{tmYwa1/+}$ mice in both sexes, possibly suggesting an incomplete penetrance and/or genetic modifier affects in the presence of the *Ednrb-tmYwa* (arrows).

Table 3.4. Comparison of gastric emptying, small intestine transit, and total gut transit between male *Ret*$^{tm1Cos/+}$ and *Ret*$^{+/+}$ mice.

Test	Genotype	n	$Mean	St Dev	p-value
Gastric emptying	*Ret*$^{tm1Cos/+}$	6	68.72	15.63	0.94
	Ret$^{+/+}$	6	67.91	18.62	
Small intestine motility score	*Ret*$^{tm1Cos/+}$	6	2.77	0.34	0.98
	Ret$^{+/+}$	6	2.78	0.51	
Total gut transit	*Ret*$^{tm1Cos/+}$	10	420.70	104.55	*<0.007
	Ret$^{+/+}$	8	264.88	102.71	

$Mean units: motility score = geometric mean; gastric emptying = %; total gut transit = minutes

Table 3.5. Comparison of gastric emptying, small intestine transit, and total gut transit between female *Ret*$^{tm1Cos/+}$ and *Ret*$^{+/+}$ mice.

Test	Genotype	n	$Mean	St Dev	p-value
Gastric emptying	*Ret*$^{tm1Cos/+}$	7	67.37	19.21	>0.56
	Ret$^{+/+}$	5	71.96	4.78	
Small intestine motility score	*Ret*$^{tm1Cos/+}$	7	2.42	0.31	>0.73
	Ret$^{+/+}$	5	2.33	0.49	
Total gut transit	*Ret*$^{tm1Cos/+}$	6	277.50	89.18	>0.56
	Ret$^{+/+}$	6	316.50	134.53	

$Mean units: motility score = geometric mean; gastric emptying = %; total gut transit = minutes

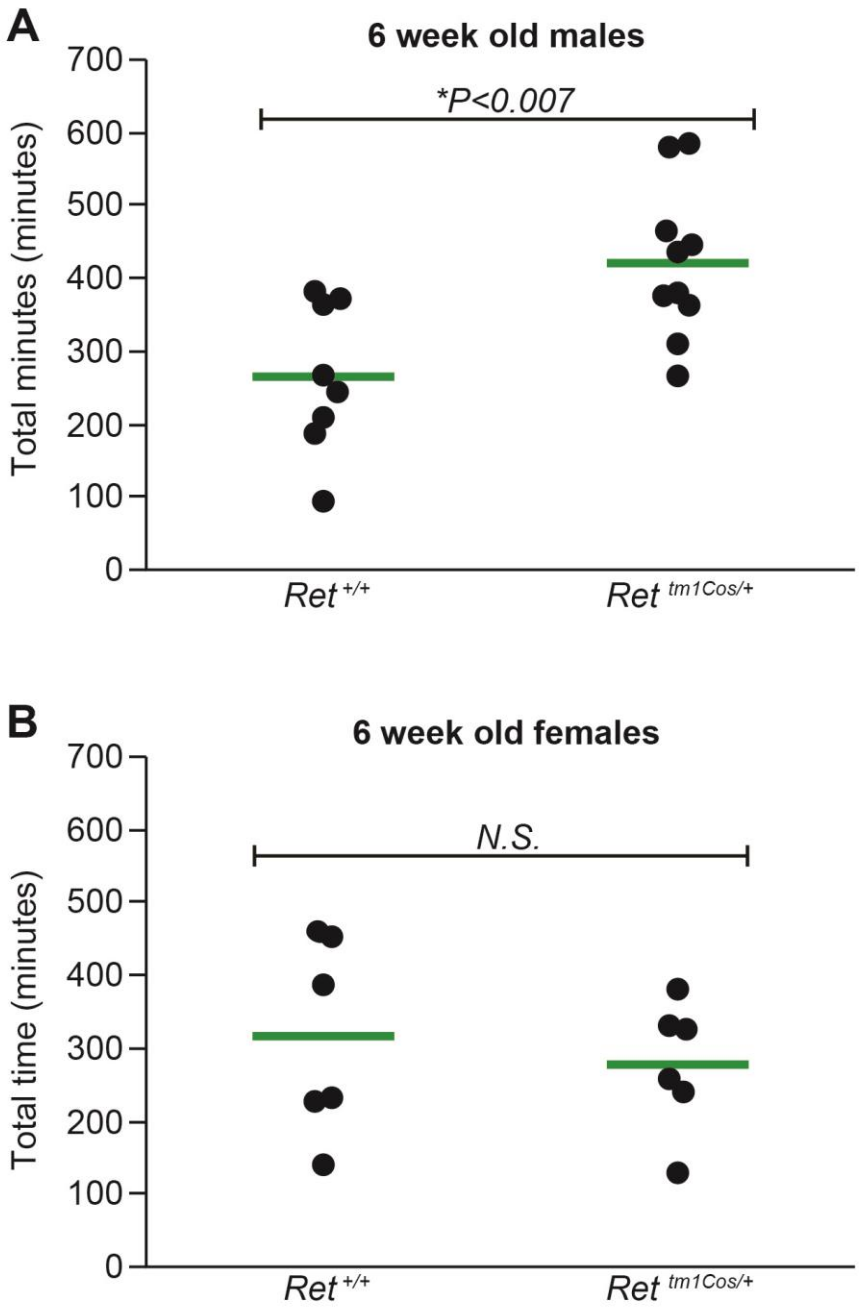

Figure 3.2. Comparsion of total gut transit time between *Ret*$^{+/+}$ and *Ret*$^{tm1Cos/+}$ adult mice. (**A**) Male *Ret*$^{tm1Cos/+}$ mice (n=10) had significantly higher total intestinal transit time when compared to *Ret*$^{+/+}$ littermates (n=8) (*P<0.007*). (**B**) *Ret*$^{+/+}$ females (n=6) and *Ret*$^{tm1Cos/+}$ females (n=6) demonstrated comparable total intestinal transit times (*P>0.56*). Green lines mark mean total gut transit for each group.

differences in GI motility parameters in male or female *Ednrb*$^{tm1Ywa/+}$ compared to wild type littermates although increased total intestinal transit was observed in a few *Ednrb*$^{tm1Ywa/+}$ mice. GI motility in *Ret*$^{tm1Cos/+}$ mice also appeared largely unaffected, except for significant increases in total intestinal transit times in *Ret*$^{tm1Cos/+}$ males, implicating a sex specific GI transit defect.

I was somewhat surprised that I observed no significant differences between *Ednrb*$^{tm1Ywa/+}$ and *Ednrb*$^{+/+}$ adult littermates in any of the physiological factors measured (gastric emptying rates, small intestine motility rates, total intestinal transit times). It could be that no differences exist in GI function between *Ednrb*$^{tm1Ywa/+}$ and *Ednrb*$^{+/+}$ of either sex. The *Ednrb*^{tm1Ywa} gene contains a Neo cassette insertion, replacing exon 3 (15). This deletion of exon 3 presumably results in haploinsufficiency of the *Ednrb* gene. It might be that increased transcription, translation, reduced breakdown, or other cellular mechanisms involving the wild type *Ednrb* gene are able to compensate for lack of *Edrnb* expression from the *Ednrb-tm1Ywa* locus. Alternatively, expression from one *Ednrb* gene locus might also be sufficient for normal development and function of the enteric nervous system. Genetic studies in humans support this hypothesis. In humans, *EDNRB* mutations are estimated to be the primary causative gene in only 6-8% of HSCR cases (2). And for most human HSCR cases that involve *EDNRB*, the disease appears only in an autosomal recessive fashion, with two mutations in the *EDNRB* needed for HSCR manifestation (1, 2). Furthermore, even in the earliest gene mapping study that led to *EDNRB* being discovered as a HSCR gene, not all family members with both copies of the mutated form of *EDNRB* had HSCR, demonstrating incomplete penetrance of the disease (14). Thus, it appears that ENS development is not as sensitive to perturbations in *EDNRB* expression and more sensitive to perturbations in other genes, such as *SOX10* and *RET*. This explanation seems plausible given our knowledge of *SOX10* and *RET*. *SOX10* is temporally upstream of *EDNRB* and, as a transcription factor, would putatively disturb more downstream targets than a mutation in *EDNRB*. And, autosomal dominant mutations in *SOX10* or *RET* mutations can cause HSCR disease (1, 2). Additionally,

although not tested, it is possible that expression of other related genes, such as *EDNRA*, could have compensatory affects when *EDNRB* expression is reduced.

Another competing hypothesis is that physiological differences in gastric motility measures exist between *Ednrb*$^{tm1Ywa/+}$ and *Ednrb*$^{+/+}$ but are more subtle and not detectable by my test methods, and/or would only be detectable under certain conditions. It is important to note that I did not incorporate additional challenges or stressors within my experimental design. Had I challenged the *Ednrb*$^{tm1Ywa/+}$ and *Ednrb*$^{+/+}$ mice, such as with a high fat diet, differences in gastric motility measures may have been observed. In humans, many GI deficits do not manifest until specific infectious or environmental challenges present. For example, gastroparesis (slowing of gastric emptying) tends to occur with a female prevalence in the context of poorly controlled diabetes (36). Future studies with such stressors or with different test methods will have to be conducted to determine if more subtle changes in GI motility exist in *Ednrb*$^{tm1Ywa/+}$ mice.

Although I saw no statistical difference in intestinal transit between *Ednrb*$^{tm1Ywa/+}$ and *Ednrb*$^{+/+}$ mice, three *Ednrb*$^{tm1Ywa/+}$ mutants did have substantially higher total intestinal transit time than the other mutant and wildtype animals (Figure 3.1A & B). These animals could represent outliers due to variations in testing conditions, but this scenario is unlikely as we did not see any wildtype outliers within *Ednrb*$^{+/+}$ tested animals nor in *Ret*$^{+/+}$ which are on the same strain background. Additionally, these three *Ednrb*$^{tm1Ywa/+}$ mice were tested on different days, further suggesting against daily variations in test conditions. As mentioned previously, HSCR disease is an oligogenic disorder—one or more mutations can cause predisposition or occurrence of the disease and other genetic variants push the predisposition to disease manifestation and/or modify the severity of the disease. Although *Ednrb*$^{tm1Ywa/+}$ mice do not suffer from aganglionosis, the increase in total intestinal transit time for the three *Ednrb*$^{tm1Ywa/+}$, but not other *Ednrb*$^{tm1Ywa/+}$ mice, could be viewed as incomplete penetrance of slow transit constipation. This hypothesis is supported by studies in *Ednrb*$^{+/+}$and *Ednrb*$^{tm1Ywa/tm1Ywa}$ mice where Hirschsprung associated-enterocolitis phenotypes appear incompletely penetrant (19, 20). In brief, Zhao and colleagues

(19) performed corrective colonic resection surgery on *Ednrb*$^{+/+}$ (control) and *Ednrb*$^{tm1Ywa/tm1Ywa}$ (short-segment aganglionosis) adult mice. Following post-surgical recovery, mice were sacrificed and small intestine and colon samples were collected and scored histologically for severity and depth of inflammation. Not surprisingly, *Ednrb*$^{tm1Ywa/tm1Ywa}$ mice were more susceptible to enterocolitis post-surgery than *Ednrb*$^{+/+}$ wild type littermates. However, this phenotype showed variable expressivity and incomplete penetrance with ~40% of *Ednrb*$^{tm1Ywa/tm1Ywa}$ suffering from enterocolitis. Even in a study where *Ednrb*$^{tm1Ywa/tm1Ywa}$ mice did not have corrective surgery (and thus were purportedly more susceptible to severe infection due to presence of aganglionosis), only 65% succumbed to gut-derived bacteremia (20). Importantly, in my study, I tested *Ednrb*$^{tm1Ywa/+}$ mice, not *Ednrb*$^{tm1Ywa/tm1Ywa}$, as the goal was to determine if these mice may have GI deficits within the context of a fully ganglionated GI tract. Roughly 18% of *Ednrb*$^{tm1Ywa/+}$ mice tested in my total intestine gut transit study had severely slowed total intestinal transit. Thus, the hypothesis that incomplete penetrance and genetic modifiers influencing total intestinal transit time in *Ednrb*$^{tm1Ywa/+}$ mice is compatible with my results and with previous studies.

Similar to my findings in *Ednrb*$^{tm1Ywa/+}$ mutants, *Ret*$^{tm1Cos/+}$ male and female mice did not differ from their wild type *Ret*$^{+/+}$ littermates in regard to gastric emptying and small intestine transit scores. However, *Ret*$^{tm1Cos/+}$ males showed significantly slower total intestinal transit time and this phenotype was not detected in *Ret*$^{tm1Cos/+}$ females. This finding is not surprising given the one in four occurrence of HSCR disease in males (1, 2), the tendency for males to be affected more often by neurodevelopmental disorders in general (37, 38), and sex differences in motility detected in *Sox10*$^{Dom/+}$ mutants (see Chapter 2). However, in adult male *Sox10*$^{Dom/+}$ mutants, I observed increased gastric emptying, a phenotype not observed in *Ret*$^{tm1Cos/+}$ males. Echoed from previous discussion above, deficits in gastric emptying or small intestine motility in these mice might not manifest unless mice are stressed or challenged. Additionally, the gut has many modes of communication and feedback mechanisms, with activity or obstruction in the distal bowel affecting activity and motility in proximal regions (39). This could explain the differences I observe

in *Ret* and *Sox10* mutants as the colons of these mice are fully ganglionic or aganglionic (obstructive) respectively.

The long total intestinal transit times in *Ret*$^{tm1Cos/+}$ males appears to be mediated primarily by slowed colonic motility since gastric emptying rates and small intestine motility rates are comparable between *Ret*$^{tm1Cos/+}$ and *Ret*$^{+/+}$ male mice. This hypothesis is corroborated by the consistency of *Ret*$^{tm1Cos/+}$ feces I saw during my studies. In general, *Ret*$^{tm1Cos/+}$ male feces appeared dryer—or had less water content—upon collection compared to *Ret*$^{+/+}$ male mice. Since the colon is largely responsible for water reabsorption, longer transit times of feces in the colon could lead to dryer feces (i.e. constipation). Previous studies have successfully measured water content of feces in mice (40), and future studies could be directed at measuring water content in *Ret*$^{tm1Cos/+}$ feces to validate if slow transit constipation is occurring in.

Although I saw no statistical differences in *Ednrb*$^{tm1Ywa/+}$ motility measures, increased total intestine transit time in a few *Ednrb*$^{tm1Ywa/+}$ mutants as well as significantly increased total transit in *Ret*$^{tm1Cos/+}$ male mice suggests that perturbations in *Ret* and *Ednrb* expression can affect ENS development and function even when aganglionosis is not present. These findings could explain clustering of constipation in families where HSCR is not present. Interestingly, at least in respect to alterations in *Ret*, only male mice showed signs of slow transit constipation. This finding mirrors sex-specific findings in *Sox10*$^{Dom/+}$ mice *(*Chapter 2) and is expected in light of the higher prevalence of HSCR disease in males. Neurodevelopmental disorders are known to show sex discrepancies, but the sex-specific factors driving differences in HSCR disease prevalence and phenotypes in HSCR mouse models have not been studied. Future studies to define these factors will not only aid in understanding HSCR outcomes, but also understanding other neurodevelopmental disorders.

References

1. Amiel, J., Sproat-Emison, E., Garcia-Barcelo, M., Lantieri, F., Burzynski, G., Borrego, S., Pelet, A., Arnold, S., Miao, X., Griseri, P., et al. 2008. Hirschsprung disease, associated syndromes and genetics: a review. *J Med Genet* 45:1-14.
2. Chakravarti, A., McCallion, A., Lyonnet, S. 2006. Scrivers' Online Metabolic & Molecular Bases of Inherited Disease. In *Multisystem Inborn Errors of Development: Hirschsprung*. D. Valle, Vogelstein, B.A., Kinzler, K.W., et al., editor: McGraw Hill Education.
3. Schuchardt, A., D'Agati, V., Larsson-Blomberg, L., Costantini, F., and Pachnis, V. 1994. Defects in the kidney and enteric nervous system of mice lacking the tyrosine kinase receptor Ret. *Nature* 367:380-383.
4. Schuchardt, A., D'Agati, V., Larsson-Blomberg, L., Costantini, F., and Pachnis, V. 1995. RET-deficient mice: an animal model for Hirschsprung's disease and renal agenesis. *J Intern Med* 238:327-332.
5. Patel, A., Harker, N., Moreira-Santos, L., Ferreira, M., Alden, K., Timmis, J., Foster, K., Garefalaki, A., Pachnis, P., Andrews, P., et al. 2012. Differential RET signaling pathways drive development of the enteric lymphoid and nervous systems. *Sci Signal* 5:ra55.
6. Jain, S., Encinas, M., Johnson, E.M., Jr., and Milbrandt, J. 2006. Critical and distinct roles for key RET tyrosine docking sites in renal development. *Genes Dev* 20:321-333.
7. Lyonnet, S., Bolino, A., Pelet, A., Abel, L., Nihoul-Fekete, C., Briard, M.L., Mok-Siu, V., Kaariainen, H., Martucciello, G., Lerone, M., et al. 1993. A gene for Hirschsprung disease maps to the proximal long arm of chromosome 10. *Nat Genet* 4:346-350.
8. Angrist, M., Kauffman, E., Slaugenhaupt, S.A., Matise, T.C., Puffenberger, E.G., Washington, S.S., Lipson, A., Cass, D.T., Reyna, T., Weeks, D.E., et al. 1993. A gene for Hirschsprung disease (megacolon) in the pericentromeric region of human chromosome 10. *Nat Genet* 4:351-356.

9. Edery, P., Lyonnet, S., Mulligan, L.M., Pelet, A., Dow, E., Abel, L., Holder, S., Nihoul-Fekete, C., Ponder, B.A., and Munnich, A. 1994. Mutations of the RET proto-oncogene in Hirschsprung's disease. *Nature* 367:378-380.

10. Romeo, G., Ronchetto, P., Luo, Y., Barone, V., Seri, M., Ceccherini, I., Pasini, B., Bocciardi, R., Lerone, M., Kaariainen, H., et al. 1994. Point mutations affecting the tyrosine kinase domain of the RET proto-oncogene in Hirschsprung's disease. *Nature* 367:377-378.

11. Emison, E.S., Garcia-Barcelo, M., Grice, E.A., Lantieri, F., Amiel, J., Burzynski, G., Fernandez, R.M., Hao, L., Kashuk, C., West, K., et al. 2010. Differential contributions of rare and common, coding and noncoding Ret mutations to multifactorial Hirschsprung disease liability. *Am J Hum Genet* 87:60-74.

12. Jain, S., Naughton, C.K., Yang, M., Strickland, A., Vij, K., Encinas, M., Golden, J., Gupta, A., Heuckeroth, R., Johnson, E.M., Jr., et al. 2004. Mice expressing a dominant-negative Ret mutation phenocopy human Hirschsprung disease and delineate a direct role of Ret in spermatogenesis. *Development* 131:5503-5513.

13. Carniti, C., Belluco, S., Riccardi, E., Cranston, A.N., Mondellini, P., Ponder, B.A., Scanziani, E., Pierotti, M.A., and Bongarzone, I. 2006. The Ret(C620R) mutation affects renal and enteric development in a mouse model of Hirschsprung's disease. *Am J Pathol* 168:1262-1275.

14. Dow, E., Cross, S., Wolgemuth, D.J., Lyonnet, S., Mulligan, L.M., Mascari, M., Ladda, R., and Williamson, R. 1994. Second locus for Hirschsprung disease/Waardenburg syndrome in a large Mennonite kindred. *Am J Med Genet* 53:75-80.

15. Hosoda, K., Hammer, R.E., Richardson, J.A., Baynash, A.G., Cheung, J.C., Giaid, A., and Yanagisawa, M. 1994. Targeted and natural (piebald-lethal) mutations of endothelin-B receptor gene produce megacolon associated with spotted coat color in mice. *Cell* 79:1267-1276.

16. Zaitoun, I., Erickson, C.S., Barlow, A.J., Klein, T.R., Heneghan, A.F., Pierre, J.F., Epstein, M.L., and Gosain, A. 2013. Altered neuronal density and neurotransmitter expression in the ganglionated region of Ednrb null mice: implications for Hirschsprung's disease. *Neurogastroenterol Motil* 25:e233-244.

17. Roberts, R.R., Bornstein, J.C., Bergner, A.J., and Young, H.M. 2008. Disturbances of colonic motility in mouse models of Hirschsprung's disease. *Am J Physiol Gastrointest Liver Physiol* 294:G996-G1008.

18. Cantrell, V.A., Owens, S.E., Chandler, R.L., Airey, D.C., Bradley, K.M., Smith, J.R., and Southard-Smith, E.M. 2004. Interactions between Sox10 and EdnrB modulate penetrance and severity of aganglionosis in the Sox10Dom mouse model of Hirschsprung disease. *Hum Mol Genet* 13:2289-2301.

19. Zhao, L., Dhall, D., Cheng, Z., Wang, H.L., Doherty, T.M., Bresee, C., and Frykman, P.K. 2010. Murine model of Hirschsprung-associated enterocolitis II: Surgical correction of aganglionosis does not eliminate enterocolitis. *J Pediatr Surg* 45:206-211; discussion 211-202.

20. Cheng, Z., Dhall, D., Zhao, L., Wang, H.L., Doherty, T.M., Bresee, C., and Frykman, P.K. 2010. Murine model of Hirschsprung-associated enterocolitis. I: phenotypic characterization with development of a histopathologic grading system. *J Pediatr Surg* 45:475-482.

21. Druckenbrod, N.R., Powers, P.A., Bartley, C.R., Walker, J.W., and Epstein, M.L. 2008. Targeting of endothelin receptor-B to the neural crest. *Genesis* 46:396-400.

22. Mulligan, L.M., Eng, C., Attie, T., Lyonnet, S., Marsh, D.J., Hyland, V.J., Robinson, B.G., Frilling, A., Verellen-Dumoulin, C., Safar, A., et al. 1994. Diverse phenotypes associated with exon 10 mutations of the RET proto-oncogene. *Hum Mol Genet* 3:2163-2167.

23. Takahashi, M., Iwashita, T., Santoro, M., Lyonnet, S., Lenoir, G.M., and Billaud, M. 1999. Co-segregation of MEN2 and Hirschsprung's disease: the same mutation of RET with both gain and loss-of-function? *Hum Mutat* 13:331-336.

24. Decker, R.A., Peacock, M.L., and Watson, P. 1998. Hirschsprung disease in MEN 2A: increased spectrum of RET exon 10 genotypes and strong genotype-phenotype correlation. *Hum Mol Genet* 7:129-134.

25. Lake, J.I., Tusheva, O.A., Graham, B.L., and Heuckeroth, R.O. 2013. Hirschsprung-like disease is exacerbated by reduced de novo GMP synthesis. *J Clin Invest* 123:4875-4887.

26. Fu, M., Sato, Y., Lyons-Warren, A., Zhang, B., Kane, M.A., Napoli, J.L., and Heuckeroth, R.O. 2010. Vitamin A facilitates enteric nervous system precursor migration by reducing Pten accumulation. *Development* 137:631-640.

27. Owens, S.E., Broman, K.W., Wiltshire, T., Elmore, J.B., Bradley, K.M., Smith, J.R., and Southard-Smith, E.M. 2005. Genome-wide linkage identifies novel modifier loci of aganglionosis in the Sox10Dom model of Hirschsprung disease. *Hum Mol Genet* 14:1549-1558.

28. Jiang, Q., Ho, Y.Y., Hao, L., Nichols Berrios, C., and Chakravarti, A. 2011. Copy number variants in candidate genes are genetic modifiers of Hirschsprung disease. *PLoS One* 6:e21219.

29. Dang, R., Torigoe, D., Sasaki, N., and Agui, T. 2011. QTL analysis identifies a modifier locus of aganglionosis in the rat model of Hirschsprung disease carrying Ednrb(sl) mutations. *PLoS One* 6:e27902.

30. Maka, M., Stolt, C.C., and Wegner, M. 2005. Identification of Sox8 as a modifier gene in a mouse model of Hirschsprung disease reveals underlying molecular defect. *Dev Biol* 277:155-169.

31. Parisi, M.A., Kapur, R.P., Neilson, I., Hofstra, R.M., Holloway, L.W., Michaelis, R.C., and Leppig, K.A. 2002. Hydrocephalus and intestinal aganglionosis: is L1CAM a modifier gene in Hirschsprung disease? *Am J Med Genet* 108:51-56.

32. de Pontual, L., Pelet, A., Trochet, D., Jaubert, F., Espinosa-Parrilla, Y., Munnich, A., Brunet, J.F., Goridis, C., Feingold, J., Lyonnet, S., et al. 2006. Mutations of the RET gene in isolated and syndromic Hirschsprung's disease in human disclose major and modifier alleles at a single locus. *J Med Genet* 43:419-423.

33. King, S.K., Southwell, B.R., and Hutson, J.M. 2006. An association of multiple endocrine neoplasia 2B, a RET mutation; constipation; and low substance P-nerve fiber density in colonic circular muscle. *J Pediatr Surg* 41:437-442.

34. Ostwani, W., Dolan, J., and Elitsur, Y. 2010. Familial clustering of habitual constipation: a prospective study in children from West Virginia. *J Pediatr Gastroenterol Nutr* 50:287-289.

35. Chan, A.O., Lam, K.F., Hui, W.M., Leung, G., Wong, N.Y., Lam, S.K., and Wong, B.C. 2007. Influence of positive family history on clinical characteristics of functional constipation. *Clin Gastroenterol Hepatol* 5:197-200.

36. Dickman, R., Wainstein, J., Glezerman, M., Niv, Y., and Boaz, M. 2014. Gender aspects suggestive of gastroparesis in patients with diabetes mellitus: a cross-sectional survey. *BMC Gastroenterol* 14:34.

37. Legato, M.J., and Bilezikian, J.P. 2004. *Principles of gender-specific medicine*. Amsterdam ; Boston: Elsevier Academic Press.

38. Gillies, G.E., and McArthur, S. 2010. Estrogen actions in the brain and the basis for differential action in men and women: a case for sex-specific medicines. *Pharmacol Rev* 62:155-198.

39. Furness, J.B. 2006. *The Enteric Nervous System*. Malden, Massachusetts: Blackwell Publishing Inc.

40. Borenshtein, D., Schlieper, K.A., Rickman, B.H., Chapman, J.M., Schweinfest, C.W., Fox, J.G., and Schauer, D.B. 2009. Decreased expression of colonic Slc26a3 and carbonic anhydrase iv as a cause of fatal infectious diarrhea in mice. *Infect Immun* 77:3639-3650.

CHAPTER IV

DEFICITS IN *SOX10*$^{DOM/+}$ PYLORIC SPHINCTER DYNAMICS

Introduction

The pyloric sphincter acts as a gatekeeper to the small intestine, opening and closing to allow stomach contents into the duodenum. Neural, musculature, and hormonal factors control pyloric sphincter dynamics (1). Developmental anomalies, disease, and trauma can affect any of these factors, leading to pyloric dysfunction such as that seen in pyloric stenosis, gastroparesis, and dumping syndrome.

Dumping syndrome, characterized by rapid gastric emptying, can manifest as a host of symptoms, including abdominal discomfort, nausea, vomiting, diarrhea, rapid heart rate, sweating, and dizziness (2). Dumping syndrome occurs commonly after major gastrointestinal surgical procedures, including Nissan duplications in the pediatric population (3) and gastric bypass surgeries used in the adult population for weight loss management (2, 4). Because the pylorus and/or innervation are modified or removed in these procedures, it comes as no surprise that dumping syndrome occurs. However, this syndrome can also be a part of other medical conditions, such as diabetes, Zollinger-Ellison, and Cyclic Vomiting syndrome (5, 6). Patients may present with dumping syndrome where gastric surgery, related medical conditions, and medications have been ruled out as a possible cause. Such cases suggest congenital defects and/or environmental causes.

We recently described increased gastric emptying in male mice with the *Sox10*^{Dom} Hirschsprung disease mutation (Chapter 2). Dumping syndrome is not commonly reported as occurring with HSCR. A literature review revealed only a handful of HSCR patients presenting with dumping syndrome (7) and most HSCR actually go on to develop gastroparesis (delayed emptying) (reviewed in (8)). Given that *SOX10* is initially expressed in all neural crest cell

populations and expression persists in several glial populations after development, it could be *SOX10* signaling has different or wider consequences on peripheral nervous system (PNS) function than other HSCR genes.

Despite numerous studies detailing *Sox10* function in the PNS, the exact affect *SOX10* mutations have on pyloric sphincter development and function have not been explored. We previously identified imbalances in neuron subtypes in the duodenum of $Sox10^{Dom/+}$ Hirschsprung mice which could be contributing to small intestinal transit slowing (Chapter 2). Although we did not evaluate neuron subtypes within the pyloric sphincter muscle walls in our previous study, we hypothesized intrinsic neurally-mediated deficits could be driving changes in pyloric sphincter function given our findings in the duodenum.

To test our hypothesis, we measured and compared pyloric sphincter opening pressures in $Sox10^{Dom/+}$ and $Sox10^{+/+}$ male mice. $Sox10^{Dom/+}$ pyloric sphincters opened at lower pressures than $Sox10^{+/+}$ pyloric sphincters, explaining the increased gastric emptying found previously in $Sox10^{Dom/+}$ mice (Chapter 2). Importantly, we devised and conducted these tests in an *ex vivo* system in order to eliminate any effects on the pyloric sphincter from extrinsic nerve inputs. Additionally, evaluation of pyloric sphincter morphology revealed no gross changes in musculature, suggesting the alteration in pyloric sphincter function in $Sox10^{Dom/+}$ mice is driven by intrinsic ENS deficits.

Methods

Pyloric Sphincter Dynamics

$Sox10^{Dom/+}$ and $Sox10^{+/+}$ mice were maintained on a C57/BL6 background. Adult (6-week to 9-week old) mice were sacrificed via isoflurane inhalation followed by cervical dislocation. The entire stomach and proximal portion of the duodenum were removed from the mouse and immediately placed in modified, deoxygenated Krebs buffer (95% N_2, 5% CO_2; 2.5 mM $CaCl_2$, 11.1 mM dextrose, 4.7 mM KCl, 1.0 mM $KH_2PO_4$109 mM NaCl, 34 mM $NaHCO_3$, 0.9 MgSO4).

Within the Krebs buffer, extraneous mesentery, pancreas, and other tissue were removed from the sample with care not to puncture any part of the gut tube. The stomach was then cut so that only the distal 0.3 to 0.5 remained. The duodenum was trimmed so the most proximal ~1.5-2 cm remained. Next, under a dissection scope, forceps were used to carefully remove as much contents as possible from the stomach and duodenum. During this step, care was taken in order to not disrupt the pyloric sphincter. (Any efforts to 'flush' the gut with liquid to remove contents will result in the pyloric sphincter shutting and are highly discouraged!) However, the dissector must not be shy in regard to trying to remove food from the pyloric sphincter area. Remaining gastric contents can clog cannulae and flow during the pyloric sphincter flow experiment, resulting in loss of the sample (usually do to bursting or extreme expansion) and demands necessary exclusion of that data from the study. Although we did not fast mice, fasting mice O/N without bedding or with bedding they will not eat could aid in keeping the cannulae from clogging.

After thorough cleaning, the gut sample was transferred to Krebs buffer within a custom designed sample bath (Figure 4.1). The cannulae within our set up were first flushed with Krebs buffer to avoid introducing a sudden increase in pressure when the gut is connected to the flow system. Strands from braided nylon sutures were used to secure the stomach and duodenum to two canula spanning the distance of the sample bath (Figure 4.1). Once secured, the sample was transported to an inverted microscope platform and connected to a flow system. (9) Gut pieces were given a minimum of 5 minutes to equilibrate within warm Krebs buffer. We started the flow at 5 mm/Hg and increased the pressure by ~5 mm/Hg at a minimum of every 2 minutes. Flow, back pressure, and forward pressure were measured throughout the study. Pyloric sphincter opening pressure was recorded as the pressure when flow reached ≥1000 ul/min. n=3 *Sox10*$^{+/+}$ and n=4 *Sox10*$^{Dom/+}$. (Initially, we had n=4 *Sox10*$^{+/+}$ mice. However, one *Sox10*$^{+/+}$ mouse was excluded from the statistical analysis because it was an outlier. Importantly, our notes indicate over-stretching of tissue from this mouse during our experimental set up, probably explaining outcomes inconsistent with other *Sox10*$^{+/+}$ mice.)

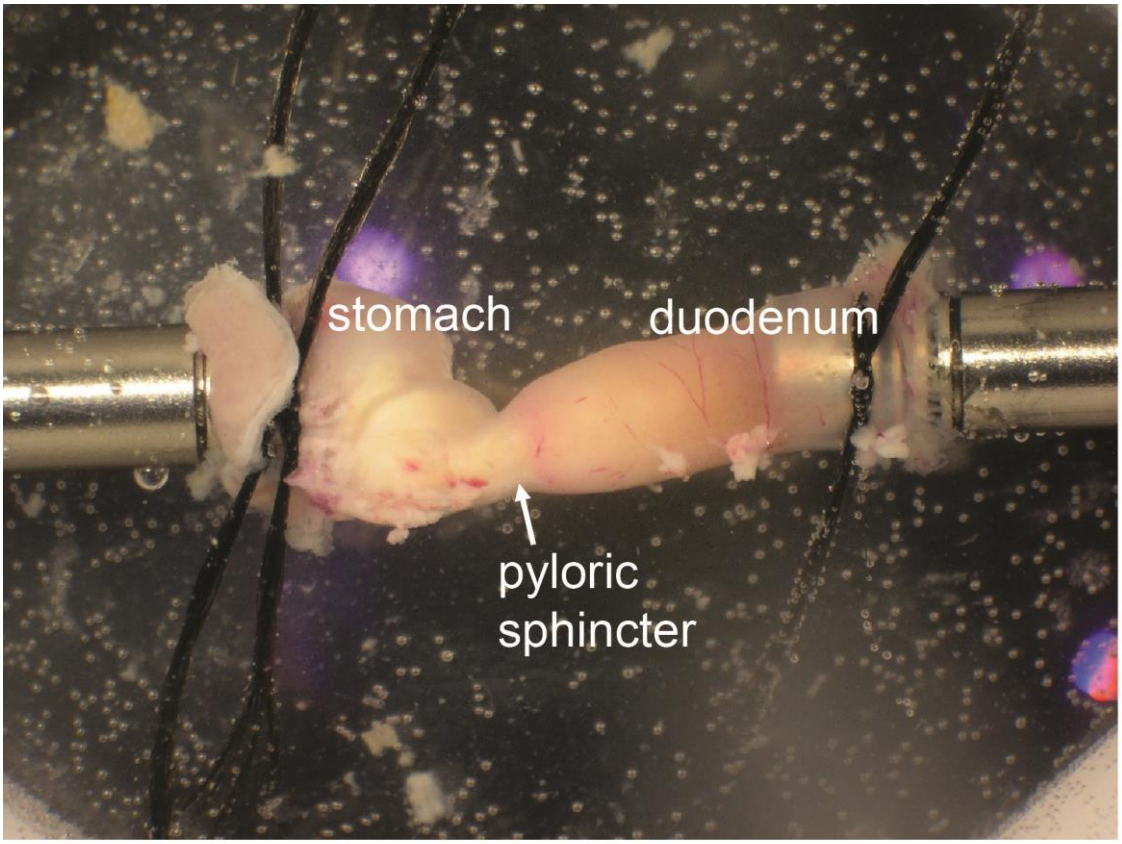

Figure 4.1. Experimental set up for testing pyloric sphincter opening pressure. The lower portion of the stomach and the proximal duodenum are tied onto canulae by surgical sutures. The pyloric sphincter is suspended in the middle (arrow). The entire tissue sample is within circulating modified Krebs buffer. Modified Krebs buffer enters the stomach through one canula and exits through the duodenum. Pressure of liquid entering the tissue and liquid flow rates through the tissue sample are monitored. Image by Elaine Shelton. Modified by M. Musser.

Muscle measurements

Stomach with intact proximal duodenum were collected from adult mice (6-week – 9-week) immediately following euthanasia. The stomach was cut in half and the remaining sample (distal stomach and duodenum) were flushed with 1XPBS to remove all gut contents. Gut samples were then placed on their sides in histology cassettes (Fisher, white, Cat. No. 15-182-702A) immediately submerged in 10% PFA, and fixed at least overnight at 4°C. Following fix, tissues were delivered to the Vanderbilt Pathology Core for processing, embedding, sectioning, and H&E staining.

To determine if gastrointestinal musculature near and within the pyloric sphincter differed between *Sox10*$^{Dom/+}$ and *Sox10*$^{+/+}$ mice, we measured the shortest distance within the antral opening (Figure 4.3). To ensure the same area of each animal was sampled for measuring, care was taken to only measure sections with visibly continuous lumen through the stomach, pyloric sphincter, and duodenum.

We did consider using the same gut samples for the pyloric sphincter dynamic studies and the muscle measurements. However, given the long hours post-sacrifice and exposure to flow pressures, we were concerned about how the pyloric sphincter flow studies could alter the muscle tissue prior to fixation. Thus, we chose to use experimentally naïve tissue for this portion of the study.

Statistics

Average pyloric sphincter pressures were statistically compared and visualized with PRISM software. Muscle measurements were statistically compared using a student's t-test assuming unequal variance (Welch's t-test) utilizing JMP v11 statistical software.

Results

Sox10$^{Dom/+}$ *pyloric sphincters open at lower pressures*

To determine if the *Sox10*$^{Dom/+}$ mutation affects pyloric sphincter opening conditions, we evaluated pyloric sphincter opening pressures in *Sox10*$^{Dom/+}$ and *Sox10*$^{+/+}$ adult male mice. To eliminate the effects of gastric hormones (such as CCK) and extrinsic neural signaling (vagal inputs), we tested pyloric opening pressures in an *ex vivo* system. Briefly, gut tissue samples that included the lower portion of the stomach, the pyloric sphincter, and the proximal duodenum were suspended between cannulae in a tissue medium bath (Figure 4.1). Modified Krebs buffer was allowed to flow into and through the gut samples—entering from the stomach and exiting through the duodenum. Flow through the sample was measured as we increased flow pressure in

~5mmHg increments. Under normal physiological fasting conditions, the pyloric sphincter is tightly closed. Many factors influence pyloric sphincter opening. However, in general, as increasing amounts of food and/or liquid enters the stomach, pressure within the stomach increases. Very high pressures eventually trigger the pyloric sphincter to open very wide, permitting gastric contents to flow into and through the small intestine. To this end, in our assay, low levels of flow indicated a closed pyloric sphincter. Abrupt, large increases in flow (>1000 ul/min) indicated pyloric sphincter opening (Figure 4.2).

Using this system, we recorded and compared pyloric sphincter opening pressures in *Sox10*$^{Dom/+}$ and *Sox10*$^{+/+}$ adult male mice. *Sox10*$^{Dom/+}$ pyloric sphincters consistently opened at lower pressures (~10 mmHg) than *Sox10*$^{+/+}$ pyloric sphincters (~15 mmHg) (Figure 4.2). When compared statistically, the difference in average pressure opening between the two groups was significant (*$P<0.05$*; Figure 4.2).

Sox10*$^{Dom/+}$ *and Sox10*$^{+/+}$ *pyloric sphincter morphology is equivalent

Although we aimed to eliminate extrinsic neural inputs and gastric signaling in our pyloric sphincter tests, the possibility remained that differences in pyloric sphincter morphology and musculature could be driving the increased gastric emptying and aberrant sphincter opening in our *Sox10*$^{Dom/+}$ males. Alterations in innervation to smooth muscle can affect musculature morphology (10, 11). In our own studies, we noticed variations in muscle thickness and texture in aganglionic regions of *Sox10*$^{Dom/+}$ colons. And in HSCR patients, aganglionic regions can contain thickened muscle (12). We have not noticed differences in muscle thickness in ganglionated regions of *Sox10*$^{Dom/+}$ intestine, but to rule out the possibility of aberrant muscle development in the pyloric sphincter region of *Sox10*$^{Dom/+}$ we collected and evaluated pyloric sphincter morphology from *Sox10*$^{Dom/+}$ and *Sox10*$^{+/+}$ adult male mice. We observed no gross morphological differences between the two genotypes (data not shown). Additionally,

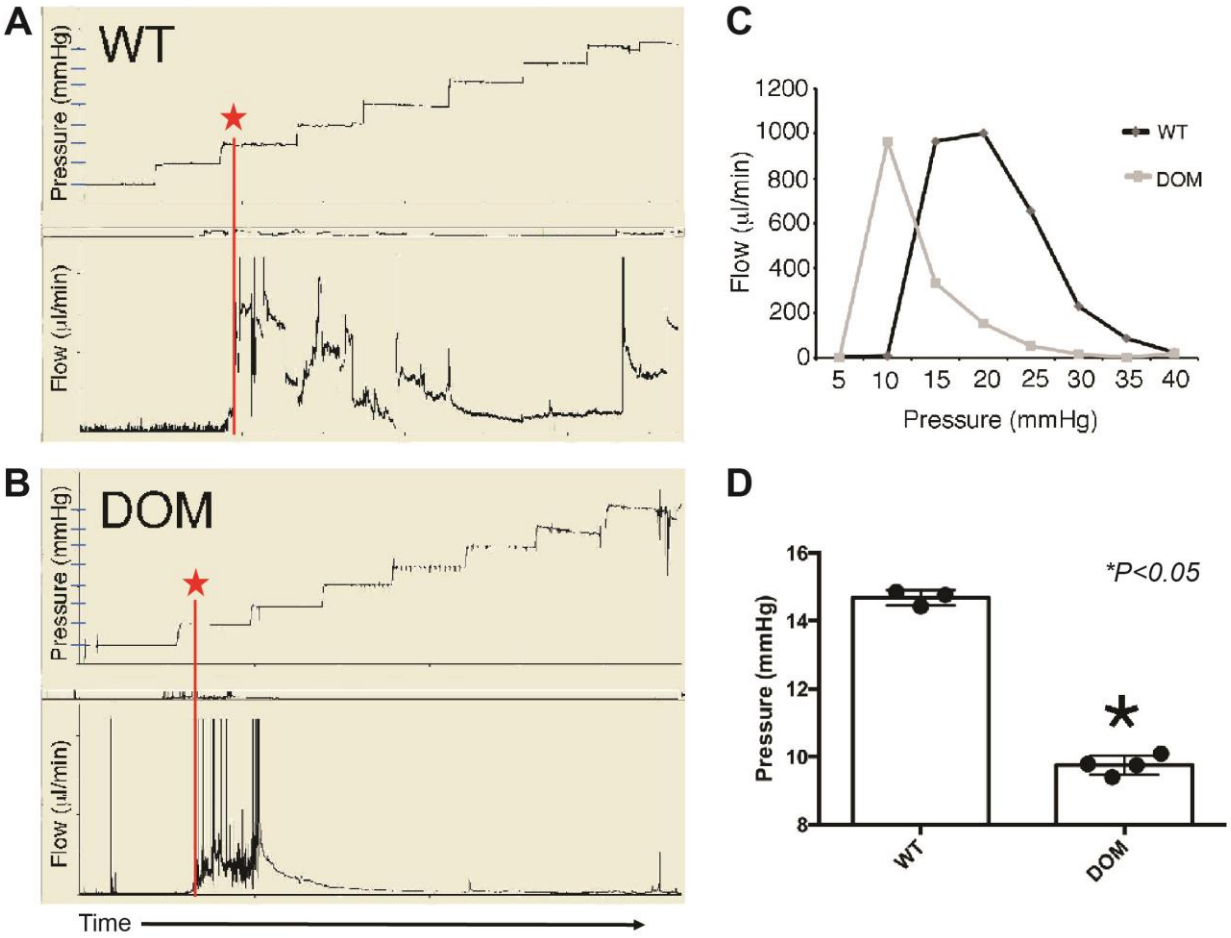

Figure 4.2. *Sox10*$^{Dom/+}$ pyloric sphincters open at lower pressures than *Sox10*$^{+/+}$ pyloric sphincters. Representative traces of (**A**) *Sox10*$^{+/+}$ and (**B**) *Sox10*$^{Dom/+}$ flow measurments through the pyloric sphincter with ~5 mmHg increases in pressure (y-axis blue hash marks) over time (x-axis). (**A**) In this *Sox10*$^{+/+}$ mouse, flow through the pyloric spincter was minimal until pressure was increased to ~15mmHg (red star and line) and flow increased dramatically, indicating opening of the pyloric sphincter. (**B**) In sharp contrast, in this *Sox10*$^{Dom/+}$ mouse, pyloric sphincter opening occured at ~10 mmHg (red star and line). (**C**) Data from panel A & B traces are represented here as flow (ul/min) at a given pressure (mmHg). (**D**) On average, *Sox10*$^{+/+}$ pyloric sphincters (n=3) opened at significantly higher pressures than *Sox10*$^{Dom/+}$ pyloric sphincters (n=4). **P<0.05*. WT= *Sox10*$^{+/+}$; DOM=*Sox10*$^{Dom/+}$. Figure generated by Elaine Shelton; modified by M. Musser.

measurements of antral opening length revealed no differences between *Sox10*$^{Dom/+}$ and *Sox10*$^{+/+}$ mice (*P=0.86*) (Figure 4.3).

Discussion

A previous study in our lab identified increased gastric emptying in adult *Sox10*$^{Dom/+}$ male mice compared to wildtype *Sox10*$^{+/+}$ mice (Chapter 2). Given neuronal subtype imbalances also identified in the small intestine of *Sox10*$^{Dom/+}$ mice (Chapter 2), we hypothesized that intrinsic, neurally mediated processes could lead to premature pyloric sphincter opening in *Sox10*$^{Dom/+}$ male mice. To test this hypothesis, we developed a novel *ex vivo* technique for applying pressure and measuring flow through the pyloric sphincter in isolated gut tissue samples (Figure 4.1). Our findings indicate that the *Sox10*$^{Dom/+}$ pyloric sphincter opens at lower pressures when compared to *Sox10*$^{+/+}$ mice. This premature opening appears to be neurally mediated as pyloric morphology and antral opening measurements are comparable between *Sox10*$^{Dom/+}$ and *Sox10*$^{+/+}$ male mice.

Our findings in the pyloric sphincter for *Sox10*$^{Dom/+}$ male mice indicate that pyloric sphincter opening is induced at lower pressures than in wildtype mice; however, we do not know if this phenomenon occurs in HSCR patients. If affecting HSCR patients, this premature opening of the pyloric sphincter could feasibly present as dumping syndrome. A few HSCR cases of dumping syndrome have been reported (7), but this raises the question as to why this phenomenon would occur only in male *Sox10*$^{Dom/+}$ mice (and not females) and only some patients. Importantly, neurodevelopmental disorders tend to affect males more severely than females and estrogen has been suggested to have a neuroprotective effect (reviewed in (13)). This sex-specific driving of phenotypes is expounded upon in detail in Chapters 2, 3 and 8 and could easily explain our findings in regard to pyloric sphincter function in *Sox10*$^{Dom/+}$ male mice. This sex-specific finding though could only partially explain the lack of HSCR patient cases with dumping syndrome in the literature. It is plausible that more HSCR patients have dumping syndrome and the lack of reporting is due to confusion of dumping syndrome symptoms, such as abdominal cramps and

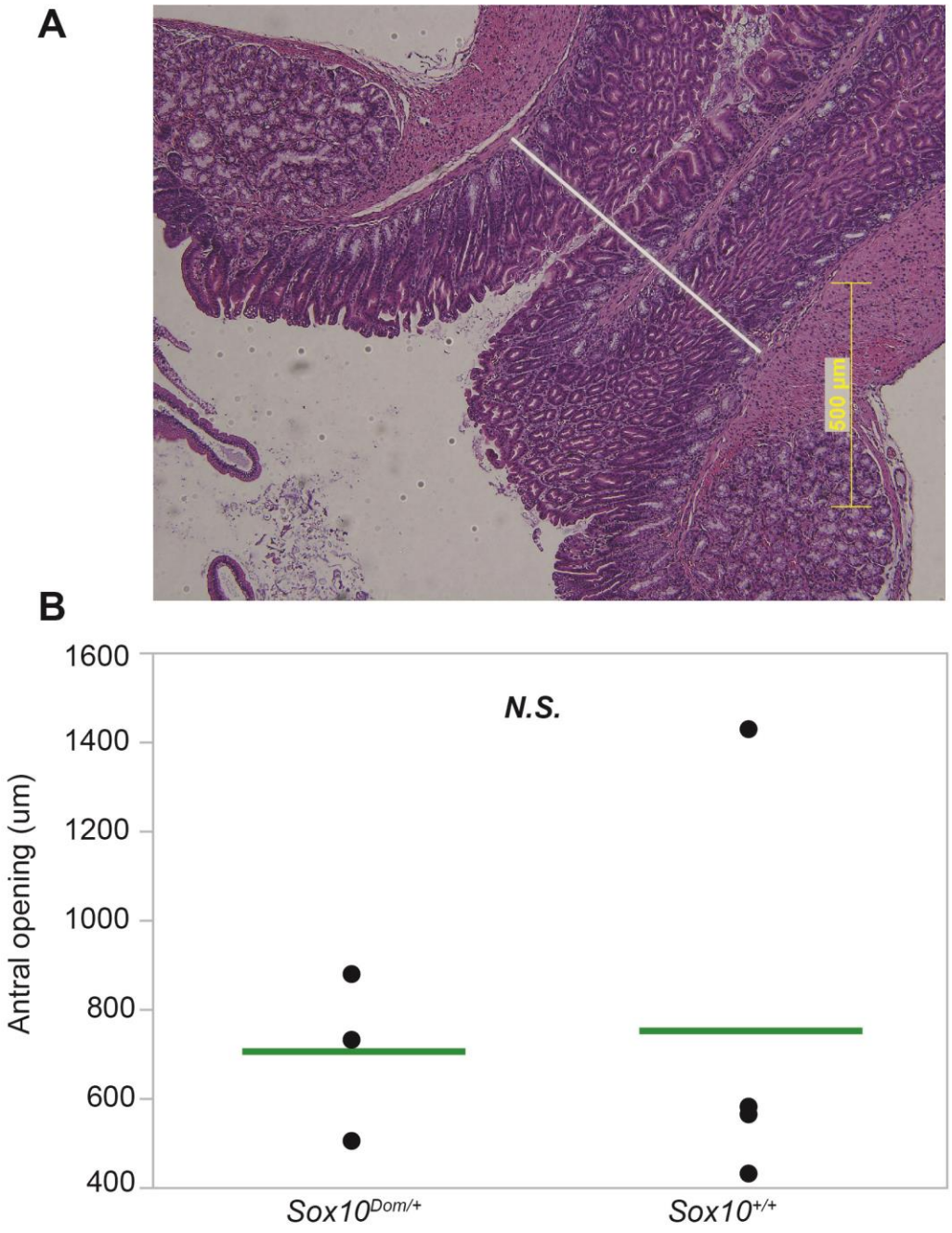

Figure 4.3. *Sox10*$^{Dom/+}$ and *Sox10*$^{+/+}$ pyloric sphincter morphology is comparable. (**A**) H&E stained transverse section of the antral openinig measured at the shortest length (white line). **(B)** Measurements (green line is the mean) of antral openings revealed no significant differences between *Sox10*$^{Dom/+}$ (706 ±109 SEM; n=3) and *Sox10*$^{+/+}$ (753 ±228 SEM; n=4) mice. *P=0.86*. N.S. = not significant.

diarrhea, with other HSCR related phenomenon. Additionally, it could be that only specific mutations along with other genetic modifiers and/or environmental influences lead to altered pyloric sphincter dynamics. This theory is compatible with what is known about *Sox10* and other HSCR genes. Because *Sox10* is a transcription factor and appears temporally before other HSCR related genes, it is possible that only *Sox10* mutations have the ability to give rise to more severe GI phenotypes such as pyloric sphincter dysfunction. Again in line with this hypothesis, it has been shown that some ENP populations are independent of specific HSCR genes or gene elements, such as Ret (14, 15) and Ednrb (16). For example, in $Ret^{-/-}$ mice, a *Ret* independent population of NCC is still able to colonize the stomach (14, 15). In mice with effectively null *Sox10*, NCC fail to reach the foregut at all, undergoing apoptosis before and during their migration from the neural tube (17, 18). Together, these findings suggest the possibility of *Sox10* mutations more severely affecting other aspects of GI function compared to other HSCR genes; however, future testing of pyloric sphincter function in other HSCR mouse models and close monitoring of HSCR patients should clarify these possible disparities.

Importantly, the premature pyloric sphincter opening in $Sox10^{Dom/+}$ male mice is most likely mediated intrinsically by the ENS given our ability to isolate gut tissue from extrinsic innervation and hormonal effects and also observed comparable pyloric sphincter morphology. As a caveat, pyloric sphincter antral opening measurements were extremely variable, most likely due to variability in slicing of tissues and cross sections available to measure. To strengthen this study, more pyloric sphincter samples from $Sox10^{Dom/+}$ and $Sox10^{+/+}$ male mice should be collected, processed, and evaluated. Additional parameters that could be measured and compared are thickness of duodenal muscle wall and gastric muscle wall. Also, H&E provides a gross overview of muscle morphology and permits some gross measurements, but more in depth evaluation of muscle fibers and structure, such as through IHC with α-actin, tubulin, or myosin-heavy chain antibodies and confocal imaging, could more strongly rule in or rule out any muscle abnormalities.

Overall, we have identified a neurally-driven pyloric sphincter defect in the *Sox10*$^{Dom/+}$ mouse model of HSCR; however, the exact neural mechanisms driving this phenotype are still unknown. Alterations in Calretinin neuron proportions in the duodenum of these mice initially led us to pursuit this study (Chapter 2) and similar analysis of neuronal subtypes and ICC cells in pyloric sphincter tissue as well as gastric tissue could aid in identifying neuronal populations contributing to the pyloric sphincter phenotype. Furthermore, our novel experimental set up could be utilized to help further define the neural networks affected—pharmacological reagents aimed at targeting specific neuronal groups could be introduced into the system and pyloric sphincter opening and flow could be measured and compared under several test conditions. Finally, although preliminary, our results indicate that some HSCR patients could suffer from the effects of rapid gastric emptying. Clinicians should bear such findings in mind when evaluating HSCR patients with GI distress post-surgery.

References

1. Furness, J.B. 2006. *The Enteric Nervous System*. Malden, Massachusetts: Blackwell Publishing Inc.
2. Tack, J., Arts, J., Caenepeel, P., De Wulf, D., and Bisschops, R. 2009. Pathophysiology, diagnosis and management of postoperative dumping syndrome. *Nat Rev Gastroenterol Hepatol* 6:583-590.
3. Pacilli, M., Eaton, S., McHoney, M., Kiely, E.M., Drake, D.P., Curry, J.I., Lindley, K.J., and Pierro, A. 2014. Four year follow-up of a randomised controlled trial comparing open and laparoscopic Nissen fundoplication in children. *Archives of Disease in Childhood* 99:516-521.
4. Ukleja, A. 2005. Dumping syndrome: pathophysiology and treatment. *Nutr Clin Pract* 20:517-525.
5. Dubois, A., Eerdewegh, P.V., and Gardner, J.D. 1977. Gastric emptying and secretion in Zollinger-Ellison syndrome. *J Clin Invest* 59:255-263.
6. Hejazi, R.A., Patil, H., and McCallum, R.W. 2010. Dumping syndrome: establishing criteria for diagnosis and identifying new etiologies. *Dig Dis Sci* 55:117-123.
7. Rlvkees, S.A., and Crawford, J.D. 1987. PATHOGENESIS OF HYPOGLYCEMIA IN CHILDHOOD DUMPING SYNDROME. *Pediatr Res* 21:276A-276A.
8. Saps, M.a.C., A. 2013. Gastric Motor Disorders: Gastroparesis and Dumping Syndrome. In *Neurogastroenterology: Gastrointestinal Motility and Functional Disorders in Children*. C.F.e. al., editor: Springer.
9. Reese, J., O'Mara, P.W., Poole, S.D., Brown, N., Tolentino, C., Eckman, D.M., and Aschner, J.L. 2009. Regulation of the fetal mouse ductus arteriosus is dependent on interaction of nitric oxide and COX enzymes in the ductal wall. *Prostaglandins Other Lipid Mediat* 88:89-96.

10. Johnston, L., Cunningham, R.M., Young, J.S., Fry, C.H., McMurray, G., Eccles, R., and McCloskey, K.D. 2012. Altered distribution of interstitial cells and innervation in the rat urinary bladder following spinal cord injury. *J Cell Mol Med* 16:1533-1543.

11. Miao, C.Y., Tao, X., Gong, K., Zhang, S.H., Chu, Z.X., and Su, D.F. 2001. Arterial remodeling in chronic sinoaortic-denervated rats. *J Cardiovasc Pharmacol* 37:6-15.

12. Chakravarti, A., McCallion, A., Lyonnet, S. 2006. Scrivers' Online Metabolic & Molecular Bases of Inherited Disease. In *Multisystem Inborn Errors of Development: Hirschsprung*. D. Valle, Vogelstein, B.A., Kinzler, K.W., et al., editor: McGraw Hill Education.

13. Garcia-Segura, L.M., Azcoitia, I., and DonCarlos, L.L. 2001. Neuroprotection by estradiol. *Prog Neurobiol* 63:29-60.

14. Durbec, P., Marcos-Gutierrez, C.V., Kilkenny, C., Grigoriou, M., Wartiowaara, K., Suvanto, P., Smith, D., Ponder, B., Costantini, F., Saarma, M., et al. 1996. GDNF signalling through the Ret receptor tyrosine kinase. *Nature* 381:789-793.

15. Schuchardt, A., D'Agati, V., Larsson-Blomberg, L., Costantini, F., and Pachnis, V. 1994. Defects in the kidney and enteric nervous system of mice lacking the tyrosine kinase receptor Ret. *Nature* 367:380-383.

16. Mundell, N.A., Plank, J.L., LeGrone, A.W., Frist, A.Y., Zhu, L., Shin, M.K., Southard-Smith, E.M., and Labosky, P.A. 2012. Enteric nervous system specific deletion of Foxd3 disrupts glial cell differentiation and activates compensatory enteric progenitors. *Dev Biol* 363:373-387.

17. Southard-Smith, E.M., Kos, L., and Pavan, W.J. 1998. Sox10 mutation disrupts neural crest development in Dom Hirschsprung mouse model. *Nat Genet* 18:60-64.

18. Kapur, R.P. 1999. Early death of neural crest cells is responsible for total enteric aganglionosis in Sox10(Dom)/Sox10(Dom) mouse embryos. *Pediatr Dev Pathol* 2:559-569.

CHAPTER V

CHARACTERIZATION AND OUTCOMES OF A HSCR PATIENT COHORT

Introduction

Scientists first described Hirschsprung disease (HSCR) hundreds of years ago, but only within the last century was the cause of congenital megacolon—absence of ganglia in the distal intestine—recognized (1). Once an almost always fatal disorder, the discovery of HSCR's etiology promptly led to the development of live saving pull-through surgeries in the 1940's through the 1960's (2-4). The vast majority of these surgeries entail removal of the aganglionic segment of the intestine followed by reanastomosis of ganglionated intestine to the anus.

Since the advent of pull-through surgeries, the survival of HSCR patients has uncovered many additional details about the disease. Clustering of the disease in multiple families and communities showed heritability of the disease, led to the discovery of HSCR gene mutations, and demonstrated that the disease was oligogenic and incompletely penetrant. The survival of HSCR patients also revealed a more insidious side of the disease. Physicians initially viewed the removal of the aganglionic segment from HSCR patients as a curative procedure; however, subsequent follow up of HSCR patients revealed adverse outcomes post-surgery, such as fecal incontinence, chronic constipation or Hirschsprung-associated enterocolitis (HAEC). Studies report chronic constipation in 7-16% of children (5, 6) and 5-30% of adults with HSCR (7-9). And HAEC, in which symptoms can include fever, severe diarrhea, and rectal bleeding, afflicts anywhere between 2-28% of patients (9-11). Not only do such outcomes burden caregivers and society in regard to healthcare resources, these outcomes can place emotional duress onto the patient and their caregivers (5, 12).

Despite the now common knowledge of poor outcomes and suboptimal quality of life suffered by many HSCR patients post-surgery, physicians and researchers only partially

understand their etiology. Recent studies in HSCR mouse models, including my study detailed in Chapter 2, have shown that the intact ENS above the area of aganglionosis is abnormal in these mice (13-16). Specifically, the balance of ENS components, or correct proportions of glia and neuronal subtypes, is skewed (13)(Chapter 2). If similar processes occur in HSCR patients, an abnormal intact ENS could partially explain changes in bowel motility as well as changes in neuromodulated inflammation. Studies in our lab are currently being conducted to evaluate ENS neuronal subtype proportions in HSCR patients and compare our findings to patient outcomes. These studies are important; however, they require extensive amounts of time, expensive reagents, and new technique development. And, even if the etiology of these outcomes becomes clearly defined, years may elapse before researchers develop and test the appropriate tissue engineering technologies or pharmaceutical therapies to target specific ENS defects. Also important, not all patients go on to develop HSCR related sequelae and some improve or worsen over time (9). Such findings suggest that other genetic and environmental factors could influence patient outcomes. Identifying such factors early in the course of the disease could help predict susceptibility of HSCR patients to such outcomes. This ability to detect patients at higher risk of developing HAEC or motility defects could aid caregivers and health care professionals by providing a guide for prophylactic treatment measures or treatment guides when unfavorable outcomes do occur.

To this end, we hypothesized that clinical variables collected from HSCR patient records could potentially inform risk for unwanted outcomes post-surgery. Some of these factors include sex, age at diagnosis, age of surgical resection, presence of other congenital anomalies, length of the aganglionic segment, family history, and pathology findings. To test this hypothesis, I defined and collected clinical data on a HSCR patient population at Monroe Carell Jr. Children's Hospital at Vanderbilt Medical Center. I used this data to characterize the pediatric HSCR patient population at Vanderbilt between January 2004-2012 and will eventually use this data to test if specific clinical variables correlate with HSCR patient outcomes.

Methods

Search Terms for Capturing HSCR Patient Population

I initially chose the following search terms—pull-through, aganglionosis and Hirschsprung—within the electronic pathology record system at the Monroe Carell Jr. Children's Hospital at Vanderbilt Medical Center to locate existing HSCR pathology specimens. I limited the search between January 2004 and January 2012 (which encompasses the oldest electronic medical records that would also potentially have "on the shelf" corresponding histology/pathology specimens to analyze.) "Pull-through" was chosen as a search term because the vast majority of HSCR pediatric patients will undergo pull-through surgery to have the aganglionic portion of their bowel removed and/or ganglionated bowel attached to the anus. Pull-through surgeries are indicated in only a few other disorders which are rare, such as imperforate anus. In the case of HSCR disease, pathologists collect interoperative biopsies during pull-through surgery to determine surgical boundaries (location of ganglionated versus aganglionated bowel.) Additionally, the surgically resected tissue undergoes full thickness biopsies post-surgery to validate surgical boundaries. Thus, most of the records captured by the search term "pull-through" were for HSCR patients with pathology specimens available for evaluation. I chose "aganglionosis" as a search term as aganglionosis of the bowel defines HSCR. However, I could not exclusively use the term aganglionosis as some pathologists use synonymous wording—such as "no ganglion cells present" or "absence of ganglia"—in their diagnosis of HSCR. I initially chose "Hirschsprung" as a search term as this term would be the most inclusive search term for capturing HSCR cases. However, while very sensitive to capturing HSCR cases, this search term was not specific. In general, pediatric patients with any GI motility disorders (obstruction, meconium plug, inflammation, etc.) will have a biopsy to "rule out Hirschsprung's." Thus, the term Hirschsprung appears in all pathology records with Hirschsprung as part of the differential diagnosis. Additionally, most of these biopsies taken to rule in or rule out HSCR were not full

thickness (through all layers of the intestine), and I would not be able to utilize them in our study. Therefore, I dropped “Hirschprung” as a search term and I captured the initial patient population with the two search terms “pull-through” and “aganglionosis.” This preliminary search led to n=90 potential HSCR cases with n=40 originating from the search term “pull-through” and n=50 originating from the search term “aganglionosis.”

Filtering for HSCR cases

All pathology records captured by the search terms “pull-through” and “aganglionosis” were manually combed and cases were further defined by meeting one or both of the following criteria:

1) Pathologist, clinical, and/or operator(ion) noted diagnosis of Hirschsprung disease
2) The terms or phrases “aganglionosis” or “no ganglion cells present” or “absence of ganglion cells” or synonymous wording within the pathologist note.

Of the initial 40 records captured by the term “pull-through,” 30 HSCR cases were validated, 4 cases were clearly not HSCR and excluded, and 6 cases were suggestive or inconclusive and warranted further investigation within the electronic medical record to verify a HSCR diagnosis. Of the initial 50 records for the term “aganglionosis,” 49 HSCR cases were validated, no cases were excluded, and 1 case was suggestive. Next, pathology record numbers were compared within and between the two search term groups to identify any duplicates or overlap that may exist. One duplicate record was found and 7 cases and 1 suggestive case overlapped between the two search term groups. Accounting for these records, n=68 HSCR cases and n=6 suggestive HSCR cases were carried through to the next filtering step. To determine if the n=6 suggestive HSCR cases were actual HSCR cases, corresponding electronic medical records (EMRs) were manually combed for these patients. Review of StarPanel EMRs revealed that n=4 of these cases were definitively HSCR cases with aganglionosis. One patient clearly had colonic

hypoganglionosis via biopsy and clinical signs and symptoms of HSCR, but no biopsy revealed overt aganglionosis. Because this case could represent a mild form of HSCR, such as ultra-short segment, it was included in this study. One suggestive case was not a HSCR case, but a pediatric patient who underwent pull-through surgery for severe ulcerative colitis. This case was excluded from the study. Given the confirmation of n=5 HSCR cases, the total number of HSCR cases carried to the next filtering step was n=73.

By comparing pathology record numbers, I could identify and eliminate duplicate or overlapping HSCR cases within or between search terms when pathology record numbers were identical. However, many HSCR patients will undergo multiple biopsies, especially if they undergo multiple surgeries to diagnose and/or treat HSCR. A unique pathology record number is assigned to the biopsies corresponding with each pathology procedure. Thus, one HSCR patient may have several pathology records. However, every patient at Vanderbilt Medical Center has a unique EMR number. Therefore, the next filtering step was to pull and compare EMR numbers within the identified HSCR cases. Correction of one incorrectly recorded EMR number along with elimination of duplicates brought the HSCR case number to n=70. This HSCR patient population was used for to determine cohort characteristics and demographics found in the results section. Figure 5.1 provides an overview of the filtering process used to define the HSCR cohort for this study.

Cohort demographics, variables, clinical outcome recordings

Study data were collected and managed using REDCap electronic data capture tools hosted at Vanderbilt University (citation). REDCap (Research Electronic Data Capture) is a secure, web-based application designed to support data capture for research studies, providing 1) an intuitive interface for validated data entry; 2) audit trails for tracking data manipulation and export procedures; 3) automated export procedures for seamless data download to common statistical packages; and 4) procedures for importing data from external sources. A list of clinical

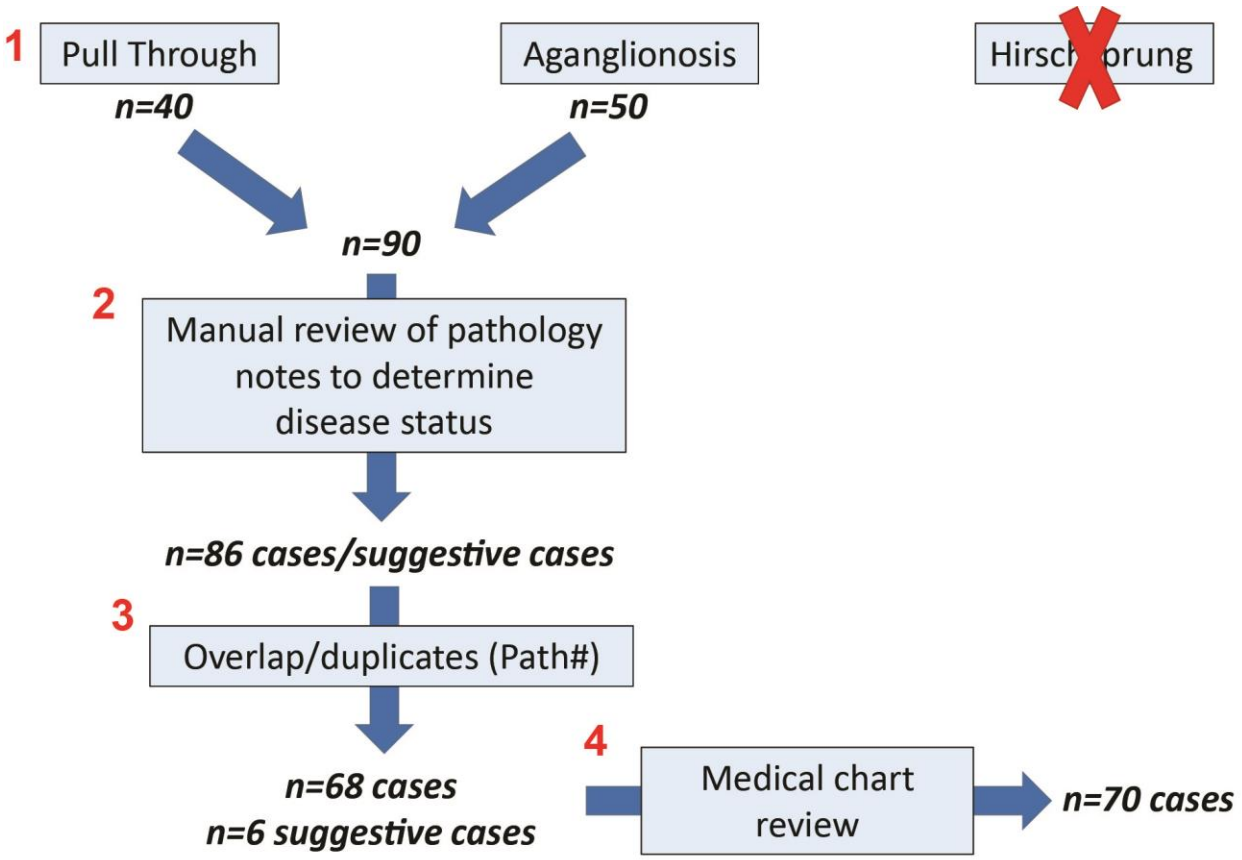

Figure 5.1. Overview of filtering process to define the HSCR patient cohort. (**1**) The search terms "pull through" and "aganglionosis" were used within the electronic pathology database at Vanderbilt University. "Hirschpsrung" was excluded as a search term due to its low specificity. (**2**) Identified pathology records were then manually combed to determine definite or probable HSCR disease status and eliminate non-HSCR cases. (**3**) HSCR patients may undergo multiple biopsies and thus be assigned multiple pathology record numbers, leading to duplicated cases. In this step, duplications and cases with overlap between the two search terms were reconciled. (**4**) Finally, any remaining discrepancies in regard to disease status or assigned medical record numbers were resolved. Thus, the final number of HSCR cases carried through for characterization was 70.

variables and outcomes collected from patient records using a custom designed data collection instrument in REDCap can be found in Table 5.1. Table 5.1 is largely a reproduction of the HAEC criteria set forth by Pastor et al. (17) with some modifications upon consultation with physicians and knowledge of material I knew should or could easily be found in the medical record.

Statistics

JMP (v10 & v11) statistical software was used for all statistical analyses. X^2 (goodness of fit) test was used to test for independence between different variables.

Study goals

The goals and focus of this study have morphed significantly since the beginning of my training. After difficulties with HSCR surgical resection staining and IHC (detailed in Chapter 7), we decided to shift the focus of this study. My main goal became running regression analysis with the collected independent clinical variables detailed above along with histological findings to determine which variables and histological findings could help predict HSCR patient long-term outcomes. Currently, histology slides from HSCR patients are being evaluated by a collaborator and this information is not available at this time. Thus, this chapter mainly serves to discuss the characteristics, known clinical variables, and outcomes of my HSCR patient cohort in anticipation of using this information for future analyses.

Results

HSCR cohort characteristics

After applying selection criteria, my HSCR cohort consisted of 70 HSCR cases with pathology and electronic medical records available. Of these 70 cases, 49 (70.0%) were males and 21 (30.0%) were females. Diagnosis of HSCR occurred in the vast majority of cases (n=49; 70.0%) near birth (less than 2 months of age) with 21 patients (30.0%) diagnosed later in life (>2

Table 5.1. HSCR cohort data collected from medical and pathological records.

Cohort Characterization Variables	Additional Details
Sex	male or female
Age of diagnosis (days)	in days
Age of initial HSCR surgery and related HSCR surgeries	in days
Initial HSCR diagnosis older than 2 mo?	
Trisomy 21	Complete? Roberstonian translocation?
Associated congenital diseases or disorders? HSCR part of a syndrome?	If genetic anomaly or syndrome noted, what one?
Family history of HSCR disease?	If so, relation to patient if noted.
Family history of Hirschsprung associated enterocolitis?	If so, relation to patient if noted.
Length of aganglionosis and transition zone?	Is the transition zone proximal to the splenic flexure?
Type of HSCR-related surgery	Swenson, Soave, Duhamel, other or not specified pull through; other
Clinical history for defining adverse outcomes	**Additional Details**
Vomiting?	
Diarrhea	Bloody? foul smelling? explosive?
Rectal bleeding without diarrhea?	
Explosive flatus?	
Fever?	
Lethargy or fatigue? (Irritability in infants?)	
Decreased peripheral perfusion?	
Distended abdomen?	
Abdomen tender to touch or palpation?	
Complaint of abdominal pain?	
Tachycardia?	
Hypotension?	
Explosive discharge of gas or stool upon rectal examination?	
Perianal excoriation present or noted?	
Lab findings	Leukocytosis, shift to left, bacteremia on blood culture, C. diff found in stool culture, other known pathogen grown from stool culture, any findings indicating enterocolitis
Radiological findings	Cutoff sign in the rectosigmoid region with absence of air distally, dilated loops of bowel, multiple air fluid levels, pneumatosis intestinalis, sawtooth appearance with irregular mucosal lining, perforated bowel
Additional biopsy findings (not HSCR surgery biopsies)	crypt dilatation, crypt abscesses, crypt with retained mucin, destruction of intestinal epithelium, transluminal necrosis or perforation, fibrinopurulent debris and mucosal ulceration, other enterocolitis related findings
Preventative/prophylactic measures?	Antibiotics, rectal washouts, probiotics, other
Treatment for stricture?	Myomectomy, myotomy, dilatation(s), botox injections, other
Did patient have known pre-operative enterocolitis?	Number of episodes?
Documented hospitalization for gastritis or enterocolitis?	
Documented occurrence of constipation? Incontinence?	
Medications (relating to intestine)	Broad spectrum antibiotics, ampicillin, gentamicin, metronidazole, vancomycin, fluconazole, norfloxacin, miralax, sodium cromoglycate, other
Other pertinent medical procedures, medications, or clinical information?	Specifically, factors that may influence or confound this study.

months of age). Typically, patients underwent their first HSCR-related surgery at a young age and close to time of diagnosis. As expected with current standard of care, almost all patients underwent a surgical pull-through procedure such as a one-stage pull-through procedure or a two-stage procedure with an initial colostomy and subsequent pull down at a later stage (n=64; 91.4%). Usually, the aganglionic segment was limited to the colon distal to the splenic flexure (n=54; 78.3%) Table 5.2 & Table 5.3 provide summaries and details in regard to these characteristics.

Table 5.2. HSCR cohort overview.

Characteristic	***n (%)***	
Sex (male/female)	49 (70.0%) / 21(30.0%)	
Trisomy 21	9 (12.9%)	
*Associated congenital disorder or disease	20 (28.6%)	
	median (range)	***average***
#Age at diagnosis (days)	7 (1 - 5839)	291
#Age of first HSCR-related surgery (days)	3 (10 - 5878)	310

*The associated congenital disorder or disease includes Trisomy 21 (Down Sydnrome) cases.
#One HSCR case was excluded from this data as the patient never underwent surgery.

Because HSCR disease segregates in families and positive family history could correlate with ultimate outcomes, I also recorded family history of HSCR when available. Within our cohort, 9 patients (12.9%) had a positive family history of HSCR. The other 61 patients either had a note in their record that stated no family history of HSCR or the family history was unknown (Table 5.3).

Table 5.3. Occurence of known or possible risk factors for adverse outcomes in a HSCR cohort.

Risk Factor	*Yes*	*No/Unknown*
Family History of HD	9 (12.9%)	61 (87.1%)
Family History of HAEC	2 (2.9%)	68 (97.1%)
Transition zone proximal to splenic flexure?	15 (21.4%)	55 (78.6%)
Initial HD diagnosis after 2 months of age?	21 (30%)	49 (70.0%)
Known pre-operative enterocolitis episode(s)?	17 (24.3%)	53 (75.7%)
Pull through surgery	64 (91.4%)	[$]6 (8.6%)

Data is presented as number of cases (percent of cases).
[$]This number includes cases where surgery type was unclear, other surgical procedures outside of pull through, as well as one case that did not undergo surgery.

HSCR in the context of other congenital disease & disorders

HSCR disease most often occurs as an isolated trait, but can occur as part of a syndromic disease. Many of the syndromic diseases that can occur with HSCR are rare, such as Congenital Central Hypoventilation Disorder (CCHD), while others are more common, such as Down Syndrome (DS). And interestingly, HSCR disease presents often in patients with Down Syndrome affecting 2.62% of all DS patients (18). This phenomenon is in stark contrast to the general population, where roughly 1 in 5000, or 0.02%, are affected with HSCR (19). In HSCR patient cohorts from other studies, the co-occurrence of DS and HSCR varies, but averages at 7.32% (18). In our study, DS patients accounted for 12.9%, or 9 out of 70 cases (Table 5.3). Of these cases, 8 were male and 1 was female. Interestingly, in our DS cases with HSCR disease, 7 of 9 (77.8%) had additional congenital heart defects and 6 of 9 (66.7%) had congenital hypothyroidism diagnoses (Table 5.4; Figure 5.2). These percentages are well above the average rates of congenital heart defects (44%)(20) and hypothyroidism (10-16%) (21, 22) reported in DS children, although a very recent study argues rates might be higher (23). Given the disparate rates of congenital heart defects and congenital hypothyroidism in our patient cohort compared to the DS

Table 5.4. Additional congenital anomalies identified in Down Syndrome patients within HSCR cohort

DS Case #	Sex	Accompanying Disorder(s)
1	M	Congenital heart defect(s); Congenital hypothyroid
2	M	Congenital heart defect(s); Bilateral hydronephrosis
3	M	Congenital heart defect(s); Congenital hypothyroid
4	M	Congenital heart defect(s); Congenital hypothyroid
5	M	Congenital hypothyroid
6	M	Congenital heart defect(s)
7	M	Congenital heart defect(s); Congenital hypothyroid
8	F	Congenital heart defect(s); Congenital hypothyroid
9	M	None

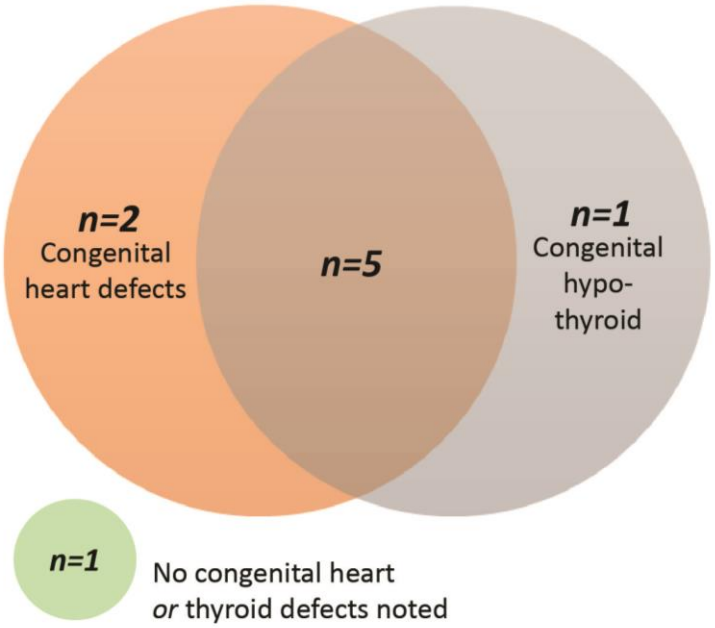

Figure 5.2. Overlap in congenital anomalies identifed in Down Syndrome patients with Hirschsprung Disease. We identified 9 cases of Down Syndrome within our HSCR cohort. Of those 9 cases, 8 were diagnosed with congenital heart defects and/or congenital hypothyroid (red and blue circles). These rates of congenital anomalies in the context of HSCR and DS significantly deviate from the rates ofthese congenital anomalies in the DS population in general (congenital heart defect *$P<0.5$; congenital hypothyroid *$P<0.001$)

population as a whole, I tested the association of HSCR disease in DS patients with the occurrence of congenital heart defects or congenital hypothyroidism in DS patients. I found that the occurrence of HSCR and congenital heart defects in DS patients was not independent. (*$P<0.05$) Additionally, the occurrence of HSCR and congenital hypothyroidism was not mutually exclusive. (*$P<0.0001$).

Outside of DS, I found 12 (17.1%) HSCR patients diagnosed with other congenital or developmental diseases and disorders. Five of these cases involved congenital heart defects and two cases involved left renal agenesis. Two of the cases had identified genetic anomalies, possibly explaining the occurrence of HSCR as well. Table 5.5 summarizes these cases and other anomalies, such as Goldenhar syndrome and chordee that may or may not relate to HSCR occurrence.

Table 5.5. Additional congenital anomalies identified in patients with HSCR.

Case #	Sex	Accompanying Disorder(s)
1	F	Coarctation of the aorta
*2	F	Coanal atresia; micrognathia; developmental delay
3	F	Right sided aortic arch, aberrant left subclavian, patent foramen ovale
4	F	Ventral septal defect
5	F	Patent ductus arteriosus
6	F	Left renal agenesis
7	M	Strabismus; abnormal facies; pyloric stenosis
8	M	Patent foramen ovale
9	M	Chordee with offset prepuce; tongue tie
10	M	Goldenhar syndrome
#11	M	Left renal agenesis; pulmonary stenosis

*Duplication of part of chromosome 4 identified
#Partial deletion of chromosome 15 long arm (includes CATSPER gene which is needed for sperm motility; loss of this gene leads to infertility and sensoryneural deafness)

HSCR cohort adverse outcomes

One difficulty in reporting HSCR patient outcomes revolves around defining an adverse event. During the course of this study, I had difficulties calling chronic constipation and fecal soiling based on medical chart information alone. Although I found numerous reports of constipation (brief and chronic) within the records, healthcare providers routinely recommended laxatives for use after surgery should any issues with constipation occur. We should applaud awareness of this possible outcome and the preventative measures taken. But, for our purposes, the broad use of laxatives would presumably lead to a gross under estimation of the rates of patients who ever report to their physicians with constipation. In this study, constipation or other motility issues were clearly noted within the medical note or communications for 28.6% of HSCR patients. However, I did not attempt to test for association or correlations between constipation and other clinical variables due to the ambiguity and probable underestimation of motility deficit prevalence in my HSCR cohort.

Defining Hirschsprung-associated enterocolitis (HAEC) came with issues as well, highlighting typical issues encountered in a retrospective study. One issue is that a definition for HAEC has not been agreed upon by the field. Pastor et al (17) recently devised a classification system for defining presence or absence of HAEC occurrence in HSCR patients. While reviewing medical charts, I collected the same variables proposed by Pastor and colleagues to aid in defining HAEC occurrence as well as pertinent data already known to influence HAEC risk (24, 25) (Table 5.1). I defined HSCR patients matching the criteria put forth by Pastor as HAEC cases. However, the medical charts did not always contain all the variables presented in Pastor's study. Thus, when I relied on these variables alone, I ran into a too conservative, unrealistic definition of HAEC which could under power future statistical modeling. Furthermore, the goal of this study is to identify patients who may experience poor outcomes, including patients who may not meet the strict criteria proposed by Pastor (17). Therefore, I adopted a more liberal definition of HAEC by also defining HAEC cases as any HSCR patient hospitalized with a diagnosis of

gastritis or enterocolitis or Hirschsrpung associated-enterocolitis. Given this broader definition of enterocolitis, I found that 18 HSCR patients (25.7%) within our HSCR cohort met the definition of HAEC. An additional 14 patients (20.0%) probably had bouts of HAEC, but the lack of information in the record, presence of comorbidities, and young age precluded me from conclusively categorizing them as HAEC cases. Also, several patients were lost to follow up or only followed shortly at Vanderbilt, leaving their HAEC status unknown.

Discussion

HSCR is defined as absence of ganglia throughout a variable length of distal colon and removal of the aganglionic portion of the bowel is the gold standard for HSCR treatment. Despite successful surgeries, many HSCR patients will suffer from short term or chronic fecal incontinence, constipation, and episodes of enterocolitis. To determine what factors might affect post-surgical outcome risk, I defined a HSCR patient cohort at the Monroe Carell Jr. Children's Hospital at Vanderbilt Medical Center. Application of the search terms "pull-through" and "aganglionosis" as well as manual combing of electronic pathology and medical records led to successful identification of 70 HSCR cases between January 2004 and January 2012. Clinical information and outcomes collected from patient records are poised for future regression analysis as we await histology evaluations. Characterization of our HSCR cohort revealed similarities in regard to demographics and clinical features previously characterized in other HSCR cohorts (19, 26) and also informed us of current medical practices and assumptions that healthcare providers may need to take into consideration. The following paragraphs provide discussion centering on this information.

HSCR—All in the family?

Within our HSCR cohort, nine patients (12.9%) reported a positive family history of HSCR. I struggled to find published percentages for isolated HSCR cases compared to familial HSCR

cases in the literature. This phenomenon can be partially explained by the relatively short time period since HSCR pull-through operations have existed. Additionally, from what I observed in the medical charts, any reporting of "isolated" occurrences called from medical records could be seriously flawed. Most medical records I observed within the system did not record the pertinent negative—no family history of HSCR disease. This finding could possibly indicate that health providers did not ask family members about HSCR family history. This possibility is certainly plausible—given the rare nature of the disease, many medical personnel probably do not realize the genetic components or heritability of the disease. Only within the last century did physicians discover the cause of HSCR and implement successful surgical procedures to save lives. Before the option of surgical intervention, the incomplete penetrance of this disease permitted the transmission of HSCR mutations through families to go largely unnoticed. However, in the near past and present, survival and subsequent passing on of genes by HSCR patients may reveal that HSCR is in fact more familial than sporadic.

This finding has key implications in regard to another finding in my study. In general, the clinical workup for the vast majority of HSCR cases in our study did not indicate genetic testing or counseling for the patients or their relatives. Because our study was retrospective in nature and patients and family could not be interviewed, the number of cases that involved genetic testing or counseling could be underestimated. However, this scenario is unlikely given that the majority of patients remained at Vanderbilt for follow-up care. Furthermore, in recent history, genetic testing for HSCR disease has not been encouraged given that the mutation rarely changes the treatment plan (unless within *RET* which can carry an additional risk for MEN2A syndrome). Additional considerations discouraging genetic testing include costs of testing, the presence of mutations in several genes and regulatory regions that can drive the disease, and the fact that many genetic mutations and/or modifiers driving HSCR disease are probably still unknown. Despite current discouragement for genetic testing in HSCR disease, the high occurrence of congenital anomalies with HSCR, familial risk, and a better understanding of the genes and

pathways contributing to HSCR is apt to eventually force genetic testing into the picture. If anything, HSCR patient families should undergo genetic counseling to understand familial risk and the likelihood of other congenital anomalies. Additionally, any physician treating a HSCR patient should keep in mind comorbidities that can occur with HSCR. Prato and colleagues (26) recently proposed a diagnostic work up for HSCR patients that takes into account the high occurrence of congenital anomalies that accompany HSCR disease (Figure 5.3). The co-occurrence of HSCR with other congenital anomalies is explored in more detail in the following paragraphs.

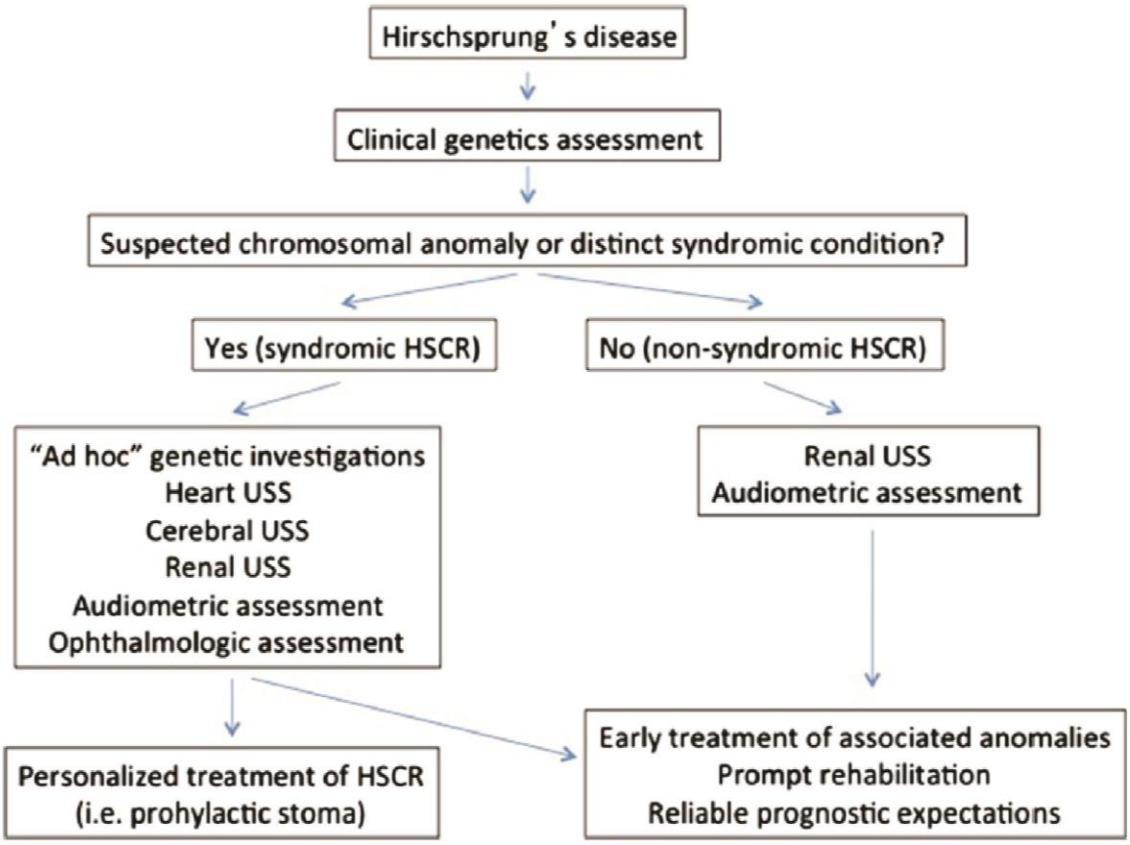

Figure 5.3. Proposed diagnostics workup for patients with HSCR. This diagram details proposed steps for physicians when assessing patients with diagnosed HSCR. Although not common practice, such steps should be taken in the light of the common co-occurence of other congenital anomalies with HSCR. This figure was adapted from Prato et. al., (2013).

HSCR & Down Syndrome (DS)

Some of the syndromic diseases that can occur with HSCR are quite rare, such as Congenital Central Hypoventilation Disorder (CCHD), while others are more common, such as Down Syndrome (DS). Interestingly, HSCR disease occurs more often in patients with Down Syndrome (DS), affecting 2.62% of all DS patients (18). This is in stark contrast to the general population, with an average incidence of 1 in 5000, or 0.02% (19). Several studies have noted the co-occurrence of DS and HSCR and although studies differ, DS and HSCR appear together in HSCR patient cohorts on average 7.32% of the time (18). Although the incidence of DS and HSCR in my study was slightly higher at 12.32%, this percent falls within published ranges (18).

The high rate of HSCR in DS patients comes as no surprise given that DS affects many NC-derived structures. For example, all DS patients have the characteristic craniofacial abnormalities, suggesting disturbance of cranial neural crest development and contribution to facial bones. Other DS comorbidities that do not occur in all DS patients, such as congenital hypothyroidism and congenital heart defects, can be linked to disturbances in NC development as the NC contributes extensively to the thyroid as well as the septum and great vessels of the heart respectively. Despite a small sample size, I found that HSCR, congenital heart defects and congenital hypothyroidism tend to present together in the context of DS. From a developmental perspective, one could expect the presence of these three congenital anomalies to happen together more often than not. The NCC that contribute to cardiac structures, the thyroid, and the ENS all originate from the vagal NC population. More explicitly, the cardiac NCC, which contribute to cardiac structures and the thyroid, is a subset of the vagal NC population. Thus, large perturbations to the vagal NC population could reasonably affect all structures the vagal NC contribute to. Although practicing clinicians are probably well versed in the risks of congenital heart defects and hypothyroidism in the DS population, our study suggests that clinicians should be hypervigilant when checking for congenital heart defects and congenital hypothyroidism when treating DS patients presenting with HSCR.

HSCR & other congenital disorders

Corroborating previous studies (19, 26, 27), I found 17.1% of HSCR patients presenting with other congenital anomalies—including congenital heart defects, abnormal facies, strabismus and left renal agenesis (Table 5.5). Interestingly, renal agenesis is typically associated with mutations in *RET* on chromosome 10 (28). One of our patients with left renal agenesis displayed a partial deletion of chromosome 4, but whether this deletion contributed to the HSCR or the left renal agenesis is unknown. I did not locate any genetic studies in the clinical history of the other HSCR patient with left renal agenesis, but a positive family history of HSCR disease could indicate a *RET* mutation driven phenotype. I found one HSCR patient with pervasive developmental disorder, but who had not undergone genetic testing. Interestingly, two case reports have noted a 20p deletion in patients exhibiting HSCR and autism (29, 30). In regard to other findings in Table 5.5, I did not find in the literature any connections of HSCR with chordee and only one unavailable case study from Poland suggests a patient with Goldenhar syndrome and HSCR.

Adverse outcomes

Although outcomes such as HAEC and constipation proved difficult to clearly define in our study, my findings for conclusive HAEC cases (25.7%) and constipation/motility issues (28.6%) falls within or near formerly published ranges of 5-30% (7-9) and 2-28% (9-11) respectively. The lack of a standard outcome criteria in the field underlies the ambiguity in defining poor outcomes (17). While many studies rely on questionnaires to HSCR patients or their family members to determine HSCR outcomes, a limitation of this study is the reliance of medical records to determine outcomes. At the same time, medical record review strengthens this study by eliminating selection and response bias. Regardless, a clear definition for HAEC is required before statistical modeling. One option for including definite and suggestive HAEC in one's model would be to assign differing likelihood or severity values to each case before running analysis. Although this type of analysis runs the risk of overfitting, this type of value assignment could help

add power to the study by permitting “suggestive” HAEC cases inclusion in the analysis and thus increasing sample size.

Overall, this study presents a method for defining a HSCR patient cohort with accompanying medical and pathology records within the Vanderbilt Medical Center that other institutions could feasibly apply in their own patient populations. Comparison of the demographic and clinical variables collected from this HSCR cohort to other previously published HSCR cohorts yielded comparable findings, suggesting satisfactory search criteria and data collection methods. In the future, the clinical data presented herein as well as additional histological findings in this HSCR cohort will serve as variables within a regression analysis study to determine what factors can readily predict patient outcome risks. Findings from this analysis should guide healthcare provider clinical practices and thus provide better care for HSCR patients.

References

1. Skaba, R. 2007. Historic milestones of Hirschsprung's disease (commemorating the 90th anniversary of Professor Harald Hirschsprung's death). *J Pediatr Surg* 42:249-251.
2. Duhamel, B. 1960. [A new surgical procedure for the treatment of Hirschsprung's disease: the exclusion of the rectum with retrorectal and transanal lowering of the colon]. *Langenbecks Arch Klin Chir Ver Dtsch Z Chir* 296:384-388.
3. Soave, F. 1964. A New Surgical Technique for Treatment of Hirschsprung's Disease. *Surgery* 56:1007-1014.
4. Swenson, O., and Bill, A.H., Jr. 1948. Resection of rectum and rectosigmoid with preservation of the sphincter for benign spastic lesions producing megacolon; an experimental study. *Surgery* 24:212-220.
5. Diseth, T.H., Bjornland, K., Novik, T.S., and Emblem, R. 1997. Bowel function, mental health, and psychosocial function in adolescents with Hirschsprung's disease. *Arch Dis Child* 76:100-106.
6. Bai, Y., Chen, H., Hao, J., Huang, Y., and Wang, W. 2002. Long-term outcome and quality of life after the Swenson procedure for Hirschsprung's disease. *J Pediatr Surg* 37:639-642.
7. Jarvi, K., Laitakari, E.M., Koivusalo, A., Rintala, R.J., and Pakarinen, M.P. 2010. Bowel function and gastrointestinal quality of life among adults operated for Hirschsprung disease during childhood: a population-based study. *Ann Surg* 252:977-981.
8. Ieiri, S., Nakatsuji, T., Akiyoshi, J., Higashi, M., Hashizume, M., Suita, S., and Taguchi, T. 2010. Long-term outcomes and the quality of life of Hirschsprung disease in adolescents who have reached 18 years or older--a 47-year single-institute experience. *J Pediatr Surg* 45:2398-2402.

9. Rintala, R.J., and Pakarinen, M.P. 2012. Long-term outcomes of Hirschsprung's disease. *Semin Pediatr Surg* 21:336-343.

10. Teitelbaum, D.H., and Coran, A.G. 1998. Enterocolitis. *Semin Pediatr Surg* 7:162-169.

11. El-Sawaf, M., Siddiqui, S., Mahmoud, M., Drongowski, R., and Teitelbaum, D.H. 2013. Probiotic prophylaxis after pullthrough for Hirschsprung disease to reduce incidence of enterocolitis: a prospective, randomized, double-blind, placebo-controlled, multicenter trial. *J Pediatr Surg* 48:111-117.

12. Hartman, E.E., Oort, F.J., Aronson, D.C., Hanneman, M.J., van der Zee, D.C., Rieu, P.N., Madern, G.C., De Langen, Z.J., van Heurn, L.W., van Silfhout-Bezemer, M., et al. 2004. Critical factors affecting quality of life of adult patients with anorectal malformations or Hirschsprung's disease. *Am J Gastroenterol* 99:907-913.

13. Zaitoun, I., Erickson, C.S., Barlow, A.J., Klein, T.R., Heneghan, A.F., Pierre, J.F., Epstein, M.L., and Gosain, A. 2013. Altered neuronal density and neurotransmitter expression in the ganglionated region of Ednrb null mice: implications for Hirschsprung's disease. *Neurogastroenterol Motil* 25:e233-244.

14. Roberts, R.R., Bornstein, J.C., Bergner, A.J., and Young, H.M. 2008. Disturbances of colonic motility in mouse models of Hirschsprung's disease. *Am J Physiol Gastrointest Liver Physiol* 294:G996-G1008.

15. Ro, S., Hwang, S.J., Muto, M., Jewett, W.K., and Spencer, N.J. 2006. Anatomic modifications in the enteric nervous system of piebald mice and physiological consequences to colonic motor activity. *Am J Physiol Gastrointest Liver Physiol* 290:G710-718.

16. Sandgren, K., Larsson, L.T., and Ekblad, E. 2002. Widespread changes in neurotransmitter expression and number of enteric neurons and interstitial cells of Cajal in lethal spotted mice: an explanation for persisting dysmotility after operation for Hirschsprung's disease? *Dig Dis Sci* 47:1049-1064.

17. Pastor, A.C., Osman, F., Teitelbaum, D.H., Caty, M.G., and Langer, J.C. 2009. Development of a standardized definition for Hirschsprung's-associated enterocolitis: a Delphi analysis. *J Pediatr Surg* 44:251-256.

18. Friedmacher, F., and Puri, P. 2013. Hirschsprung's disease associated with Down syndrome: a meta-analysis of incidence, functional outcomes and mortality. *Pediatr Surg Int* 29:937-946.

19. Amiel, J., Sproat-Emison, E., Garcia-Barcelo, M., Lantieri, F., Burzynski, G., Borrego, S., Pelet, A., Arnold, S., Miao, X., Griseri, P., et al. 2008. Hirschsprung disease, associated syndromes and genetics: a review. *J Med Genet* 45:1-14.

20. Freeman, S.B., Bean, L.H., Allen, E.G., Tinker, S.W., Locke, A.E., Druschel, C., Hobbs, C.A., Romitti, P.A., Royle, M.H., Torfs, C.P., et al. 2008. Ethnicity, sex, and the incidence of congenital heart defects: a report from the National Down Syndrome Project. *Genet Med* 10:173-180.

21. Stirn Kranjc, B. 2012. Ocular abnormalities and systemic disease in Down syndrome. *Strabismus* 20:74-77.

22. Jaruratanasirikul, S., Patarakijvanich, N., and Patanapisarnsak, C. 1998. The association of congenital hypothyroidism and congenital gastrointestinal anomalies in Down's syndrome infants. *J Pediatr Endocrinol Metab* 11:241-246.

23. Purdy, I.B., Singh, N., Brown, W.L., Vangala, S., and Devaskar, U.P. 2014. Revisiting early hypothyroidism screening in infants with Down syndrome. *J Perinatol*.

24. Laughlin, D.M., Friedmacher, F., and Puri, P. 2012. Total colonic aganglionosis: a systematic review and meta-analysis of long-term clinical outcome. *Pediatr Surg Int* 28:773-779.

25. Menezes, M., Pini Prato, A., Jasonni, V., and Puri, P. 2008. Long-term clinical outcome in patients with total colonic aganglionosis: a 31-year review. *J Pediatr Surg* 43:1696-1699.

26. Pini Prato, A., Rossi, V., Mosconi, M., Holm, C., Lantieri, F., Griseri, P., Ceccherini, I., Mavilio, D., Jasonni, V., Tuo, G., et al. 2013. A prospective observational study of associated anomalies in Hirschsprung's disease. *Orphanet J Rare Dis* 8:184.

27. Pini Prato, A., Gentilino, V., Giunta, C., Avanzini, S., Mattioli, G., Parodi, S., Martucciello, G., and Jasonni, V. 2008. Hirschsprung disease: do risk factors of poor surgical outcome exist? *J Pediatr Surg* 43:612-619.

28. Jain, S. 2009. The many faces of RET dysfunction in kidney. *Organogenesis* 5:177-190.

29. Michaelis, R.C., Skinner, S.A., Deason, R., Skinner, C., Moore, C.L., and Phelan, M.C. 1997. Intersitial deletion of 20p: new candidate region for Hirschsprung disease and autism? *Am J Med Genet* 71:298-304.

30. Garcia-Heras, J., Kilani, R.A., Martin, R.A., and Lamp, S. 2005. A deletion of proximal 20p inherited from a normal mosaic carrier mother in a newborn with panhypopituitarism and craniofacial dysmorphism. *Clin Dysmorphol* 14:137-140.

CHAPTER VI

DISCRETE POPULATIONS OF NEURAL CREST CELLS CONTRIBUTE TO THE ENS

Introduction

Early studies assessing NC cell migration and contributions to the ENS led scientists to believe that the ENS is totally NC derived (1-4). However, more recent studies have suggested that cells from the ventral region of the neural tube may also be contributing to peripheral nervous system components long believed to be only NC-derived. These cells, termed VENT cells by their discoverers, have been shown in avian species to contribute to numerous cranial nerves (5, 6), the otic vesicle (7), and the ENS (8). However, if these cells exist in mammals and whether they contribute to the ENS is not known.

Stepping away from VENT cells, many questions surround NC subpopulations. It is known that certain regions of the NC (cranial, vagal, lumbar, etc.) innervate specific organs and give rise to certain cell types. But defining subpopulations within these spatially defined groups is novel work. Within vagal and sacral enteric NC-derived cell populations, an outstanding question exists—how “stem-like” or specified are NC-cells as they migrate from the neural tube to different regions of the gut? One extreme hypothesis is that all enteric neural progenitors (ENPs) are equal in their ability to give rise to different neuron types and glia until they reach the end of their migration in the intestine. However, as the ENS field has progressed, studies have shown that the NC-derived cells that populate the gut may not show equal potency, or ability to differentiate into different cell types. For example, it was long thought that all enteric bound ENPs express Nestin and Ednrb. However, Lei and colleagues demonstrated that a *Nestin* independent population of ENPs exists and that this population can partially rescue ENS development when Hand2 expressing-Nestin dependent cells are genetically ablated (9). Mundell et. al., determined that not all ENPs require a well known *Ednrb* enhancer region. These *Ednrb* enhancer

independent ENPs are also able to partially compensate for deficits in the ENS when *Ednrb* enhancer dependent NC cells are genetically ablated (10).

Early in my studies, I noticed regions of the ENS in P17-20 *Sox10*-Cre; *R26R*^{tdTom} mice (with or without the *Sox10Dom* mutation) where reporter expression was not evident. Indeed, certain areas of the intestine are known to contain no or very few neurons and only nerve fibers, such as Peyer's patches (11, 12) (Figure 6.1). However, in my studies, I noted consistent areas with particular patterning that had no or little reporter expression and that were not within Peyer's patches (Figure 6.2). IHC with a marker specific for neurons (Hu) revealed neurons in these areas (Figure 6.3). Interestingly, these areas seemed to be expanded and more prevalent in older animals. Given the recent studies detailed above as well as my own findings, we hypothesized that these areas could contain neural cell types deriving from VENT populations or a Sox10 independent NC population.

To test this hypothesis, I evaluated for presence or absence of enteric neurons in mutant *Foxd3*$^{flox/-}$*; Wnt1*-Cre mice, where NC specific ablation of *Foxd3* leads to supposed loss of all NC-derived ENS components (13). Absence of enteric neurons in the small and large intestine suggested that ENPs are entirely NC derived or that non-NC cell populations contributing to ENS rely on similar genetic signaling pathways as NCC. However, presence of neurons in the stomach of some of mutants with NC specific Foxd3 ablation at early embryonic stages revealed a previously unrecognized NCC population that was not dependent upon Foxd3 for early migration, but ultimately required for survival.

Methods

Animals

Timed crosses were performed between *Foxd3*$^{flox/flox}$*; R26R*$^{YFP/YFP}$ and *Foxd3*$^{+/-}$*; Wnt1*-Cre mice to generate embryos with genetically ablated NC-derived ENPs. Crosses were performed

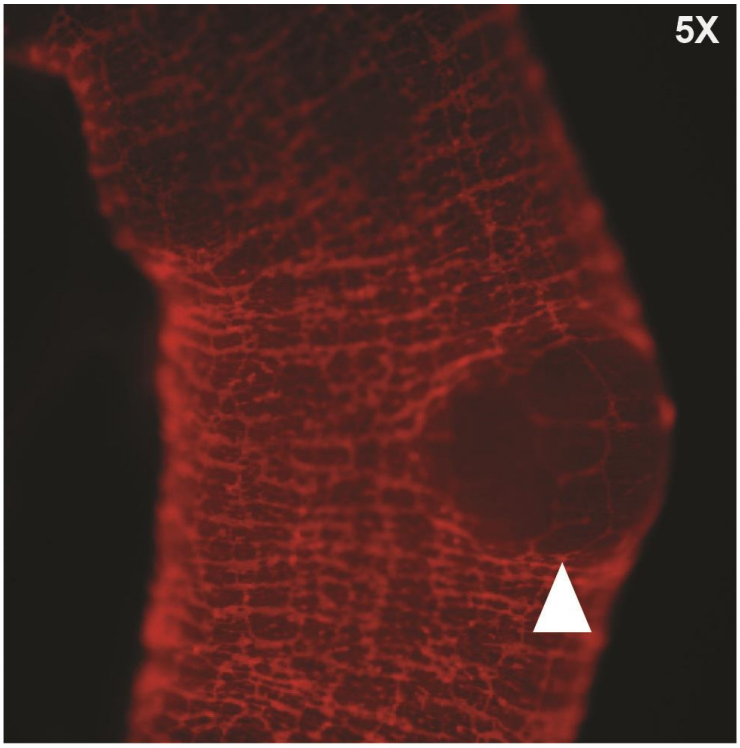

Figure 6.1. Peyer's patches are sparsely innervated. In this wholemount colon, *Sox10*-Cre transgene driven expression of the $R26R^{tdTom}$ can be clearly seen throughout the ENS. Peyer's patches tend to be sparsely innervated, with few neurons but many nerve fibers located throughout the lymphoid structure (arrow).

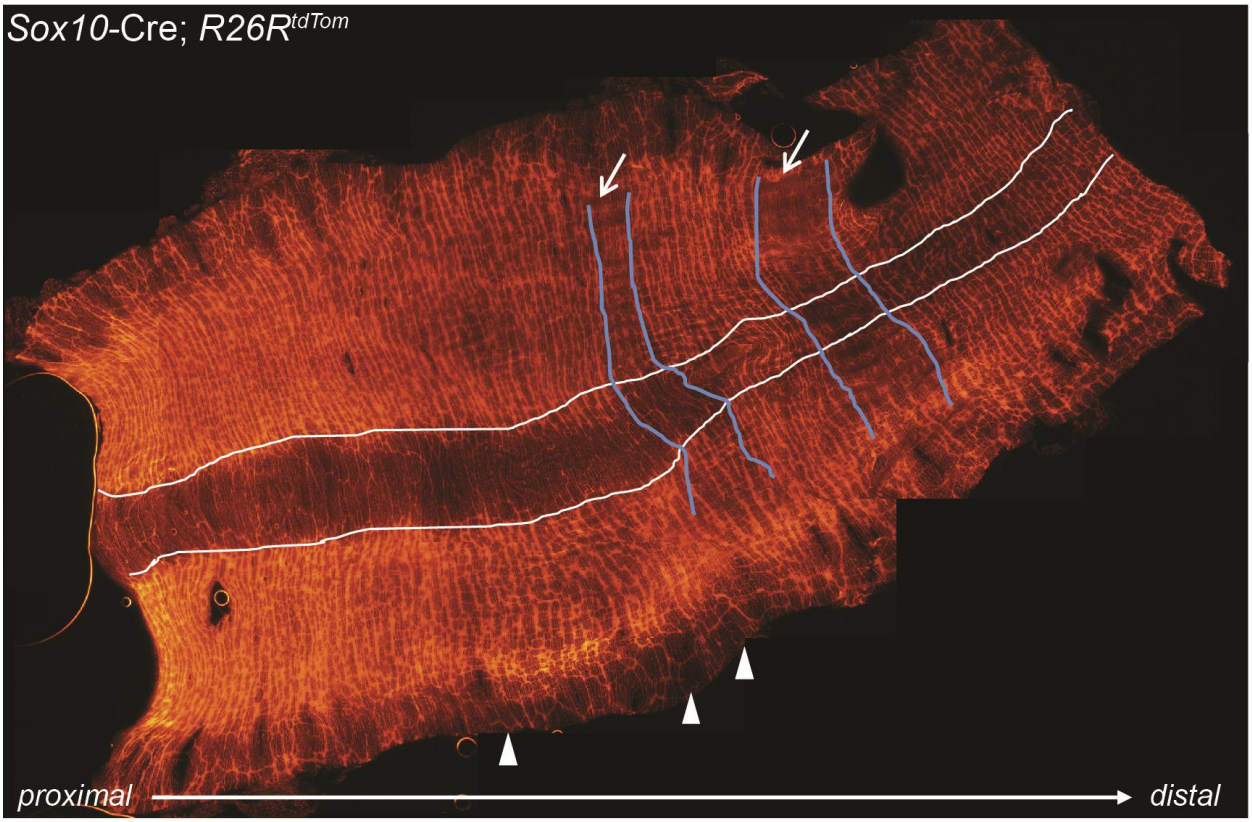

Figure 6.2. Overview of *Sox10*-Cre driven *R26R*^{tdTom} expression in the colon. TdTomato reporter expression in the ENS is observed throughout the vast majority of colon. ENS is present and expresses the tdTomato reporter but is less dense along the anti-mesenteric line (arrowheads) as well as the mesenteric line (area between solid white lines). This is particularly obvious in more proximal regions of the colon. Thin stripes of low or no tdTomato expression are seen in banded patterns, pointed out by the arrows and between the blue lines. These areas typically contained neurons with little or no tdTomato expression. Additionally, they were rare in younger pups (P15-17) but were increased dramatically in number in older pups (P18-21). This image is a tiled composite of multiple images.

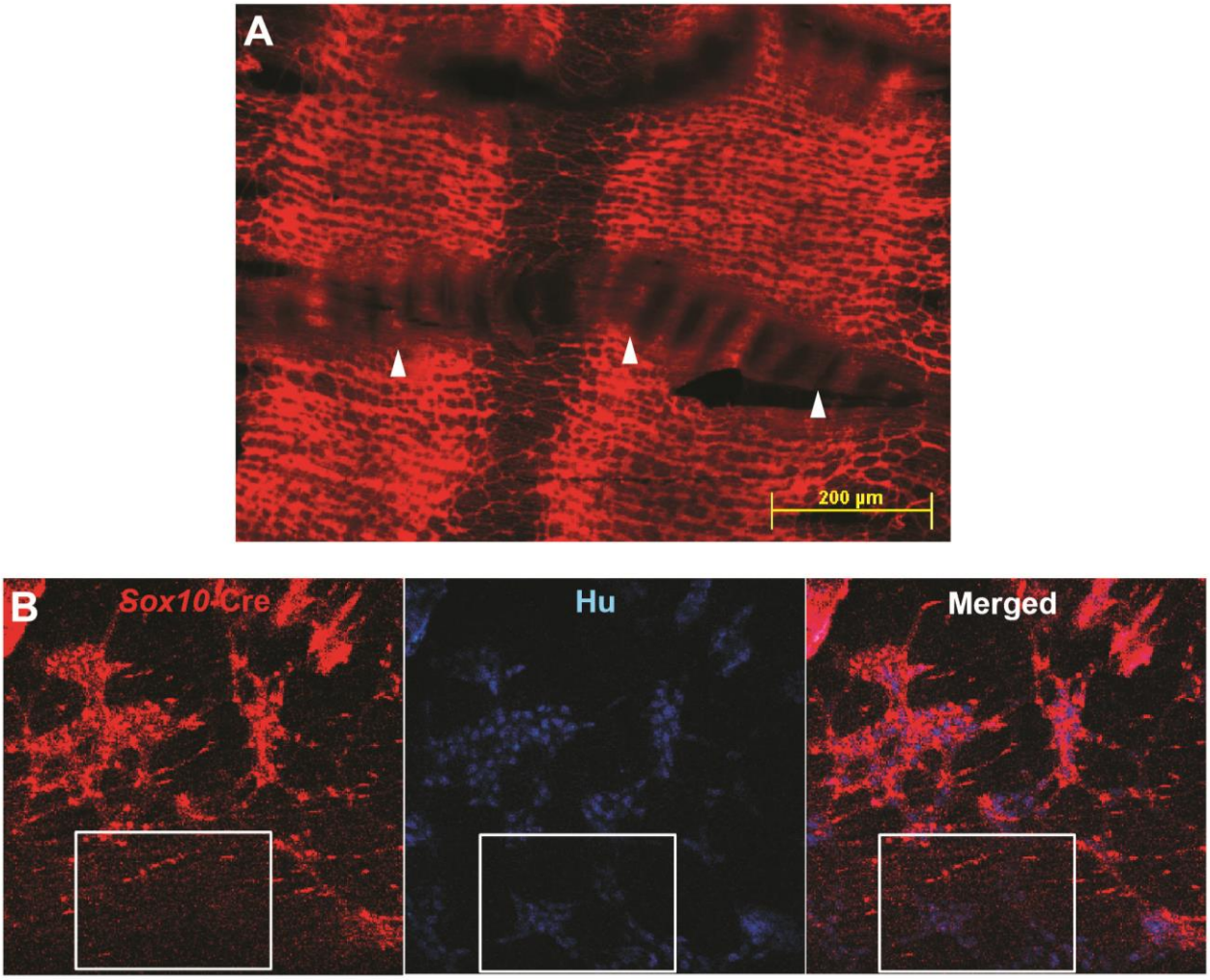

Figure 6.3. Absence of *Sox10*-Cre driven reporter expression in colonic enteric neurons. (**A**) In the colon, *Sox10*-Cre driven tdTomato expression is absent in bands with specific patterning (arrowheads). These areas could be found in the small intestine, but were quite rare. (**B**) IHC with a Hu antibody revealed that these areas are not missing ENS components, but in fact contain neurons at what appears to be a normal density (inset boxes).

and pregnant females were kindly provided by the T. Labosky lab. For all mice, the morning of plug formation was designated as E 0.5.

Dissections and IHC

Pregnant females were sacrificed with isoflurane followed by cervical dislocation and embryos were collected and immediately placed in cold 1XPBS. Mutants were noted by craniofacial features (13). Pups were then decapitated and tail/limb buds were collected for genotyping. Since I obtained experimental mice from a lab that was closing their mouse colony, I was limited to a small sample size for each age tested. Total number of embryos from pregnant dams received along with their embryonic age and genotype can be found in (Table 6.1).

Table 6.1. Summary of *Foxd3*$^{flow/+}$; *Wnt1*-Cre (control) and *Foxd3*$^{flox/-}$; *Wnt1*-Cre (mutant) embyros received for ENS analysis.

Age	Control	Mutant
E14.5	2	4
E16.5	10	2
E17.5	6	4

For each embryo, the abdominal cavity was fully opened. To remove as much intact GI tract as possible, the esophagus was first gently, but firmly, tugged loose. Most of the time, this firm tugging resulted in the entire esophagus remaining intact, although sometimes the esophagus did tear. Next, perianal tissue was cut loose from the rest of the embryo without disturbing the anus. Then, the whole GI tract was pulled gently away from the peritoneal cavity. This was best accomplished by using forceps to scoop behind the liver and using the liver and the kidneys as a barrier between the forceps and the GI tract as the entire peritoneal contents was pulled from the embryo. Once the GI tract and other organs and tissue had been scooped

from the peritoneal cavity, forceps were used to gently remove extraneous organs and tissue from the GI tract. The mesentery was cut to allow the GI tract to uncoil. Following complete isolation of the GI tract for each pup, entire guts were fixed in sterile filtered 4% PFA for at least 4 hours at 4°C. After fixation, guts were rinsed in 1XPBS for at least 10 min at RT followed by two rinses in 1XPBS/0.1% Triton X-100 for at least 10 min/rinse. Next, samples were blocked for at least 1 hr at RT in NDS block (0.1 g BSA, 0.5 mL Normal Donkey Serum, 9.5 mL 1XPBS/0.1% Triton X-100.) Guts were then subjected to incubation in 1:800 Hu antibody dilution (gift of V. Lennon through M. Epstein) in NDS block O/N at 4°C. The next day, guts were rinsed four times in 1XPBS/0.1% Triton X-100 for at least 10 min/rinse followed by incubation in chick anti-GFP antibody (Abcam, Cat. No. AB13970) at 1:500 in NDS block. Following primary antibody incubation, guts were rinsed four times in 1XPBS/0.1% Triton X-100 for at least 5 min/rinse and then incubated in secondary donkey anti-human TexasRed (Jackson Immuno, Cat. No. 709-075-149) at 1:100 in NDS block for 1 hr at RT. Following four additional rinses in 1XPBS/0.1% Triton X-100 for at least 5 min/rinse, guts were incubated in donkey anti-chick FITC (Jackson Immuno, Cat. No. 703-096-155) at 1:400 in NDS block for 1 hr at RT. Finally, guts were rinsed for 15 min in 1XPBS/0.1% Triton X-100 followed by three 10 minutes rinses in 1XPBS. Guts were stored at 4°C until imaging. For imaging, guts were laid on a slide, wetted with 1XPBS, and a cover slip was gently laid on top and fluorescent signaling was visualized on a BX41 Olympus fluorescent microscope. After imaging, guts were placed back into 1XPBS and stored indefinitely at 4°C. During the IHC process, a *Wnt-1*Cre negative gut sample was subjected to secondary antibody incubations only to serve as a negative control.

Results

Genetic ablation of enteric NC-derived cells

By ablating enteric NC derivative populations, one may determine if other cell populations, such as VENT (VEntral Neural Tube) cells, are contributing neurons to the ENS. The *Foxd3* gene

is required for embryonic stem cell maintenance as well ENS precursor survival (13-15). To effectively ablate NC-derived ENS cells while avoiding embryonic lethality, we used a previously established system of crosses in mouse mutants (13). Briefly, *Foxd3*$^{flox/flox}$*; R26R*$^{YFP/YFP}$ mice were crossed to *Foxd3*$^{+/-}$*; Wnt1*-Cre mice. In mutant *Foxd3*$^{flox/-}$*; Wnt1*-Cre; *R26R*^{YFP} (~25% of offspring), Cre-recombinase expression driven from the *Wnt1*-Cre transgene results in ablation of Foxd3 expression within NC derivatives and subsequent death of NC-derived cells bound for the ENS. At the same time, Cre-recombinase acts on the floxed *R26R*^{YFP}, resulting in YFP labeling of NC derivatives. For controls, I used *Foxd3*$^{flox/+}$*; Wnt1*-Cre; *R26R*^{YFP} mice (~25% of offspring) which have intact NC-derived ENS cells as well as YFP labeling of NC derivatives. In avian models, VENT cells migrate after NC populations have already migrated from the neural tube (reviewed in (16)). Presumably, if VENT cells exist in the mouse, migration of VENT cells to peripheral nervous system (PNS) structures would take place after NC migration from the neural tube. Vagal and rostral truncal NC cells that contribute to the ENS start migrating from the neural tube and reach the foregut between E8.5-9.5 (17) and sacral NC cells reach the hindgut by E14.5 (4). Thus, the time window for possibly observing VENT cells migration to and through the gut would be no earlier than E9.5. Additionally, although it is possible VENT cells proliferate and contribute to PNS near or after birth, the presence of *Foxd3*$^{flox/-;}$ *Wnt1*-Cre leads to perinatal lethality. Thus, the time window I set for analyzing possible presence of VENT cells within the ENS of mice was E10.5 – E19.5. Due to additional restrictions (mouse colony closing), I limited my analysis to embryos at E14.5, E16.5, and E17.5.

Time dependent presence of neurons in the stomach, but not intestines, of Foxd3$^{flox/-;}$ Wnt1-Cre mice

To test for the presence or absence of enteric neurons, I performed IHC to label neurons (Hu+ cells) in the intestines of mutant (*Foxd3*$^{flox/-;}$ *Wnt1-Cre; R26R*^{YFP}*)* and control *(Foxd3*$^{flox/+;}$ *Wnt1-Cre; R26R*^{YFP}) embryos at E14.5, E16.5, and E17.5. In all mutants at all ages examined, I

observed no Hu+ cells nor YFP+ cells within most the length of the small intestine and large intestine (Figure 6.4) Interestingly, all mutants examined at E14.5 had NC-derived neurons throughout their stomach with a few neurons reaching past the pyloric sphincter into the proximal duodenum (n=4). At E16.5, mutants had reduced numbers of neurons within the ENS of their stomachs compared to control littermates (n=2) (Figure 6.4). At E17.5, only 1 mutant had any gastric ENS neurons—which were extremely sparse—while all other mutants had no detectable gastric neurons (n=3).

Discussion

I undertook this study to determine if VENT cells or a Sox10 independent NC-derived population contributes to the ENS. Although I observed no Foxd3 independent cell populations contributing to the ENS in the guts of *Foxd3*$^{flox/-;}$ *Wnt1-Cre; R26R*^{YFP} mutants, the possibility remains that non-NC cells, such as VENT cells, exist and contribute to PNS structures. For example, these cells could also rely on Foxd3 and Wnt1 expression. Thus, genetic ablation of NC Foxd3+ cells would also ablate Foxd3+ non-NC cells contributing to the ENS. Additionally, the VENT cells could rely on appropriate signaling from NC or other tissues for appropriate specification and successful migration. NCC ablation or unsuccessful colonization of PNS structures could prevent VENT cells from migrating or properly differentiating.

An interesting, but unexpected, outcome of my *Foxd3*$^{flox/-}$*; Wnt1-Cre; R26R*^{YFP} analysis was the presence of neurons in the esophagus, stomach, and sometimes very proximal duodenum of all E14.5 mutants examined (n=4). The sparser gastric neuron density in E16.5 mutants followed by complete absence of neurons in mutants by E17.5 suggests that at least some NC-derivatives are migrating to the foregut and they or daughter cells differentiate into neurons, but succumb to early cell death. I had initially expected to see no gastric neurons as a previous study noted complete absence of the entire ENS in *Foxd3*$^{flox/-}$*; Wnt1-Cre; R26R*^{lacz} embryos (13). However, this study limited analysis of the stomach to E17.5, effectively preventing

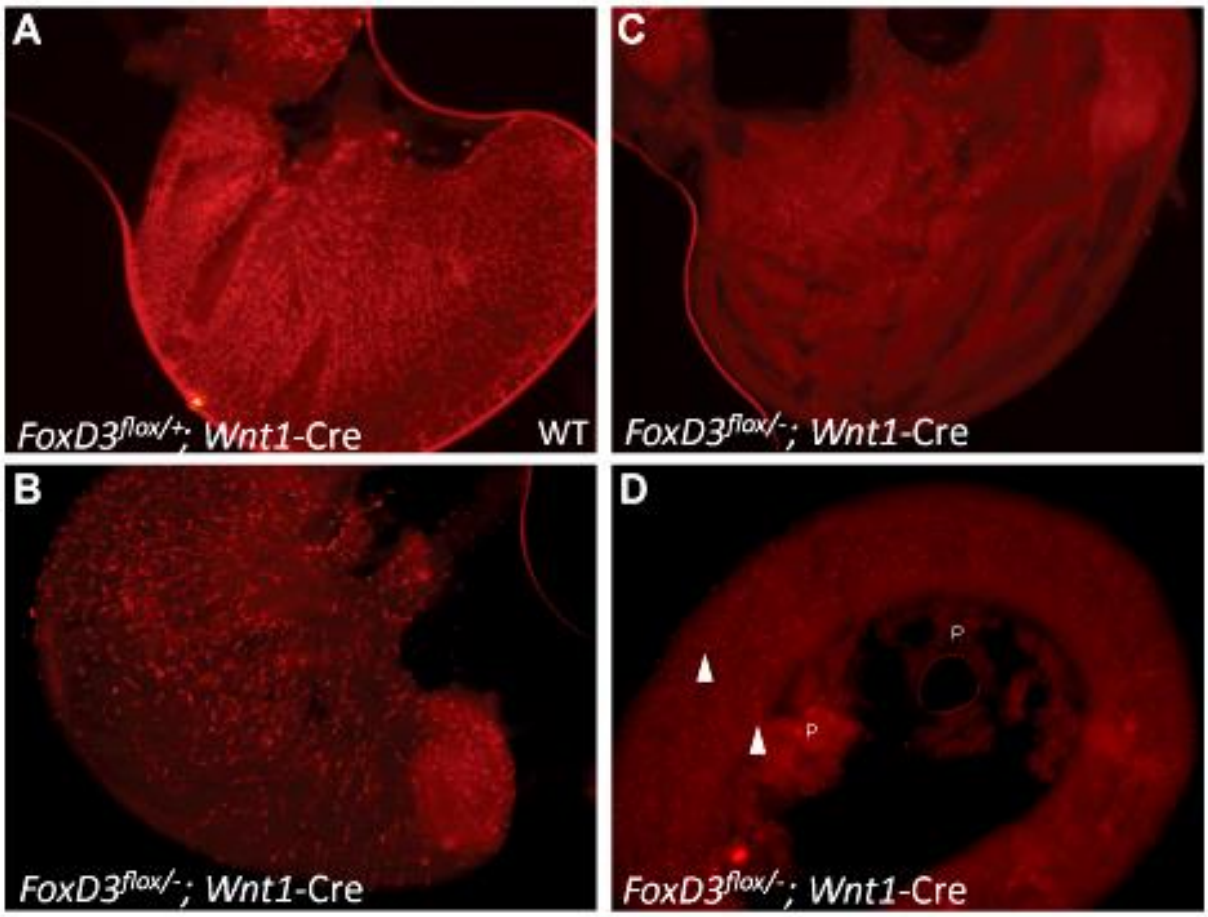

Figure 6.4. ENS neurons in E16.5 *Wnt1*-Cre; *Foxd3*$^{flox/+}$ and *Foxd3*$^{flox/-}$; *Wnt1*-Cre embryos. IHC for neurons (Hu+ red) reveals (**A**) neurons at normal density and number within the gastric ENS of an E16.5 wild type embryo. E16.5 embryos with genetic ablation of NC *Foxd3* expression showed varying levels of neuronal density within the ENS of the stomach. (**B**) Some embryos had neurons throughout their stomach, but had an obvious decrease in neuronal density. (**C**) Other embryos were severely affected and had no or very few neurons in the stomach. (**D**) The large and small intestines of *Foxd3*$^{flox/-}$; *Wnt1-Cre* mutant embryos were largely devoid of neurons, although occasionally a few strings of neurons (arrows) could be found in the most proximal portion of the duodenum. (P=pancreas) (5X objective)

any chance that gastric neurons could be observed in these mutants. Interestingly, this same study noted a reduction in cardiac NC-derivative numbers in these mutants, but these cells were eventually able to proliferate and nearly completely compensate for the initial reduction. It could be that a unique population of NC-derivatives reaches the foregut in *Foxd3$^{flox/-}$; Wnt1-Cre* mutants and that they are near or part of the same vagal, cardiac population that migrates to the heart. In line with this hypothesis, previous studies have identified unique NC-derived cell populations in ENS mutants that only colonize the esophagus and stomach (17, 18). In *Ret$^{-/-}$* mice, where Ret expression has been completely obliterated, E10.5 and E13.5 embryos as well as new born pups were reported to have total intestinal aganglionosis, but neurons were still detected in the stomach and esophagus (17, 18). Interestingly, the Ret independent population of cells that colonized the foregut did not appear to derive from vagal neural crest cells, but rather proximal truncal neural crest cells (17) (Figure 6.5).

Gdnf is a ligand for Ret and thus it comes as no surprise that reduction or ablation of Gdnf signaling leads to phenotypes that closely mimic those of *Ret$^{-/-}$* mice. However, conflicting studies exist for *Gdnf* null, or *Gdnf$^{-/-}$,* embryos in regard to ENS presence or absence in the stomach. Moore et al (1996) reported total intestinal aganglionosis in *Gdnf$^{-/-}$* and sparse neurons were detected in the stomachs of *Gdnf$^{-/-}$* mice from E12.5 – P0, although this data is not shown (19). Similarly, Sanchez et. al., (1996) reported total intestinal aganglionosis in *Gdnf$^{-/-}$* embryos at all stages observed. However, in line with my findings in *Foxd3$^{flox/-}$; Wnt1*-Cre mutants, Sanchez and colleagues observed neurons in the esophagus and stomach of young *Gdnf$^{-/-}$* embryos from E9.5 to E13.5, but detected no neurons in the lower esophagus or stomach of older, newly born *Gdnf$^{-/-}$* pups (20). Deficiencies in Gfra, the primary co-receptor for Ret:Gdnf binding in ENS development, also leads to deficits similar to those seen in *Ret$^{-/-}$* mice. *Gfra1$^{-/-}$* mice at E17 and at birth have total intestinal aganglionosis, but some neurons in the foregut (21, 22). To summarize, mice with components of the Ret signaling pathway eliminated have what appears to be a Ret independent population of NCC that colonizes the foregut and gives rise to neurons;

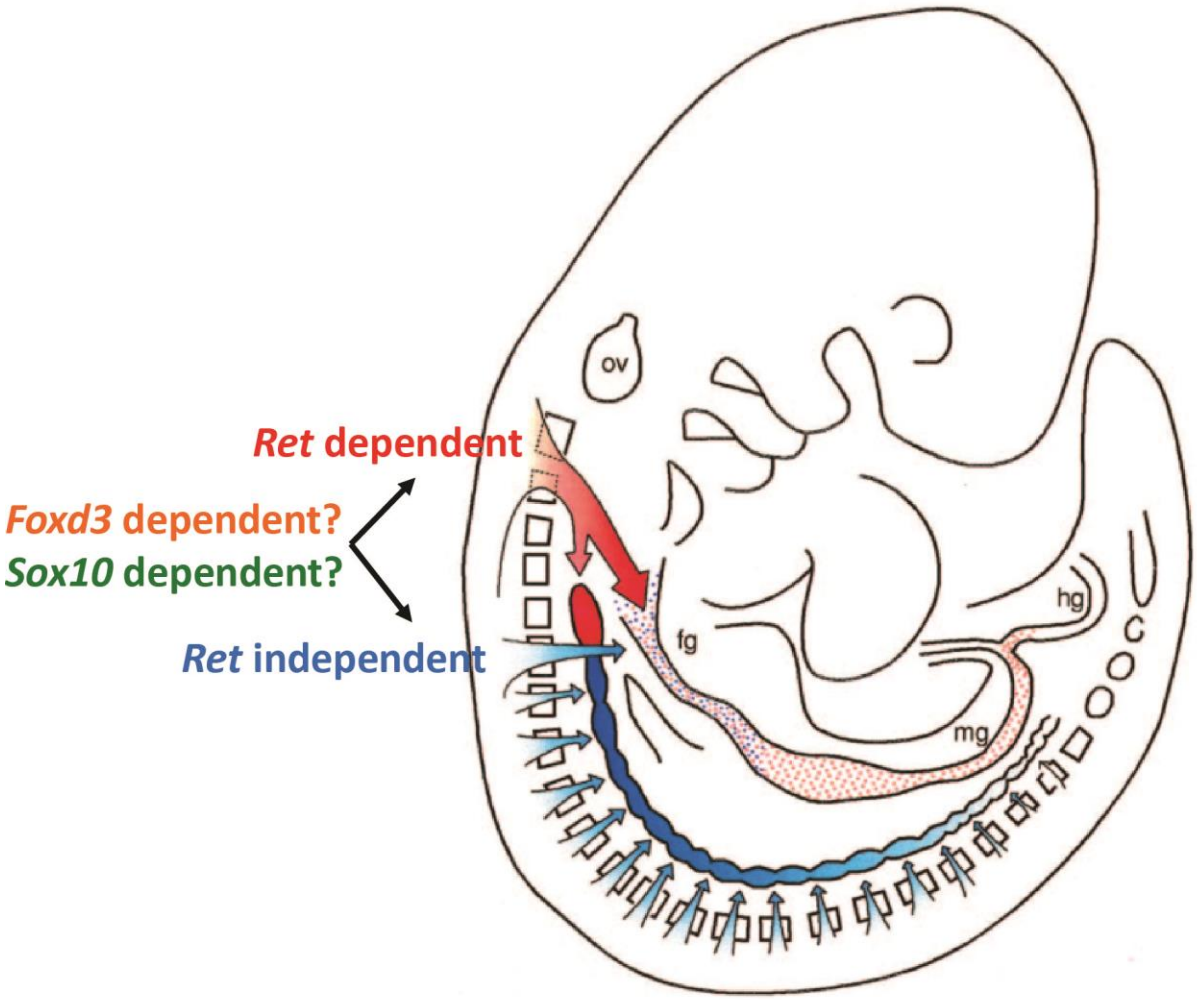

Figure 6.5. Unique vagal and truncal NC population contribute to the ENS. A vagal NC population that is *Ret* dependent contributes extensively to ENS components in the foregut, midgut, and hindgut (red). A truncal NC population that is *Ret* independent is known to contribute to foregut ENS populations (blue). A NC cell population is known to migrate into the foregut independent of Foxd3 expression. However, the origin of this NC population along the neural tube is unknown. Furthermore, it is unknown as to whether a Sox10 independent line of NCC exists. fg = foregut, mg = midgut, hg = hindgut (This figure is modified from a previous version found in Durbec et. al., 1996.)

however, while this population persists in *Ret*$^{-/-}$ and *Gfra1*$^{-/-}$ mice, this population disappears with time, presumably due to cell death, in *Gdnf*$^{-/-}$ mice. *Foxd3*$^{flox/-}$*; Wnt1*-Cre mutants closely mimic these mouse models, particularly *Gdnf*$^{-/-}$ mice as neurons are detected at early stages (E14.5 and E16.5) but not later stages (E17.5). This close resemblance in phenotype could mean that the *Ret* independent NC population originating from truncal NC may also be a *Foxd3* independent population. Conversely, it is also possible that in *Foxd3*$^{flox/-}$*; Wnt1*-Cre mutants, the *Foxd3* independent population is part of a separate Ret dependent, vagal NC population (Figure 6.5). Future experiments could answer this question and are explored in Chapter 8.

Despite my findings in regard to foregut NC-derived populations in *Foxd3*$^{flox/-}$*; Wnt1-Cre; R26R*^{YFP} mutants, the question persisted as to the origin of ENS populations in *Sox10*-Cre; *R26R*^{tdTom} animals that did not express the tdTomato fluorophore. The possibility remained that these neurons that lack reporter expression derive from a *Sox10* independent population of ENPs (Figure 6.5). However, other explanations emerged later in my work that could more readily explain these strange areas. One possible explanation is tissue integrity. Neurons tend to be highly sensitive to osmotic changes during washes and fixations (personal communications, Mike Gershon and Kara Margolis.) Large changes in osmolarity can cause neuron membranes to burst, expelling proteins into the environment. It could be that my fixing conditions initially led neurons in certain areas (where tissue was thin or more prone to mechanical forces) to “leak” reporter if their membranes burst. Similarly, another plausible explanation is that the fix time was inadequate to permeate through certain regions of the tissue and bind the fluorescent reporter within neurons (personal communications, Guoqiang Gu.) Importantly, I did see some reduction in these reporter absent areas in later experiments where an additional fix time (+12 hours at 4°C) after gut muscle strip subdissection was added. (During my initial observations, gut muscle strips were only fixed on ice for 20-25 minutes.) However, this reduction was small and these areas still persisted. Given that these areas tended to occur more often in older animals (>P19) and were

present, but quite rare, in younger animals (P15-17), other biological explanations for these areas relate to transgene and reporter expression. One explanation is the existence of *Sox10* independent NC-derived cell types that never express Cre-recombinase and proliferate later in life, primarily in the postnatal period. However, this seems unlikely. Even though ENS cell birth and turnover occurs throughout the life of the mouse, the number of new neurons is very small and could not account for such large areas that do not express *Sox10*. Alternatively, *ROSA26* expression is not ubiquitous in all cell types and *R26R* reporter expression could be downregulated or switched off over the course of development. This would readily explain the appearance of areas without reporter expression and why older pups had increases in the number and size of these reporter absent areas.

In summary, I set out in this study to determine whether VENT cells contribute the ENS of the mouse and to determine if a Sox10 independent population of cells contribute to the ENS. Unfortunately, these questions remain unanswered. Serendipitously, this study did uncover a previously unrecognized population of NC-derived cells that do not require *Foxd3* for NCC migration into the foregut but ultimately require *Foxd3* for survival. The biological underpinnings that allow a small group of NC cells to migrate to the foregut, but then disappear after supposed differentiation, remains to be determined. As the field moves forward, future studies should aim to further define unique populations of NC cells and the factors that drive their potency, specification, and differentiation.

References

1. Burns, A.J. 2005. Migration of neural crest-derived enteric nervous system precursor cells to and within the gastrointestinal tract. *Int J Dev Biol* 49:143-150.
2. Yntema, C.L., and Hammond, W.S. 1954. The origin of intrinsic ganglia of trunk viscera from vagal neural crest in the chick embryo. *J Comp Neurol* 101:515-541.
3. Le Douarin, N.M., and Teillet, M.A. 1973. The migration of neural crest cells to the wall of the digestive tract in avian embryo. *J Embryol Exp Morphol* 30:31-48.
4. Kapur, R.P. 2000. Colonization of the murine hindgut by sacral crest-derived neural precursors: experimental support for an evolutionarily conserved model. *Dev Biol* 227:146-155.
5. Ali, M.M., Farooqui, F.A., and Sohal, G.S. 2003. Ventrally emigrating neural tube cells contribute to the normal development of heart and great vessels. *Vascul Pharmacol* 40:133-140.
6. Sohal, G.S., Bockman, D.E., Ali, M.M., and Tsai, N.T. 1996. DiI labeling and homeobox gene islet-1 expression reveal the contribution of ventral neural tube cells to the formation of the avian trigeminal ganglion. *Int J Dev Neurosci* 14:419-427.
7. Ali, M.M., Jayabalan, S., Machnicki, M., and Sohal, G.S. 2003. Ventrally emigrating neural tube cells migrate into the developing vestibulocochlear nerve and otic vesicle. *Int J Dev Neurosci* 21:199-208.
8. Sohal, G.S., Ali, M.M., and Farooqui, F.A. 2002. A second source of precursor cells for the developing enteric nervous system and interstitial cells of Cajal. *Int J Dev Neurosci* 20:619-626.
9. Lei, J., and Howard, M.J. 2011. Targeted deletion of Hand2 in enteric neural precursor cells affects its functions in neurogenesis, neurotransmitter specification and gangliogenesis, causing functional aganglionosis. *Development* 138:4789-4800.

10. Mundell, N.A., Plank, J.L., LeGrone, A.W., Frist, A.Y., Zhu, L., Shin, M.K., Southard-Smith, E.M., and Labosky, P.A. 2012. Enteric nervous system specific deletion of Foxd3 disrupts glial cell differentiation and activates compensatory enteric progenitors. *Dev Biol* 363:373-387.

11. Krammer, H.J., and Kuhnel, W. 1993. Topography of the enteric nervous system in Peyer's patches of the porcine small intestine. *Cell Tissue Res* 272:267-272.

12. Kulkarni-Narla, A., Beitz, A.J., and Brown, D.R. 1999. Catecholaminergic, cholinergic and peptidergic innervation of gut-associated lymphoid tissue in porcine jejunum and ileum. *Cell Tissue Res* 298:275-286.

13. Teng, L., Mundell, N.A., Frist, A.Y., Wang, Q., and Labosky, P.A. 2008. Requirement for Foxd3 in the maintenance of neural crest progenitors. *Development* 135:1615-1624.

14. Liu, Y., and Labosky, P.A. 2008. Regulation of embryonic stem cell self-renewal and pluripotency by Foxd3. *Stem Cells* 26:2475-2484.

15. Hanna, L.A., Foreman, R.K., Tarasenko, I.A., Kessler, D.S., and Labosky, P.A. 2002. Requirement for Foxd3 in maintaining pluripotent cells of the early mouse embryo. *Genes Dev* 16:2650-2661.

16. Dickinson, D.P., Machnicki, M., Ali, M.M., Zhang, Z., and Sohal, G.S. 2004. Ventrally emigrating neural tube (VENT) cells: a second neural tube-derived cell population. *J Anat* 205:79-98.

17. Durbec, P., Marcos-Gutierrez, C.V., Kilkenny, C., Grigoriou, M., Wartiowaara, K., Suvanto, P., Smith, D., Ponder, B., Costantini, F., Saarma, M., et al. 1996. GDNF signalling through the Ret receptor tyrosine kinase. *Nature* 381:789-793.

18. Schuchardt, A., D'Agati, V., Larsson-Blomberg, L., Costantini, F., and Pachnis, V. 1994. Defects in the kidney and enteric nervous system of mice lacking the tyrosine kinase receptor Ret. *Nature* 367:380-383.

19. Moore, M.W., Klein, R.D., Farinas, I., Sauer, H., Armanini, M., Phillips, H., Reichardt, L.F., Ryan, A.M., Carver-Moore, K., and Rosenthal, A. 1996. Renal and neuronal abnormalities in mice lacking GDNF. *Nature* 382:76-79.

20. Sanchez, M.P., Silos-Santiago, I., Frisen, J., He, B., Lira, S.A., and Barbacid, M. 1996. Renal agenesis and the absence of enteric neurons in mice lacking GDNF. *Nature* 382:70-73.

21. Enomoto, H., Araki, T., Jackman, A., Heuckeroth, R.O., Snider, W.D., Johnson, E.M., Jr., and Milbrandt, J. 1998. GFR alpha1-deficient mice have deficits in the enteric nervous system and kidneys. *Neuron* 21:317-324.

22. Cacalano, G., Farinas, I., Wang, L.C., Hagler, K., Forgie, A., Moore, M., Armanini, M., Phillips, H., Ryan, A.M., Reichardt, L.F., et al. 1998. GFRalpha1 is an essential receptor component for GDNF in the developing nervous system and kidney. *Neuron* 21:53-62.

Chapter VII

Summary and Future Directions

HSCR is an example of a complex disease where aberrant ENP migration and differentiation leads not only to aganglionosis, but also anomalies in the ganglia that are present. Basic science studies in HSCR mouse models as well as clinical studies in HSCR patient cohorts have served to not only better define the disease, but also shed light on the mechanisms and processes that drive ENS development. In this Chapter, I endeavor to provide brief synopses of my findings for particular topics along with their potential impact and ideas for future directions.

NC lineage imbalance

Previous studies have suggested that abnormal enteric NC differentiation occurs in HSCR and non-HSCR mouse models (reviewed in (1)). In our lab, a previous study demonstrated that enteric ENPs isolated from *Sox10*$^{Dom/+}$ and *Sox10*$^{+/+}$ embryos differ in their *in vitro* developmental capacity, with fewer neurons and glia and more myofibroblasts being generated from *Sox10*$^{Dom/+}$ ENPs compared to *Sox10*$^{+/+}$ ENPs (2). Part of my study efforts were to extend these studies and determine if this difference in developmental potential manifested as ENS defects *in vivo*. Fate-mapping NC derivatives and utilizing IHC for specific ENS cell types in *Sox10*$^{Dom/+}$ and *Sox10*$^{+/+}$ pups revealed that indeed NC derivatives were affected in their ability to differentiate into correct cell types in the context of HSCR. Imbalances in neural crest derivatives were regionally specific, and interestingly, imbalances encountered in the colon correlated with extent of aganglionosis.

However, in regard to ENS cell type imbalance in *Sox10*$^{Dom/+}$ and *Sox10*$^{+/+}$ and other HSCR mouse models, much is left to be determined. Initially, I sought to characterize numerous neuronal cell types within the ENS. Several factors led me to limit my analysis to neurons, glia, and nNOS- and Calretinin-expressing neuronal subtypes. First, I had difficulties in locating

appropriate antibodies and optimizing IHC. Second, we had expected an obvious phenotype in regard to *Sox10*$^{Dom/+}$ ENS patterning and skew in ganglia components. However, I did not observe any obvious ENS patterning defects and only time-intensive counting of ganglia components in numerous animals revealed skewing of some ganglia cell types. Despite these difficulties, future studies would benefit from knowing all the neuronal subtypes that are affected in HSCR. Such knowledge would help determine how much the local environment and/or timing of differentiation affect resultant ganglia constituents. To be specific, we know that early born neuron types, such as serotonergic neurons, affect the proportions of later born neuron types (3). The two neuronal subtypes I analyzed, Calretinin- and nNOS-expressing neurons, are at least born between E12-P4 and E11-P0 respectively (4-6). In regard to birth dates, these neuronal subtypes have a rather broad range when compared to other neuron subtypes such as Serotonergic neurons (born E8-E14) or Neuropeptide Y neurons (born E10-18). Knowing which populations of neuronal subtypes are actually affected in HSCR will not only tell us more about the disorder, but also reveal more about discrete NC populations and how they interact.

Furthermore, even though much work has gone into characterizing neuronal subtypes and their birthdates in the ENS (4-7), relatively little is known about enteric glia. It is known that glia modulate inflammatory processes as ablation of enteric glia leads to severe jejuno-ileitis (8, 9). And glia or glia-like cells generate new neurons after traumatic injury (10). However, birthdates of glia, their exact roles in modulating neuron signaling, and the specific genes they express are just now being examined. My lab group is currently investigating the expression patterns of ENPs that express high and low levels of *Phox2b,* which are believed to correspond to future neurons and glia respectively. This work will be extremely important as arguably very few genes have been discovered or studied in these pathways in regard to ENS development, especially when compared to what is known about CNS development. While this *Phox2b* study will shed light on developmental processes, future studies could also serve to define characteristics of enteric glia in adult mice. Similar to the *Phox2b*-centric study mentioned above, flow-sorting of enteric glia

from adult mice using a glia-specific marker followed by subsequent RNA seq or reverse-transcriptase PCR for plausible glial genes should provide a basis for the genes that are expressed by some or all enteric glia. (Surprisingly, only about a dozen known enteric glial markers have been documented. These markers include GFAP, SOX2, SOX10, BFABP, FOXD3, FABP7, BLBP, ERBB3, PHOX2B and S100A&B subtypes.)

Glia birthdates could be determined through simple experiments incorporating BrdU technology and IHC, similar to previous neuron-birthdating studies (4-6). As a reminder, the birthdate of a specific cell type can be defined as the time period that a cell ceases to divide and starts to take on the characteristics of the cell type it is destined to become. To this end, BrdU can be injected into pregnant dams at different developmental time points. Postnatally, pups from injected dams are sacrificed and the ENS is subjected to IHC to detect glia and BrdU. Should BrdU be detected in glia from a specific time period, such as E8, one can conclude that at least some ENP cells underwent final mitotic division and were differentiating into glia at E8. By conducting this experiment at numerous time points during development, one can define the window of time a specific cell type is born. Admittedly, if one uses a pan-glial marker, this experiment would first only define the time period all glia are born and the relative amounts of glia born at certain time periods. Unfortunately, very few studies have identified glia subtypes by marker expression and those that have relied on more complicated means than strictly IHC, such as electrophysiological identification or changes in glia marker expression levels due to a biological stressor such as inflammation (11-14). Some studies, including one published within the last month, have classified enteric glia based on location and morphology (15, 16). By identifying specific glia subtypes by location and morphology or by population-specific markers (once discovered), a similar type of experiment could be conducted to determine glia subtype birthdates. In total, these experiments will not only shed light on ENS developmental processes, but could also explain why glia proportions are only disturbed in the colon of *Sox10*$^{Dom/+}$ mutants. Additionally, once glia subtypes are further defined, the exact processes that specific suptypes

contribute to, such as inflammation or modulation of neuron signaling, can be more readily explored.

Defining NC populations

Along with characterizing individual cell types within enteric NC populations comes the task of characterizing discrete NC populations. In Chapter 6, I described a NC population that did not require *Foxd3* for migration into the foregut, but ultimately required *Foxd3* expression for survival. This population, along with the *Ret*-dependent and independent populations discussed in Chapter 6 (Figure 6.5), raises many interesting questions and possibilities for future directions in this work

First, the question remains as to whether the population of NC cells I observed in the stomachs of *Foxd3$^{flox/-}$; Wnt1*-Cre embryos originates from the vagal or rostral truncal NC populations. To test this hypothesis, one could use DiI injections to label neural crest in either the vagal or truncal populations in *Foxd3$^{flox/-}$; Wnt1*-Cre and *Foxd3$^{flox/+}$; Wnt1*-Cre embryos before NC migrate from the neural tube. Mouse embryos can transiently develop and survive in culture for at least a couple days (up to E10.5), permitting DiI-labeled and unlabeled NC cells to migrate to the foregut. The presence of DiI-labeled cells from vagal and/or truncal regions in the foregut post-migration will reveal the origins of the NC cell population. However, DiI-labeling can be non-specific and dilutes over multiple cell divisions, and culturing whole embryos is difficult. Other approaches to answering this questing include different labeling techniques, such as GFP-tagged adenovirus vectors (although speficity is also an issue here) and utilizing transgenic mouse lines that have reporter expression specific to the ventral neural tube. The use of transgenic mouse lines would eliminate the need for *ex vivo* culturing of embryos; however, several transgenic lines may need to be tested as a pan-ventral neural tube marker is not currently known.

Furthermore, it is fascinating that NC cells within *Foxd3$^{flox/-}$; Wnt1*-Cre go as far as differentiating into neurons within the stomach before they appear to undergo apoptosis.

Experimentally, the presence of apoptosis could be investigated through TUNEL assays within the stages that these NC cell populations seem to disappear (possibly E16-E17). The more important question, as to why these cells do die, will be harder to establish. It could be that lack of *Foxd3* eventually leads to aberrant signaling between NC cells and the molecular signals in their environment (non-NC cells) which leads to cell death. Or, aberrant signals between NC cells or signals needed from an absent NC population result in cell death. These hypotheses could initially be explored through IHC staining of NC and non-NC cell populations in *Foxd3*$^{flox/-}$*; Wnt1*-Cre and *Foxd3*$^{flox/+}$*; Wnt1*-Cre at different stages to determine if known regulatory receptors and their ligands (such as *Ret:Gdnf* or *Ednrb:Edn3*) are present at the correct time in the correct cell populations. A more specific experiment would be to first define the NC cell population present in *Foxd3*$^{flox/-}$*; Wnt1*-Cre through flow-sorting for these cells and then performing RNAseq analysis to determine grossly genes expressed at high levels in this cell population. This population can also be further defined by using IHC to determine if any glia or specific neuronal subtypes are present within this population. This type of experiment could be important as it is known that a "transiently catecholaminergic" cell population gives rise to specific early born neuron types in the developing gut such as serotonergic neurons (17). Ablation of "transiently catecholaminergic" in *Mash1*$^{-/-}$ (or *Ascl1*$^{-/-}$) mice results in the absence of serotonergic neurons, but presence, and importantly, survival of other neuron types such as CGRP expressing neurons (17). By comparing the types of neurons present in *Foxd3*$^{flox/+}$*; Wnt1*-Cre before they succumb to cell death to those neuron types described in *Mash1*$^{-/-}$ mice would help to further define this NC cell population.

Finally, elimination of *Foxd3* expression at different time points, either through an inducible mutation or use of alternate *Cre* alleles with the *Foxd3-flox* allele, would help determine exactly when *Foxd3* is directly or indirectly acting on specific NC processes such as migration and differentiation. For example, previous members of my lab group generated an inducible *Sox10*-Cre/ert2 transgene. This transgene can be induced at specific developmental time points in *Foxd3*$^{flox/+}$ or *Foxd3*$^{flox/-}$ embryos by tamoxifen gavage to the mother. Inclusion of a Cre-loxP driven

ROSA26 reporter in this scheme would permit visualization of NCC location and number as well as provide evidence that induction of the *Sox10*-Cre/ert2 was successful.

GI motility studies

In this study, we found that young, 4-week old *Sox10*$^{Dom/+}$ mice had significantly slower small intestinal transit times when compared to *Sox10*$^{+/+}$ mice. However, older 6-week old females did not have any small intestinal transit slowing and, interestingly, I observed increased gastric emptying in 6-week old male *Sox10*$^{Dom/+}$ mice. Although a surprise, possible defects in pyloric sphincter function are compatible with Sox10's biological roles and expression patterns and the neural lineage imbalance we identified in the nearby duodenum. Differences in circulating sex hormones was put forward as a hypothesis to explain this discrepancy between findings in adult mice. However, we never tested this hypothesis. Because sex differences are seen so often in neurodevelopmental disorders and because the protective effects of female specific sex hormones are not well understood, this finding would be interesting and important to follow up. There are a couple of possible ways to rule in or rule out a role for sex hormones in pyloric sphincter and small intestinal transit changes in *Sox10*$^{Dom/+}$ mice. First, *Sox10*$^{Dom/+}$ males could be subjected to hormone injections during periods of time that correspond to onset of circulating sex hormones in females. Males subjected to hormone injections as well as untreated *Sox10*$^{Dom/+}$ (and wildtype equivalents for each group) could be tested for changes in pyloric sphincter dynamics and small intestinal transit using tests previously described in Chapters 2, 3, and 7. In this study, if sex hormones are playing a role, I would expect to observe similar gastric emptying, pyloric sphincter measures, and small intestinal transit assays in *Sox10*$^{Dom/+}$ mice when compared to wildtype *Sox10*$^{+/+}$ mice and female *Sox10*$^{Dom/+}$ mice. Conversely, *Sox10*$^{Dom/+}$ female mice could undergo ovarectomies prior to puberty onset. Loss of ovaries would lead to significant decreases in female sex hormones. Thus, when testing for GI motility deficits, *Sox10*$^{Dom/+}$ females should

mimic findings in untreated *Sox10*$^{Dom/+}$ males should hormones be playing a role. For this type of study, it will be important to monitor hormone levels in all untreated and treated mice involved to ensure physiological levels of hormones in treated mice coincide with levels in untreated mice.

As a side note, if a group were to test varying levels of testosterone (such as through castration in males or injection to females) in these types of studies, they should proceed with caution. Both females and males synthesize testosterone and testosterone is an intermediate in estradiol (estrogen) biosynthesis pathway. And estradiol has been implicated as the molecule responsible for the "neuroprotective effect" (reviewed in (18)). Thus, results from studies where testosterone is introduced may not be easy to interpret (i.e. Were changes due to testosterone? Or due to estradiol synthesis resulting from excess testosterone?) Although determining how near complete absence of sex hormones affects neurodevelopment could be interesting, the global impact of such a loss would make findings difficult to interpret. Furthermore, because both females and males produce testosterone and the sheer amount of literature that suggests estradiol as the "neuroprotective" factor, the clinical relevance of testing decreased testosterone levels is lacking at this time.

Revisiting the slow intestinal transit in 4-week *Sox10*$^{Dom/+}$ old mice, we have yet to determine the exact cause of slower transit within the small intestine of these mice. We put forth the hypothesis that imbalances in inhibitory (nNOS+) and excitatory (Calretinin+) neurons could be at least partially driving this alteration in motility. However, other neuron types can affect GI motility and slower transit could result from different movement alterations, such as uncoordinated peristalsis or slower or less peristalsis. Several lab groups have developed methods to trace rates of peristalsis, such as generating spatiotemporal maps of muscle constriction (19) or physically marking intestine pieces and tracing marker movements (20). We could use similar methods in our lab to look at peristalsis dynamics in *Sox10*$^{Dom/+}$ mice. I think a more important question for potential pharmaceutical targets in the ENS is to determine if the changes we observed in inhibitory (nNOS+) and excitatory (Calretinin+) neurons (and possibly other neuron

types) cause a physiological affect. To get closer to answering this question, one could use a "force" assay where a piece of duodenum is hung between two hooks (within a tissue culture bath) and force generated by constriction of the muscle is measured after application of various pharmaceutical reagents. For example, in *Sox10*$^{Dom/+}$ mice, we observed an equal proportion of nNOS neurons in the duodenum when compared to *Sox10*$^{+/+}$ littermates, but increased Calretinin neurons. Therefore, one could eliminate the contribution of nNOS neurons to gut movement by applying L-NAME (a readily available nNOS inhibitor) to duodenum pieces. This loss of inhibitory neuron contribution would feasibly lead to the loss of relaxation by the intestinal muscle. The resultant constriction force, primarily due to Calretinin neurons, would then be measured. Since *Sox10*$^{Dom/+}$ mice have more Calretinin neurons than *Sox10*$^{+/+}$, one would expect the constriction force in *Sox10*$^{Dom/+}$ mice to be greater.

In regard to GI motility tests in other mouse models, I found no differences in small intestinal transit in *Ednrb*$^{tm1Ywa/+}$ and *Ret*$^{tm1Cos/+}$ males and females compared to their wildtype littermates. When testing for total intestinal transit time, *Ednrb*$^{tm1Ywa/+}$ male and female mice were comparable to their wildtype littermates and the same was observed in *Ret*$^{tm1Cos/+}$ females and wildtype littermates. Intriguingly, *Ret*$^{tm1Cos/+}$ males had significantly higher total transit times than their wildtype counterparts. Given that *Ednrb*$^{tm1Ywa/+}$ and *Ret*$^{tm1Cos/+}$ mice are reported to have no aganglionosis (21, 22), this finding in *Ret*$^{tm1Cos/+}$ males could help explain familial constipation and, similar to findings in *Sox10*$^{Dom/+}$, suggests sex-specific severity of phenotypes in the ENS. Finding the cause of constipation and defining the constipation type in *Ret*$^{tm1Cos/+}$ mice will be the initial steps in establishing this mouse as a model for studying familial constipation. First, *Ret*$^{tm1Cos/+}$ mice have no aganglionosis, but their ENS neurons tend to be smaller on average compared to wildtypes (22). We can further characterize the ENS of *Ret*$^{tm1Cos/+}$ mice using IHC (similar to that carried out in *Sox10*$^{Dom/+}$ mice) to identify skews in ganglia constituents that could drive constipation. Additionally, if slowing of fecal contents is occurring in the colon, one would expect fecal material to be drier in *Ret*$^{tm1Cos/+}$ mice than in *Ret*$^{+/+}$ mice. One may easily measure the water

contents of fecal material by collecting fresh feces and weighing it, eliminating water from the feces via desiccation, and then weighing dried feces (23).

Inflammatory responses

Interestingly, I observed no difference in inflammation in *Sox10*$^{Dom/+}$ and *Sox10*$^{+/+}$. Some possible explanations for this finding are expounded upon in Chapter 2, and this finding emphasizes the importance of genetic and environmental interactions. In my review of clinical charts for HSCR patients, I noticed a recurring event. Many times, reports of HSCR patients hospitalized for gastritis and enterocolitis carried a note that other family members had just suffered from a bout of gastritis or other GI discomfort. However, other family members did not require hospitalization for their symptoms. While some of this can be attributed to vigilant caretakers realizing enterocolitis can be a life threatening event in HSCR, it also suggests that HSCR patients may have an increased or aberrant inflammatory response to infectious agents when compared to the general population. It has become apparent in recent years that the ENS modulates inflammatory responses in the bowel (24, 25) and studies in mice and humans could help reveal how the ENS modulates inflammation in the context of HSCR.

For example, the interaction between environment and inflammatory response could be tested in *Sox10*$^{Dom/+}$ and *Sox10*$^{+/+}$ mice in several ways. In many mouse studies, evaluation to determine differences in inflammatory responses is conducted by introducing a stressor that induces inflammation. Examples of stressors include chemical insults such as introduction of DSS or TNBT or introduction of an infectious agent, such as *C. difficile*, that would normally elicit inflammatory processes in the bowel. One could introduce similar stressors to *Sox10*$^{Dom/+}$ and *Sox10*$^{+/+}$ mice and then evaluate colonic inflammation. Additionally, although I used H&E to grade inflammation, other tests are available that could also show if inflammatory processes are altered in these mice. For example, differing levels in cytokine levels could be tested via RT-PCR or ELISA (26) or one could stain for myeloperoxidase (MPO) (27). Furthermore, the microbiome of

Sox10$^{Dom/+}$ and *Sox10*$^{+/+}$ mice could differ, leaving the HSCR mouse mutant more susceptible to inflammation. Several studies have used RNAseq to determine the relative quantities of specific strains and species of flora in different disease states (28-30) and a similar approach could be taken in HSCR mouse models. Once differences in flora are determined, more specific studies could be carried out defining the interactions between specific microbiome organisms and the ENS.

Ethical considerations preclude using environmental reagents to inflict unnecessary inflammation or pain (biopsy) to test possible inflammation triggers in HSCR patients. However, simple additions to HAEC standard of care could reveal the infectious agents that most often lead to HAEC. For example, stool samples from patients being admitted with HAEC could undergo laboratory testing to determine infectious agents present. Infectious agents that appear most often in hospitalized patients could indicate that HSCR patients are more susceptible to inflammation when that particular agent is present. Additionally, since the infectious agent will most likely be well characterized, such information could clue researchers into the biological pathways (neural and immune) that are affected and interacting in the context of HSCR. Furthermore, when HSCR patients present to the hospital or clinic with gastritis symptoms, implementing simple surveys that address environmental exposures (such as the presence of gastritis in other family members) as part of their care could clue physicians and caregivers into extra measures that may need to be taken in the home environment to help reduce the risk of HAEC in HSCR patients.

Clinical considerations

In Chapter 5, I described clinical information from a HSCR cohort that could be helpful in determining comorbidities and what patients would go on to suffer from adverse outcomes, such as HAEC. Although I focused my attention on clinical variables that could be collected from electronic medical records, more clinical and pathology data exists that could be collected and

tested for correlation with enterocolitis. For example, the current focus while interpreting HSCR biopsies is to assess for presence or absence of ganglia. However, many times, other pathological findings are noted within HSCR patient biopsies, such as eosinophilia, “foamy” cells within ganglia, and overt ganglionitis (personal communications, Hernan Correa.) The reason for such findings is currently unknown and no study has evaluated their value in determining patient outcomes. Interestingly, it is known that standing inflammation in the GI tract can lead to more severe inflammation after a stressor such as surgery or infection. Thus, it is plausible such pathological findings have real value in predicting patient outcomes post-surgery. To this end, I am in an active collaboration with Dr. Hernan Correa (Pediatrics Pathology Director, Vanderbilt Medical Center), to grade surgical HSCR biopsies for pathological features and inflammation. The long term goal is to apply regression analysis to determine the independent variables (histology findings, sex, length of aganglionosis, etc.) that can predict or contribute to patient outcomes (enterocolitis).

Also, early in my graduate school training, the initial focus of the HSCR population study was to define patterning and ENS deficits in HSCR patient resections. However, difficulties with HSCR surgical resection staining and IHC, issues with power, and recent discoveries in HSCR mouse models (21) as well as my own findings in the *Sox10*$^{Dom/+}$ HSCR model led us to rethink this project. Specifically in regard to HSCR mouse models, Zaitoun et. al., (2013) observed a significant increase in colonic nNOS neurons within the *Ednrb*$^{-/-}$ HSCR mouse when compared to *Ednrb*$^{+/-}$ littermates. I also observed an increase in colonic nNOS neuron proportions in the *Sox10*$^{Dom/+}$ HSCR mouse mutant. But more specifically than the Zaitoun study, I found that this increase correlated highly with the extent of colonic aganglionosis. In other words, the longer the aganglionic segment, the higher the proportion of nNOS neurons. Fortuitously, I have had success with NADPH-β staining on HSCR surgical resections (Chapter 7). NADPH-β staining permits visualization of individual nNOS expressing neurons, and thus I can also determine if nNOS neuron numbers correlate with aganglioniosis extent in HSCR patients. Such information

could hold great clinical relevance as patients with longer lengths of aganglionosis could be experiencing a “double whammy’— greater lengths of aganglionosis not only means removal of more colon (and associated side effects), but more severe defects in the ENS of the colon that is remaining.

Currently, I am grading nNOS expressing neuron density as part of a previous study. (The lab just recently received IRB approval for connecting our findings to clinical outcomes.) There are a few caveats and modifications that one needs to consider while conducting this type of study. In my mouse studies, I was able to calculate the proportion of nNOS neurons to total neurons. I do not currently have a stain to use in tandem with the NAPDH- β stain to detect and quantify all neurons. Thus, nNOS neuron measurements will have to be made by comparing nNOS neuron numbers to total ENS area or ganglia area. This feat is possible given that nNOS neuron connectives are plentiful and provide a clear outline of individual ganglia as well as other ENS components (Chapter 7, Figure 7.9). Furthermore, in my mouse studies, I could calculate the percent of colon that was aganglionic because I could measure the total length of the colon. Of course, these types of measurement are not available for HSCR surgical resections. However, information in regard to length of hypoganglionosis and aganglionosis (in cm) from the rectum can be teased from the surgical pathology records.

The colon—the final frontier

Throughout my studies and discussion herein, I hugely ignored a population of NC cells that has only recently been recognized. Midway through my graduate training, a paper was published detailing the presence of trans-mesenteric NC cells (31). While for decades it has been assumed that NC exclusively travel caudally or rostrally along gut mesenchyme once they enter the gut, Nishiyama and colleagues discovered a population of NC cells that actually take a ‘short cut’ to the colon (31). These NC cells enter the foregut, migrate to the gut mesentery along the duodenum, and then track across the gut mesentery into the colon, bypassing the jejunum and

ileum altogether. (This path is possible as the duodenum and colon lay directly juxtaposed.) The role of this NC population and how they might be affected in the context of HSCR has not been explored. Nishiyama and our lab group have hypothesized that this NC population could explain "skip lesions" in HSCR, where areas of colon alternate between ganglionated and aganglionated (1, 31). Further characterizing this population of NC cells in wildtype animals as well as within HSCR is an open field for researchers. Relatively little is known about why these NC cells migrate into the mesentery and others do not, the intrinsic and extrinsic cues that guide their migration, and the ENS cell types they eventually give rise to. Do these cells fail to reach the colon in HSCR? Or do they reach the colon but succumb to cell death like the *Foxd3* dependent cells in the stomach? To begin to answer these questions, one may evaluate the migration patterns of NCC in the gut tube as well as within the mesentery at different developmental time points in HSCR mouse models. Such a study could easily be completed with mouse crosses similar to ones I completed within Chapter 2, where nearly all ENPs and their daughter cells express the tdTomato reporter.

Concluding Remarks

Overall, this study has moved the ENS field forward by defining alterations in ENS subpopulations and functional parameters within the ganglionated regions of the *Sox10*$^{Dom/+}$ mouse model. Attempts to define and correlate HSCR patient variables with adverse outcomes were met with difficulties, but initial work here has laid the foundation for future studies. Furthermore, work within non-HSCR mouse models has provided a possible explanation and model for familial constipation and defined a new NC population that does not rely on *Foxd3* for cell migration or differentiation, but ultimately relies on *Foxd3* for viability. Future efforts to further define effects of HSCR genes on ENS development should positively impact HSCR patient care and shed light on other GI disorders.

References

1. Musser, M.A., and Michelle Southard-Smith, E. 2013. Balancing on the crest - Evidence for disruption of the enteric ganglia via inappropriate lineage segregation and consequences for gastrointestinal function. *Dev Biol* 382:356-364.
2. Walters, L.C., Cantrell, V.A., Weller, K.P., Mosher, J.T., and Southard-Smith, E.M. 2010. Genetic background impacts developmental potential of enteric neural crest-derived progenitors in the Sox10Dom model of Hirschsprung disease. *Hum Mol Genet* 19:4353-4372.
3. Li, Z., Chalazonitis, A., Huang, Y.Y., Mann, J.J., Margolis, K.G., Yang, Q.M., Kim, D.O., Cote, F., Mallet, J., and Gershon, M.D. 2011. Essential roles of enteric neuronal serotonin in gastrointestinal motility and the development/survival of enteric dopaminergic neurons. *J Neurosci* 31:8998-9009.
4. Chalazonitis, A., Pham, T.D., Li, Z., Roman, D., Guha, U., Gomes, W., Kan, L., Kessler, J.A., and Gershon, M.D. 2008. Bone morphogenetic protein regulation of enteric neuronal phenotypic diversity: relationship to timing of cell cycle exit. *J Comp Neurol* 509:474-492.
5. Pham, T.D., Gershon, M.D., and Rothman, T.P. 1991. Time of origin of neurons in the murine enteric nervous system: sequence in relation to phenotype. *J Comp Neurol* 314:789-798.
6. Bergner, A.J., Stamp, L.A., Gonsalvez, D.G., Allison, M.B., Olson, D.P., Myers, M.G., Jr., Anderson, C.R., and Young, H.M. 2014. Birthdating of myenteric neuron subtypes in the small intestine of the mouse. *J Comp Neurol* 522:514-527.
7. Li, Z., Caron, M.G., Blakely, R.D., Margolis, K.G., and Gershon, M.D. 2010. Dependence of serotonergic and other nonadrenergic enteric neurons on norepinephrine transporter expression. *J Neurosci* 30:16730-16740.

8. Bush, T.G., Savidge, T.C., Freeman, T.C., Cox, H.J., Campbell, E.A., Mucke, L., Johnson, M.H., and Sofroniew, M.V. 1998. Fulminant jejuno-ileitis following ablation of enteric glia in adult transgenic mice. *Cell* 93:189-201.

9. Bush, T.G. 2002. Enteric glial cells. An upstream target for induction of necrotizing enterocolitis and Crohn's disease? *Bioessays* 24:130-140.

10. Heanue, T.A., and Pachnis, V. 2011. Prospective identification and isolation of enteric nervous system progenitors using Sox2. *Stem Cells* 29:128-140.

11. Costagliola, A., Van Nassauw, L., Snyders, D., Adriaensen, D., and Timmermans, J.P. 2009. Voltage-gated delayed rectifier K v 1-subunits may serve as distinctive markers for enteroglial cells with different phenotypes in the murine ileum. *Neurosci Lett* 461:80-84.

12. Nasser, Y., Keenan, C.M., Ma, A.C., McCafferty, D.M., and Sharkey, K.A. 2007. Expression of a functional metabotropic glutamate receptor 5 on enteric glia is altered in states of inflammation. *Glia* 55:859-872.

13. Nasser, Y., Fernandez, E., Keenan, C.M., Ho, W., Oland, L.D., Tibbles, L.A., Schemann, M., MacNaughton, W.K., Ruhl, A., and Sharkey, K.A. 2006. Role of enteric glia in intestinal physiology: effects of the gliotoxin fluorocitrate on motor and secretory function. *Am J Physiol Gastrointest Liver Physiol* 291:G912-927.

14. Tjwa, E.T., Bradley, J.M., Keenan, C.M., Kroese, A.B., and Sharkey, K.A. 2003. Interleukin-1beta activates specific populations of enteric neurons and enteric glia in the guinea pig ileum and colon. *Am J Physiol Gastrointest Liver Physiol* 285:G1268-1276.

15. Boesmans, W., Lasrado, R., Vanden Berghe, P., and Pachnis, V. 2014. Heterogeneity and phenotypic plasticity of glial cells in the mammalian enteric nervous system. *Glia*.

16. Hanani, M., and Reichenbach, A. 1994. Morphology of horseradish peroxidase (HRP)-injected glial cells in the myenteric plexus of the guinea-pig. *Cell Tissue Res* 278:153-160.

17. Blaugrund, E., Pham, T.D., Tennyson, V.M., Lo, L., Sommer, L., Anderson, D.J., and Gershon, M.D. 1996. Distinct subpopulations of enteric neuronal progenitors defined by

time of development, sympathoadrenal lineage markers and Mash-1-dependence. *Development* 122:309-320.

18. Garcia-Segura, L.M., Azcoitia, I., and DonCarlos, L.L. 2001. Neuroprotection by estradiol. *Prog Neurobiol* 63:29-60.

19. Roberts, R.R., Ellis, M., Gwynne, R.M., Bergner, A.J., Lewis, M.D., Beckett, E.A., Bornstein, J.C., and Young, H.M. 2010. The first intestinal motility patterns in fetal mice are not mediated by neurons or interstitial cells of Cajal. *J Physiol* 588:1153-1169.

20. Dominik, S., Markus, K., Kerstin, L., Jasmin, C., Michael, B., and Karl-Herbert, S. 2014. The mesenterially perfused rat small intestine: A versatile approach for pharmacological testings. *Ann Anat* 196:158-166.

21. Zaitoun, I., Erickson, C.S., Barlow, A.J., Klein, T.R., Heneghan, A.F., Pierre, J.F., Epstein, M.L., and Gosain, A. 2013. Altered neuronal density and neurotransmitter expression in the ganglionated region of Ednrb null mice: implications for Hirschsprung's disease. *Neurogastroenterol Motil* 25:e233-244.

22. Gianino, S., Grider, J.R., Cresswell, J., Enomoto, H., and Heuckeroth, R.O. 2003. GDNF availability determines enteric neuron number by controlling precursor proliferation. *Development* 130:2187-2198.

23. Zhou, M., Jia, P., Chen, J., Xiu, A., Zhao, Y., Zhan, Y., Chen, P., and Zhang, J. 2013. Laxative effects of Salecan on normal and two models of experimental constipated mice. *BMC Gastroenterol* 13:52.

24. Lomax, A.E., Fernandez, E., and Sharkey, K.A. 2005. Plasticity of the enteric nervous system during intestinal inflammation. *Neurogastroenterol Motil* 17:4-15.

25. Sharkey, K.A., and Mawe, G.M. 2002. Neuroimmune and epithelial interactions in intestinal inflammation. *Curr Opin Pharmacol* 2:669-677.

26. Leng, S.X., McElhaney, J.E., Walston, J.D., Xie, D., Fedarko, N.S., and Kuchel, G.A. 2008. ELISA and multiplex technologies for cytokine measurement in inflammation and aging research. *J Gerontol A Biol Sci Med Sci* 63:879-884.

27. Garrity-Park, M., Loftus, E.V., Jr., Sandborn, W.J., and Smyrk, T.C. 2012. Myeloperoxidase immunohistochemistry as a measure of disease activity in ulcerative colitis: association with ulcerative colitis-colorectal cancer, tumor necrosis factor polymorphism and RUNX3 methylation. *Inflamm Bowel Dis* 18:275-283.

28. McNulty, N.P., Yatsunenko, T., Hsiao, A., Faith, J.J., Muegge, B.D., Goodman, A.L., Henrissat, B., Oozeer, R., Cools-Portier, S., Gobert, G., et al. 2011. The impact of a consortium of fermented milk strains on the gut microbiome of gnotobiotic mice and monozygotic twins. *Sci Transl Med* 3:106ra106.

29. Macklaim, J.M., Fernandes, A.D., Di Bella, J.M., Hammond, J.A., Reid, G., and Gloor, G.B. 2013. Comparative meta-RNA-seq of the vaginal microbiota and differential expression by Lactobacillus iners in health and dysbiosis. *Microbiome* 1:12.

30. Castellarin, M., Warren, R.L., Freeman, J.D., Dreolini, L., Krzywinski, M., Strauss, J., Barnes, R., Watson, P., Allen-Vercoe, E., Moore, R.A., et al. 2012. Fusobacterium nucleatum infection is prevalent in human colorectal carcinoma. *Genome Res* 22:299-306.

31. Nishiyama, C., Uesaka, T., Manabe, T., Yonekura, Y., Nagasawa, T., Newgreen, D.F., Young, H.M., and Enomoto, H. 2012. Trans-mesenteric neural crest cells are the principal source of the colonic enteric nervous system. *Nat Neurosci* 15:1211-1218.

CHAPTER VIII

EXTENDED METHODS & SHORT STUDIES

Animals

Genotyping

Genomic DNA was collected from tail snips (postnatal mice) or limb buds (embryonic mice). Tissues were placed in tail digest buffer (10 mM Tris pH 8.0, 10 mM EDTA, 0.5% SDS, 100 nM NaCl) and incubated with Proteinase K (Fisher, BP1700 100; Gojira, PK 1001) at 55°C for a minimum of 2 hours. Digestion of tissues was followed by phenol-chloroform extraction and EtOH precipitation of the DNA. DNA was then resuspended in 250 µL TE buffer, pH 7.5. Conditions for PCR genotyping for specific transgenic and mutant lines are listed below. All primer sets used for genotyping can be found in Table 8.1. All PCR products were ran on a non-denaturing acrylamide gel (10% gel in 1X TBE buffer) unless otherwise specified.

Sox10-Cre

For *Sox10*-Cre primer sets (Table 8.1), thermocycler PCR conditions were as follows: 94°C for 5 min; [94°C for 30 sec, 55°C for 30 sec, 0.5°C/sec ramp up to 72°C, 72°C for 30 sec, 0.5°C/sec ramp up to 94°C] repeated 34 times; 72°C for 10 min, 4°C indefinitely. In cases where it was necessary to determine if mice were homozygous or heterozygous for the transgene, DNA quantity was measured post-extraction on a NanoDrop 2000 spectrophotometer (Thermo Scientific). DNA quantity for PCR was equalized (150 ng/tube) and cycling repeats were reduced to 25. Intensity of the resulting bands on acrylamide gel compared to control DNAs was used to determine homozygous or heterozygous state. In my attempts, Sp6 primers produced the clearest difference in band intensity in heterozygous versus homozygous mice. This method for determining homozygosity was validated when I bred a putatively homozygous male and all his

Mouse line	Product Amplified	Assigned name	Forward primer (5' to 3')	Reverse primer (5' to 3')
Wnt1-Cre	Transgene fragment-Cre 475 bp	WNT1CRE F & WNT1CRE R	ATTCTCCCACCGTCAGTACG	CGTTTTCTGAGCATACCTGGA
Sox10-Cre	Transgene fragment-Sp6 arm 227 bp	Sp6 MS2 & 28o11 BAC left/Sp6 Rev	GTTTTTTGCGATCTGCCGTTTC	GGCACTTTCATGTTATCTGAGG
	Transgene fragment-T7 arm 202 bp	28o11 BAC Right/T7 Rev & SacBII promo Rev	AAGAGCAAGCCTTGGAACTG	TCGAGCTTGACATTGTAGGAC
	Transgene fragment-Cre 400 bp	AfpCreFor & AfpCreRev	GCGGCATGGTGCAAGTTGAAT	CGTTCACCGGCATCAACGTTT
Sox10^{Dom}	*Sox10* 34 bp mutant; 33 bp wildtype	dcgs10 Bh2midFa & dcgs10 Bh2mid RB	CGGATGCAGCACAAAAAGGACC	GGCCAGGTGGGCACTCTTGTA
Ret^{tm1Cos} *Ednrb*^{tm1Ywa}	Neo cassette 366 bp	Neo_Fwd_041510 & Neo_Rev_041510	CCTGCCGAGAAAGTATCCATC	TTCAGCAATATCACGGGTAGC
Ret^{tm1Cos} *Ednrb*^{tm1Ywa}	*Rapsn* (control) 592 bp	Rapsyn sense & Rapsyn a-sense	AGGACTGGGTGGCTTCCAACTCCCAGACAC	AGCTTCTCATTGGTGCGCGCCAGGTTCAGG
Phox2b^{CFP} *Sox10*^{YFP}	Transgene fragment-H2BGFP 580 bp	H2BGFPSac & H2BGFPNot	CTGGTCGAGCTCGACGGCGACGTA	AGTCGCGGCCGCTTTACTTG
R26R^{tdTom}	*ROSA* (wild type) 196 bp	oIMR9020_WT_Rtom_F & oIMR9021_WT_Rtom_R	AAGGGAGCTGCAGTGGAGTA	CCGAAAATCTGTGGGAAGTC
	ROSA (mutant) 297 bp	oIMR9103_Mutant_Rtom_R & oIMR9105_Mutant_Rtom_F	GGCATTAAAGCAGCGTATCC	CTGTTCCTGTACGGCATGG

Table 8.1 Oligonucleatide primers for PCR genotyping. This table includes primer information for mouse lines mentioned throughout this work (Chapters 1-7). "Assigned name" of the primers within the Southard-Smith lab is included to aid lab members in locating these primers in the future.

offspring (2 litters) harbored the transgene.

Sox10Dom

Sox10$^{Dom/+}$ genotypes were confirmed by PCR for pups used in analysis that had white paws and belly stripes or spots, but did not have obvious hypoganglionosis and/or aganglionosis when viewed under a dissection scope. (The vast majority of pups in my studies with white paws and belly markings displayed overt hypoganglionosis and/or aganglionosis. On very rare occasion, some pups with these markings did not display an overt ENS phenotype; however, these rare mice always tested positive for the *Sox10Dom* mutation via PCR genotypes.) Thermocycler PCR conditions for *Sox10Dom* genotyping were as follows: 92°C for 5 min; [92°C for 30 sec, 58°C for 30 sec, 0.5°C/sec ramp up to 72°C, 72°C for 30 sec, 0.5°C/sec ramp up to 94°C] repeated 27 times; 72°C for 10 min, 10°C indefinitely.

Wnt1-Cre

For *Wnt1*-Cre primer sets, thermocycler PCR conditions were as follows: 94°C for 3 min; [94°C for 30 sec, 55°C for 1 min, 0.5°C/sec ramp up to 72°C, 72°C for 1 min 30 sec, 0.5°C/sec ramp up to 94°C] repeated 35 times; 72°C for 5 min, 4°C indefinitely.

Ednrb$^{tmYwa1/+}$ & Ret$^{tmCos1/+}$

For *Ednrb*$^{tmYwa1/+}$ and *Ret*$^{tmCos1/+}$ mice, primer sets, a portion of the Neo cassette sequence was amplified to identify knockout mice. Additionally, a portion of the *Rapsn* gene was amplified in parallel as a control. Thermocycler PCR conditions were as follows: 94°C for 5 min, [(94°C for 30 seconds, *55°C for 30 sec, ramp to 72°C at 0.5°C per second, 72°C for 30 seconds, ramp to 94°C at 0.5°C per second) x 25-35 times], 72°C for 10 minutes, 4°C indefinitely. *This PCR protocol is notorious for producing non-specific bands. Although the genotype of the mice can usually still be interpreted with these non-specific bands. When I first joined the lab group, I ran this protocol with annealing temperatures at 55°C. However, I eventually starting running this protocol with annealing temperatures at 58°C. The more stringent annealing temperature led to less non-specific amplification of other gene products. Also important, similarities within the

Neomycin cassette and Kanamycin cassette result in amplification of the Kanamycin cassette when this primer set is used. This was discovered when I tried to genotyping pups from *Sox10*-Cre x *Ednrb*$^{tm1Ywa/+}$ crosses. The *Ednrb*^{tm1Ywa} locus contains a Neomycin cassette (Chapter 3) from which our genotyping protocol in lab is based off of. Unbeknownst to me, the *Sox10*-Cre transgene contains a Kanamycin cassette. I noticed within crosses from these litters that many more pups than expected, (expected = 50%; observed =~70%), were genotyping "positive" for presence of the Neomycin cassette and that nearly 100% of mice that tested positive for the *Sox10*-Cre transgene also tested positive for presence of the Neomycin cassette. Subsequent requests for information about the transgene sequence, which revealed that a Kanamycin cassette was within the transgene, led me to realize the overlap between genotyping products. Thus, any crosses between *Sox10*-Cre mice to mice that contain a Neo cassette must include more specific primer sets in order to differentiate mouse genotypes.

Phox2b^{CFP} & Sox10^{YFP}

For *Phox2b^{CFP} & Sox10^{YFP}* primer sets, thermocycler PCR conditions were as follows: 94°C for 5 min; [94°C for 45 sec, 55°C for 45 sec, 72°C for 45 sec,] repeated 35 times; 72°C for 5 min, 10°C indefinitely. More details in regard to these transgenic lines and genotyping can be found in the thesis of a previous Southard-Smith lab member (1).

R26R^{tdTom}

During my studies with *R26R$^{tdTom/tdTom}$* mice, we had several issues in this line including increased occurrence of bifurcated vaginas in females leading to poor breeding or infertility and dystocia. I also had issues with very small litter sizes, cannibalism, poor maternal care, and hydrocephalus. We hypothesized that some of these issues may have occurred due to multiple generations of inbreeding in this mouse line. (Small litter sizes are not uncommon on the C57/B6 background.) Efforts were made at one time to outbreed the line to C57/B6 stock without the *R26RtdTom* gene. Unfortunately, the outbred line appeared to have the hydrocephalus phenotype carried through to the second outcross. And, careful monitoring of females for

bifurcated vaginas as well as attempts to not breed brother-sister pairs improved some of our breeding issues in our lines that were not outbred. Because of the issues in our outbred line as well as improvement in our inbred lines, we chose to discontinue our outbreeding efforts. However, if these issues resulting from inbreeding occur again, primer sequences for genotyping for outbreeding may be found in Table 8.1 and thermocycler conditions are as follows: HOT START; 94°C for 5 min, [(94°C for 30 seconds, 61°C for 30 sec, ramp to 72°C at 0.5°C per second, 72°C for 30 seconds, ramp to 94°C at 0.5°C per second) x35 times], 72°C for 10 minutes, 10°C indefinitely.

Crosses & mouse selection

The progeny for my enteric NC-derived lineage analysis were derived from a series of crosses For NC-derivative studies, B6.*Sox10*$^{Dom/+}$ males were first mated to C3Fe.*Sox10*-Cre (line F) females. B6.*Sox10*^{Dom}; C3.*Sox10*-Cre males produced from these crosses were then crossed to homozygous *B6.Cg-Gt(ROSA)26Sor*$^{tm9(CAG-tdTomato/Hze/J}$, hereafter B6.*R26R*$^{tdTom/tdTom}$, females. Pups harboring the *Sox10Dom* or *Sox10* wild types allele, *Sox10*-Cre transgene, and *R26R*^{tdTom} were used in assessing enteric NC-derivative cell type proportions. These crosses are detailed in Figure 8.1. While the vast majority of test animals came from this type of cross, a couple litters were generated by mating a *Sox10*$^{Dom/+}$ male that was homozygous for the *Sox10*-Cre transgene to *R26R*$^{tdTom/tdTom}$ females.

Early in my studies, I had to identify a reporter line that would appropriately and clearly label NC-derivatives within the ENS. Initially, I attempted crosses with *Wnt1-Cre* or *Sox10*-Cre to *B6.129-Gt(ROSA)26Sor*^{tm1Joe}*/J*, hereafter *R26R*$^{GNZ/GNZ}$. We thought the *R26R*$^{GNZ/GNZ}$ line would work well as the GFP reporter included a nuclear localization signal, presumably leading to clear, nuclear labeling and easy quantification of cells. Unfortunately, the signal from these crosses was weak. Even in combination with IHC (primary antibody to GFP; secondary Cy2 antibody),

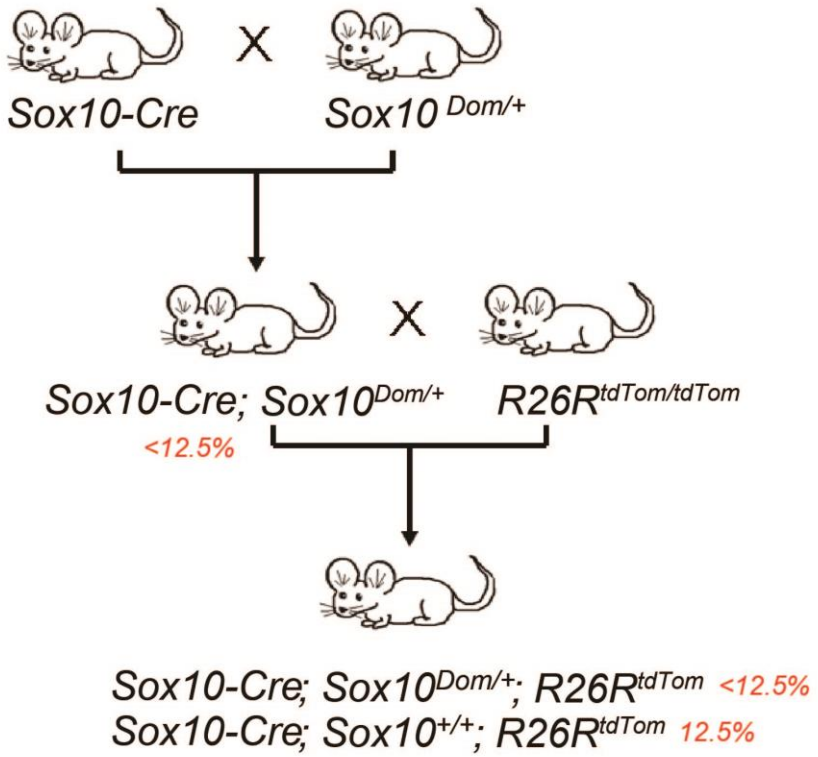

Figure 8.1. Mouse crosses for NC lineage analysis. Female mice harboring the *Sox10*-Cre transgene were crossed with $Sox10^{Dom/+}$ mice to produce *Sox10*-Cre; $Sox10^{Dom/+}$ males. These males were mated to homozygous $R26R^{tdTom/tdTom}$ females to produce progeny used in NC lineage analysis. Percentages in red represent expected yield of mice with specific genotypes to be utilized in crosses or NC lineage analysis. Inevitably, some pups with a *Sox10Dom* mutation will succumb to their disease before breeding or experimental age.

In general, the reporter mainly appeared localized to parts of the nucleus instead of labeling the whole nucleus. I also attempted *Sox10*-Cre crosses with *B6.129-Gt(ROSA)26Sor*$^{tm1(EYFP)Cos}$*/J*, hereafter *R26R*$^{YFP/YFP}$ mice. This reporter line worked much better in regard to labeling the ENS; however, additional IHC to the YFP reporter (primary antibody to GFP; secondary Cy2 antibody) was necessary for optimal signal visualization (Figure 8.2B). Also, use of an additional antibody to visualize the YFP reporter reduces the antibody choices to label NC-derived cell types. I therefore turned to evaluating the *R26R*$^{tdTom/tdTom}$ line. We were optimistic about this reporter line evidence from personal communications as well as the literature promised better reporter expression. More specifically, the *R26R*^{tdTom} contains an additional CAG sequence with the R26R reporter sequence has been reported to increase reporter expression above that when CAG and *R26* are used on their own to drive expression (reviewed in (2)). *Sox10*-Cre and *R26R*$^{tdTom/tdTom}$ crosses produced progeny (~50%) with clearly labeled ENS (Figure 8.2C) without the need for additional IHC. Unexpectedly, but fortuitously, the nuclei of many cells appeared to have differential reporter expression compared to their processes, making quantification of cell types

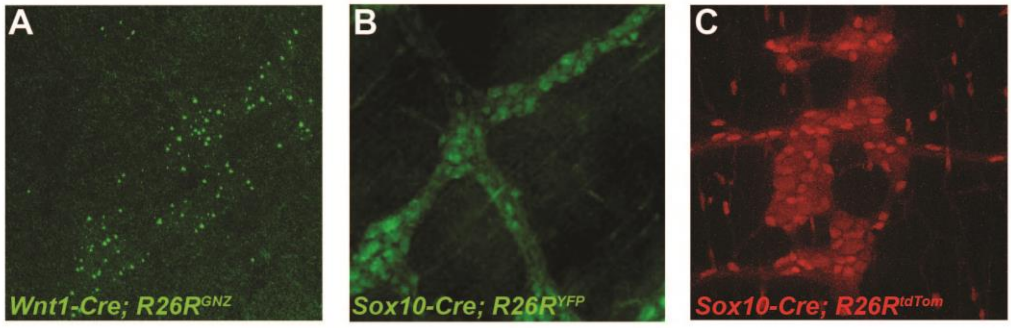

Figure 8.2. *ROSA26 Reporter* comparisons within the enteric nervous system. Three reporters were tested with *Wnt1-Cre* and/or *Sox10*-Cre. (**A**) *R26R*^{GNZ} expression appeared limited to small, discrete locations possibly within the nucleus of ENS cells and also did not appear to mark all ENS cells. In general, this led to a speckled appearance. (**B**) Reporter signal through *R26R*^{YFP} clearly labeled ENS cells and processes; however, weak signal led to prerequisite use of additional IHC (anti-GFP antibody with fluorescent secondary antibody.) This additional IHC needed to intensify the signal limited choices of other IHC reagents in future experiments, making this reporter acceptable, but not ideal. (**C**) *R26R*^{tdTom} expression clearly labeled ENS cell bodies and processes wihtout additional IHC, making it the optimal reporter out of those tested for ENS lineage analysis. (20X objective with software (LSM and/or Microsoft Powerpoint) zoom and selection.)

easier. Additionally, glia tended to have brighter signals than neurons, also making cell types easier to differentiate during quantification. Although unexpected, I hypothesize that glia have a brighter signal due to cell volume. Glia have much smaller processes than neurons, whose axons and dendrites can extend for several centimeters. Other possible explanations include differential expression of the reporter or differential turnover of the reporter driven by cell type specific mechanisms.

Once I had crosses with the appropriate mutation, it was important to determine if the *Sox10*-Cre transgene produced any additional adverse phenotypes or death within the *Sox10*$^{Dom/+}$ mice. (This possibility is explored and explained in depth in Chapter 2.) In my own personal observations of the mouse crosses, *Sox10*$^{Dom/+}$ mice with the transgene did not appear physically different or more runted than their *Sox10*$^{Dom/+}$ littermates without the transgene. To test this statistically, when I first began these crosses, I recorded the number of *Sox10*$^{Dom/+}$ mice with or without the transgene that survived to time of experiment (P15-P21). If the *Sox10*-Cre transgene was causing lethal phenotypes or worst aganglionosis in *Sox10*$^{Dom/+}$ animals, I would expect more *Sox10*$^{Dom/+}$ mice with the transgene to succumb to death before time of experiment when compared to *Sox10*$^{Dom/+}$ mice without the transgene. I statistically tested this possibility (X^2 goodness of fit; JMP v11) and found no significant difference in the number of *Sox10*$^{Dom/+}$ mice with or without the transgene (*P=0.2413*; n=25 *Sox10*$^{Dom/+}$Cre+ and n=34 *Sox10*$^{Dom/+}$Cre-). Also see Table 2.5.

Analysis of myenteric plexus NC-derived lineages

Sample Collection

P15-19 day mice were sacrificed with isoflurane and pieces of the duodenum, ileum, and the entire cecum and colon were immediately removed and placed into 1XPBS. For the duodenum, 1.5-2.0 cm was taken starting ~0.5 cm distal to the pyloric sphincter. For the ileum,

1.5-2.0 cm was taken starting ~1.5 cm proximal to the cecum and then heading more proximally. Before taking the mid-colon region in *Sox10^{Dom}* mice, the entire cecum and colon was placed on a slide and viewed on a BX41 Olympus fluorescent microscope with a 5X objective. A Sharpie™ marker or equivalent was used while viewing to mark the beginning of aganglionosis and/or hypoganglionosis in each sample if applicable. The sample was then placed on a ruler to determine the entire length of the colon (end of cecum to anus), the length of aganglionosis, and the length of hypoganglionosis. Then, ~1.5 cm of mid-colon was taken. In P15-16 mice, the mid-colon was defined as starting 1.5 cm distal to the cecum. In P17 and older mice, the mid-colon was defined as starting 2.0 cm distal to the cecum. All regions of the gut were then flushed with 1XPBS and immediately placed into NBF/0.5% Triton X-100 (NBF, Sigma, HT50112; Triton X-100, MP Biomedical, 819620) on ice for a minimum of 20 minutes. Gut pieces were then moved into 1XPBS on ice until subdissection in 1XPBS and cut along the mesenteric line. Gut muscle strips (GMS), also known as laminar muscle preparations, were then subdissected from all gut regions. (Gut muscle strips include the serosa, longitudinal muscle, myenteric plexus, and circular muscle layers of the gut. All other layers were discarded.) Efforts were made to remove as much extraneous tissue (mesentery, blood vessels, etc.) as possible from the GMS. Subsequent fix times and IHC differed depending on the antibodies being used. Details can be found in proceeding sections of this chapter.

IHC for neurons and glia

Following subdissection, GMS were placed back into NBF with 0.5% TritonX-100 and fixed O/N at 4°C. GMS were then rinsed once in 1XPBS and twice in 1XPBS/0.1% TritonX-100 for a minimum of 10 minutes per rinse. GMS were then placed in filtered NDS block (0.1 g BSA, 0.5 mL Normal Donkey Serum, 9.5 mL 1XPBS/0.1% Triton X-100) for 1.5 hr at RT. Next, GMS were placed in Human anti-Hu primary antibody to label neurons (Table 8.2) for at least O/N at 4°C.

Antigen	Host	Supplier	Catolog	Dilution	Tissue fix times	*Reusable?
Phox2b	Rabbit (polyclonal)	gift of P. Chambon	n/a	1:750	20-25 min at RT	yes
HuC/D	Human	gift of V. Lennon	n/a	1:10000	20-25 min at RT or O/N at 4°C	yes
FoxD3	Rabbit (polyclonal)	gift of T. Labosky	n/a	1:400	O/N at 4°C	no
Calretinin	Goat (polyclonal)	Millipore	AB1550	1:2500	20-25 min at RT	yes
NOS1 (K-20)	Rabbit (polyclonal)	Santa Cruz	sc-1025	1:600	O/N at 4°C	yes
s100A1	Sheep (polyclonal)	QED Biosciences (H.Young)	56201	1:3000	O/N at 4°C	yes
s100B	Rabbit (polyclonal)	DAKO	Z 0311	1:500	20-25 min at RT or O/N at 4°C	no
ChAT	Rabbit (polyclonal)	Millipore	AB143	1:250	20-25 min at RT	?
vAChT	Rabbit (polyclonal)	SYSY	139 103	1:1000	20-25 min at RT	?
**SERT	Guinea pig (polyclonal)	Frontier Institute	HTT-GP-Af1400	1:1000	20-25 min at RT	?
cKit (CD 117)	Rat ($IgG2b_{Kappa}$)	Millipre	CBL1360	1:250-500	20-25 min at RT	?
TH	Sheep (polyclonal)	Millipore	AB1542	1:100	20-25 min at RT	?
GFP	Chicken (polyclonal)	AbcAM	AB13970	1:500	20-25 min at RT	?

Table 8.2. Primary antibodies for IHC. This table includes information in regard to primary antibodies used for IHC (Chapters 1-7). Antibodies that were tested but failed to clearly label cell types in our test conditions are not included on this list. *Dilutions of antibodies that could be used multiple times are indicated as such under the reusable column. ?=untested for multiple use. **This antibody works best if tissues are fixed in a 4% PFA/3% sucrose solution.

During this time, extra GMS tissue was placed in freshly diluted (1:400) Rabbit anti-FoxD3 antibody (Table 8.2) in NDS block and placed with other samples at 4°C O/N. (Use of this "pre-incubated" anti-FoxD3 dilution significantly reduced background in GMS samples, especially in the colon.) Following the first primary antibody incubation, the GMS were rinsed four times for a minimum of 5 minutes in 1XPBS/0.1% TritonX-100. GMS were then placed in the second primary antibody, Rabbit anti-FoxD3 (the same dilution prepared with extra GMS tissue) to label glia for at least O/N at 4°C. The GMS were then rinsed four times for a minimum of 5 minutes in 1XPBS/0.1% TritonX-100. Next, GMS were placed in secondary antibody Donkey anti-Human DyL649 (Table 8.3) for 1.5 hours at RT followed by four rinses for a minimum of 5 minutes in 1XPBS/0.1% TritonX 100. GMS were then placed in secondary antibody Donkey anti-RabbitAlexa488 (Table 8.3) for 1.5 hours at RT. GMS were then rinsed for at least 10 minutes in 1XPBS/0.1% TritonX-100 and twice for at least 10 minutes in 1XPBS. GMS were then placed in fresh 1XPBS and placed at 4°C. Efforts were made throughout the IHC procedure to guard GMS and secondary antibodies from light. Anti-FoxD3 antibody dilution was only used once and then discarded. Attempts to reuse this antibody produced very weak signals.

Detection and Type	Supplier	Cat.No.	*Dilution
Alexa488 Donkey Anti-Rabbit IgG (H+L)	Jackson Immuno	711-545-152	1:400
Alexa488 Donkey Anti-Sheep IgG (H+L)	Jackson Immuno	713-545-147	1:400
Alexa488 Donkey Anti-Guinea Pig IgG	Jackson Immuno	706-545-148	1:400
Cy2 Donkey Anti-Chicken	Jackson Immuno	no longer available	1:200
FITC Donkey anti-Chicken IgY F(ab') 2 fragment	Jackson Immuno	703-096-155	1:400
Cy2 Donkey Anti-Goat	Jackson Immuno	705-225-147	1:600
Alexa647 Donkey Anti-Rabbit IgG (H+L)	Jackson Immuno	711-605-152	1:200
DyLight649 Donkey Anti-Human IgG (H+L)	Jackson Immuno	709-495-149	1:200
Texas Red Donkey Anti-Human IgG (H+L)	Jackson Immuno	709-075-149	1:100
Cy3 Donkey Anti-Rat igG (H+L)	Jackson Immuno	712-165-153	1:500
Cy3 Donkey Anti-Sheep IgG (H+L)	Jackson Immuno	713-165-147	1:1000
Cy3 Donkey Anti-Rabbit IgG (H+L)	Jackson Immuno	711-165-152	1:1000

Table 8.3. Secondary antibodies for IHC. This table includes information in regard to secondary antibodies used for IHC (Chapters 1-7). Those secondary antibodies with similar fluorescent excitation/emission spectrums are color blocked together. *All secondary antibody dilutions listed are based on an initial 1:1 dilution in glycerol.

IHC for Calretinin expressing neurons

Following subdissection, GMS were immediately rinsed once in 1XPBS and twice in 1XPBS/0.1% TritonX-100 for a minimum of 10 minutes per rinse. GMS were then placed in NDS block for either one hour at RT or O/N at 4°C. GMS were then placed in Human anti-Hu primary antibody for a minimum of 4 hours at RT or at least O/N at 4°C. Following the first primary antibody incubation, the GMS were rinsed four times for a minimum of 5 minutes in 1XPBS/0.1% TritonX-100. GMS were then placed in a second primary antibody, Goat anti-Calretinin (Table 8.2) for a minimum of 4 hours at RT or O/N at 4°C. The GMS were rinsed four times for a minimum of 5 minutes in 1XPBS/0.1% TritonX-100. GMS were then placed in secondary antibody Donkey anti-Human DyL649 (Table 8.3) for 1 hour at RT followed by four rinses for a minimum of 5 minutes in 1XPBS/0.1% TritonX-100. GMS then incubated in secondary antibody Goat anti-Cy2 for 1 hour at RT followed by a rinse for at least 10 minutes in 1XPBS/0.1% TritonX-100 and two rinses for at least 10 minutes in 1XPBS. GMS were then placed in fresh 1XPBS and placed at 4°C. Efforts were made throughout the IHC procedure to guard GMS and secondary antibodies from light. Of note, all antibodies were diluted in NDS block and both primary anti-Hu and anti-Calretinin antibodies were used multiple times (5+) before replacing.

IHC for nNOS expressing neurons

Following subdissection, GMS were placed back into NBF with 0.5% TritonX-100 and fixed O/N at 4°C. GMS were then rinsed once in 1XPBS and twice in 1XPBS/0.1% TritonX-100 for a minimum of 10 minutes per rinse. GMS were blocked in NDS block for 1.5 hr at RT. GMS were then placed in Human anti-Hu primary antibody for at least O/N at 4°C. Following the first primary antibody incubation, the GMS were rinsed four times for a minimum of 5 minutes in 1XPBS/0.1% TritonX-100. GMS were then placed in a second primary antibody, Rabbit anti-nNOS (Table 8.2)

for at least O/N at 4°C followed by four rinses for a minimum of 5 minutes/rinse in 1XPBS/0.1% TritonX-100. GMS were then placed in secondary antibody Donkey anti-Human DyL649 (Table 8.3) for 1.5 hour at RT followed by four rinses for a minimum of 5 minutes in 1XPBS/0.1% TritonX 100. GMS were then placed in secondary antibody Donkey anti-Rabbit Alexa488 (Table 8.3) for 1.5 hours at RT. GMS were then rinsed for at least 10 minutes in 1XPBS/0.1% TritonX-100 and twice for at least 10 minutes in 1XPBS. Following rinses, GMS were placed in fresh 1XPBS and stored at 4°C. Efforts were made throughout the IHC procedure to guard GMS and secondary antibodies from light. Of note, all antibodies were diluted in NDS block and both primary anti-Hu and anti-nNOS antibody dilutions were used multiple times (5+) before replacing.

IHC for Interstitial Cells of Cajal

Early in my studies, I recognized the possible necessity of analyzing Interstitial Cells of Cajal (ICC) number and morphology. ICC cells are largely responsible for the slow wave movement and pace maker activity of the gut (3). Additionally, they are found closely juxtaposed to ENS neurons and muscle. In regard to muscle movement, enteric neurons may signal directly onto smooth muscle cells or onto ICC that in turn signal onto smooth muscle cells (3). The role of ICC in HSCR is disputed. Many studies note reductions in ICC in hypoganglionic and/or aganglionic portions of human HSCR intestine (4-7). One study has highlighted changes in ICC architecture (8) while another study suggested ICC, while possibly reduced in number, were regularly distributed and patterned (9). ICC cells have been evaluated in the aganglionoic region of *Ednrb*$^{ls/ls}$ HSCR mice, but not in ganglionated regions (10). Because I saw the possibility of having to analyze ICC in our HSCR mouse samples, I optimized IHC with a cKit (CD 117) antibody on gut muscle strips (Figure 8.3) as well as sections. cKit is a tyrosine protein kinase purportedly expressed in a subset of ICC in the myenteric plexus (3). IHC on GMS for cKit is identical to the

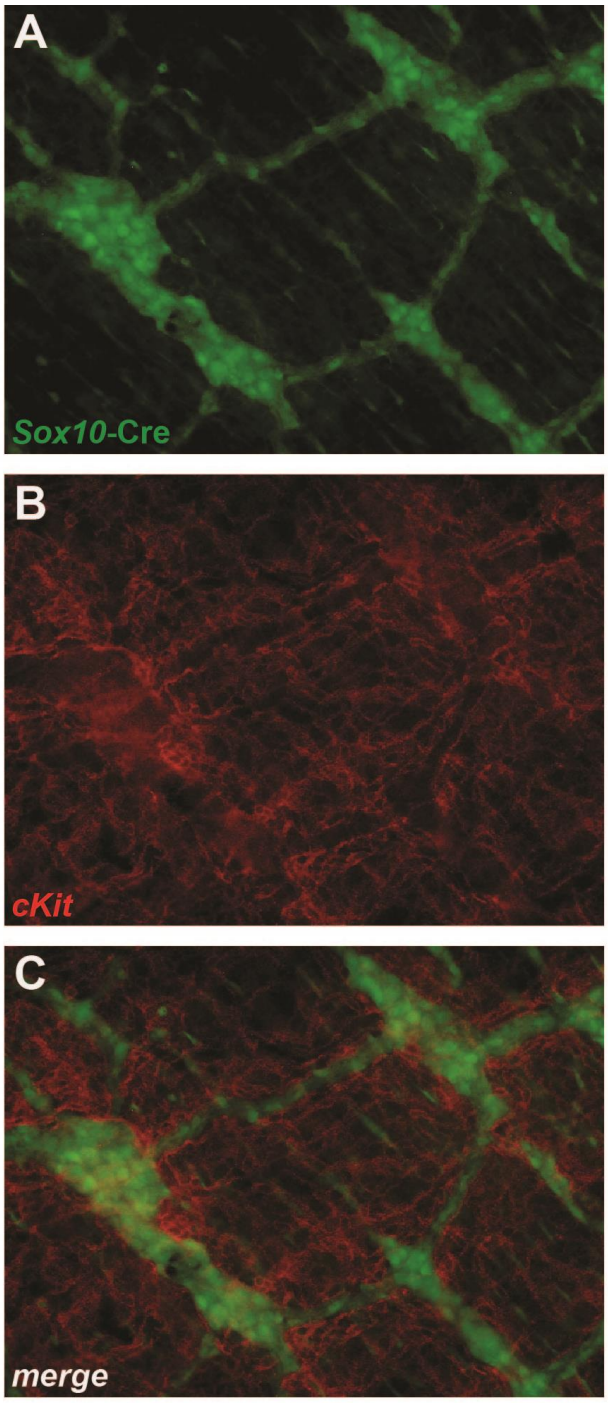

Figure 8.3. Interstitial cells of cajal (ICC) surround the myenteric plexus ganglia and processes. (**A**) The *Sox10*-Cre transgene drives YFP reporter from *R26R*^{YFP} in the myenteric plexus. (**B**) IHC with the an antibody to cKit labels ICC-MY (ICC cells within the myenteric plexus) bodies and processes. (**C**) The merged image detail the intricate relationships of ICC-MY with myenteric plexus neurons and processes.

protocol outlined above for Calretinin neurons, except for the primary and secondary antibodies used (Tables 8.2 & 8.3).

For cKit IHC on sections, I first dissected whole guts into 1XPBS followed by fix in NBF/0.5% Triton X-100 on ice. Fixation was followed by four 5 minute rinses in 1XPBS at RT and a one hour rinse in 1XPBS at 4°C. Guts were then placed in 30% sucrose O/N at 4°C. Following equilibration, sampled were embedded in OCT tissue embedding medium. After freezing, samples were sectioned on a cryostat, allowed to dry on a slide warmer for at least 30 minutes, and blocked in 1% donkey serum in 1XPBS/0.1% Triton X-100. Samples were then incubated in cKit antibody (1:500 dilution in block) O/N at 4°C followed by secondary antibody incubation (Table 8.3) for 30 minutes at RT. Slides were then rinsed in 1XPBS. Importantly, attempts by other lab members and labs to use this antibody were not always successful in different tissues or slice types. The Bob Coffey lab had clear staining with this antibody if tissue was fresh frozen and sliced followed by fixation in either PFA or acetone (Jumpei Kondo, personal communications).

IHC for other cell types (SERT, TH, ChAT, vAChT)

During my studies, I tested and attempted to optimize numerous antibodies to label specific neurons subtypes and other cell types. Here, I provide details for additional antibodies not used ultimately in my analysis of NC derived lineages, but that could potentially be used in future studies. SERT antibody was used to label serotonergic neurons within the myenteric plexus. For IHC with the SERT (serotonin transporter) antibody (Table 8.2), the protocol was identical to that of Calretinin IHC except for the type of fix used. Fixing tissues in NBF/0.5% TritonX-100 led to suboptimal staining, but fixing tissues in 4%PFA/3% sucrose led to clearer staining. (With thanks to Mike Gershon and Kara Margolis for this suggestion.) Ultimately though, SERT signal is strong in neuronal processes and does not label cell bodies as clearly as one

would like to quantify this cell type. This same type of issue arose when I attempted IHC with a TH (tyrosine hydroxylase) antibody (Table 8.2) to label dopaminergic neurons. Neuronal processes were clearly labeled, but cell bodies only had punctate signal, making quantification difficult. On the other hand ChAT (choline transferase) and vAChtT antibodies (Table 8.2) clearly labeled cholinergic neuron cell bodies and processes (Figure 8.4). The ChAT antibody tended to label both neuron cell bodies and processes with high expression in both. The vAChT antibody clearly labeled both, but with less signal emanating from cell bodies. This outcome was expected though as the vAChT antibody specifically labels vesicular acetyl choline transporters, which in neurons will be found prominently in neuronal processes as vesicles filled with acetylcholine are trafficked to axonal boutons. The ChAT antibody is less specific, labeling all ChAT (found outside and insides vesicles) within the neuron. The IHC protocol for TH, ChAT, and vAChT is identical to the Calretinin protocol above except for the primary and secondary antibodies used.

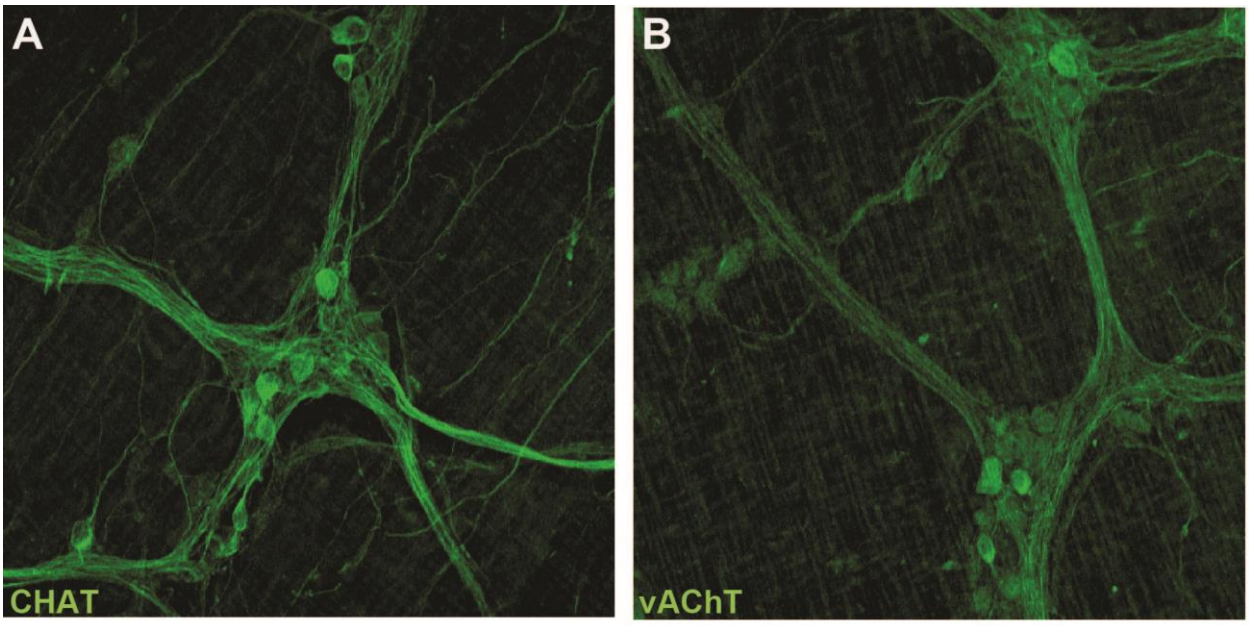

Figure 8.4. IHC for cholinergic neurons in the myenteric plexus. (**A**) The CHAT antibody labels cholinergic neurons. Expression is concentrated in the soma, but is also clearly seen in cellular processes. (**B**) vAChT, as expected, is expressed in axonal processes and less strongly within cell bodies compared to the CHAT antibody used in panel A.

IHC with s100B

I initially set out to label and quantify glia in *Sox10^{Dom}* and *Sox10$^{+/+}$* pups with a well known glial maker in the ENS, s100B. The IHC protocol for the s100B is identical to the Calretinin protocol above except for the primary and secondary antibodies used. Additionally, longer fixation times do not seem to impact labeling. For the most part, I obtained clear labeling of glia within all regions of the intestine along with successful labeling of neurons (Hu+) (Figure 8.5). However, while trying to complete this analysis, I noticed some samples did not "label as well" with the s100B antibody as other samples (Figure 8.6). I initially thought this might be an issue with my IHC technique, such as gut muscle strips not being completely submerged within antibody incubation solutions. However, once this difference in labeling occurred a few times, despite careful attention to IHC technique, I unblinded myself to mouse phenotype and genotype. Interestingly, I immediately noticed that my "problem" samples all originated from *Sox10$^{Dom/+}$* pups. Thus, the difference in s100B signal intensity in my imaging was probably biologically driven and not a result of poor lab technique. This discovery led me to abandon labeling glia with s100B for my studies. Instead, I utilized a FoxD3 antibody. FoxD3, unlike s100B, is temporally upstream of Sox10, and thus expression is less likely perturbed by the *Sox10Dom* mutation.

Mounting & Imaging

Following IHC, GMS were flat-mounted onto slides (Fisherbrand, Cat.No. 12-550-15) with Aqua Poly/Mount (Polysciences, Cat. No. 18606-20) and cover slipped (Fisherbrand, Cat.No. 12-545-F). Clear nail polish was used to seal the edges of the cover slip and slide in order to prevent drying out of the mounting medium and samples. All samples for NC-lineage analysis were imaged on an LSM 510 Meta Inverted Confocal Microscope system at 200X (20X objective; 10X eyepiece) with a 1.5 software zoom with LSM software. For each region of the gut, areas were

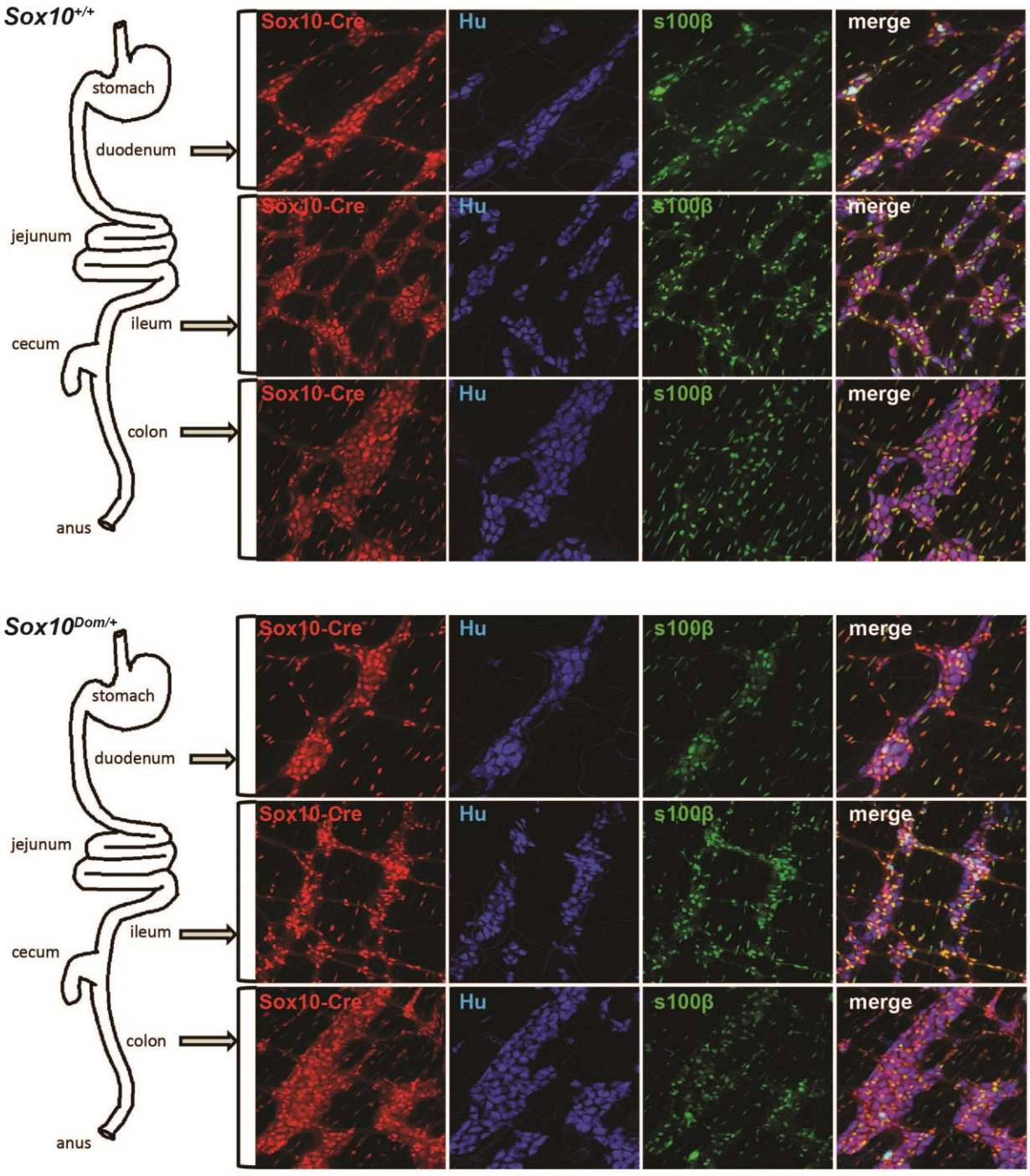

Figure 8.5. Overview of *Sox10*$^{+/+}$ and *Sox10*$^{Dom/+}$ reporter expression and IHC. For NC-derived lineage analysis, samples were collected from the duodenum, ileum, and mid-colon of (**A**) *Sox10*$^{+/+}$ and (**B**) *Sox10*$^{Dom/+}$ pups that harbored the *Sox10*-Cre transgene and *R26R*^{tdTom} (red). IHC was carried out to label neurons (Hu) and glia (s100β).

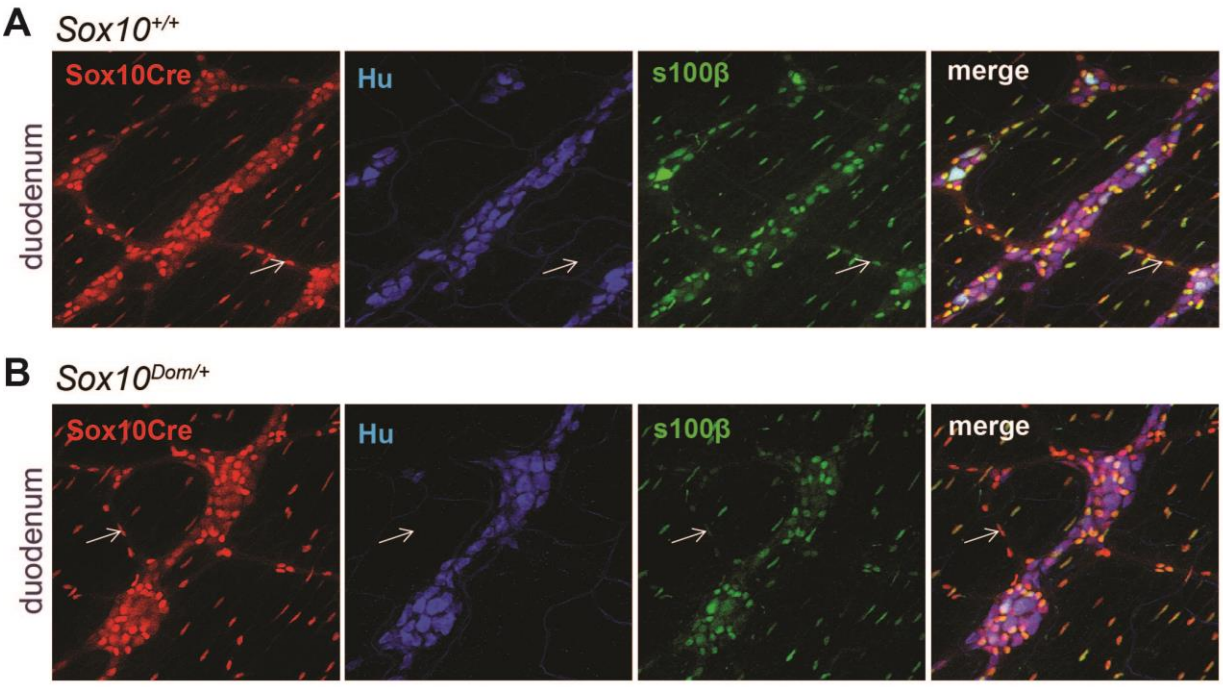

Figure 8.6. Differential expression of s100β in *Sox10*$^{+/+}$ and *Sox10*$^{Dom/+}$ pups. *Sox10*-Cre driven expression from *R26R*^{tdTom} labels all NC-derived cells. IHC was used to label neurons (Hu) and glia (s100β). (**A**) In *Sox10*$^{+/+}$ pups, s100β signal appears strong in in glia within ganglia and connectives (arrow). (**B**) In contrast, some glia in *Sox10*$^{Dom/+}$ pups had little or weak s100β expression (arrow).

randomly selected to image and noted during imaging to avoid image redundancy. Areas were randomly selected by visualization of the *ROSA26R-tdTomato* reporter under the Cy3 filter. Random selection via this channel ensured the imager was not biasing imaging based on neural crest derivative types (neurons, glia, neuron subtypes) since the only signal visible during selection was that generated from *tdTomato* expression within all neural crest derivatives. Due to fixation issues or unknown reasons, sometimes *tdTomato* expression was not consistently observed in patches of neurons, especially in the ileum and colon. To avoid this issue, I moved my analysis to an earlier developmental time period (P15-17 from P17-P20.) I also noted that expression was better with a longer fixation period. However, since some antibodies worked better with a shorter fix period, the best option was to move the analysis earlier. Additionally, lack

of tdTomato reporter expression appeared to occur primarily along the anti-mesenteric line. And, blood vessels and mesentery made imaging directly next to the mesenteric line difficult. Thus, for consistency, images were randomly selected from in between the mesenteric and anti-mesenteric lines in the ileum and colon. For all images, pinhole and laser power were adjusted accordingly for optimal signal capture. (Individual LSM files contain these parameters. To easily access these settings, open an image file in the LSM Image Browser and click on the "info" icon in the lower right hand corner of the image viewer window. In general, I aimed for a pinhole setting of near 1.0 for each laser channel. The 633 nm wavelength laser could typically, but not always, be set at a lower power (2-4%) while 488 nm and 543 nm wavelength lasers were typically more mid-range (5-14%)). Set parameters included: 4X averaging, 512x512 resolution or higher, "optimal slice interval" selection through the LSM software, 20X objective with 1.5X software zoom.

Image processing & counting

Z-stack images were converted to 3D projections using LSM software. Separate channel images were exported from LSM and adjusted in Adobe PhotoShop for brightness and contrast and merged. Cell types were counted manually in Adobe PhotoShop with a manual cell counter. Layer(s) with dots denoting each cell counted were added in Adobe PhotoShop. Cells were only counted if they were in the same layer as myenteric plexus ganglia. For neuron and glia analysis, neurons and glia were only counted if they were contained in ganglia and primary connectives. (Initial counting of all glia in all layers in each image introduced large intragroup variance. Also, samples differed in thickness due to fix times as well as phenotype. For example, *Sox10*^{Dom} mutants have thinner muscle in hypoganglionic and aganglionic regions. Thus, preliminary tests indicated that analysis should be limited to ganglia and primary connectives.)

Western Blot

Although I chose not to use s100B for IHC studies, the biological relevance of reduced s100B expression in glia of *Sox10Dom* pups is intriguing. S100B has been implicated in numerous processes that could be relevant to my studies, such as cell migration, proliferation, and differentiation (reviewed in (11)). Interestingly, Sox family genes, although not Sox10, have been implicated in downregulating s100B expression (reviewed in (12). Although differences in IHC signaling hinted that s100B expression is perturbed in *Sox10*$^{Dom/+}$ mice, measurements of fluorescent signaling within IHC images is not easily compared between samples. Variations in IHC from experiments on different days typically leads to slightly altered confocal microscope specifications for optimal imaging. And, sheer measuring of fluorescent intensity does not take into account the number or size of cells within an image. Furthermore, because s100B can act extracellularly, differences seen in fluorescent signal intensity in glia may not be caused by glia in *Sox10*$^{Dom/+}$ mice producing less s100B, but rather be caused by glia extruding more s100B into the extracellular space. A more accurate measurement of s100B protein within GI tissue can be obtained through Western blotting. My attempts at Western blotting are most accurately labeled as “partially successful.” In my cleanest attempt, the control protein neuronal β-tubulin bands are evident in duodenal samples and very clean and evident in ileal samples. Additionally, presumed s100B dimer bands were visualized for some wild type samples for the duodenum, but not for *Sox10*$^{Dom/+}$ samples, suggesting a true decrease of this protein in *Sox10*$^{Dom/+}$ mice (Figure 8.7). However, results were not clean enough to conclusively make this statement. Here, I include a full protocol for Western Blot analysis with the caveat that more stringent denaturing conditions might be needed to visualize monomer (non-dimerized) s100B and that modifications/alternatives to imaging blots might be needed for publication quality data. I would be remiss if I did not acknowledge Byron Knowles (Jim Goldenring lab) and Eric Armour (Kevin Ess lab) for sharing

Western Blot protocols. All my protocols related to Western Blots are unchanged or modified versions of recipes and protocols from these two lab groups.

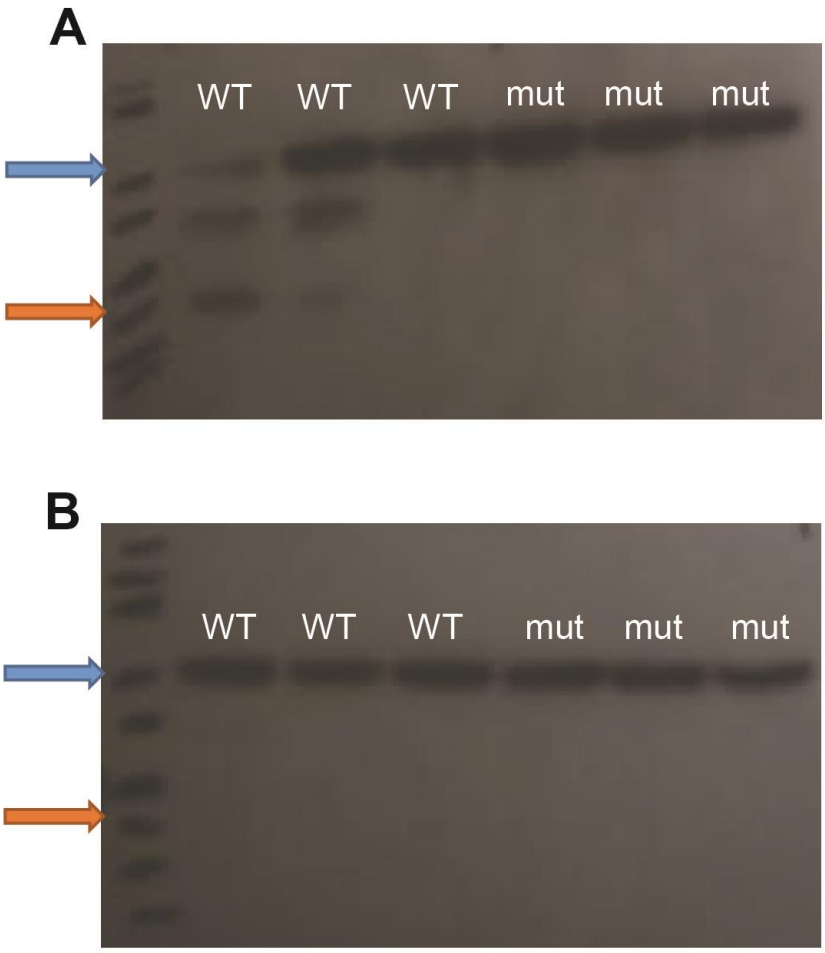

Figure 8.7. Western blot attempts for neuronal β-tubulin and s100B. Attempts were made to quantify protein expression levels via Western blot from *Sox10*$^{+/+}$ (WT) and *Sox10*$^{Dom/+}$ (mut) intestinal segments. (**A**) In the duodenum, control protein expresison of neuronal β-tubulin appears at ~50 kDA for all samples (blue arrows) while presumed s100B dimers at ~21 kDA only appear in WT samples (orange arrows). (**B**) In the ileum, control protein expression is clear in all samples tested, but testing parameters were not optimal to visualize s100B protein dimers. (Exposure time = 1 second)

Protein Isolation

Sox10$^{Dom/+}$ or *Sox10*$^{+/+}$; *Sox10*-Cre; *R26R*^{tdTom} pups (P16-17) were euthanized quickly with isoflurane followed immediately by cervical dislocation. Sections of the duodenum, ileum, and colon (identical to those described for IHC protocols) were immediately removed and placed in ice cold 1XPBS. *Sox10*$^{Dom/+}$ colons were immediately viewed under a BX41 Olympus fluorescent microscope as quickly as possible to assess length of hypoganglionosis and aganglionosis. These parameters were measured for two reasons. First, hypoganglionosis and/or aganglionosis in the colon has to be taken into consideration as a sheer decrease in glia number would appear as decreased s100B expression on a Western blot when compared to controls. Second, given the correlations I observed between small intestine neuronal subtypes and extent of aganglionosis in *Sox10*$^{Dom/+}$ animals, I wanted to be able to test for correlations between s100B expression levels and aganglionosis should *Sox10*$^{Dom/+}$ animals have visible variability in s100B expression in different regions of the small intestine.

Immediately following dissection and/or measurement of aganglionosis, in cold 1XPBS, the entire gut muscle strip was removed from each section of the gut collected. The gut muscle strip was immediately placed in and along the side of a pre-labeled 1.5 mL microtube. A pipette was used to remove as much 1XPBS as possible from the sample and microtube. Once the microtube cap was securely screwed into place, the sample was flash frozen in liquid nitrogen. (Do NOT attempt to use 1.7 mL centrifuge (snap cap) tubes for flash freezing and double check screw caps to make sure they are closed. Centrifuge tubes with snap caps tend to not seal as well as screw cap tubes. If the tube is not adequately sealed, liquid nitrogen will enter the tube and the tube will explode when removed from the liquid nitrogen. This inevitably leads to loss of your sample and possibly your eye.) This procedure was repeated for each section of the gut. Samples were allowed to stay in liquid nitrogen until all GMS dissections were completed. Once all dissections were complete, samples were moved into a tube rack and stored at -80°C.

Importantly, this whole procedure was done as carefully, but as quickly as possible in order to avoid protein degradation. Also, I chose to use GMS since the only cells that purportedly express s100B in these samples would be glia in the myenteric plexus. Whole gut samples would also include the submucosal plexus and epithelium which contain glia and other cell types that express s100B and other s100 proteins (13-15).

To isolate protein from tissues, I first placed my samples from -80°C onto ice. I then added to 200 µL of pre-made RIPA buffer (Table 8.4) and 2 µL of Inhibitor Cocktail (Thermoscientific, Pierce, Halt Protease Inhibitor Cocktail, Cat. No. 87785) to each sample and placed back on ice for 30 minutes. (Note: It is important to mix the inhibitor cocktail and RIPA buffer immediately BEFORE placing into sample tubes. Enzyme activity of inhibitors can be lost if mixed before the day of your experiment and protein can be lost if you add inhibitors after you add RIPA buffer to your samples.) At the start of this 30 minute interval, I used a filter pipette tip to mechanically dissociate the tissue in each tube. This pulverization was done gently and the RIPA solution was relied upon to do most of the cell lysing. Approximately 15 minutes into the 30 minute interval, each sample tube was flicked multiple times. Tubes were flicked again at the end of 30 minutes before centrifugation for 10 minutes at 10,000G at 4°C. Importantly, the amount of RIPA buffer and Inhibitor Cocktail can be adjusted for these steps depending on tissue size. Additionally, one can add a small amount of RIPA buffer and Inhibitor Cocktail initially and pulverize tissue, followed by addition of more RIPA buffer. After centrifugation, I placed supernatant in new, labeled 1.5 mL tubes. To avoid multiple freeze thaws to the protein, I eventually chose to aliquot each sample into multiple tubes and to place 5 uL of each sample's supernatant in a tube for subsequent protein quantification. If I was not using protein immediately, I stored at -80°C. If protein was to be used in the next day or two, I stored it at -20°C.

To quantify protein, I prepared samples with the Biorad DC Protein assay system (Cat. No. 500-0113 & 500-0114) and measured protein quantities on a NanoDrop 2000 (Thermoscientific). Within the NanoDrop software, I chose the “Protein Bradford” application to measure my protein amounts. In addition to the protein from my samples, I made serial dilutions (2, 1, 0.5, 025, 0.125, 0.0625 µg/mL) of BSA protein (Sigma-Aldrich, Cat.No. #A2153) to establish a standard curve. Detailed instructions on how to measure proteins on the NanoDrop 2000 using the “Protein Bradford” application are available within the NanoDrop 2000 manual as well as at nanodrop.com.

Reagent	Amount
1XPBS	89 mL
10% NP40	10 mL
Sodium Deoxycholate	0.5 g
10% SDS	1 mL

Table 8.4. RIPA buffer recipe. This RIPA recipe makes 100 mL of RIPA buffer. Based on the availability of reagents in lab and percentages of stock solutions, this recipe can be adjusted as long as the buffer ultimately contains 1% NP40, 0.5% Sodicum Deoxycholate, 0.1% SDS in 1XPBS. The RIPA buffer should be sterile filtered and stored at 4°C. Phophotase and protease inhibitors should only be added to this buffer immediately prior to protein isolation.

Gels & Transfer

On days I was going to perform SDS-PAGE to separate my proteins, I first mixed and poured my gels. I chose to run my samples through a 6% stacking gel and 12% resolving gel (Table 8.5). However, percentages and reagents should be adjusted based on the size and possible separation/denaturing needed for the protein of interest. A handy tool for quickly calculating gel ingredient amounts at specific percentages can be found at Cytographica.com. When pouring gels, I allowed the resolving gel to set slightly before pouring the stacking gel. I

also used a squirt bottle to add 100% EtOH across the top of the resolving gel. The EtOH effectively evens out the top surface of the gel which enables proteins to run more evenly. After pouring the stacking and gel and while my gel was setting, I measured out equal amounts (10 ng) of my protein samples (if I had not already). To these samples, I added 5X Laemli Sample Buffer (SB). I added 5X SB up to bring my final sample size to 40 µL. Once SB was added, samples were gently flicked and placed at 70°C for at least 10 minutes in a heat block that had been pre-heated with tube holes filled with water. Following this incubation, samples were loaded into gels along with a ladder (Biorad, Precision Plus Protein Dual Color Sandards Ladder, Cat. No. 151-0374). Samples were run on the gel at 100 volts at RT in 1XTGS. Due to the high percentage of my resolving gel and the small size of my protein of interest, I ran the gel at least 3 hours. (Usually, 1hr 30 min to 2 hr is sufficient.)

Reagent	12% Resolving Gel	6% Stacking Gel
ddH_20	13.7 mL	11.6 mL
40% Bis-Acrylamide	9.6 mL	3 mL
1.5 M Tris, pH 8.8	8 mL	-
0.5 M Tris, pH 6.8	-	5 mL
10% SDS	320 µL	200 µL
10% APS	320 µL	200 µL
TEMED	32µL	20 µL
Total volume	32 mL	20 mL

Table 8.5. Polyacrylamide gel recipes for SDS-PAGE. Gel recipes listed above are intended for use with smaller proteins. For larger proteins, the resolving gel percentage can be reduced.

While the gel is nearing the end of its run, protein membranes can be prepped if needed. I chose to use the Immobilon-P PVDF membrane (0.45 µm pore size, Millipore, Cat. No. IPVH00010) which is suggested for small proteins. Immobilon membranes must be soaked for at least 15 seconds in 100% methanol followed by a 2 minute soak in MilliQ water and then at

least 5 minutes in transfer buffer. (I used 1XTGS with 2X methanol for my transfer buffer.) For the transfer step, I first cut off extra gel (stacking gel) from the gel on which I ran my proteins. In a large tub with transfer buffer, I stacked the following in this order:

Back (black) side of transfer cassette

Sponge

Absorbent gel blot paper

Gel

Immobilon membrane

Absorbent gel blot paper

Sponge

Front (white or red) side of transfer cassette

Care was taken to try to eliminate bubbles between gel and membrane. This can be done carefully with gloved hands. After stacking and elimination of bubbles, the cassette was closed and inserted into the transfer rig with transfer buffer. The cassette was moved up and down within the rig to try to ensure complete submersion (without bubbles) of the gel and membrane. The transfer was then run at 250 mA for ~1 hr 45 min. The transfer rig was kept on top of a stir plate with a large stir bar stirring inside. Post transfer, the presence of ladder bands on the membrane indicated transfer had successfully taken place.

Blot

After transfer, the membrane was rinsed 4 times in 1XTBST for at least 5 minutes/rinse with slow horizontal shaking. After rinsing, the membrane was trimmed and cut into two pieces (one with duodenum samples and one with ileum samples.) These smaller membrane pieces enabled conservation of reagents (antibodies) and fit better into crystal plastic boxes used in subsequent steps. Membrane pieces were then blocked for 30 minutes at RT on the horizontal shaker in 1XTBST/5% powdered milk (Kroger brand, instant non-fat).

Following block, membranes were subjected to O/N incubation at 4°C on a horizontal shaker in 1:5000 control antibody dilution in block. I chose to use Rabbit anti-neuronal β-tubulin (COVANCE #PRB-435P) as a control. Another lab (Goldenring lab) has had great success with this antibody in Western blots. Additionally, this is a better control than many housekeeping gene controls as it is specific to neuronal cell types. Other control antibodies, such as GADPH or actin, are found in many other cell types. *Sox10*$^{Dom/+}$ mice have thicker muscle and different tissue consistency in some areas of their intestine, indicating that other tissue types outside the ENS may be altered or overgrown, making GADPH and actin poor choices for controls. Furthermore, at 50kDA, the control protein is small and runs near the dimer (~21 kDA) of s100B, permitting me to blot less membrane and thus conserve reagents.

After incubation, control antibody dilution was sucked off samples and saved for later use at 4°C. Membranes were then rinsed 4 times in 1XTBST for at least 5 minutes/rinse. Membranes were then incubated in 1:5000 s100B antibody (DAKO, Z0311) dilution O/N at 4°C on a horizontal shaker. The next day, membranes were rinsed 4 times in 1XTBST for at least 5 minutes/rinse. Next, membranes were placed in a 1:10,000 secondary antibody dilution (Donkey anti-Rabbit-HRP, Jackson Immuno, Cat.No. #711-035-152) for 1.5 hr at RT (covered). Following secondary antibody application, membranes were rinsed 4 times in 1XTBST for at least 5 minutes/rinse. Samples were then subjected to ECL substrate (Biorad, Clarity ECL Substrate system) incubation for 5 minutes followed immediately by a quick rinse in 1XTBST. Membranes were then placed between layers of Saran wrap, laid into cassettes (FisherBiotech, Electrophoresis System, Autoradiography Cassette, FBAC 810) and film (KODAK, 8 x 10 inch BioMAx MR Film, Cat. No. 870 1302) was exposed to the membrane in a dark room at roughly 1 sec, 10 sec, 30 sec, etc. intervals until optimal film exposure was reached. For my films, I was looking for evidence of bands at 50 kDA (β-tubulin control protein), 21 kDA (s100B dimer) and 10 kDA (s100B monomer). In my attempts, most of the control bands were clearly evident and worked well. I also saw

evidence of s100B dimers in my wild type duodenal samples, but not my *Sox10*$^{Dom/+}$ samples (Figure 8.7). This result was encouraging given that I expected less s100B expression in my *Sox10*$^{Dom/+}$ samples. However, I never fully optimized the procedure in order to visualize s100B dimer bands from the *Sox10*$^{Dom/+}$ or to visualize monomer s100B bands. More stringent conditions during gel running may be required to de-dimerize s100B. Additionally, alterations in the amount of protein loaded, antibody concentrations, rinses post ECL treatment, developing time, or imaging methods could lead to clearer s100B signal.

Gastric emptying & small intestine transit assay

Prior to the experiment, 2% methylcellulose (Sigma Aldrich Cat. No. 274429-5G) was dissolved in water at RT. To ensure full dissolution, the 2% methylcellulose mixture was either mixed for 4 or more hours at room temperature and stored at 4°C prior to use or mixed O/N. Rhodamine B Dextran (Invitrogen Cat. No. D-1841) was added and mixed into the 2% methylcellulose the following day at 2.5 mg/mL. For each mouse, 4 ml of filtered 0.9% NaCl solution (Corning 1L filter system; 0.22 µm; Cat. No. 431098) was placed in eleven 15-mL conical tubes (Corning CentriStar, 15-ml polypropylene, Cat. No.05-598-59B). For each mouse, tubes were labeled with an identifier for that mouse as well as the numbers 1-10 to denote small intestine segments and 11 to denote the stomach. Another tube was filled with at least 7 mL of 1XPBS and labeled 12 for the cecum and colon. Additionally, a “cardboard ruler” was prepared in order to divide the small intestine into 10 equal segments the day of the experiment. This cardboard ruler included several measurements of equal segments of 10. For example, one set of lines had each segment equaling 2 cm and another set of lines had 1.5 cm segments. Because the age and strain of the mouse significantly affects the length of the intestine, having several sets of equal segments allows the experimenter to quickly dissect and divide the intestine without having to pull out a ruler and draw new sets of lines in the middle of the experiment. The cardboard ruler

was covered in Saran™ wrap to allow for easy cleaning with 100%EtOH after each mouse dissection.

The day before the experiment, adult mice (4-8 weeks) were fasted overnight in cages with CAREfresh® or Purcell bedding and then water deprived for 3 hours prior to the experiment. Each mouse was gavaged (BD 1 ml Syringe Ref. No. 309602; Instech Plastic Feeding Needle Ref. No. FTP 22-30) with 200 µl of the Rhodamine B Dextran/2% methylcellulose solution and allowed to survive for 15 minutes singularly in a cage with CAREfresh® bedding with no food or water. (Gavage needles were replaced between mice if bent or damaged. Mice that spit up the gavage solution or had solution come through their nasal cavity were excluded from the study.) At 15 minutes, mice were placed in a chamber and exposed to isoflurane (Piramal Healthcare) for 30 seconds and then immediately underwent cervical dislocation.

Post-sacrifice, the ventral side of the mouse was wetted down and cleaned with 100% EtOH. The abdominal cavity was opened and the esophagogastric junction, pyloric sphincter, and ileocecal junction were immediately clipped (Dieffenbach Serrefine Artery Clamps, ordered through Amazon.com, Part No. SBD-225) to prevent further movement of gastrointestinal contents. Extraneous tissue (mesentery, blood vessels, pancreas, spleen) was then removed with a dissection scissor and forceps. The cecum and colon were submerged in 1XPBS in a 15 mL conical tube for later use. The stomach was removed above the pyloric sphincter clip and placed in the tube labeled 11 for the stomach. The remaining small intestine was divided into ten equal segments using the cardboard ruler and placed in tubes labeled 1-10, with 1 denoting the most proximal segment and 10 denoting the most distal segment. All segments were emerged in the 4 mL of 0.9% NaCl solution as soon as possible and covered with aluminum foil to avoid exposure to light.

Once all segments were collected, each segment was homogenized in the 4 mL 0.9% NaCl solution (IKA-WERKE® ULTRA-TURRAX®, T-25 at approximately 19,000 rotations/minute). Tissue was homogenized for a minimum of 3 seconds. Between each

segment, the probe was washed with deionized water, 0.9% NaCl, and then again with 0.9% NaCl. Between each mouse, tissue stuck to the probe was removed with forceps and the deionized water was replaced. (Because the stomach usually caused the most tissue to stick to the probe, it was homogenized last for each mouse.) Homogenized tissue was then spun down for a minimum of 10 minutes at a minimum of 2000 RPM in a SORVALL RT7 tabletop centrifuge. 15 µl of supernatant from each tube was placed in a well of a 384-well PCR plate (Phenix, Cat. No. MPS-3898BLK). Additionally, the equivalent of 200µl of rhodamine B dextran/2% methylcellulose solution in 4 mL of 0.9% NaCl solution and 0.9% NaCl solution were placed in at least three wells to serve as 'maximum possible fluorescence' and blank controls respectively. Fluorescence intensity was read the day of or plates were covered and placed at 4°C until read. (Plates never sat more than two days at 4°C before being read.) Plates were read on a Molecular Devices/LJL Analyst HT (Molecular Devices, Union City, CA, USA). For the LJL Analyst, Phenix plate dimensions were entered and saved. Settings for readings were as follows:

Averaging: 3 reads per well

Excitation Filter: 7 TAMRA

Emission Filter: 620-635

Read location: Top well read

Time between readings: 100 ms

Motion settling time: 25 ms

Shake time: none (0 s)

Attenuator mode: high

Data from fluorescence reads was then used to calculate gastric emptying and a small intestine motility score. To calculate gastric emptying, the total fluorescent count (all fluorescence detected in the stomach and small intestine) was calculated first:

$C_{all} = \sum (C_{segment})$

where C_{all} is the total fluorescence count and $C_{segment}$ is the fluorescence count in each segment.

Gastric emptying (the percent of fluorescent signal that has left the stomach) was then calculated:

Gastric emptying = $[(C_{all} - C_{stomach})/ C_{all}] \times 100$

where $C_{stomach}$ is the fluorescence reading for the stomach

A small intestine motility score was calculated for each mouse based on the geometric center (mean) of fluorescence in the small intestine:

Geometric center (mean) = $\sum[(C_{segment} \times \text{segment number})/C_{SI}]$

where C_{SI} is the total fluorescence count in the small intestine.

This method to determine gastric emptying and small intestine motility in rats was first described in detail by Miller and colleagues (16) and have been used more recently in mouse (17). I tested for differences in gastric emptying rates and small intestine motility scores using a Student's t-test assuming unequal variance (also known as Welch's t-test) in JMP version 10 (SAS Institute Inc., Cary, NC, USA.)

To generate heat maps used to depict gastric emptying and small intestine motility data, I first determined the percent contribution of each intestine segment to the transit score for each mouse (ie intestine segments with large amounts of the fluorescent meal contribute greatly to the score; while those with little fluorescent meal contribute little.) I chose "percent contribution" as our measurement in generating these maps as fluorescence intensity itself is a relative measurement and "percent contribution" normalizes the data. Once I determined the percent

contribution for each intestine segment for each mouse, I averaged the percent contributions within each genotype for each intestine segment. Using MATLAB (Mathworks, Natwick, MA, USA) to generate a heat map, we assigned higher average percent contributions the color red (representing greater fluorescent reads) and lower average percent contributions no color (representing no or little fluorescent reads.) These colors (averages) were then interpolated across segment numbers to generate a heat map. This type of schematic can be generated using the following code (with labels and data included here as an example) within MATLAB:

```
close all
clear all

data= [ 4.0416096 14.28408441 4.295096182 12.09379354 7.553430393 6.350554323 4.700948565 7.68474756
22.0739831 38.5162063 20.70632278 35.45094993 22.77372882 30.86191969 16.00892165 20.95407008
24.88038928 26.29393612 29.94567845 36.40508425 25.01027451 32.51049307 16.02055989 18.80964905
31.21113151 9.992309122 28.44167445 8.089767516 15.53496235 7.549006448 15.71863551 12.81208631
12.25236999 6.451572256 9.80013087 1.453495287 9.358071659 15.34240155 10.54429915 2.365436026
1.05727502 0.62966815 0.797701269 0.588716867 6.735494095 3.434370837 0.668142608 0.384875792
0.676744389 0.7652144 0.649828756 0.570780285 6.947050581 1.052032025 1.054545974 0.55150921
1.212253706 0.761793527 1.485846914 1.241554973 2.24019892 0.593656462 0.936757664 0.884501296
1.502352027 1.13635819 2.008245828 2.394361344 1.983012587 1.065398182 0.918010851 1.39678111
1.091891383 1.168857521 1.869474496 1.711496006 1.863776084 1.240167411 0.962616775 1.628591084
];


labels=[4 wk male WT' '4 wk male Dom' '4 wk female WT' '4 wk female DOM' '6 wk male WT' '6 wk male Dom' '6 wk
female WT' '6 wk female DOM];

custcolor=[1.0000    1.0000    1.0000
    1.0000    1.0000    1.0000
    1.0000    1.0000    1.0000
    1.0000    1.0000    1.0000
    1.0000    1.0000    1.0000
    1.0000    1.0000    1.0000
    1.0000    1.0000    1.0000
    1.0000    0.9750    0.9865
    1.0000    0.9500    0.9730
    1.0000    0.9250    0.9596
    1.0000    0.9000    0.9461
    1.0000    0.8750    0.9326
    1.0000    0.8500    0.9191
    1.0000    0.8250    0.9056
    1.0000    0.8000    0.8922
    1.0000    0.7750    0.8787
    1.0000    0.7500    0.8652
    1.0000    0.7250    0.8517
    1.0000    0.7000    0.8382
    1.0000    0.6750    0.8248
    1.0000    0.6500    0.8113
    1.0000    0.6250    0.7978
    1.0000    0.6000    0.7843
    1.0000    0.5875    0.7603
    1.0000    0.5750    0.7363
    1.0000    0.5625    0.7123
    1.0000    0.5500    0.6882
    1.0000    0.5375    0.6642
    1.0000    0.5250    0.6402
    1.0000    0.5125    0.6162
```

```
    1.0000    0.5000    0.5922
    1.0000    0.4875    0.5681
    1.0000    0.4750    0.5441
    1.0000    0.4625    0.5201
    1.0000    0.4500    0.4961
    1.0000    0.4375    0.4721
    1.0000    0.4250    0.4480
    1.0000    0.4125    0.4240
    1.0000    0.4000    0.4000
    1.0000    0.3750    0.3750
    1.0000    0.3500    0.3500
    1.0000    0.3250    0.3250
    1.0000    0.3000    0.3000
    1.0000    0.2750    0.2750
    1.0000    0.2500    0.2500
    1.0000    0.2250    0.2250
    1.0000    0.2000    0.2000
    1.0000    0.1750    0.1750
    1.0000    0.1500    0.1500
    1.0000    0.1250    0.1250
    1.0000    0.1000    0.1000
    1.0000    0.0750    0.0750
    1.0000    0.0500    0.0500
    1.0000    0.0250    0.0250
    1.0000         0         0
    0.9375         0         0
    0.8750         0         0
    0.8125         0         0
    0.7500         0         0
    0.6875         0         0
    0.6250         0         0
    0.5625         0         0
    0.5000         0         0];


for iii=1:8



MUTmat=ones(10,100);
tem=data(:,iii);

for i=1:100
   for j=1:10
      columncontmut(j,i)=tem(j)*MUTmat(j,i);

   end
end

figure(iii)

[hC hC] = contourf(transpose(columncontmut),500);
set(hC,'LineStyle','none');5
title(labels(iii));
%colormap(custcolor);
fnam= num2str(cell2mat(labels(iii)));

saveas(hC,fnam,'pdf');

end
```

Total GI tract transit assay

Prior to the experiment, 0.5% methylcellulose (Sigma-Aldrich, Cat. No. 274429-5G) solution was made in filtered 0.09% NaCl (saline) solution (Corning 1L Filter System, Cat. No. 431098) by O/N stirring. Carmine (Sigma-Aldrich, Cat. No. C1022-5G) was added to make a 6% carmine red solution and allowed to either stir O/N the day before the experiment or vortexed vigorously the day of the experiment to ensure uniform mixing of the carmine into the solution. Solution was either used directly after addition of Carmine or stored at 4°C for future use. If the 6% Carmine solution was stored in 4°C for future use, it was allowed to warm to RT before beginning the experiment.

Cages were prepared by removing bedding and cleaning the interior with 100% EtOH. Whatman paper (Whatman, Cat.No. 3030-392) was placed in the bottom of the cage to enhance visualization of fecal pellets. A numbered sticky note was placed on each cage to record the mouse assigned to that cage, gavage time, and time of appearance of red fecal pellets. Water bottles and low-fat mouse chow were available in the food and water bottle holder so mice could eat and drink *ad libitum* during the experiment. A 15-mL clear canonical tube filled with tap water was numbered corresponding to the cage number and set on top of the food in its corresponding cage.

Day of the experiment, 6 week old mice were brought from the mouse facility in either cages or buckets and immediately placed singularly in experimental cages. Unlike the gastric emptying and small intestine transit assay, I did not fast mice O/N prior to testing. (Although, if I were testing other mouse disease models, I would consider fasting before and/or during the experiment if regular feeding behaviors are known to differ. For example, ob/ob mice overeat due to leptin deficiency. Overeating would cause an increase in total gut transit due to sheer volume of food being ingested and not necessarily changes in ENS function.) Mouse information (breeding cage, ear punch, etc.) was added to each sticky note on each cage. I gavaged (BD 1 ml Syringe Ref. No. 309602; Instech Plastic Feeding Needle Ref. No. FTP 22-30) each mouse with 300 µl of 6% Carmine solution and recorded the time at which the gavage was complete on

each cage sticky note. Gavage needles were replaced in between mice if visibly bent or damaged. Any animals that spit up solution or had solution come through their nasal cavity were excluded from the study. For the first one or two experiments for each phenotype tested in these studies, stool was checked for and collected starting 1 hour after gavage and then repeated 30 minutes later. Then cages were checked every 10 minutes until the first appearance of red fecal pellets. Then cages were checked at least every 10 minutes or more often after that. These checks included visualization of the underside of mouse cages beneath the Whatman paper since fecal pellets occasionally were located beneath the paper. Fecal pellets were collected via forceps and placed in the 15 ml canonical tubes with tap water for easy visualization of Carmine within the pellet. The time of fecal Carmine visualization was recorded on the sticky note under gavage start time. The total time in minutes from gavage to excretion of red fecal pellets was then calculated. All mouse information and recorded times were also written down on lab notebook paper during the experiment to ensure no data would be lost.

Because strain background plays a large role in total transit time, the first check for fecal pellets was adjusted accordingly throughout the course of these experiments. (For example, after two experiments, the fastest transit time I recorded for *129SvEdrnb*$^{+/+}$ mice was 2 hours and 56 minutes. Thus, the next time I performed this assay on *129SvEdrnb*$^{+/+}$ mice, I did not check for fecal pellets after one hour, but started at 1 hour and 45 minutes post-gavage. Conversely, if you predict a fast transit time in your animals, consider checking for fecal pellets prior to the suggested 1 hour post-gavage.) Additionally, large variation can exist in this experiment and other labs suggest repeating in mice 5-6 days following the first gavage if possible. However, I was limited to one test per animal due to IACUC guidelines and mouse facility requirements within my institution.

Transit time between HSCR mutants and WT littermates for each gender were compared using a student's t-test assuming unequal variance (Welch's t-test) using JMP version 10 and 11 (SAS Institute Inc., Cary, NC, USA.)

Histology

Intestine "jelly rolls"

Adult mice (6-8 weeks) were sacrificed with isoflurane. Two regions of gut—the distal half of the small intestine and the large intestine—were immediately dissected out into 1XPBS and gently flushed with 1XPBS. Care was taken to flush gently since forceful flushing can disturb gut epithelium. Guts were then flushed once with 10% NBF to help preserve the integrity of the gut epithelium. Flushed gut pieces were cut along the mesenteric line and then laid out flat using forceps onto Whatman paper. Using curved tip forceps, gut pieces were then rolled into "jelly rolls" starting from the most distal section and working proximally. As the gut was rolled, the forceps were used to flatten the gut and pull the roll tight. Care was taken not to roll the gut piece too tight as "tenting"—where inner rolls get squeezed out from the entire roll—can occur. Once gut pieces were completely rolled, a syringe needle was pushed through the roll and the proximal plastic portion of the syringe needle removed. Pinned, rolled intestines were placed in cassettes with the edges of the rolled intestine against the surface of the cassette. Cassettes with samples were submerged completely in 10% NBF in plastic containers or glass beakers and placed in 4°C O/N. Whittem and colleagues (2010) provide an excellent video detailing the process of "jelly rolling" intestines should future lab members need a visualization of this technique (18).

Post-fix, samples in cassettes were delivered to the Translational Pathology Shared Resource (TPSR) Core facility at Vanderbilt University for processing and embedding. Initially, samples were embedded in paraffin wax, picked up at the TPSR facility, and stored at RT or -20°C until sectioned. Samples were sectioned on a microtome at 5-13 µm. A heated water bath was used to mount sections onto slides. Sections were allowed to dry on a slide warmer for a minimum of 1 hour before being stored at RT or undergoing H&E staining. Ultimately, we had the

TPSR Core process, embed, section, and stain samples to insure consistency in sectioning and staining as well as save time.

Pyloric sphincter collection for H&E

Pyloric sphincter samples were typically collected at the same time as intestine "jelly roll" samples. For each animal, the gastrointestinal tract was cut at the esophagus and ~1 cm below the duodenum and removed from the animal and placed in 1XPBS. Once in 1XPBS, I cut off the proximal 0.5-0.75 of the stomach and gently swished the sample around in 1XPBS to remove large food items from the stomach. After swishing, I used a syringe with 1XPBS to rinse the inside of the stomach and gently flushed through the pyloric sphincter. I also gently flushed 1XPBS in the opposite direction through the duodenum to remove as much food stuffs as possible from the sample. Importantly, when I first attempted to collect pyloric sphincter samples, I left the entire stomach intact. I inserted a syringe into the stomach and tried flush the entire stomach with 1XPBS to remove food stuffs. Interestingly, in my first attempt with a *Sox10*$^{+/+}$ mouse sample, the pyloric sphincter snapped shut and the stomach became engorged with liquid. The next sample I attempted was from a *Sox10*$^{Dom/+}$ mouse. Here, I once again attempted to clear the stomach totally intact; however, in this mouse, the liquid immediately went through the pyloric sphincter. In an attempt later with another *Sox10*$^{Dom/+}$ mouse sample, liquid was able to make it through the pyloric sphincter again, but in very quick spurts as the pyloric sphincter visibly contracted and relaxed multiple times. This observation, in combination with the increased gastric emptying observed in 6-week+ male *Sox10*$^{Dom/+}$ mice (Chapter 2), led us to pursue further studies in pyloric sphincter dynamics (Chapter 4). In regard to experiment design for pyloric sphincter collection, leaving the entire stomach intact not only led to difficulties in cleaning out food material from the stomach, but also led to difficulties in sectioning (as wax had issues permeating into the lumen of the stomach.) These technical issues, as well as the fact the proximal stomach was not needed for evaluation, led me to alter the protocol to remove the majority of the stomach from the

sample before flushing. After samples were thoroughly (but gently) flushed, they were laid in cassettes on their sides. Cassettes with samples were submerged completely in 10% NBF in plastic containers or glass beakers, placed at 4°C O/N, and then delivered to the TPSR facility for processing, embedding, sectioning, and H&E staining. Attempts were made by myself and by the TPSR core staff to section samples so that the lumen of the GI tract was visible and continuous throughout the distal stomach, pyloric sphincter, and duodenum for the section. This quality control, in theory, would reduce variability in measurements (muscle thickness, antral opening, etc.) due to samples being cut at different angles.

Hematoxylin & Eosin staining

Throughout the H&E procedure, I used slide carriers and solution basins from the Tissue-Tek® Manual Slide Staining Set. Slides were deparrafinized by placing slides into xylenes (Fisher, Cat. No. X3P1Gal) for 2 minutes and then repeating this step in a new xylene bath. Gentle swishing for a few seconds immediately upon submersion and immediately before removal helped to insure complete removal of all paraffin wax. This step was performed in the chemical hood, and xylenes were reused several times for this step. However, when it was noted that the reused xylenes were not removing wax very efficiently, reused xylenes were properly disposed of and fresh xylenes were used. Sections were rehydrated in a series of ethanol dilutions (100%, 90%, 70%, 50%) and then placed in deionized water. Slides were in each ethanol and water bath for 2 minutes.

Next, sections were stained with filtered Harris hematoxylin (VWR Scientific, Cat. No. 84000090) for 3 minutes. Following hematoxylin staining, slides were immediately immersed in a slide basin with tap water and then brought over to the sink. In the sink, tap water was allowed to wash over the slides for 10 minutes. Care was taken to avoid direct contact of sections with the faucet water stream as this can cause sections to fall off slides. However, attempts were made to keep the water pressure coming from the faucet high so that water was constantly

circulating throughout the entire basin. Next, slides were dipped 4 times in 1% acid alcohol (1mL 12N HCl in 99 mL 70% EtOH) followed by a 45 second rinse in 0.1% Na bicarbonate. Then, as previously described, slides were washed with running tap water for 10 minutes. Slides were then immersed in 80% ethanol for 2 minutes followed by eosin (1% alcoholic, HARLECO®, VWR Scientific, Cat. No. 15204-132) stain for 2 minutes. Finally, slides were dehydrated in a series of ethanol dilutions (90%, 95%, 100%) and two basins of xylenes. Slides were in each dilution for 2 minutes. Slides were then laid out on paper towels to dry in the chemical hood for at least 1 hour or O/N. Coverslips were mounted onto sections in the chemical hood with Permount mounting medium (Fisher, Cat. No. SP15-100). Importantly, the protocol above was derived from a series of H&E optimization attempts by myself and another graduate student, Elaine Ritter, in lab. H&E staining improved drastically over these series of optimizations. However, although this H&E staining was a simple procedure, it was time intensive, my H&E staining had not reached "text book" or "publication quality", and the TPSR Core at Vanderbilt offers H&E staining services at very reasonable prices. We ultimately decided to have the TPSR Core at Vanderbilt section and H&E stain samples when it came to samples for analysis and publications. A comparison of H&E staining from our protocol compared to that of the TPSR Core is provided in Figure 8.8.

HSCR Surgical Resections

Sample acquisition

Following surgery and pathology evaluation, full length surgical resections from colons of Hirschsprung patients were collected from the Pediatric Pathology Suite of the Monroe Carell Jr. Children's Hospital at Vanderbilt. Samples were either collected and placed on ice immediately after pathologist evaluation or were placed into a 4°C fridge and acquired at the earliest convenience of the investigator. (Longest time to collection was after a weekend (~2.3 days) due to a long surgical procedure followed by confusion over storage location.) The vast majority of samples were acquired the same day as surgery; however, a few samples were collected up to 2

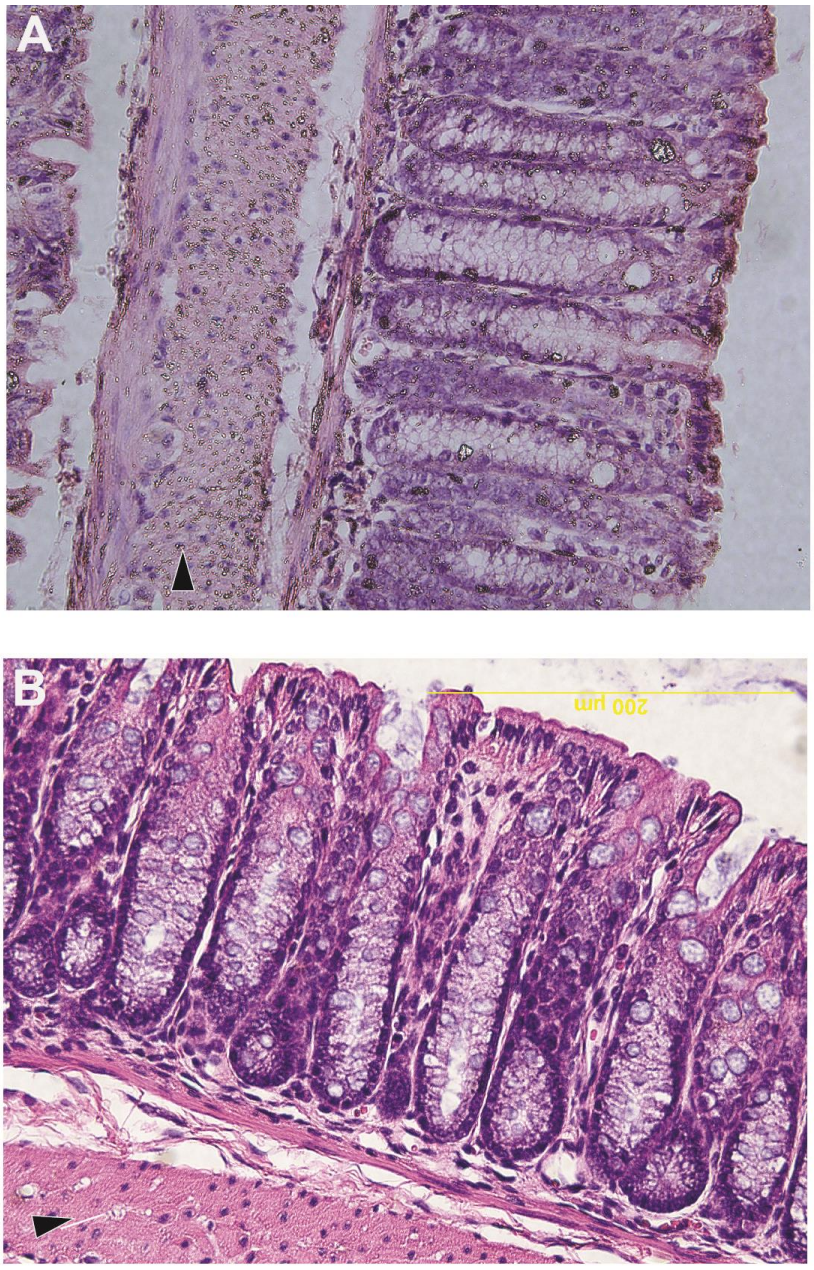

Figure 8.8. H&E staining comparison in the colon. (**A**) In our hands, sectioning was clean and H&E staining clearly labeled cells. However, eosin staining was too light as exemplified in the circular muscle layer (arrowheads, pink color). Residue (of unknown source) was also visualized throughout the sample after mounting. (**B**) TPSR Core sectioning and staining protocols produced clean sections with deeper and richer H&E staining.

days post-surgery. Collection time did not seem to affect subsequent NADPH-β staining. These results are in line with a study by Wester and colleagues wherein pediatric autopsy colonic tissue collected several hours after time of death still successfully stained with NADPH-β staining (19). The maximum length of time from surgery to sample collection and fix to still achieve successful acetylcholinesterase (AChE) stain or immunohistochemistry is unknown. Samples I performed successful AChE stain or IHC on were collected and fixed day of surgery. Obstacles with AChE staining and IHC led me to abandon these techniques early in the study, leaving samples collected and fixed at later times (1-2 days post-surgery) untested with these techniques.

Control (autopsy) samples were collected during autopsy from the Autopsy Suites at Vanderbilt University Hospital or after autopsy from a 4°C fridge in the Pediatric Pathology Suite of the Monroe Carell Jr Children's Hospital at Vanderbilt. Samples were collected as close to 'time of death' as possible, usually the morning or afternoon following death when autopsies are routinely performed.

Sample fixation and dissection

All samples were transported on ice to the laboratory, immediately rinsed at least once in 1XPBS, and then fixed in 4% PFA. (1XPBS rinses prior to fixation can be increased if samples contain a lot of fecal material or blood. Although fecal material and blood do not seem to affect fixation or future staining, tissue is much more pleasant to manipulate if relatively clean.) Initially, samples acquired early in the study were fixed 15-30 minutes in 4% PFA, partially dissected (serosa, mucosa and some muscle fibers removed), and then fixed an additional 30 min – 1.5 hours in 4% PFA at RT. Although this fix time was adequate for successful IHC, AChE stain, and NADPH-β stain, it was not adequate for long term storage of tissue. Typically, tissue not fixed overnight started to disintegrate and grow mold. Once I dropped AChE staining and IHC from the study and also discovered O/N fixing of samples in 4% PFA did not affect the NADPH-β stain, all collected samples from that point on were fixed at least O/N in 4% PFA at 4°C. Fixation of tissue

was followed by at least three rinses in 1XPBS for samples or sample pieces undergoing IHC or NADPH-β stain. Samples or sample pieces undergoing AChE staining were additionally rinsed in tap H_20 or dH_20 and then stored in saturated sodium sulfate solution at 4°C as per standard procedures (20, 21). Most samples were sub-dissected several times to aid in exposing the myenteric plexus to stain or IHC reagents. Typically, post 15-45 minutes fix, pieces of the serosa, mucosa and some muscle fibers were removed. Following O/N fix and/or immediately prior to staining, additional muscle fibers were removed (from the circular and/or longitudinal muscle layer depending on the thickness of the sample.) Finally, for NADPH-β stain, samples were sub-dissected during the stain. (See NADPH-β stain section below for more details.)

IHC on human intestine samples

Colonic tissue samples subjected to IHC were rinsed with 1XPBS, blocked in NDS block for 1 hour at RT or O/N at 4°C, and then incubated in primary antibody O/N at 4°C. Primary antibodies tested on human tissues include: Rabbit anti-Phox2b, Human anti-HuC/D, and Rabbit anti-s100 (Table 8.2). Primary antibody incubation was followed by rinses in 1XPBS/0.1% TX-100 (x4), incubation in secondary antibody, one rinse in 1XPBS/0.1% TX-100 and two rinses in 1XPBS. Tissues were stored in fresh 1XPBS at 4°C until imaging. Successful IHC was only attained with the Rabbit anti-Phox2b antibody (Figure 8.9C'&C''). Several factors may have influenced my results with the other antibodies. To my knowledge, none of antibodies had ever been tested on human tissue and thus the binding dynamics of the antibody to the protein of interest, concentration of antibody needed, and optimal fix time for tissue before IHC was attempted were unknown. All samples that I performed IHC on were fixed under two hours. Longer fix times in the future could influence results. Additionally, the thickness of the human tissue could make it difficult for primary and secondary antibodies to permeate the tissue and come in contact with the myenteric plexus (MP). Although efforts were made to remove muscle fibers and expose parts of the MP, the inability to see the MP while dissecting often times led to

too much muscle still covering the MP or disruption and destruction of the MP if too much muscle was removed. Besides appropriately dissecting off muscle fibers, longer incubation times in primary and secondary antibodies and/or stronger detergents to break up tissue could potentially resolve some of the permeation issues.

AChE staining on human intestine samples

Following storage in saturated Sodium Sulfate solution at 4°C, samples were rinsed in MilliQ filtered H_20 and then incubated in incubation buffer for 2.5 – 3 hours at 50-60 rpm on a horizontal shaker. (Incubation buffer: 0.886% Sodium Acetate Trihydrate, 0.075% Glycine, 0.05% Cupric Sulfate, 0.1156% Acetylthiocholine iodide, 0.0072% Ethopropazine in MilliQH_20, pH 5.5. pH adjusted with 1.7 N Acetic Acid.) Following incubation, in a chemical hood, samples were rinsed in MilliQ H_20, immersed 1 – 3 minutes in freshly made 1.25% Sodium Sulfide solution, pH 6.0, and rinsed six times in MilliQ H_20. Samples were then stored in scintillation vials in autoclaved 50% glycerol solution at 4°C until they were imaged. AChE staining was successfully performed on samples where the muscle layers were very easily separated without disturbing the MP, such as premature fetal autopsy samples, or in older patient samples where some muscle fibers were removed to successfully uncover part of the MP so that it was easily exposed to AChE staining reagents (Figure 8.9A). Unfortunately, because removal of muscle fibers was very difficult to complete without disturbing the MP and extremely time intensive, AChE staining on human tissues was dropped midway through the study.

NADPH-β stain on human intestine samples

Following fixation and rinses in 1XPBS (see “Sample fixation and dissection” section for details), samples subjected to NAPDH-β were rinsed in fresh 1XPBS day of NAPDH-β staining and then placed in 10 mL of NAPDH-β incubation buffer at RT on a nutator (Table 8.6). During incubation, samples were checked multiple times for appearance of stain in the MP on the edges

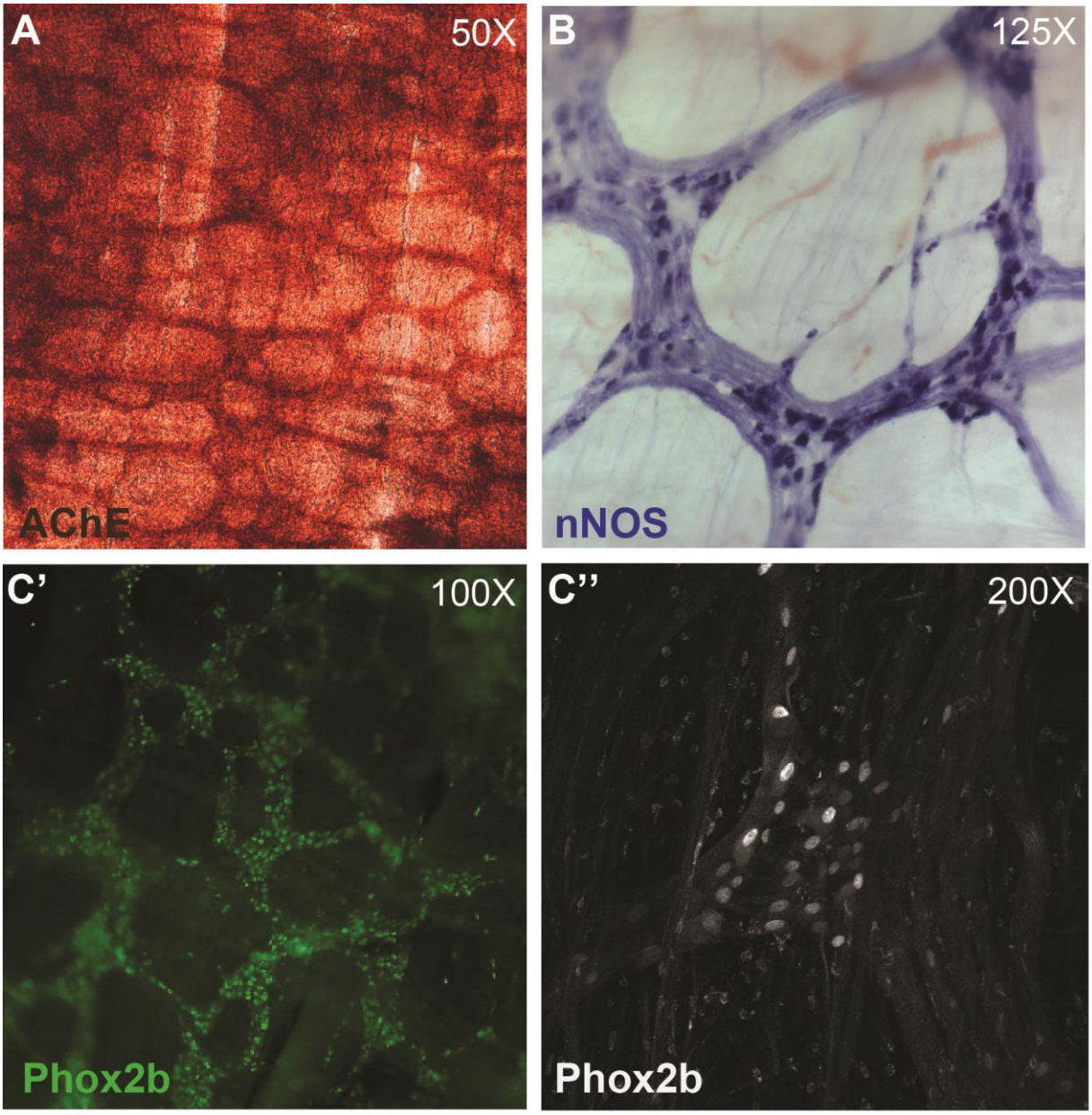

Figure 8.9. Successful stains and IHC on human colonic tissue. Stains and IHC with several antibodies were attempted on human ccolonic tissue. (**A**) Acetycholinesterase staining (AChE), which labels cholinergic neurons and processes, was successful in samples where the myenteric plexus could be exposed pior to staining. (**B**) Similarly, NADPH-B staining labels nNOS expressing neuron bodies (dark purple) and processes (light purple) when the myenteric plexus is exposed during the staining process. (**C' & C"**) IHC with a Phox2b antibody, which labels both neurons and glia, was successful. However, smooth muscle tended to obscure Phox2b expressing ganglia cells unless completely removed.

of the sample between the longitudinal and circular muscle layers (Figure 8.10A). Once the MP was visible, muscle fibers from the longitudinal and/or circular muscle layers were removed from the sample under a dissection microscope to help expose more of the internal MP to incubation buffer. (MP stain visibility varied with samples, but stain will probably not appear for at least 15 minutes and usually took longer. Additionally, in my experience, it is best to allow the stain reaction at least 45 minutes – 1 hour to start. If no MP is visible by that time, chances are the tissue will fail to stain at all.) The stained MP on the edges of the sample was used as a guide for the dissection to avoid accidentally dissecting off or tearing the MP in the sample (Figure 8.10B). Additionally, samples were kept in incubation buffer during dissection, allowing for MP to continue to stain and further aid in dissection. Samples were periodically returned to the nutator after dissection and allowed to stain more undisturbed. This process of alternating between dissecting and undisturbed staining was repeated multiple times until the majority of MP on a sample was visible and stained (Figure 8.10C&D). Typically, stain times ran over 200 minutes. To quench the staining process, samples were rinsed three times in 1XPBS, fixed 1.5 – 2 hour fix in 4% PFA, rinsed three times in 1XPBS, and then placed in fresh 1XPBS and stored at 4°C until clearing. For clearing samples, samples were placed in the following glycerol solution gradient:

Reagent	Amount	Vendor	Catolog #
NADPH-β	10 mg	Sigma-Aldrich	N1630
NBT/BCIP	13.3 ul	Roche	11 681 451 001
10% Triton X-100	3 mL	Fisher	BP157-500
1XPBS	fill to 10 mL	Sigma	P4417

Table 8.6. NADPH-β stain reagents. This recipe for NADPH-β diaphorase stain yields 10 mL of staining solution, but may be adjusted appropriately for tissue size. NADPH-β is an expensive reagent and staining solution cannot be stored for later use. Thus, care should be taken to make the least amount of staining solution possible for the experiment.

15% glycerol in 1XPBS, 25% glycerol in 1XPBS, 50% glycerol in H_20, and 70% glycerol in H_20. For each glycerol solution, samples were allowed to equilibrate at 4°C on a nutator O/N.

NADPH-β stain sample imaging

Following NADPH-β staining and clearing, samples were mounted between two large glass slides (Ted Pella, Inc., 152 x 114 mm, No. 260233). Samples were kept moist while mounted on slides with 70% glycerol solution or 1XPBS. Samples images were captured on a Nikon AZ 100 M wide field microscope (Vanderbilt CISR) with a Nikon DS-Ri1 color camera using NIS-Elements software.

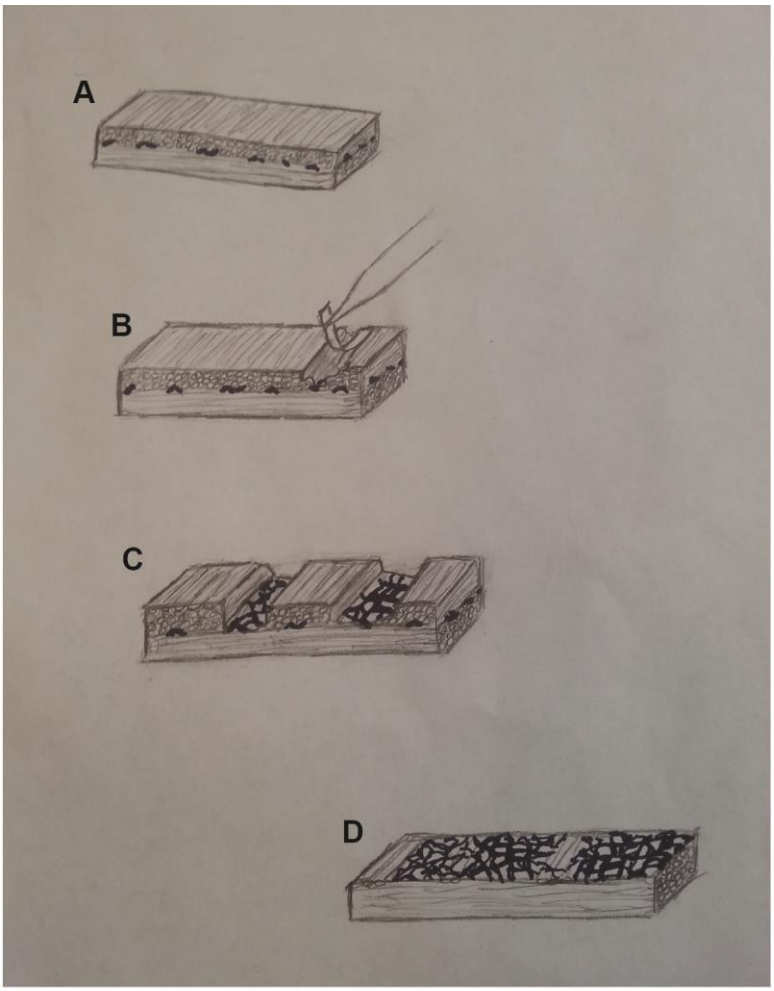

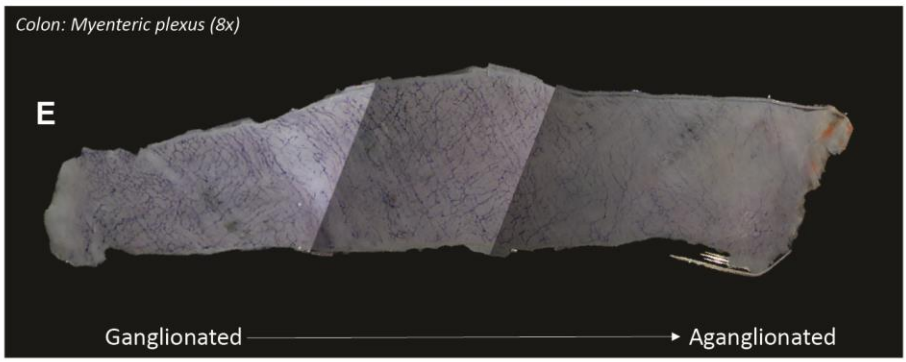

Figure 8.10. Dissection of gut muscle during NAPDH-β staining. (**A**) Initially, during NADPH-β staining, only neurons on the edge of the sample in the myenteric plexus (between cirucluar and longitudinal muscle layers) can be visualized. (**B**) These neurons that stain along the edges can be used as a guide to remove strips of muscle to expose more myenteric plexus for staining. (**C**) Removal of muscle followed by more staining eventually leads to entire ganglia and and their connectives being exposed to stain. (**D**) After many rounds of removing strips of muscle and staining, nearly the entire myenteric plexus can be viewed. (**E**) Actual surgical resection following NADPH-β staining.

References

1. Corpening, J.C. 2007. Transgenic studies to investigate timing of lineage divergence in the enteric nervous system. In *Neuroscience*: Vanderbilt University.
2. Dymecki, S.M., Ray, R.S., and Kim, J.C. 2010. Mapping cell fate and function using recombinase-based intersectional strategies. *Methods Enzymol* 477:183-213.
3. Sanders, K.M., Ward, S.M., and Koh, S.D. 2014. Interstitial Cells: Regulators of Smooth Muscle Function. *Physiol Rev* 94:859-907.
4. Nemeth, L., Maddur, S., and Puri, P. 2000. Immunolocalization of the gap junction protein Connexin43 in the interstitial cells of Cajal in the normal and Hirschsprung's disease bowel. *J Pediatr Surg* 35:823-828.
5. Yamataka, A., Kato, Y., Tibboel, D., Murata, Y., Sueyoshi, N., Fujimoto, T., Nishiye, H., and Miyano, T. 1995. A lack of intestinal pacemaker (c-kit) in aganglionic bowel of patients with Hirschsprung's disease. *J Pediatr Surg* 30:441-444.
6. Vanderwinden, J.M., Rumessen, J.J., Liu, H., Descamps, D., De Laet, M.H., and Vanderhaeghen, J.J. 1996. Interstitial cells of Cajal in human colon and in Hirschsprung's disease. *Gastroenterology* 111:901-910.
7. Piotrowska, A.P., Solari, V., de Caluwe, D., and Puri, P. 2003. Immunocolocalization of the heme oxygenase-2 and interstitial cells of Cajal in normal and aganglionic colon. *J Pediatr Surg* 38:73-77.
8. Rolle, U., Piotrowska, A.P., Nemeth, L., and Puri, P. 2002. Altered distribution of interstitial cells of Cajal in Hirschsprung disease. *Arch Pathol Lab Med* 126:928-933.
9. Horisawa, M., Watanabe, Y., and Torihashi, S. 1998. Distribution of c-Kit immunopositive cells in normal human colon and in Hirschsprung's disease. *J Pediatr Surg* 33:1209-1214.

10. Taniguchi, K., Matsuura, K., Matsuoka, T., Nakatani, H., Nakano, T., Furuya, Y., Sugimoto, T., Kobayashi, M., and Araki, K. 2005. A morphological study of the pacemaker cells of the aganglionic intestine in Hirschsprung's disease utilizing ls/ls model mice. *Med Mol Morphol* 38:123-129.

11. Donato, R., Cannon, B.R., Sorci, G., Riuzzi, F., Hsu, K., Weber, D.J., and Geczy, C.L. 2013. Functions of S100 proteins. *Curr Mol Med* 13:24-57.

12. Donato, R., Sorci, G., Riuzzi, F., Arcuri, C., Bianchi, R., Brozzi, F., Tubaro, C., and Giambanco, I. 2009. S100B's double life: intracellular regulator and extracellular signal. *Biochim Biophys Acta* 1793:1008-1022.

13. Roh, J., Knight, S., Chung, J.Y., Eo, S.H., Goggins, M., Kim, J., Cho, H., Yu, E., and Hong, S.M. 2014. S100A4 expression is a prognostic indicator in small intestine adenocarcinoma. *J Clin Pathol* 67:216-221.

14. Leach, S.T., Yang, Z., Messina, I., Song, C., Geczy, C.L., Cunningham, A.M., and Day, A.S. 2007. Serum and mucosal S100 proteins, calprotectin (S100A8/S100A9) and S100A12, are elevated at diagnosis in children with inflammatory bowel disease. *Scand J Gastroenterol* 42:1321-1331.

15. Borthwick, L.A., Neal, A., Hobson, L., Gerke, V., Robson, L., and Muimo, R. 2008. The annexin 2-S100A10 complex and its association with TRPV6 is regulated by cAMP/PKA/CnA in airway and gut epithelia. *Cell Calcium* 44:147-157.

16. Miller, M.S., Galligan, J.J., and Burks, T.F. 1981. Accurate measurement of intestinal transit in the rat. *J Pharmacol Methods* 6:211-217.

17. D'Autreaux, F., Margolis, K.G., Roberts, J., Stevanovic, K., Mawe, G., Li, Z., Karamooz, N., Ahuja, A., Morikawa, Y., Cserjesi, P., et al. 2011. Expression level of Hand2 affects specification of enteric neurons and gastrointestinal function in mice. *Gastroenterology* 141:576-587, 587 e571-576.

18. Whittem, C.G., Williams, A.D., and Williams, C.S. 2010. Murine Colitis modeling using Dextran Sulfate Sodium (DSS). *J Vis Exp*.

19. Wester, T., O'Briain, S., and Puri, P. 1998. NADPH diaphorase-containing nerve fibers and neurons in the myenteric plexus are resistant to postmortem changes: studies in Hirschsprung's disease and normal autopsy material. *Arch Pathol Lab Med* 122:461-466.

20. Cantrell, V.A., Owens, S.E., Chandler, R.L., Airey, D.C., Bradley, K.M., Smith, J.R., and Southard-Smith, E.M. 2004. Interactions between Sox10 and EdnrB modulate penetrance and severity of aganglionosis in the Sox10Dom mouse model of Hirschsprung disease. *Hum Mol Genet* 13:2289-2301.

21. Owens, S.E., Broman, K.W., Wiltshire, T., Elmore, J.B., Bradley, K.M., Smith, J.R., and Southard-Smith, E.M. 2005. Genome-wide linkage identifies novel modifier loci of aganglionosis in the Sox10Dom model of Hirschsprung disease. *Hum Mol Genet* 14:1549-1558.